Polish Academy of Sciences
University of Engineering and Economics in Rzeszów

TEKA

COMMISSION OF MOTORIZATION AND ENERGETICS IN AGRICULTURE

AN INTERNATIONAL QUARTERLY JOURNAL ON MOTORIZATION, VEHICLE OPERATION, ENERGY EFFICIENCY AND MECHANICAL ENGINEERING

Vol. 13, No 2

LUBLIN – RZESZÓW 2013

Editorial Office address

Commission of Motorization and Energetics in Agriculture
Wielkopolska Str. 62, 20-725 Lublin, Poland
e-mail: eugeniusz.krasowski@up.lublin.pl

ISSN 1641-7739

Edition 150+16 vol.

TEKA. COMMISSION OF MOTORIZATION AND ENERGETICS IN AGRICULTURE – 2013, Vol. 13, No. 2, 3–6

The physical properties of starch biocomposite containing PLA

Maciej Combrzyński, Leszek Mościcki

Department of Food Process Engineering, Faculty of Production Engineering,
University of Life Sciences in Lublin, Doświadczalna 44, 20-280 Lublin, maciej.combrzynski@up.lublin.pl

Received May 6.2013; accepted June 14.2013

Summary. The paper presents the results of measurements of selected mechanical properties of biodegradable starch film produced from thermoplastic starch with 20% addition of polylactide (PLA). TPS was produced on a single screw extrusion-cooker with L/D = 16. Film blowing was processed on the plastic extruder, with L/D = 36. The measurements of the mechanical properties were performed on the Universal Testing Machine Zwick BDO-FBO0.5TH. The films produced with the addition of PLA were characterized by poor tensile strength, they easily cracked and were brittle.
Key words: PLA, biodegradable, extrusion, TPS.

INTRODUCTION

Initial production of biodegradable polymers dates back to the late twentieth century. The year 1995 can be considered as the date of manufacture of bioplastics for packaging production on a small scale [2, 3, 4, 20]. The price of bioplastics is currently one of the key market barriers that have an impact on their application. A significant and growing position in the production of degradable in the natural environment of packaging materials occupy polysaccharides of vegetable origin, in particular cellulose and starch derivatives [5, 8, 10, 11, 19]. Modification of the polymerization process and the use of new technology allow you to increase the area of applications for biodegradable plastics. Still, on the overall biopolymers market, the strongest in demand are those that are generated by biological processes. This segment is mainly dominated by polylactide (PLA) [6, 7].

Polylactide is an aliphatic polyester obtained by direct condensation of lactic acid [4, 7]. Methods for the preparation of this polymer are different, for example by a biotechnological process, which is analogous to the fermentation production of ethyl alcohol. In the global market there are different types of polylactide called NatureWorks, which produces U.S. company Cargill Dow LLC. These polymers are adapted to be processed by various techniques (injection-moulding, extrusion, thermoforming, blowing) in the typical equipment used in plastics processing [12, 14].

The advantage of packaging made from the PLA is mainly meeting the requirements relating to the environment [3, 4, 9]. The material allows the use of renewable raw materials in biological processes, reducing CO_2 emissions, organic recycling of packaging waste, it is compostable. PLA also has its drawbacks: it is quite brittle and rigid (needs a number of functional additives to be used in the packaging industry) and, most significantly, it is expensive [7, 20]. Its current net price is 4.2 Euro per 1 kg of PLA, an 6,0 Euro for 1 kg of PLA film. Potentially, one of the best solutions can be application of thermoplastic starch mixed with PLA, which has to reduce the cost of production of biodegradable packaging materials. Oniszczuk et al. [13] has described advantages of the TPS in the production of bioplastics using conventional equipment (as in the case of PLA). Application of potato TPS together with pure PLA without other excipients in production of biodegradable film was the main scope of the trials reported.

MATERIALS AND METHODS

The basic raw material for the production of TPS was potato starch (PZPZ Łomża), mixed with a plasticizer – glycerol of 99.5% purity (Odczynniki Chemiczne Lublin), added in an amount of 20 % wt. The bland was processed using a modified single screw food extruder TS-45 (Fig. 1) with L / D = 16, equipped with an additional cooling zone. TPS granules were produced at temperatures of 85 -100 °C with a constant screw rotational speed of 80 r. p. m., and the die hole diameter φ=3 mm.

Polylactide 2003D Ingeo ™ Biopolymer (Nature Works LLC) was added in an amount of 20% by weight to the TPS granules during a film blowing on a plastics extruder Savo

(Polish design) with L / D = 36 (Fig. 2). The film was produced at variable screw rotation (50- 80 r.p.m.), at temperature range from 80 till 140 °C, using a blow die gap of 0.6 mm.

Fig. 1. Food extruder TS-45

Fig. 2. Stand for film blowing

The measurements of selected mechanical properties of the obtained films were done following the Polish standards and methodology described in the literature [1, 15, 16, 17]. The tests were carried out using the Universal Testing Machine Zwick type BDO-FBO0.5®, just as in the studies carried out by Rejak et al. [18]. The film samples were cut longitudinally and transversely to the direction of the film blowing. The results were verified statistically using software – Statistica 6.0.

RESULTS

Tensile strength of films cut transversely decreased with the increasing of the screw speed (Figure 3). In the case of samples cut longitudinally, the applied screw rotation speed had a small effect on the value of the characteristic. Greater differences were observed in the samples which were cut longitudinally.

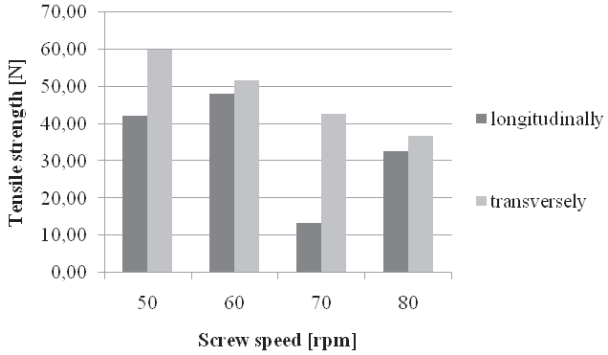

Fig. 3. Tensile strength of the film samples with PLA produced at different screw rotation

The results of measurements on the film elongation susceptibility presented in Fig. 4 showed bad mechanical properties of the obtained products. The statistical analysis showed no correlation between the used screw rotations and the value of the elongation at tensile strength. Destructive tests have confirmed these findings (Figure 5).

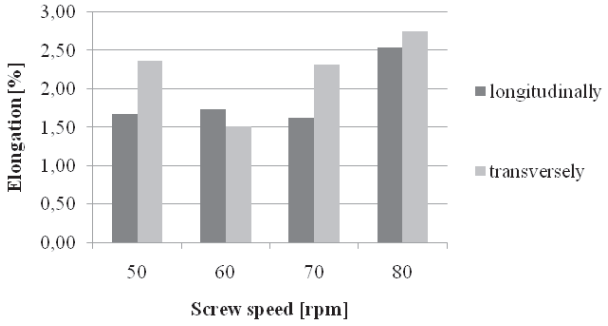

Fig. 4. Elongation at tensile strength of the films samples with PLA produced at different screw rotation

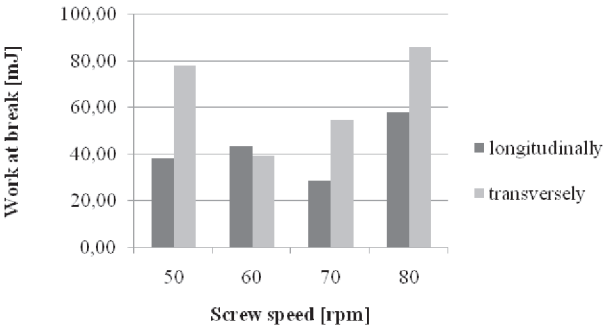

Fig. 5. Work at break of the films in the processed samples with PLA produced at different screw rotation

CONCLUSIONS

The TPS films produced with the addition of PLA were characterized by poor tensile strength, quickly cracked and were brittle. However, the obtained results have confirmed the possibility of thermoplastic starch and polylactide use for the production of biodegradable packaging material. However, it needs additional components such as selective polymers or oligomers in order to achieve a commercially acceptable product. In other words, since the fragility of the obtained film resulted from the properties of PLA pellets, their use would require a variety of other functional additives.

The screw rotation had a slight impact on the measured mechanical properties of the films (except for the measurement of tensile strength).

Further research is needed for proper selection of the bland composition and processing parameters in order to improve the quality of this promising material, to make it more accessible and thus useful for manufacturers of biodegradable packaging.

REFERENCES

1. **Broniewski T., Kapko J., Płaczek W., Thomalla J., 2000:** Metody badań i ocena właściwości tworzyw sztucznych. WNT-Warszawa.
2. **Combrzyński M., 2012:** Opakowania biodegradowalne. Przegląd Zbożowo-Młynarski, 4, 4-5.
3. **Duda A. 2003:** Polilaktyd – tworzywo sztuczne XXI wieku? Przem. Chem., 82, 905-907.
4. **Garlotta D. 2001:** A literature review of poly(lactid acid). J.Polym. Environ., 2, 63-84.
5. **Janssen L.P.B.M., Mościcki L. (Eds.), 2009:** ThermoplasticStarch, Wiley-VCH Verlag GmbH & Co. KGaA, Weinheim, Germany.
6. **Kowalczuk M. M., 2009:** Prace badawcze nad polimerami biodegradowalnymi. Opakowanie, 9, 46-48.
7. **Kowalczuk M., Żakowska H. (Eds.), 2012:** Materiały opakowaniowe z kompostowalnych tworzyw polimerowych. Centralny Ośrodek Badawczo-Rozwojowy Opakowań, Warszawa.
8. **Lawton J. W. 1996:** Effect of starch type on the properties of starch containing films. Carbohydrate Polymers, 29, 203-208.
9. **Martin O., Averous L., 2001:** Poly(lactic acid): plasticization and properties of biodegradable multiphase systems. Polymer, 42, 6209-6219.
10. **Mościcki L (Ed), 2011:** Extrusion-Cooking Techniques, Wiley-VCH Verlag GmbH & Co. KGaA, Weinheim, Germany.
11. **Mościcki L., Mitrus M., Wójtowicz A., 2007:** Technika ekstruzji w przemyśle rolno-spożywczym, PWRiL, Warszawa.
12. **Mościcki L., Mitrus M., Wójtowicz A. 2008.** Biodegradable Polymers and Their Practical Utility. W: Janssen L.P.B.M., Moscicki L. (Eds), in Thermoplastic Starch. Wiley-VCH Verlag GmbH & Co. KGaA, Weinheim, Germany, 1-29.
13. **Oniszczuk T., Wójtowicz A., Mitrus M., Mościcki L., Combrzyński M., Rejak A., Gładyszewska B. 2012:** Influence of process conditions and fillers addition on extrusion-cooking efficiency and SME of thermoplastic potato starch. TEKA Commision of Motorization and Power Industry in Agriculture, Vol. 12, No. 1, 181-184.
14. **Petersen K., Vaeggemose Nielsen P., Bertelsen G., Lawther M., Olsen M.B., Nilson N.H., Mortensen G. 1999:** Potential of biobased materials for food packaging. Tr. Food Sci. Tech., 10, 52-68.
15. PN-68/C-89034. Tworzywa sztuczne. Oznaczanie cech wytrzymałościowych przy statycznym rozciąganiu.
16. PN-81/C-89092. Folie z tworzyw sztucznych. Oznaczanie cech wytrzymałościowych przy statycznym rozciąganiu.
17. **Rejak A., Mościcki L., Wójtowicz A., Oniszczuk T., Mitrus M., Gładyszewska B., 2012:** Influence of keratyn addition on selected mechanical properties of TPS film. TEKA Commision of Motorization and Power Industry in Agriculture, Vol. 12, No. 1, 219-224.
18. **Rejak A., Mościcki L. 2011:** Selected mechanical properties of TPS films stored in the soil envifonment. TEKA Commision of Motorization and Power Industry in Agriculture, Vol. 11c, s. 264-272.
19. **Roper H., Koch H. 1990.** The role of starch in biodegradable thermoplastic materials. Starch, 42, 4, 123-140.
20. **Świerz-Motysia B., Jeziórska R., Szadkowska A., Piotrowska M. 2011:** Otrzymywanie i właściwości biodegradowalnych mieszanin polilaktydu i termoplastycznej skrobi. Polimery, 56, nr 4, 271-280.

WŁAŚCIWOŚCI FIZYCZNE BIOKOMPOZYTU SKROBIOWEGO Z DODATKIEM PLA

Streszczenie. W pracy przedstawiono wyniki pomiarów wybranych właściwości mechanicznych biodegradowalnych folii skrobiowych wytłaczanych ze skrobi termoplastycznej z 20% dodatkiem polilaktydu (PLA). Granulat skrobi termoplastycznej wytworzono na ekstruderze jednoślimakowym o L/D=16. Folie wytłoczono metodą rozdmuchu na wytłaczarce o L/D=36. Badania właściwości mechanicznych przeprowadzono na urządzeniu wytrzymałościowych Zwick typ BDO-FBO0.5TH. Wyprodukowane z dodatkiem PLA folie charakteryzowały się słabą odpornością na rozciąganie, szybko pękały i były kruche.
Słowa kluczowe: PLA, biodegradowalność, ekstruzja, TPS.

TEKA. COMMISSION OF MOTORIZATION AND ENERGETICS IN AGRICULTURE – 2013, Vol. 13, No. 2, 7–12

Selected mechanical properties of starch films

Maciej Combrzyński, Leszek Mościcki, Andrzej Rejak, Agnieszka Wójtowicz, Tomasz Oniszczuk

Department of Process Engineering, University of Life Sciences in Lublin, Doświadczalna 44, 20-280 Lublin, Poland, maciej.combrzynski@up.lublin.pl

Received April 10.2013; accepted June 14.2013

Summary. This paper presents the results of measurements of selected mechanical properties of biodegradable starchy films (TPS), enriched by functional additives, produced at different screw rotation of the extruder. TPS granules were processed using a modified single screw extrusion-cooker TS-45 with L/D = 16. The following functional additives were used during the production: polylactide, polyvinyl alcohol and guar gum. Film blowing was carried out on the plastic extruder with L/D = 36. The obtained films were evaluated by mechanical properties test. Tensile strength, elongation, strain at break, elongation at break, work at tensile strength and work at break were measured. The best results were noticed for the film samples containing polyvinyl alcohol. The films with PLA addition were more brittle and weaker than the ones containing guar gum.

Key words: thermoplastic starch, extrusion-cooking, mechanical properties, PLA, polyvinyl alcohol, guar gum, film blowing.

INTRODUCTION

Application of biodegradable polymers, including starch, is becoming more and more popular during packaging production [2, 8]. Their use is important for ecological reasons, therefore innovative solutions aimed to reduce packaging waste are being searched. Studies on the possibility of increasing natural ingredients addition to produce more ecologic packaging are being carried out. The best, for economy and cost reasons, seems to be thermoplastic starch (TPS). Currently there are no chances to make pure starch material without plastic addition [4, 14, 17, 18]. Starch additive is only a filler, its content in the final materials is lower than 50%. During starch degradation to CO_2 and water, the materials disintegrate into smaller pieces.

Starch, as a biodegradable component of plastic materials, can fulfill the raw material function, it can also be physically or chemically connected with the synthetic polymer [7, 9]. It can be done using extrusion-cooking technique, which is one of the most commonly used methods for forming synthetic materials. That method has an important advantage – TPS can be produced using traditional machinery and equipment, typical for synthetic polymers manufacturing. Many publications and solutions presented on the international conferences confirm TPS functionality.

Oniszczuk et. al. [11] has described a wide application of TPS in biodegradable packaging materials production. It can be used as an additive which improves the degradation of plastics or as a stand-alone packing material. Starch biodegrades to CO_2 and water in a relatively short time. To improve the flexibility of ready materials and improve the production process, plasticizers are used. The most popular is glycerol. For improving the mechanical properties of the rigid forms of packaging based on TPS, the functional additives are used such as emulsifiers, cellulose, plant fiber, bark, kaolin or pectin [10].

In numerous scientific centers of the world scientists are searching for polymers based on natural raw materials. Recently, polylactide (PLA) is used as one of the most popular functional additives or as a stand-alone packaging material.

PLA is an aliphatic polyester obtained by condensation of milk acid [6, 19, 20]. Its production is carried out on a massive scale. PLA, due to its properties, is particularly useful in the manufacture of food packaging. The polymer can be used for packing fruit and food. From PLA thermoformed trays, containers are made. It can be also used to produce shopping bags and labels. Packaging from PLA is compostable. The advantage of this material is its ecologic aspect. PLA is based on natural raw ingredients , so the requirements of environment are achieved, e.g. natural biological processes to obtain half-ready product, use of renewable raw materials, reduction of CO_2 emissions, organic recycling of packaging waste. The disadvantages of PLA are: price, tenderness and stiffness. However, there is the possibility of using PLA in the packaging industry through other functional additives [5].

MATERIALS AND METHODS

The basic raw material used for TPS production was potato starch Superior produced by PPZ Bronislaw Sp. z o.o. During the production the plasticizer – glycerol of 99.5% purity, was used. In order to obtain a film with similar properties to typical synthetic material, 3 functional additives were used: polylactide 2003D Ingeo ™ Biopolymer (NatureWorks LLC), polyvinyl alcohol and guar gum.

Potato starch, glycerol and functional additives were mixed in a batch mixer accordingly to the recipe presented in Table 1. PLA was added to pure TPS after extrusion-cooking before film blowing.

Table 1. Recipes of TPS applied for biodegradable film blowing

Sample	Potato starch [%]	Glycerine [%]	Ingeo™ 2003D [%]	Polyvinyl alcohol [%]	Guar gum [%]
a4	58	22	20	-	-
c4	76	22	-	2	-
e4	77	22	-	-	1

In order to enhance penetration of glycerol and additives into starch, the obtained blends were kept in sealed plastic bags for 24 hours before processing, than processed on a modified single screw extrusion-cooker TS-45 (Polish design) with L/D = 16 (see Fig. 1) in the temperature range of 85-100°C and a screw rotation of 80 rpm. Extrudates were cut using high-speed cutter, adapted to achieve small size granules. Further cooling was used to avoid the sticking together of granulates. Dried TPS granules, a half product for film blowing, were stored in plastic containers.

Fig. 1. Single screw extrusion-cooker TS-45 with L/D = 16 made by Z.M.Ch. Metalchem

Film blowing was carried out on a plastic extruder with L/D = 36. During extrusion the die-mold with a nozzle diameter of 80 mm and the working slot of 0.6 mm was used. The applied screw rotation was variable: 50, 60, 70 and 80 rpm. Each sample of the collected products (film sleeve about 200 cm lengths) was dried for 24 hours at ambient temperature (Fig. 2). After that it was cut into pieces of film (15 cm length and 2 cm width), assembled and stored in the open containers.

Fig. 2. TPS film slave sample

The mechanical properties of the film samples were measured on the Zwick Universal Testing Machine type BDO-FBO0.5TH (Fig 3). The samples were cut longitudinally and transversely to the direction of extrusion blown film. The tensile strength, elongation, strain at break, elongation at break and work done to achieve the targets were measured according to the Polish standards and methodology described by Rejak et al. [1, 3, 12, 13, 15, 16]. The results were statistically analyzed using *Statistica 6* tool.

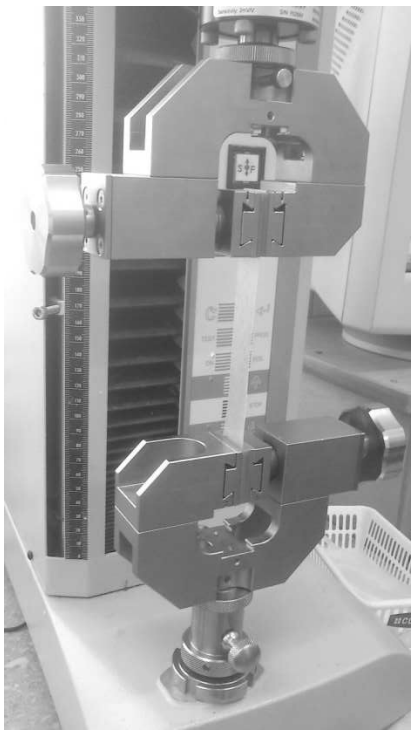

Fig. 3. Universal Testing Machine Zwick BDO-FBO0.5TH

RESULTS

The results of measurement of the tensile strength of samples processed with different extruder screw rotations are presented in Fig. 4. Maximum values of the tensile strength (the maximum value of the tensile force) were obtained for c4 samples processed at 80 rpm (72.65 N – sample cut lon-

gitudinally; 63.88 N – sample cut transversely). The lowest values of tensile strength occurred in the film samples produced at 70 rpm (13.26 N – a4 longitudinally; 16.07 N – c4 transversely). The statistical analysis showed that the tensile strength of samples which were cut longitudinally and contained the polyvinyl alcohol increased with higher rotation of the screw (correlation coefficient 0.75). To the contrary, the tensile strength of samples with the addition of PLA cut transversely decreased (correlation coefficient -0.93). In the remaining samples, statistical analysis showed no relationship between the speed rotation and the value of the test.

Elongation at tensile strength is the value of the elongation at the maximum value of the tensile force. Results of elongation measurement are shown in Figure 5. The highest elongation values occurred in the samples enriched by polyvinyl alcohol, processed at 70 rpm (value of 5.88% for samples cut longitudinally and 22.55% for samples cut transversely). Samples cut transversely had a larger elongation. The lowest value of elongation was observed for the samples containing polylactide (1.63% – samples cut longitudinally produced at 70 rpm, 1.51% – samples cut transversely produced at 60 rpm). Unfortunately, the low values of correlation coefficients indicated a lack of correlation between the screw speed and elongation.

The strain at break is defined as the value of tensile force at maximum elongation at break. The obtained results are shown in Figure 6. The highest values were reported for samples with guar gum addition (20.34 MPa and 20.50 MPa for the samples produced at 70 rpm cut longitudinally and transversely). The lowest values of strain at break were noticed for film samples containing a polyvinyl alcohol, processed at 70 rpm (3.88 MPa – samples cut longitudinally, 2.70 MPa – samples cut transversely). Only for the films produced at 80 rpm and cut lengthwise the inverse relationship was noted – the highest value of strain at break occurred in sample c4 (16.52 MPa) and the lowest in sample e4 (7.83 MPa). The statistical analyzes showed no significant relationship between the screw rotation and strain at break of the films.

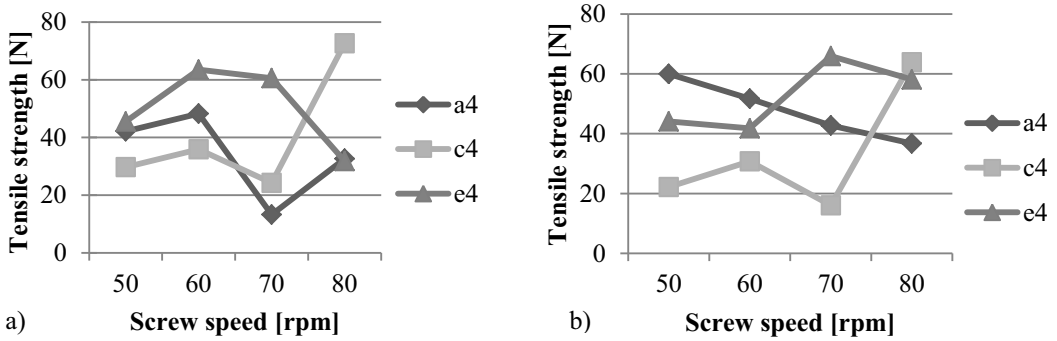

Fig. 4. Tensile strength of the film samples produced at different screw rotations (a – sample cut longitudinally, b – sample cut transversely)

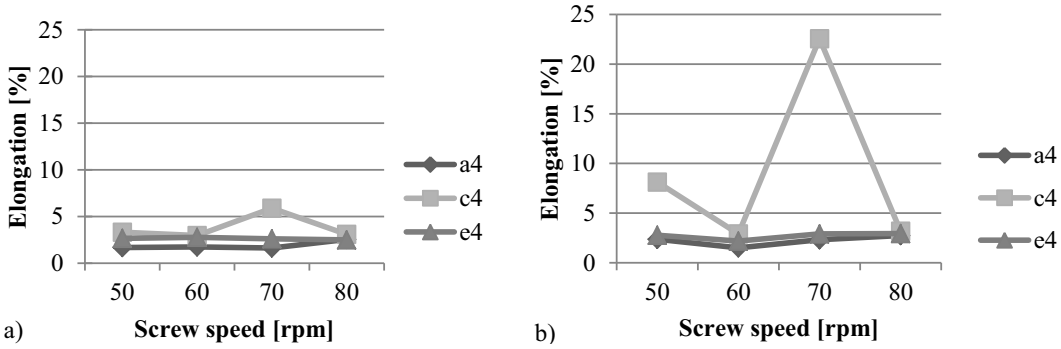

Fig. 5. Elongation of the film samples processed at different screw rotation (a – sample cut longitudinally, b – sample cut transversely)

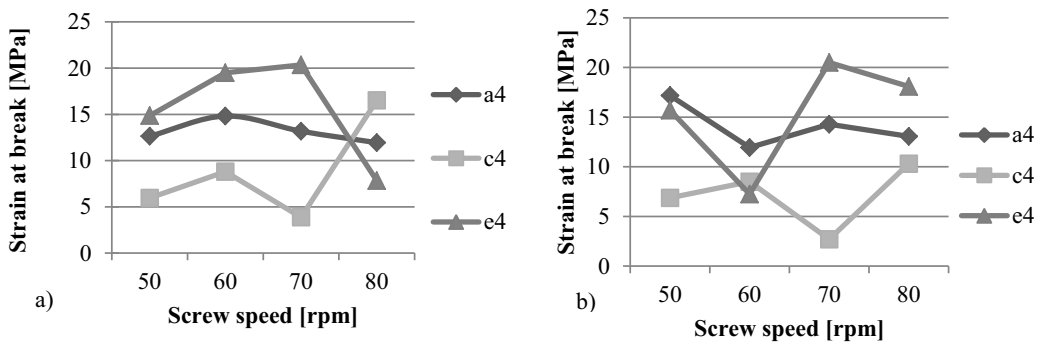

Fig. 6. Strain at break of the film samples processed at different screw rotation(a – sample cut longitudinally, b – sample cut transversely)

Elongation at break is the maximum tensile elongation. Figure 7 shows the results of measurement of that mechanical parameter. The samples a4 and e4 did not show an impact value of the screw speed on these characteristics. For samples cut longitudinally and transversely similar results were noted. The lowest values of elongation at break were reported for samples with PLA addition (1.66% at 70 rpm –samples cut longitudinally, 1.54% at 60 rpm –samples cut transversely). The highest value was observed for the samples c4 prepared at 70 speed (19.80% – samples cut longitudinally; 26.87% – samples cut transversely). Unfortunately, a low value f correlation coefficients was noticed during the measurements, which did not allow to estimate clear relationship between the screw rotation and the screw rotation and elongation at break.

Work at tensile strength defines value of the area under the curve of the maximum tensile force. Results of the measurement of this parameter are shown in Figure 8. The highest value was noticed for the film samples containing the polyvinyl alcohol (137.46 mJ at 80 rpm – samples cut longitudinally; 283.26 mJ at 70 rpm – samples cut transversely). The lowest results were noted for sample a4 (37.30 mJ at 50 rpm – longitudinally, and 38.75 mJ at 60 rpm – transversely). Looking for the relationship between the value of work at tensile strength and the applied screw rotation, only the measurements of the films with the polyvinyl alcohol cut transversely showed satisfactory value of the correlation coefficients (0.88). For the other results values of the correlation coefficients were too low.

Work at break is the value of area under the entire curve of the tensile force to break. The screw speed had the impact on the value of work at break in the case of films with the addition of polyvinyl alcohol (Figure 9). For samples c4 the highest values of the work at break was noticed (429.57 mJ at 70 rpm – lengthwise; 475.37 mJ at 80rpm – transversely). The film samples containing PLA were characterized by

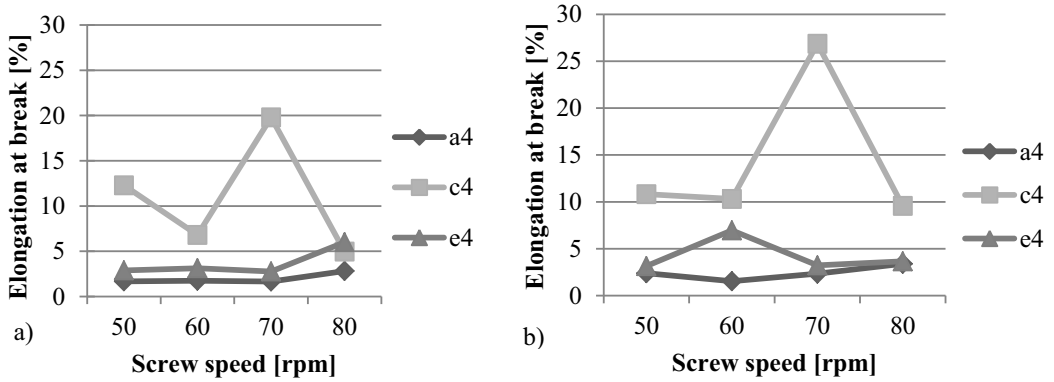

Fig. 7. Elongation at break of films with functional additives produced at different speeds (a – sample cut longitudinally, b – sample cut transversely)

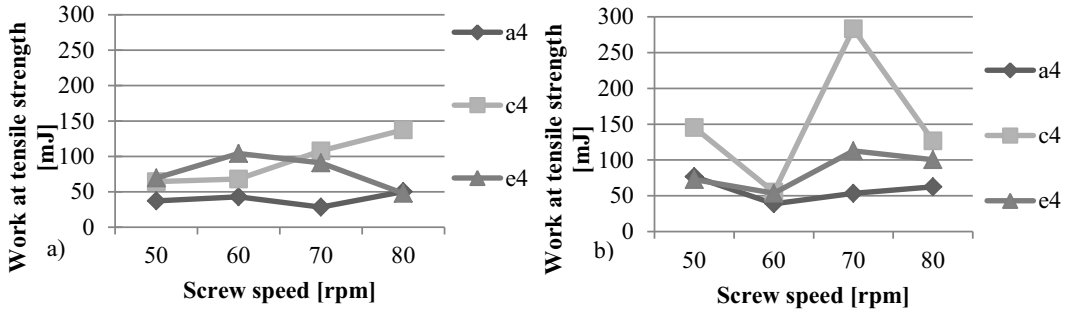

Fig. 8. Work at tensile strength of the film samples processed at different screw rotation (a – sample cut longitudinally, b – sample cut transversely)

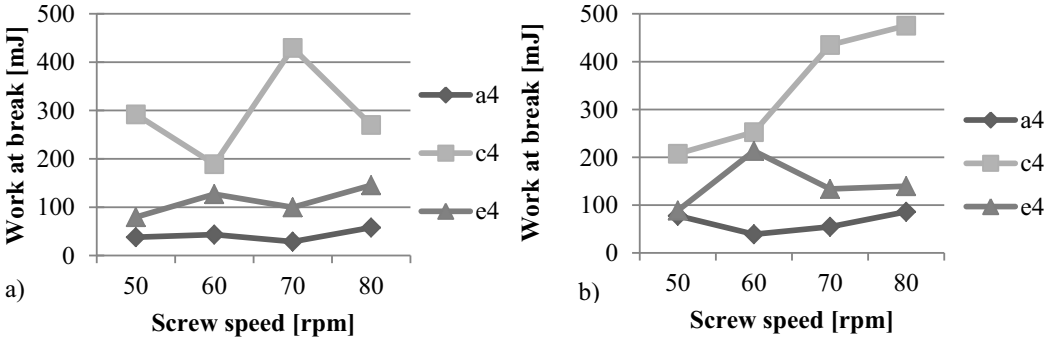

Fig. 9. Work at break of the film samples processed at different screw rotation (a – sample cut longitudinally, b – sample cut transversely)

the lowest value of the measured parameter (28.66 mJ at 70 rpm – lengthwise; 39.09 mJ at 60 rpm – transversely). The highest value of the correlation coefficient (0.77) was obtained for the films containing the polyvinyl alcohol and cut transversely (the value of work at break grew with the increase almost linearly with the screw speed).

CONCLUSIONS

Application of variable screw rotation speed during TPS films blowing influenced their mechanical properties. Samples containing PLA were characterized by average strength properties compared to the films produced from other blends. The best results for the films with PLA were obtained only during the tensile strength test.

The films containing the guar gum were the most elastic, which allowed obtaining a packaging material of better mechanical characteristics than the one containing 20 % of PLA.

The best results of mechanical properties were shown by the film samples containing 2 % of polyvinyl alcohol. The statistical analysis indicated that during this type of film processing, the screw rotation speed had a significant, positive influence on its mechanical properties. The combined application of the extrusion-cooking technique and typical "plastic" film blowing has allowed for the conclusion that TPS processing in order to produce biodegradable packaging materials is promising and gives acceptable results. However, further studies are needed to improve the stability of both the process and physical parameters of the obtained products.

REFERENCES

1. **Broniewski T., Kapko J., Płaczek W., Thomalla J. 2000.** Metody badań i ocena właściwości tworzyw sztucznych. WNT-Warszawa.
2. **Combrzyński M., Mitrus M., Mościcki L., Oniszczuk T., Wójtowicz A. 2012.**Selected aspects of thermoplastic starch production.TEKA Commision Motorization and Power Industry in Agriculture, Vol. 12, No 1, 25-29.
3. **Gładyszewska B., Stropek Z. 2010.** The influence of the storage time in selected mechanical properties of apple skin. TEKA Commision of Motorization and Power Industry in Agriculture, 10, 59-65.
4. **Janssen L.P.B.M., Mościcki L. (Eds.) 2009.** ThermoplasticStarch, Wiley-VCH Verlag GmbH & Co. KGaA, Weinheim, 1-29.
5. **Kowalczuk M., Żakowska H. (Eds.) 2012.** Materiały opakowaniowe z kompostowalnych tworzyw polimerowych. Centralny Ośrodek Badawczo-Rozwojowy Opakowań, Warszawa.
6. **Martin O., Averous L. 2001.** Poly(lactic acid): plasticization and properties of biodegradable multiphase systems. Polymer, 42, 6209-6219.
7. **Mitrus M., Oniszczuk T. 2007.** Wpływ obróbki ciśnieniowo – termicznej na właściwości mechaniczne skrobi termoplastycznej. Właściwości geometryczne, mechaniczne i strukturalne surowców i produktów spożywczych. Wyd. Nauk. FRNA, Lublin, 149-150.
8. **Mościcki L (Ed) 2011.** Extrusion-Cooking Techniques, Wiley-VCH Verlag GmbH & Co. KGaA, Weinheim.
9. **Mościcki L., Mitrus M., Wójtowicz A. 2007.** Technika ekstruzji w przemyśle rolno-spożywczym,PWRiL, Warszawa.
10. **Oniszczuk T., Mitrus M., Mościcki L. 2008.** Influence of Natural Fibres Addiction on Mechanical Properties of Biodegradable Packaging Materials. Polish Journal of Environmental Studies, 17, 1B, 257-262.
11. **Oniszczuk T., Wójtowicz A., Mitrus M., Mościcki L., Combrzyński M., Rejak A., Gładyszewska B. 2012.** Biodegradation of TPS mouldings enriched with natural fillers. TEKA Commision of Motorization and Power Industry in Agriculture, Vol. 12, No. 1, 175-180.
12. PN-68/C-89034. Tworzywa sztuczne. Oznaczanie cech wytrzymałościowych przy statycznym rozciąganiu.
13. PN-81/C-89092. Folie z tworzyw sztucznych. Oznaczanie cech wytrzymałościowych przy statycznym rozciąganiu.
14. **Rejak A., Mościcki L. 2006.** Biodegradable foil extruded from thermoplastic starch. TEKA Commision of Motorization and Power Industry in Agriculture, 6, 123-130.
15. **Rejak A., Mościcki L. 2011.** Selected mechanical properties of TPS film stored in the soil environment. TEKA Commision of Motorization and Power Industry in Agriculture, 11c, 264-272.
16. **Rejak A., Mościcki L., Wójtowicz A., Oniszczuk T., Mitrus M., Gładyszewska B. 2012.** Influence of keratyn addition on selected mechanical properties of TPS film. TEKA Commision of Motorization and Power Industry in Agriculture, Vol. 12, No. 1, 219-224.
17. **Roper H., Koch H. 1990.** The role of starch in biodegradable thermoplastic materials. Starch 42, 4, 123-140.
18. **Żakowska H. 2003**. Opakowania biodegradowalne. Wyd. Centralny Ośrodek Badawczo-Rozwojowy opakowań, Warszawa, 7-17.
19. **Żakowska H. 2006.** Biodegradowalne opakowania z polilaktydu (PLA) do owoców i warzyw. Przemysł Fermentacyjny i Owocowo-Warzywny, 7-8, 34-36.
20. **Żakowska H. 2008.** Materiały biodegradowalne wykorzystywane do produkcji opakowań kompostowalnych. Przemysł Fermentacyjny i Owocowo-Warzywny, 7-8, 50-53.

WYBRANE WŁAŚCIWOŚCI MECHANICZNE SKROBIOWYCH FOLII

Streszczenie. W pracy zaprezentowano wyniki pomiarów wybranych właściwości mechanicznych biodegradowalnych folii skrobiowych wzbogaconych dodatkami funkcjonalnymi wyprodukowanych przy różnych obrotach wytłaczarki. Granulat skrobi TPS wytworzono na jednoślimakowym, zmodyfikowanym ekstruderze TS-45 o L/D=16. Zastosowano dodatki funkcjonalne w postaci polilaktydu, alkoholu poliwinylowego oraz gumy guar. Proces wytłaczania folii z rozdmuchem wykonywano na wytłaczarce o L/D = 36. Wytworzone folie poddano testom na

rozciąganie. Zbadano cechy wytrzymałościowe folii, tj. wydłużenie przy wytrzymałości na rozciąganie i wydłużenie niszczące, wytrzymałość na rozciąganie i naprężenie przy zniszczeniu oraz pracę przy wytrzymałości na rozciąganie i pracę zniszczenia. Najlepsze wyniki odnotowano w przypadku folii z dodatkiem alkoholu poliwinylowego. Folie z dodatkiem PLA odznaczały się większą kruchością i gorszą wytrzymałością niż folie z dodatkiem gumy guar.

Słowa kluczowe: skrobia termoplastyczna, ekstruzja, właściwości mechaniczne, PLA, alkohol poliwinylowy, guma guar.

TEKA. COMMISSION OF MOTORIZATION AND ENERGETICS IN AGRICULTURE – 2013, Vol. 13, No. 2, 13–16

Innovations in the construction of pelleting and briquetting devices

Roman Hejft, Sławomir Obidziński

Department of Agricultural and Food Techniques, Faculty of Mechanical Engineering,
Bialystok University of Technology, 45C Wiejska Street, 15-351 Bialystok, Poland,
tel. +48 0857469282, fax: +48 0857469210, e-mail: r.hejft@pb.edu.pl

Received May 8.2013; accepted June 14.2013

Summary. Waste materials of plant origin: sawdust, shavings, wood dust, corn, rape straw, buckwheat hulls, etc. can be used as a valuable ecological fuel. Combustion of different forms of materials of plant origin, i.e. biomass, is beneficial from the ecological point of view and is a rich source of energy. This paper presents selected issues concerning the modernization of the process of producing heating pellets and briquettes (ecological solid fuel) from biomass. Devices with an immovable flat matrix working system are a beneficial solution in the production of solid fuel in small- and medium-sized plants.
Key words: solid fuels, biomass, waste, pelletisation, pellets, briquettes.

1. INTRODUCTION

Waste materials of plant origin: sawdust, shavings, wood dust, corn, rape straw, buckwheat hulls, etc. can be used as a valuable ecological fuel. Combustion of different forms of materials of plant origin, i.e. biomass, is beneficial from the ecological point of view and is a rich source of energy (for instance, the calorific value of straw is 15-17 $MJ \times kg^{-1}$ at a moisture content of approx. 10%).

The production of solid fuels through pelletisation and briquettisation of materials of plant origin (biomass) has found widespread applications. Pelletisation (briquettisation) of materials of plant origin is a process in the course of which shredded material, as a result of external and internal forces, undergoes densification, and the obtained product acquires a specific, permanent geometrical form.

Depending on the size of a product from biomass, it is called pellets (e.g. a diameter of 2 to 12-15 mm) or briquette (over 15-20mm) – fig. 5 [1, 2, 3, 4].

The mechanism of the densification of materials of plant origin is presented in fig.1.

On the basis of fig.1, it can be noticed that as the segment x is increasing, the values of pressure p_x in the densified material are decreasing.

The experimental verification of the distribution of the forces at work in the densification process is shown in fig. 2.

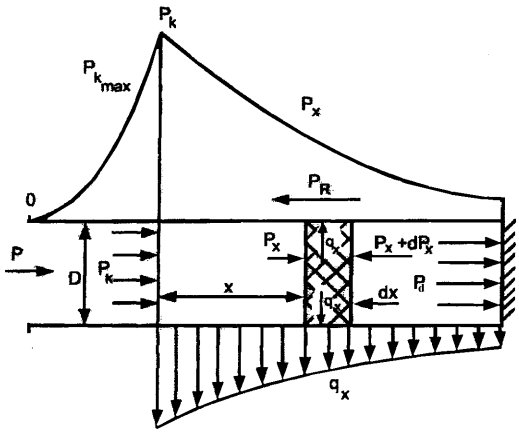

Fig. 1. The scheme of pressures in a densified material [Hejft, 2002]: p_k – densifying pressures, p_x – axial stresses, q_x – lateral pressures, P_d – pressures on the bottom of the chamber, D – chamber diameter, P_R – friction forces

Fig. 2. Destruction of the chamber during densification (p_k – approx. 145 MPa)

Technical and technological progress depends on the details implemented in production plants of pellets (briquettes) in the areas of the design and operation of machines, process engineering, as well as the modification of material characteristics of biomass.

This paper presents selected issues concerning the production of pellets and briquettes.

2. The production of pellets and briquettes

The flow chart of the production of pellets and briquettes from biomass is presented in fig. 3.

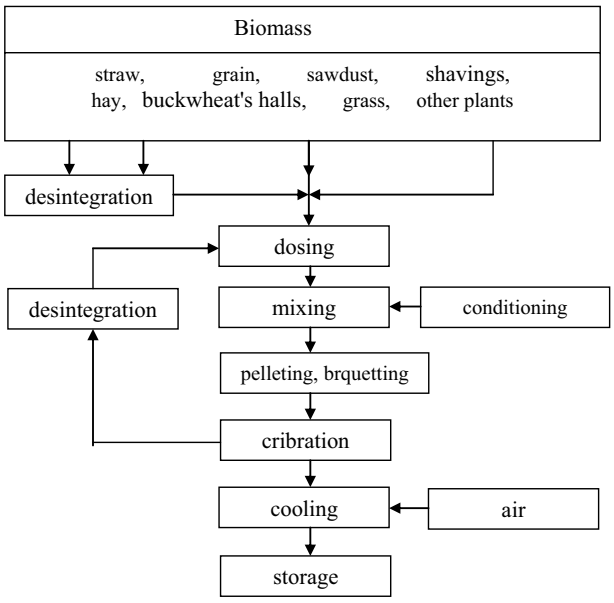

Fig. 3. The flow chart of the production of pellets and briquettes (it was assumed that the moisture content of biomass is lower than 20% and it does not require drying) [2]

Fig. 4 shows a stand for performing the tests of the processes of pelletisation and briquettiation of materials of plant origin (biomass).

The device consists of an immovable matrix 3 and two densification rolls 2. The set of densification rolls is driven by the shaft 9, bearing-supported in the shaft jacket 4, through the belt transmission 6 from the electric motor 8. The device is equipped with a feeder 1, whose position relative to the cone mounted in the upper part of the transmission shaft 9 can be continuously variably adjusted (continuously variable control of the quantity of the fed material). Technical data: power – 15 kW, speed of the set of densification rolls – 210 rpm, roll width – 102 mm, B, D-process temperature recorder, C- power recorder

The example of the matrices using in the universal pelletising and briquetting device shown in fig. 5.

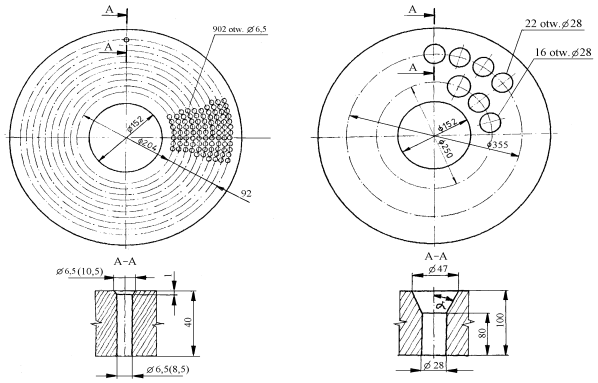

Fig. 5. Example matrices [2]

SHREDDING

The average size of particles undergoing pelletisiation or briquettisation has a significant influence on the course of the processes and the quality of the product. The degree of shredding of biomass needs to be determined in laboratory tests (in pelletising and briquetting devices, e.g. in the one presented in fig. 4). With a certain approximation it can be initially assumed that the average size of particles is about 0.5 of the diameter of the matrix openings.

The high diversity of materials of plant origin, as far as their biological structure, chemical composition, physical properties are concerned, as well as, additionally, their high

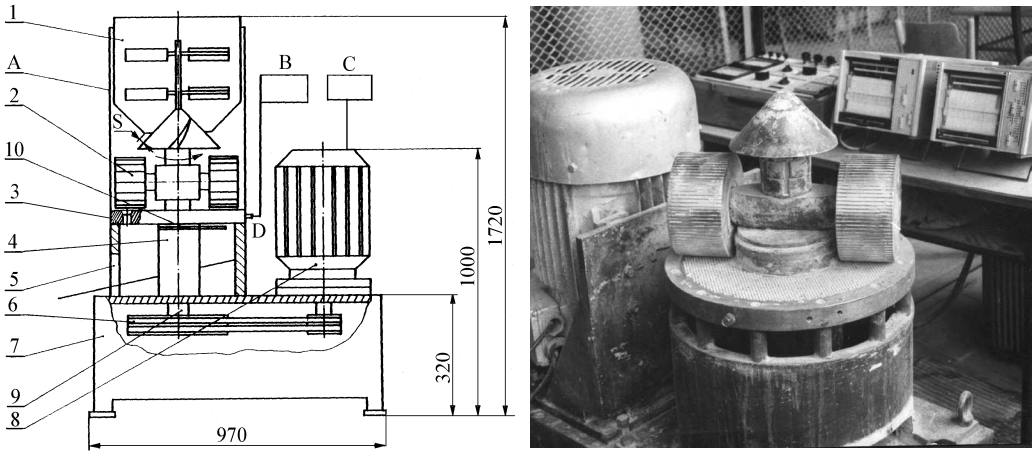

Fig. 4. The scheme and view (without a feeder) of a universal pelletising and briquetting device [2]

changeability during the pelletisation or briquettisation process are make it difficult to determine which of the binding mechanisms would be dominant (this pertains, above all, to mixtures of different components).

For example: during the pelletisation of biomass with a content of e.g. shredded corn grains (starch content – binder additive), the contribution of bindings from the field of cohesion forces is an important factor.

During the briquettisation of shredded straw, there appear mechanical bindings. The durability of agglomerate is influenced by mechanical coupling and locking of particles, internal pressure between particles, binder additives and capillary forces.

For example: in the densification of biomass with a 60% content of straw shredded on a beater shredder using a sieve mesh of a)10 mm and b)6 mm, the proportional content of individual fractions of shredded straw is: a) 0-5 mm – 38.1%, 5-10 mm – 40.3%, 10-20 mm – 17.3%, 20-30 mm – 3.9%, above 30mm – 0.4% and b) 0-5 mm – 58.1%, 5-10 mm – 30.2%, 10-20 mm – 10.9%, 20-30 mm – 0.8) density of briquettes decreases (in the b) case) by approx. 10 $kg \times m^{-3}$.

MIXING

Densified biomass belongs to the so-called difficult materials, i.e. it requires high densifying pressures (from 80 to 150 MPa and higher). Therefore, it would be advisable to create mixtures, e.g. shredded waste paper. This method also allows to eliminate a significant portion of dusty fractions (they appear in smaller or greater amounts during shredding), through their non-pressure agglomeration into particles of sizes multiple times smaller than those of the components (e.g. shredded straw – grain processing and milling industry waste, sawdust, shavings – potato pulp, sawdust – buckwheat hulls – fig. 6).

The mixing process is also significant as far as reducing the moisture content of a biomass mixture is concerned (mixing components of an increased moisture content with components of a low moisture content has a positive influence on the process of pelletisation or briquettisation). Conditioning of biomass by means of superheated water vapour can also be used in the mixing process. Its purpose is to plasticise the particles of plant components.

Fig. 6. Briquettes (from spruce sawdust, from spruce sawdust with a buckwheat hulls content) [2]

PELLETISATION, BRIQUETTISATION

The high dynamic loads of the pelletising and briquetting working systems cause their relatively fast wear, at simultaneously high production costs.

Research studies carried out by a team of authors and their collaborators allow to promote universal low-output devices for the pelletisation and briquettisation of materials of plant origin, which can produce solid ecological fuel (also from waste material) as well as industrial fodder on medium- and big-sized agricultural farms and in small- and medium-sized plants processing materials of plant origin.

Hence, special attention needs to be paid to working systems with a flat immovable matrix (a simple design; in the case of many products both sides of the matrices can be used; the matrix and the densification rolls can be replaced easily; a significantly lower price in comparison with other designs, etc.). Pellets and briquettes obtained in a working system with a flat immovable matrix are shown in fig. 7.

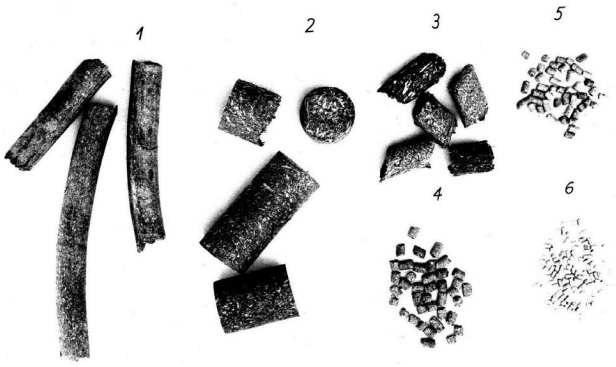

Fig. 7. Examples of pellets (4,5,6 – a diameter of 4;6,5; 8.5mm) and briquettes (1,2,3 – a diameter of 28mm; 50mm) from biomass

For the briquettes with a diameter of 28mm and 50 mm matrices with muffs were used (fig. 8)

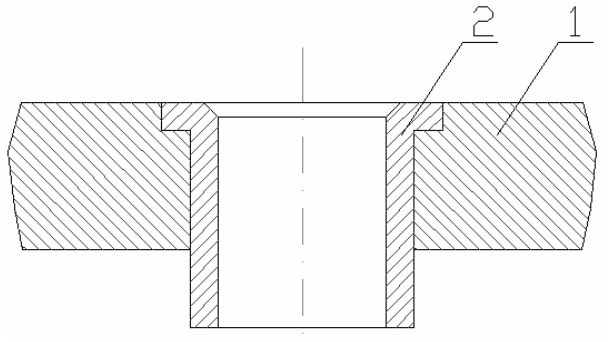

Fig. 8. A cross-section of a matrix with a briquetting muff [2]

SIEVING

The obtained pellets (briquettes) can undergo sieving – the ones that fulfil the norms are cooled, while the rest are shredded and recycled within the process (fig. 3).

COOLING

Pellets, as well as briquettes, undergoing cooling acquire a better durability (a greater resistance to crumbling).

3. SUMMARY

The paper presents selected aspects of the modernization of the process of producing heating pellets and briquettes (ecological solid fuel) from biomass. The presented suggestions are the result of many years of research of both the process of pelletisation and briquettisation and the design solutions of prototype universal pelletising and briquetting devices. The devices with a flat immovable matrix working system are a beneficial solution in the production of solid fuels in small – and medium-sized plants.

REFERENCES

1. **Chłopek M., Dzik T., Hryniewicz M., 2012**. The method for selection of the working system components for a pellet press with flat die. Chemik 2012, 66,5, 493-500.
2. **Hejft R., 2002**. The pressure agglomeration of vegetable materials (in Polish). The Library of Exploitation Problems, ITE Radom.
3. **Hejft R., Obidziński S., 2012**. The pressure agglomeration of the plant materials – the technological and technical innovations. Part 1. Journal of Research and Applications in Agricultural Engineering", Vol. 57(1), 63-65
4. **Obidziński S., Hejft R., 2012**. The influence of technical and technological factors of the fodders pelleting process on the quality of obtained product. Journal of Research and Applications in Agricultural Engineering", Vol. 57(1), 109-114.

INNOWACJE W KONSTRUKCJI URZĄDZEŃ DO PELLETOWANIA I BRYKIETOWANIA

Streszczenie. Odpadowe materiały pochodzenia roślinnego: trociny, wióry, pyły drzewne, słomy zbóż, rzepaku, łuski gryki, itp. mogą stanowić cenny, ekologiczny opał. Spalanie odpadów pochodzenia roślinnego -biomasy, w różnych jego postaciach, jest korzystne ze względów ekologicznych i stanowi bogate źródło energii. W pracy przedstawiono wybrane aspekty modernizacji procesu wytwarzania peletów i brykietów opałowych (ekologicznego paliwa stałego) z biomasy. Urządzenia z układem roboczym płaska nieruchoma matryca, są korzystnym rozwiązaniem przy produkcji paliwa stałego w małych i średnich zakładach.
Słowa kluczowe: paliwo stałe, biomasa, odpady, pelletowanie, pellety, brykiety.

Research carried out within the framework of independent research MNiSzW Nr N N504488239.

TEKA. COMMISSION OF MOTORIZATION AND ENERGETICS IN AGRICULTURE – 2013, Vol. 13, No. 2, 17–22

Model validation of the SI test engine

Arkadiusz Jamrozik

Institute of Thermal Machinery, Czestochowa University of Technology
Armii Krajowej Av. 21, 42-201 Czestochowa, e-mail: jamrozik@imc.pcz.czest.pl

Received April 5.2013; accepted June 14.2013

Summary. The results of thermal cycle modelling of spark ignition internal combustion engine are presented. The modelling was carried out in the AVL FIRE. The object of investigation was a S320 spark-ignited internal combustion engine powered by gasoline. The author considered the effort to generate a complete mesh for the test engine, including the intake and exhaust ports and the valves. This involved generation of four computational domains. A local and temporary thickening of the mesh was included, which contributed to more accurate solutions and shortening of computing time, as well as the engine calculations cycle. The numerical analysis results were juxtaposed with the results of indicating the engine on the test stand. The created model of SI engine was successfully verified.
Key words: engine, simulation, modelling, combustion.

INTRODUCTION

Engines are designed to maximize power and economy while minimizing exhaust emissions. This is due to the growing concern with decreasing energy resources and environmental protection. For this reason, intensive research is being carried out and development is in progress on internal combustion engines. The engine should operate with the greatest efficiency with the least toxic compound emissions. Research on improving the combustion process, introducing a new fuel such as hydrogen, and optimization of the engine parameters is still being carried out. Maximizing the performance of the engine (BMEP) usually causes the occurrence of the so-called knock combustion. Therefore, intensive researches and development in internal combustion engines are carried out.

Researches based on numerical simulations using advanced mathematical models have recently been developed very intensively. The development of numerical modelling is heightened by increasing computational power that allows not only the modelling of flow processes but also combustion in 3D [1, 2, 3]. One of more advanced numerical models used for combustion process in internal combustion engines modelling is AVL FIRE [4]. In 2009 the Institute of Internal Combustion Engines and Control Engineering of Czestochowa University of Technology began University Partnership Program with AVL Company. This has allowed the use of the Fire software to IC engine thermal cycle modelling [5, 6, 7]. The AVL FIRE software belongs to programs which are used to modelling of thermal cycle of internal combustion engines. FIRE allows the modelling of flows and thermal processes occuring in the intake and exhaust manifold and in combustion chamber of internal combustion engine. This program allows for the modelling of transport phenomena, mixing, ignition and turbulent combustion in internal combustion engine. Homogeneous and inhomogeneous combustion mixtures in spark ignition and compression ignition engine can be modelled using this software, as well. Kinetics of chemical reactions phenomena is described by combustion models which take oxidation processes in high temperature into consideration. Several models apply to auto ignition processes. AVL FIRE allows modelling knock process which occur in the combustion chamber of IC engine. This program allows for the creation of three-dimensional computational mesh, description of boundary conditions of surfaces as well as of the initial conditions simulation.

OBJECT OF INVESTIGATION

The test engine was constructed on the basis of a four-stroke compression-ignition engine S320 manufactured by "ANDORIA" Diesel Engine Manufacturers of Andrychow. After some constructional changes, this engine was redesigned for the combustion of gasoline as a spark-ignition engine. For this reason, the engine was equipped with a new fuel supply system and an ignition installation [8]. As a result of modernization, the shape of the combustion chamber

and the compression ratio was reduced from 17 to 9. This is a stationary engine, equipped with two valves with horizontal cylinder configuration. The engine is equipped with a cooling system based on the evaporation of liquid.

Figures 1 and 3 show a serial engine manufactured by ANDORIA. Figure 2 shows the modernized combustion chamber with spark plug location of the test engine. On the basis of the test engine geometry the computational mesh was created (Fig. 5). Valve lifts curves were determined by measuring the engine cams. The modelling takes into account only the intake and exhaust channels located in the engine head.

Table 1. Main engine parameters

Parameters	Value
bore cylinder	100 mm
stroke piston	120 mm
connecting rod length	216 mm
direction of cylinders	horizontal
squish	11 mm
compression ratio	9
engine speed	1000 rpm
number of cylinders	1

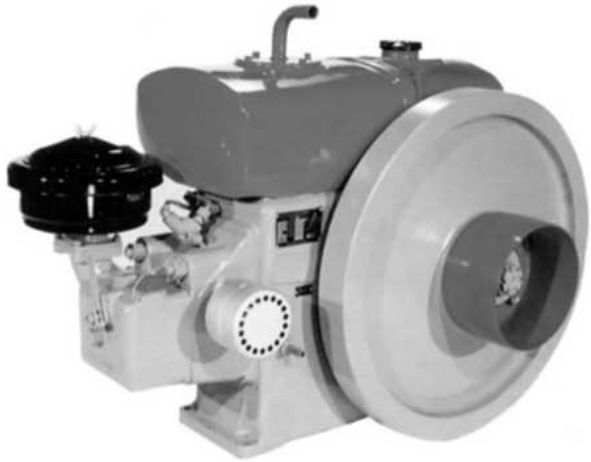

Fig. 1. Engine of S320 Andoria – catalog view

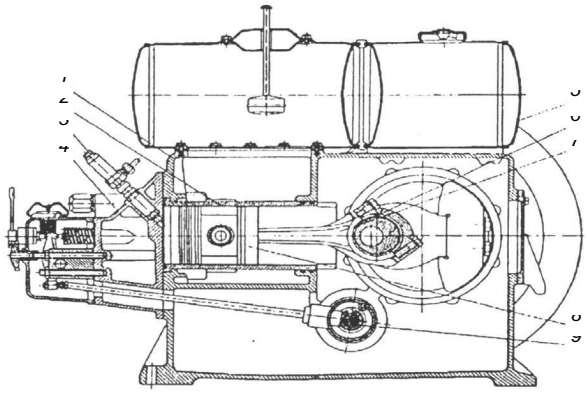

Fig. 2. Cross-section of the engine head after modernization 1 – spark plug, 2 – combustion chamber in the cylinder, 3 – combustion chamber in the piston

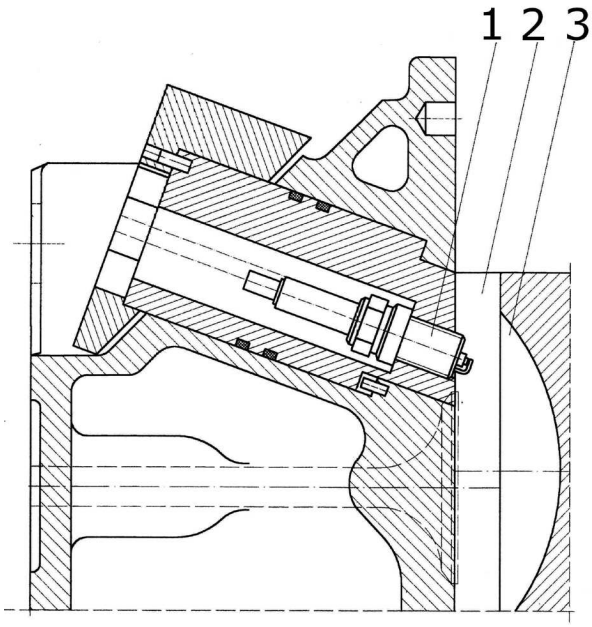

Fig. 3. Engine of S320 Andoria – cross-section of factory engine 1 – engine block, 2 – cylinder sleeve, 3 – injector, 4 – cylinder head, 5 – fuel tank, 6 – rod, 7 – crankshaft, 8 – piston, 9 – camshaft

TFSCM COMBUSTION MODEL

For the simulation of homogeneously/inhomogeneously premixed combustion processes in SI engines, a turbulent flame speed closure model (TFSCM) is available in FIRE [4]. The kernel of this model is the determination of the reaction rate based on the approach depending on parameters of turbulence, i.e. turbulence intensity and turbulent length scale, and of flame structure like the flame thickness and flame speed, respectively. The reaction rate can be determined by two different mechanisms via: Auto-ignition and Flame propagation scheme.

The auto-ignition scheme is described by an Arrhenius approach and the flame propagation mechanism depends mainly on the turbulent flame speed. The larger reaction rate of these two mechanisms is the dominant one. Hence, the fuel reaction rate ω_{fuel} can be described using a maximum operator via:

$$\omega_{fuel} = \max\{\text{Auto} - \text{ignition}\ \omega_{AI}, \text{Flame Propagation}\ \omega_{FP}\}.$$

The first scheme is only constructed for air/fuel equivalence ratios from 1.5 up to 2.0 and for pressure levels between 30 and 120 [bar], respectively. The auto-ignition reaction rate ω_{AI} can be written as:

$$\omega_{AI} = a_1 \rho^{a_2}\, y_{fuel}^{a_4}\, y_{O_2}^{a_4}\, T^{a_5} \exp\left(-\frac{T_a}{T}\right),$$

where: a_1 to a_5 are empirical coefficients and T_a is the activation temperature, T is the temperature, r is the density, y_{fuel} is the fuel mass fraction and y_{O2} is the oxygen mass fraction.

The reaction rate ω_{FP} of the flame propagation mechanism, the second one in this model, can be written as the

product of the gas density, the turbulent burning velocity S_T and the fuel mass fraction gradient ∇y_{fuel} via:

$$\omega_{FP} = \rho S_T \nabla y_{fuel}.$$

NUMERICAL MODEL OF ENGINE

The computational mesh can be obtained as surface or volume discretization. In AVL FIRE the Finite Volume Method (FVM) is used to calculate the heat flows. For four-stroke engine four computational domains are required. The first domain includes the intake stroke until closing the intake valves. The second domain is used since the closure of the inlet valve until the exhaust valve timing, at a time when the valves are closed. The third domain is used since the opening of the exhaust valve to the end of the exhaust stroke. And finally, the fourth domain is required for the whole engine cycle. The division cycle of three domains eliminates the problem of return flows in the crevices between the valve train and valve seat.

The first step is to draw the engine workspace (Fig. 4). Due to software, valves must be slightly open. This geometry is loaded into the preprocessor of FIRE program. On the basis of this geometry the computational moving mesh is generated (Fig. 5).

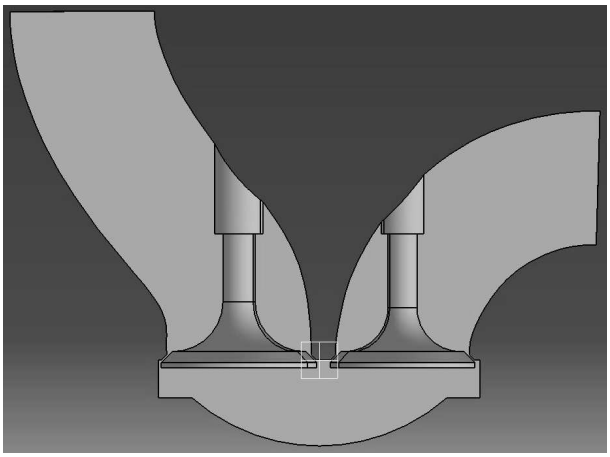

Fig. 4. Geometry of engine in CAD

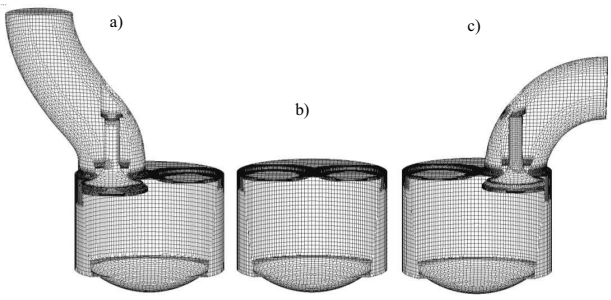

Fig. 5. Computational mesh of engine, a) intake, b) compression, c) exhaust

The computational mesh around valves was concentrated to obtain more accurate results. FIRE gives the possibility of temporary thickening of the grid.

Table 2. Modelling parameters

Parameters	Value
ignition advance angle	12 deg
fuel	gasoline
fuel temperature	320 K
initial pressure	0.095 MPa
initial temperature	365 K
excess air factor	1.0, 1.1, 1.2, 1.3
density	1.19 kg/m^3

Table 3. Submodels

Model	Name
combustion model	TFSCM
turbulence model	k-zeta-f
NO formation model	Extended Zeldovich Model
soot formation model	Lund Flamelet Model
evaporation model	Dukowicz
breakup model	Wave

RESULTS

As a result of numerical analysis a number of characteristic quantities of combustion process in the engine were obtained such as: pressure, temperature, parameters of flow field, turbulence, heat transfer, species, toxic parameters and other. In Figures 6 and 7 the results of model validation are presented. To model validation, the courses of pressure formed in real test engine were taken. As additional param-

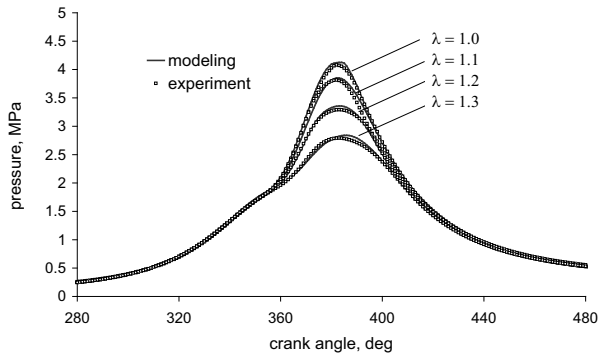

Fig. 6. Pressure courses for the four values of excess air factor

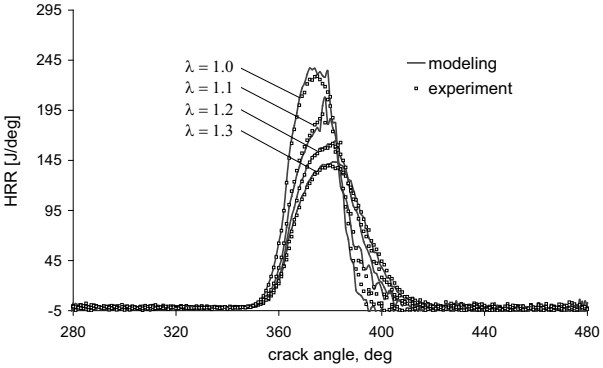

Fig. 7. Heat release rate courses for the four values of excess air factor

eters, the courses of the pressure rise and heat release rate HRR were taken as well. The researches were conducted for four values of excess air factor equal 1.0, 1.1, 1.2 and 1.3.

SI engine model of the AVL FIRE software pretty accurately reflects the real processes in the compression ignition engine. The satisfactory qualitative and quantitative compatibility between the pressure courses was achieved. For the pressure rise and heat release rate quite good agreement was achieved, as well.

Analyzing the results of modelling and experimental studies it should be mentioned that the results of indication of IC engine, in particular, the results of the analysis of thermal processes taking place in the cylinder are subject to some error resulting from the measurement accuracy and hence the uncertainty of the result.

In Figure 8 the flow field in the modelled engine during intake and compression stroke is presented. The main swirl process by the streamlines is underlined. There, the so-called tumble swirl is visible. This swirl is responsible for flame kernel direction propagation.

Figure 9 shows the cross sections of the engine cylinder where the temperature field is presented. The first three pictures show flame propagation in the combustion chamber. The direction of flame propagation is determined by fluid flows generated during intake stroke (Fig. 8). In Figure 8 the tumble flow is highly visible. The other two pictures show the exhaust stroke when the exhaust valve starts to open and when it is fully open.

CONCLUSIONS

AVL FIRE program is a research tool that can be successfully used to model the thermal cycle of the internal combustion engine. The AVL FIRE up-to-date numerical code used during research made it possible to generate 3D geometric mesh of combustion chambers of the test engine and allowed to perform numerical calculations of processes occurring in this engine. Simulations of combustion process have delivered information concerning spatial and time-de-

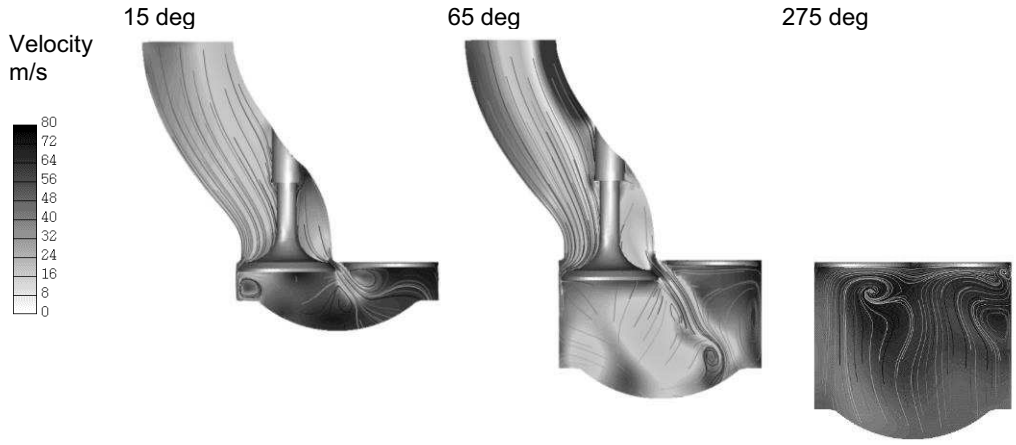

Fig. 8. Cross sections of the engine cylinder during intake and compression stroke – velocity field with streamlines

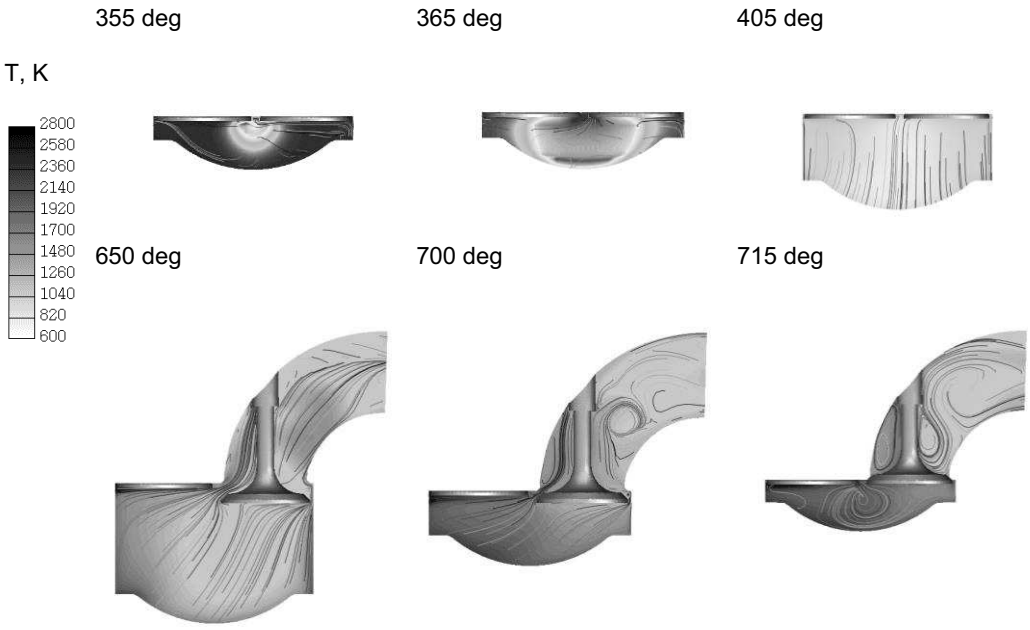

Fig. 9. Cross sections of the engine cylinder at the beginning of combustion and during exhaust stroke – temperature

pendent pressure and temperature distribution in combustion chamber. This information would be extremely difficult to obtain by experimental methods. It allows analyzing not only the combustion chamber but also the intake and exhausting process.

The paper presents results of SI engine modelling using CFD software. Pressure, temperature, heat release rate and other parameters in function of crank angle as well as spatial distribution of the above-mentioned quantities at selected crank angles were determined. The created model of SI engine was successfully verified. The resulting differences are acceptable. The results of modelling allow for an analysis of engine operation both in terms of thermodynamic and flow.

REFERENCES

1. **Jamrozik A., 2009**: Modelling of two-stage combustion process in SI engine with prechamber. MEMSTECH 2009, V-th International Conference Perspective Technologies and Methods in MEMS Design, Lviv-Polyana, 13-16.
2. **Jamrozik A., 2008**: Analiza numeryczna procesu tworzenia i spalania mieszanki w silniku ZI z komorą wstępną. Teka Komisji Motoryzacji Polskiej Akademii Nauk, Zeszyt Nr 33-34, 143-150.
3. **Tutak W., 2009**: Modelling of flow processes in the combustion chamber of IC engine. Proceedings of the 5th International Conference MEMSTECH'2009. Perspective Technologies and Methods in Mems Design. Lviv–Polyana, Ukraine, 45-48.
4. AVL FIRE version 2009, ICE Physics & Chemistry, Combustion, Emission, Spray, Wallfilm. AVL LIST GmbH, 2009.
5. **Jamrozik A., Tutak W., 2010**: Modelling of combustion process in the gas test engine. Proceedings of the VI-th International Conference MEMSTECH 2010 Perspective Technologies and Methods in Mems Design. Lviv–Polyana, 14-17.
6. **Tutak W., Jamrozik A., 2010**: Numerical analysis of some parameters of gas engine. Teka Commission of Motorization and Power Industry in Agriculture, Volume X, Polish Academy of Science Branch in Lublin. Lublin, 491-502.
7. **Tutak W., Jamrozik A., 2010**: Modelling of the thermal cycle of gas engine using AVL FIRE Software. Combustion Engines, No. 2/2010 (141), 105-113.
8. **Jamrozik A., Tutak W., 2011**: A study of performance and emissions of SI engine with two-stage combustion system. Chemical and Process Engineering. Vol. 32, No 4, 453-471.
9. **Tutak W., Jamrozik A., Kociszewski A., Sosnowski M., 2007**: Numerical analysis of initial swirl profile influence on modeled piston engine work cycle parameters. Combustion Engines, 2007-SC2, 401-407.
10. **Kociszewski A., Jamrozik A., Sosnowski M., Tutak W., 2007**: Simulation of combustion in multi spark plug engine in KIVA-3V. Combustion Engines. 2007-SC2, 212-219.
11. **Jamrozik A., Tutak W., Kociszewski A., Sosnowski M., 2006**: Numerical Analysis of Influence of Prechamber Geometry in IC Engine with Two-Stage Combustion System on Engine Work Cycle Parameters. Journal of KONES Powertrain and Transport, Vol 13, No 2, 133-142.
12. **Jamrozik A., Kociszewski A., Sosnowski M., Tutak W., 2006**: Simulation of combustion in SI engine with prechamber. XIV Ukrainian-Polish Conference – CAD in Machinery Design Implementation and Educational Problems CADMD'2006. Polyana, Ukraine, 66-69.
13. **Cupiał K., Jamrozik A., 2002**: SI engine with the sectional combustion chamber. Journal of Kones, Internal Combustion Engines. Vol 9, No 3-4, 62-66.
14. **Szwaja S, Jamrozik A., 2009**: Analysis of Combustion Knock in the SI Engine. Combustion Engines, 2009-SC2, 128-135.
15. **Tutak W., Jamrozik A., Kociszewski A., Sosnowski M., 2007**: Numerical analysis of initial swirl profile influence on modelled piston engine work cycle parameters. Combustion Engines, 2007-SC2, 401-407.
16. **Szwaja S., 2010**: Studium pulsacji ciśnienia spalania w tłokowym silniku spalinowym zasilanym wodorem. Serie monografie nr 182, Częstochowa.
17. **Tutak W., 2008**: Thermal cycle of SI engine modelling with initial swirl process into consideration. Combustion Engines, 1/2008 (132), 56-61.
18. **Kociszewski A., 2008**: Numerical analysis of spark plugs number influence on selected parameters of combustion in piston engine. Combustion Engines, 1/2008 (132), 50-55.
19. **Szwaja S., Bhandary K.R., Naber J.D., 2007**: Comparison of hydrogen and gasoline combustion knock in a spark ignition engine. Int. J. Hydrogen Energy Vol. 32 nr 18.
20. **Szwaja S., 2009**: Combustion Knock – Heat Release Rate Correlation of a Hydrogen Fueled IC Engine Work Cycles. 9th International Conference on Heat Engines and Environmental Protection. Proceedings. Balatonfured, Hungary.
21. **Styła S., Walusia S., Pietrzyk W., 2008**: Computer simulation possibilities in modelling of ignition advance angle control in motor and agricultural vehicles. Teka Commission of Motorization and Power Industry in Agriculture, 8, 231-240.
22. **Jamrozik A., Tutak W., Kociszewski A., Sosnowski M., 2013**: Numerical simulation of two-stage combustion in SI engine with prechamber. Applied Mathematical Modelling, Volume 37, Issue 5, 2961–2982.
23. **Szwaja S., Jamrozik A., Tutak W., 2013**: A Two-Stage Combustion System for Burning Lean Gasoline Mixtures in a Stationary Spark Ignited Engine. Applied Energy, 105 (2013), 271-281.

WALIDACJA MODELU BADAWCZEGO SILNIKA ZI

Streszczenie. W pracy przedstawiono wyniki modelowania obiegu cieplnego tłokowego silnika spalinowego o zapłonie iskrowym. Modelowanie przeprowadzono w programie AVL Fire. Obiektem badań był silnik S320 o zapłonie iskrowym zasilany benzyną. Au-

tor pojął trud wygenerowania kompletnej siatki dla posiadanego silnika spalinowego, z uwzględnieniem kanałów wymiany ładunku wraz z zaworami. Wymagało to wygenerowania czterech domen obliczeniowych. Uwzględniono miejscowe i chwilowe zagęszczanie siatki, co przyczyniło się do uzyskania dokładniejszych rozwiązań oraz skrócenia i tak długiego czasu obliczeń cyklu silnika. Wyniki analizy numerycznej zostały zestawione z wynikami indykowania silnika na stanowisku badawczym. Stworzony model silnika SI został pomyślnie zweryfikowany.
Słowa kluczowe: silnik, symulacja, modelowanie, spalanie.

Acknowledgements

The authors would like to express their gratitude to AVL LIST GmbH
for Providing a AVL Fire software under the University Partnership Program.

TEKA. COMMISSION OF MOTORIZATION AND ENERGETICS IN AGRICULTURE – 2013, Vol. 13, No. 2, 23–28

The effect of exposing wheat and rye grains to infrared radiation on the falling number and moisture content in the flour

Mariusz Kania[1], Dariusz Andrejko[1], Beata Ślaska-Grzywna[1], Izabela Kuna-Broniowska[2], Katarzyna Kozłowicz[3]

[1]Department of Biological Bases of Food and Feed Technologies
[2]Department of Applied Mathematics and Computer Science
[3]Department of Refrigeration and Food Industry Energetics
University of Life Sciences in Lublin

Received April 15.2013; accepted June 14.2013

Summary. The work presents the results of research on the effect of processing wheat and rye grains with infrared radiation on the falling number in flour. The research material was provided by wheat of "Waluta" variety and rye of "Dańkowskie Diament" variety. The grain was moisturized to 14, 16 and 18% and exposed to infrared radiation for the period of 0, 30, 60, 90 and 120 s at the temperature of 150°C. Next, the samples were milled and the falling number in the obtained flour was determined. On the basis of study results it was recorded that heating the grain with infrared radiation prior to milling resulted in a significant increase in the value of the falling number, as well as in lower moisture of the flour.
Key words: wheat, rye, falling number, infrared radiation.

INTRODUCTION

Falling number is one of indicators determining the bread making quality of flour. This value is expressed in seconds which are equivalent to the mixing time and the time needed by a viscosimetric stirrer to reach the bottom in hot starch pap. The value of the falling number is affected by the amylolytic activity of flour. Alpha- and beta-amylase occurring in flour are enzymes which break the starch down. Their excessive activity leads to decomposition of starch into simple sugars, which deteriorates the bread making quality of flour [17].

The main reason for high amylase activity, and for low value of the falling number, is pre-harvest germination within the grain head. This happens in a situation when unfavorable weather conditions delay the harvest. High temperature and moisture in the air activate alpha- and beta-amylase, as well as proteases, which leads to degrading proteins and starch [16]. Frequently, grain which was originally meant for consumption has to be qualified for feed manufacturing. This is an unfavorable phenomenon, particularly in the face of worldwide food problems (according to FAO, in 2010 there were 925 m people suffering malnutrition) [6]. The factors which affect the falling number include:

– altitude – the falling number increases as elevation increases,
– nitrogen fertilization rate – the falling number increases or decreases,
– late maturity of alpha-amylase – the falling number decreases,
– fungicide treatment – the falling number declines,
– fusarium infection – minor decrease in the falling number [8].

One of the methods used to process plant materials, such as cereal grain, legume seeds and cocoa seeds are heating them with infrared radiation. This enables us to develop desired qualitative features in the product. Using this method for processing cereal grains affects, among others, modifying physical properties in the products of milling, and also energy consumption of milling or granulometric composition [3, 4, 5, 7, 18]. Therefore, some attempts have been made to improve the quality of cereal through exposing it to infrared radiation [14, 15].

PURPOSE AND METHODS

The aim of the study was to determine the relationship between the time of exposing wheat and rye grains of different moisture to infrared radiation and the activity of amylases present in the flour produced from those grains, as well as flour moisture.

The material studied was the grain of spring wheat of "Waluta" variety and of winter wheat of "Dańkowskie Diament" variety. Before starting the analyses the moisture of the grain was determined (according to PN-86/A-74011 norm), which was ca. 12%. Then the samples were moisturized up to 14, 16 and 18% [10].

After moisturizing and mixing the grain, the sample was stored in a tightly closed container placed in a cool-

ing chamber at the temperature of ca. 4°C. In order to obtain equal required moisture in the whole volume the sample was shaken several times each day. An hour prior to measurement, the sample was taken out of the cooling chamber to make its temperature uniform with that of the environment.

The grain prepared in this way was next exposed to infrared radiation in a laboratory device for IR processing of grainy plant materials [1, 2]. After reaching the temperature of 150°C, the grain was supplied in a single layer onto the conveyor belt moving below the radiators. The speed of conveyor belt's movement was adjusted in such a way that the grain should stay within the radiation area for the time of 30, 60, 90 and 120 s. Then the grain was ground with the help of Brabender Junior laboratory mill.

After completing the milling process, the moisture of the obtained flour was determined according to PN-86/A-74011 [10] and the falling number was calculated following PN-ISO 3039 [13].

RESULTS

Figures 1 and 2 present how the time of exposing cereal grains to infrared radiation affects the value of the falling number of flour obtained from that cereal.

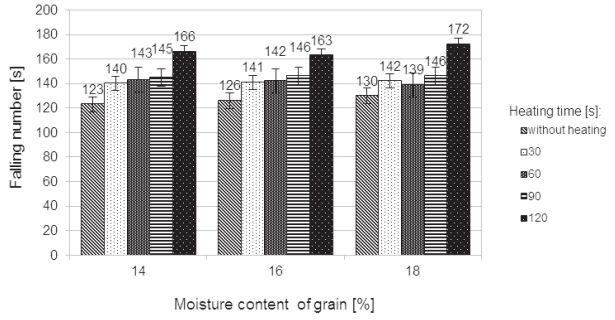

Fig. 1. Falling number of rye flour, depending on the time of heating the grain

The data presented in Figure 1 reveal that the lowest value of the falling number was recorded for rye flour obtained from the grain which had not been exposed to thermal processing. Depending on the moisture of the grain, the falling number for this flour ranged between 123 and 130 s,

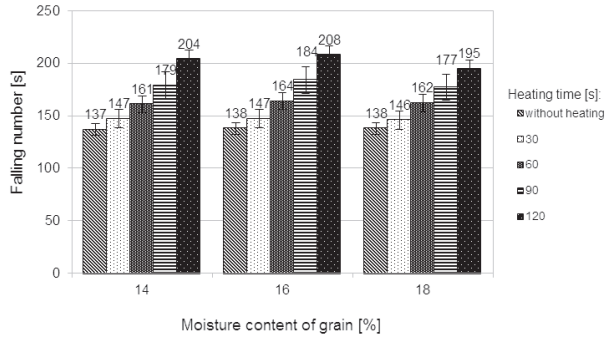

Fig. 2. Falling number of wheat flour, depending on the time of heating the grain

which suggests average activity of alpha-amylase and, at the same time, its low bread making utility. Heating the grain, irrespective of its initial moisture, clearly resulted in a higher value of the falling number. The highest increase in this value was observed when the grain had been heated for 120 s. This resulted in the falling number reaching the level of 163-172 s.

Wheat flour obtained from the grain which had not been thermally processed was characterized by the falling number at the level of 137 to 138 s, depending on the initial moisture, which, according to PN-A-74022:2003 [11], makes it useless as a material for making bread. Using infrared radiation led to increasing the value of the falling number. It was observed that each time prolonging the heating time by 30 s within the range of 30 to 120 s clearly contributed to increasing the value of the falling number, irrespective of the initial moisture of the grain. Maximum values of the analyzed parameter were noted after heating the grain for 120 s and they ranged from 195 to 208 s, depending on the initial moisture of the grain.

The changes observed in the falling number of flour suggest a clearly lower activity of the amylases present in that flour, which is directly reflected in bread making quality of the flour. The obtained values will qualify flour for making bread [11].

Figures 3 and 4 present the effect of the time of heating cereal grains with IR on the content of moisture in the flour produced from those cereals.

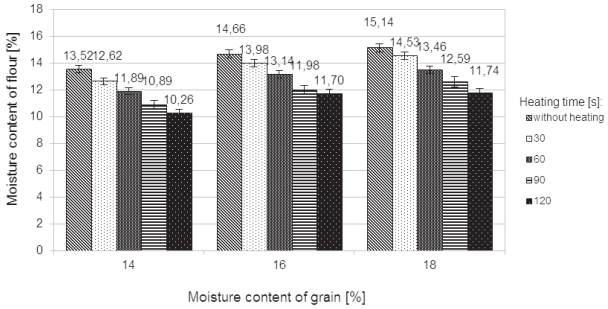

Fig. 3. Moisture content of rye flour, depending on the time of heating the grain

The moisture of flour obtained from rye which had not been thermally processed ranged from 13.52 to 15.14%. In each of the analyzed variants the moisture of the flour was lower than the moisture of the grain. This resulted from partial evaporation of water during and immediately following milling. Prolonging the time of exposing the grain to heating resulted in decreased flour moisture. Heating the grain for 120 s let us reduce the moisture of the flour to the level of 10.26% for the grain of initial moisture amounting to 14%, and to 11.74% for the grain of initial moisture of 18%. According to the Polish Norm for rye flour [12], the required moisture must not exceed 15%. In our analyses this value was exceeded only in the flour obtained from the grain of initial moisture of 18% which had not been subject to heating. The product of milling reached the value of moisture equal to 15.14%.

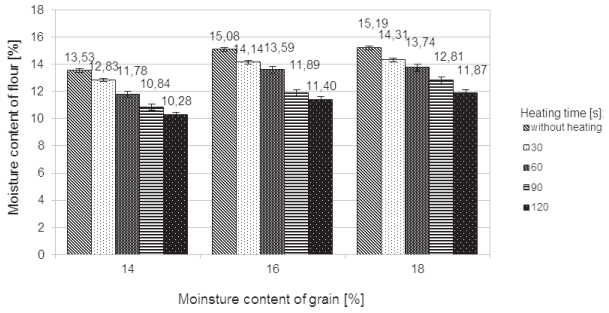

Fig. 4. Moisture content of wheat flour, depending on the time of heating the grain

The moisture of wheat flour obtained from grain which had not been thermally processed ranged from 13.53 to 15.19%. Irrespective of the initial moisture of the grain, prolonging the time of exposing the grain to heating resulted in decreased moisture of flour. With the longest variant of processing the grain for 120 s, the moisture of the flour was noted at the level of 10.28% to 11.87%. Considering the Polish Norm, the requirements regarding acceptable moisture were not met by the flour obtained from the grain with the moisture of 16% and 18% which had not been subject to heating, since the values exceeded the level of 15%.

STATISTICAL ANALYSIS

The experiment was performed in the system of three-factor cross-classification. The experimental factors considered were two varieties of grain, three levels of moisture (14%, 16%, 18%) and four processing periods (30 s, 60 s, 90 s and 120 s). The experiment also involved control groups (unprocessed) created by the grain of two varieties with three analyzed moisture levels. As the model for the experiment, the following linear model was adopted:

$$y_{ijkl} = \mu + \alpha_j + \beta_k + \gamma_l + \alpha\beta_{jk} + \alpha_{jl} + \beta_{jkl} + \alpha\beta\gamma_{jkl} + e_{ijkl},$$

where:

y_{ijkl} – moisture of flour (or the falling number) of *j-this* grain variety with *k-this* moisture undergoing *l-this* processing time,
μ – mean moisture of flour,
a_j – effect of *j-this* grain variety,
b_k – effect of *k-this* grain moisture,
g_l – effect of *l-this* processing time,
ab_{jk} – effect of interaction of *j-this* grain variety with *k-this* grain moisture,
$a\,g_{jl}$ – effect of interaction between *j-this* grain variety and *l-this* processing time,
$b\,g_{kl}$ – effect of interaction between *k-this* grain variety and *l-this* processing time,
e_{ijkl} – experimental error.

For the needs of the adopted experimental model, we verified hypotheses regarding the significance of the particular components of the model. To verify those hypotheses, we used multivariate analysis of variance because we were analyzing two features of grain which were correlated (r_s=-0.68). Wilk's and F Snedecore's tests were applied as test functions. The results of the calculations are presented in the table below.

None of the zero hypotheses assuming the lack of significance of the considered effects of the model was rejected (p = 0.000), so it was concluded at the significance level of 0.01 that both grain variety and grain moisture, as well as processing time, result in a significant variation of at least one of the examined properties: grain moisture or the falling number.

In order to verify which of the analyzed agents significantly diversifies the values of these properties, one-dimensional tests of variance analysis were performed (Table 2).

Table 1. Multivariate analysis of variance for the analyzed flour properties

Effect	Test	Value	F	Effect df	Error df	p
Free term	Wilksa	0,000	524765,590	2,000	29	0,000
Species	Wilksa	0,016	865,707	2,000	29	0,000
Moisture content	Wilksa	0,016	101,019	4,000	58	0,000
Heating time	Wilksa	0,000	326,771	8,000	58	0,000
Species*Moisture content	Wilksa	0,522	5,577	4,000	58	0,001
Species*Heating time	Wilksa	0,042	28,200	8,000	58	0,000
Moisture content*Heating time	Wilksa	0,414	2,007	16,000	58	0,028
Species*Moisture content*Heating time	Wilksa	0,274	3,302	16,000	58	0,000

Table 2. One-dimensional tests of significance for flour moisture and falling number

Effect	Moisture content F	Moisture content p	Falling number F	Falling number p
Free term	551241,8	0,000	369072,2	0,000
Species	4,7	0,038	1715,9	0,000
Moisture content	873,8	0,000	1,2	0,329
Heating time	1216,1	0,000	1229,7	0,000
Species*Moisture content	1,1	0,359	11,6	0,000
Species*Heating time	2,1	0,110	142,7	0,000
Moisture content*Heating time	3,4	0,007	1,2	0,340
Species*Moisture content*Heating time	3,4	0,006	3,9	0,003

The tests did not reveal any interaction between the variety of the grain and its moisture, or between the variety and heating time that would be significant for flour moisture. At the significance level of 0.01 it may be claimed that flour moisture for both varieties changed similarly along with changed grain moisture, as well as along with changed processing time (Table 2).

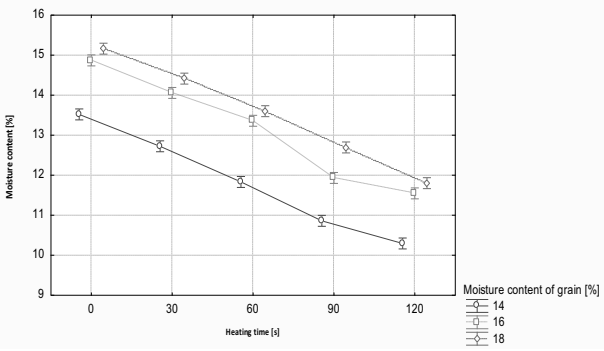

Fig. 5. Changes in the value of mean flour moisture for grain at the analyzed moisture levels, depending on heating time

As far as the falling number is concerned, the analyzed levels of grain moisture and the interaction between grain moisture and heating time turned out to be insignificant. At the significance level of 0.01, it may be claimed that the analyzed levels of grain moisture do not result in any significant variation of the falling number. Additionally, it may be assumed that the falling number in the flour of particular initial level of grain moisture changed in the same way along with the change in processing time (Fig. 6).

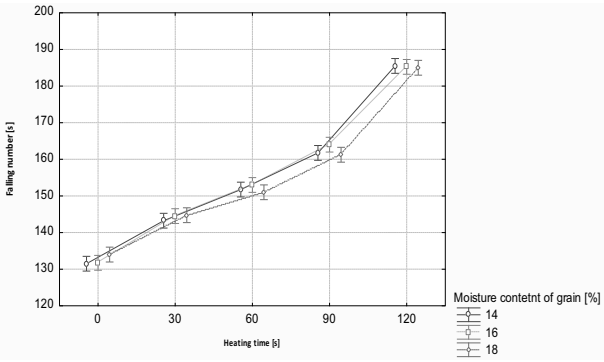

Fig. 6. Changes in the value of the falling number for grain at the analyzed moisture levels, depending on heating time

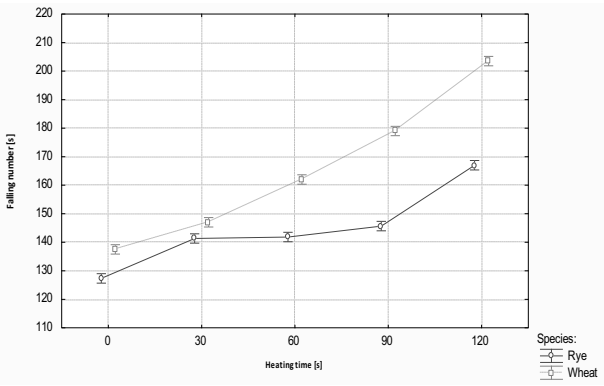

Fig. 7. Changes in the value of the falling number for wheat and rye, depending on heating time

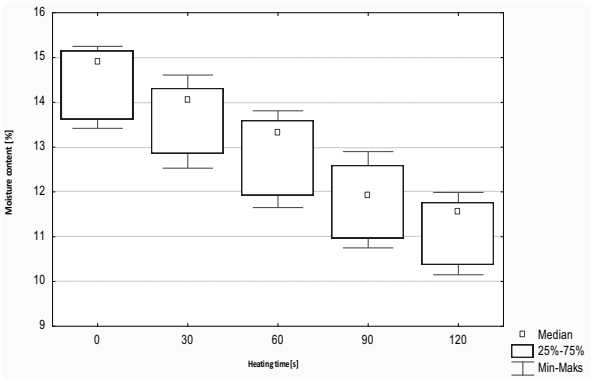

Fig. 8. Box plot diagrams for flour moisture, depending on heating time

Flour moisture decreased along with prolonged heating time and the character of changes in moisture was similar to linear (Fig. 8).

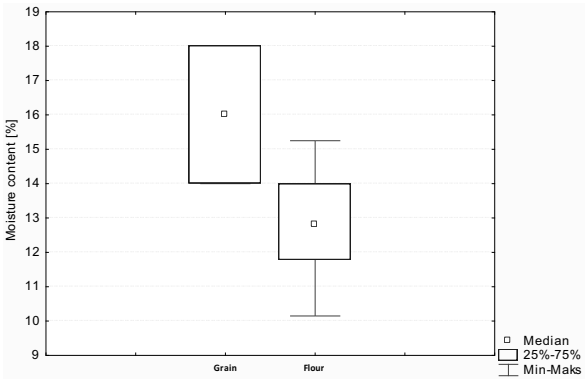

Fig. 9. Flour moisture and initial grain moisture

Half of the analyzed grain samples with the moisture of 14% to 18% were characterized by flour moisture at the level of 12% to 14% (Fig. 9). The numbers in individual sub-classes amounting to n=2 were too low to determine if the assumptions for the variance analyses, i.e. normality of distribution and homogeneity of variances for studied properties had been fulfilled. The F Test is highly resistant to deviations from normality [9].

Table 3. Contrast evaluations

Contrast	Evaluation	Statistical error	t	p	-95% Confidence Interval	+95% Confidence Interval
Moisture content	8,363	0,173	48,342	0,000	8,010	8,717
Falling number	-114,000	2,555	-44,619	0,000	-119,218	-108,782

Irrespective of variance analysis tests, we performed a planned comparison of mean moisture and the falling number in flour from the grain that had not been subject to processing with the mean value of these properties in flour from the grain heated for 30, 60, 90 and 120 s.

In order to do this, we analyzed significance for the following contrast: $4 \cdot \mu_0 - \mu_{30} - \mu_{60} - \mu_{90} - \mu_{120}$, where μ_t are mean values of a property for respective heating periods (t=0; 30;

60; 90; 120). The value of this comparison for flour moisture was significant (p=0.000) and it amounted to 8.36% (2.9% on the average). Also, the difference between the value of the falling number in unprocessed grain and the falling number in heated grain was statistically significant (p = 0.000) and it was -114 (-28.5 on the average). The mean value of the falling number was statistically lower for the flour from unprocessed grain, as compared with the falling number in the flour from heated grain.

On the basis of the contrast analysis it may be claimed that the process of grain heating results in a statistically significant reduction in flour moisture, while it causes a statistically significant increase in the falling number (Table 3).

CONCLUSIONS

The following conclusions were drawn on the basis of the studies discussed above:

1. Heating wheat and rye grains with infrared radiation leads to a statistically significant increase in the falling number of flour.
2. Both with wheat and rye grains, a statistically significant decrease is observed in the moisture of the flour obtained from heated grain.
3. The initial moisture of grain does not affect the value of the falling number in the analyzed cereals.
4. Heating grain with infrared radiation may be an effective method of increasing the value of the falling number and, consequently, the bread making quality of flour.

REFERENCES

1. **Andrejko D., 2005**: Zmiany właściwości fizycznych nasion soi pod wpływem promieniowania podczerwonego. Rozprawy Naukowe AR w Lublinie, ISSN 0860- 4355, 288.
2. **Andrejko D., Ślaska-Grzywna B., 2008**: An influence of heating using IR radiation on pea seeds moisturizing process. TEKA Komisji Motoryzacji i Energetyki Rolnictwa PAN V/VIII, 7-17.
3. **Andrejko D., Kania M., Łatka A., Rydzak L., 2011**: Wpływ obróbki cieplnej promieniami podczerwonymi na proces przemiału ziarna pszenicy odmiany Korynta. MOTROL, Motoryzacja i Energetyka Rolnictwa 13, 7-13.
4. **Dziki D., Laskowski J., 2004**: The energy – consuming indexes of wheat kernel grinding process. TEKA Komisji Motoryzacji i Energetyki Rolnictwa PAN V/IV, 62-70.
5. **Dziki D., Laskowski J., 2005**: Influence of selected factors on wheat grinding energy requirements. TEKA Komisji Motoryzacji i Energetyki Rolnictwa PAN V/V, 56-64.
6. http://www.fao.org/docrep/012/al390e/al390e00.pdf
7. **Kusińska E., Zawiślak K., Sobczak P., 2008**: Energy consumption of maize grain crushing depending on moisture content. TEKA Komisji Motoryzacji i Energetyki Rolnictwa PAN V/VIII, 129-134.
8. **Kweon M., 2010**: Falling number in wheat. USDA, ARS, Soft Wheat Quality Lab., Wooster, OH, USA.
9. **Lindman H. R., 1974**: Analysis of variance in complex experimental designs. W. H. Freeman, San Francisco.
10. Polska Norma PN-86/A-74011: – Ziarno zbóż, nasiona roślin strączkowych i przetwory zbożowe. Oznaczenie wilgotności.
11. Polska Norma PN-A-74022: 2003 – Przetwory zbożowe. Mąka pszenna
12. Polska Norma PN-A-74032: 2002 – Przetwory zbożowe. Mąka żytnia.
13. Polska Norma PN-ISO 3039:– Ziarna zbóż. Oznaczanie liczby opadania.
14. **Rydzak L., Andrejko D., 2011a**: Effect of different variants of pretreatment of wheat grain on the particle size distribution of flour and bran. TEKA Komisji Motoryzacji i Energetyki Rolnictwa PAN V/XIC, 283-290.
15. **Rydzak L. Andrejko D., 2011b**: Effect of vacuum impregnation and infrared radiation treatment on energy requirement in wheat grain milling. TEKA Komisji Motoryzacji i Energetyki Rolnictwa PAN V/XIC, 291-299.
16. **Thomason W.E., Hughes K.R., Griffey C.A., Parrish D.J, Barbeau W.E., 2009**: Understanding Pre-harvest Sprouting of Wheat. http://www.ext.vt.edu, Publication 424-060.
17. **Wang J., Pawelzik E., Weinert J., Zhao Q., Wolf G.A., 2008**: Factors influencing falling number in winter wheat. Eur. Food Res. Technol. 226:1365–1371
18. **Zawiślak K., Sobczak P., Andrejko D., Rydzak L., 2011**: Energochłonność procesu rozdrabniania wybranych odmian pszenicy. MOTROL, Motoryzacja i Energetyka Rolnictwa 13, 336-341.

WPŁYW OGRZEWANIA ZIARNA PSZENICY I ŻYTA PROMIENIAMI PODCZERWONYMI NA LICZBĘ OPADANIA I WILGOTNOŚĆ MĄKI

Streszczenie. W pracy przedstawiono wyniki badań wpływu obróbki promieniami podczerwonymi ziarna żyta i pszenicy na liczbę opadania uzyskanej następnie mąki. Materiałem badawczym była pszenica odmiany Waluta oraz żyto odmiany Dańkowskie Diament. Ziarno dowilżono do 14, 16 i 18% i poddano obróbce promieniami podczerwonymi przez okres 0, 30, 60, 90 i 120 s w temperaturze 150°C. Następnie dokonano przemiału próbek i oznaczono liczbę opadania uzyskanej mąki. Na podstawie wyników badań stwierdzono, że ogrzewanie ziarna promieniami podczerwonymi przed przemiałem powoduje istotny wzrost wartości liczby opadania oraz spadek wilgotności mąki.
Słowa kluczowe: pszenica, żyto, liczba opadania, obróbka promieniami podczerwonymi.

TEKA. COMMISSION OF MOTORIZATION AND ENERGETICS IN AGRICULTURE – 2013, Vol. 13, No. 2, 29–34

Optimization of work parameters of gaseous SI engine

Arkadiusz Kociszewski

Institute of Thermal Machinery, Czestochowa University of Technology
Armii Krajowej Av. 21, 42-201 Czestochowa, e-mail: kocisz@imc.pcz.czest.pl

Received May 15.2013; accepted June 14.2013

Summary. Results of numerical analysis of methane combustion in SI engine are presented in the paper. Work parameters of engine fuelled with methane lean mixtures of $\lambda = 1.4$ for several ignition advance angles are compared. The results of analysis proved that using ignition advance 6° CA before TDC, caused that engine work parameters (pressure, temperature and pressure growth speed) are correct and optimal. Simultaneously, the emission of nitric oxide was decreased compared to early ignition advance angles.
Key words: SI engine, methane, numerical modelling, lean mixture.

INTRODUCTION

One of the research activities carried out in the Institute of Thermal Machinery is 3D modelling of combustion in spark ignition engine fuelled with gasoline, gas and lean mixtures this fuels [1-15]. The calculations are performed in KIVA-3V and AVL FIRE programs [16-22].

The paper aims an analysis of influence of the ignition advance angle to stationary gaseous engines parameters, operating at constant rotational speed and driving electric generators. Such engines can be fuelled with natural gas, biogas (waste dump gas, sewage gas) or mine gas as well as fuels containing methane. The containment of methane in above mentioned fuels differs according to the origin of the fuel. The natural gas contains approx. 98% of methane, biogas contains approx. 40-60%, and main gas obtained during the exploitation of the mine contains approximately 25-60% of methane. The containment of methane in mine gas differs for different coal deposits, the way it is exploited and time.

The paper is the continuation of numerical analysis of combustion in gaseous SI engine model fuelled with lean mixtures [23, 24].

MODEL OF ENGINE

The engine model was prepared according to the test engine data. The test engine was designed as the modified single-cylinder, high-pressure S320ER engine, which has been rebuilt in order to apply multipoint spark ignition [25]. The main engine parameters are presented in Table 1.

Table 1. Main engine parameters

Engine capacity	1810 cm^3
Number of cylinders	1
Cylinder alignment	horizontal
Cylinder diameter	120 mm
Crank throw	80 mm
Crankshaft length	275 mm
Piston stroke	160 mm
Compression ratio	8.5
Rotational speed	1000 rev/min

The application of multipoint spark ignition in the test engine allowed to fuel the engine with lean mixtures of liquid and gaseous fuels of air excess factor $\lambda \leq 2.0$ [25].

The numerical modelling was performed in KIVA-3V program [26]. The software enabled 3D modelling of flow in piston engine combustion chambers of various geometry with taking turbulence and heat exchange into consideration.

The geometric mesh (Figure 1) describing the combustion chamber of the test engine was generated in the pre-processor of KIVA-3V package.

COMBUSTION MODELLING

The simulation of combustion process was performed for gaseous fuel (methane) at air excess factor value $\lambda =$

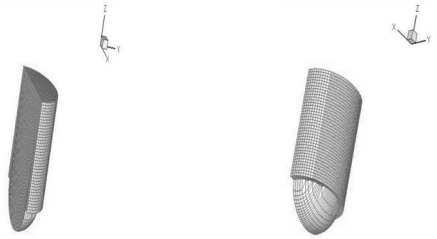

Fig. 1. Geometric mesh in cartesian co-ordinate system

1.4, one central spark plug and eight values of the ignition advance angles – 2, 4, 6, 8, 10, 12, 14, 16 deg CA before top dead center (TDC).

The chemical reaction of methane combustion model in KIVA-3V takes into account four kinetic reactions and six equilibrium reactions. The first kinetic reaction describes the oxidation of fuel and the following three reactions describe the NO formation according to extended Zeldowich mechanism [27].

$$CH_4 + 2O_2 \Rightarrow CO_2 + 2H_2O,$$
$$O + N_2 \Leftrightarrow N + NO,$$
$$N + O_2 \Leftrightarrow O + NO,$$
$$N + OH \Leftrightarrow H + NO.$$

The equilibrium reactions are [27]:

$$H_2 \Leftrightarrow 2H,$$
$$O_2 \Leftrightarrow 2O,$$
$$N_2 \Leftrightarrow 2N,$$
$$O_2 + H_2 \Leftrightarrow 2OH,$$
$$O_2 + 2H_2O \Leftrightarrow 4OH,$$
$$O_2 + 2CO \Leftrightarrow 2CO_2.$$

The coefficients of NO formation kinetic reaction rate are necessary to perform the calculations and they were chosen on the basis of the literature studies [28].

The results of numerical modelling are presented in graphical form. The distribution of temperature and nitric oxide concentration in the combustion chamber are presented using Tecplot 360 postprocessing software [29]. The courses of pressure, temperature, NO and CO_2 concentration (averaged values for the volume of combustion chamber) in function of crank angle are also presented.

NUMERICAL ANALYSIS RESULTS

The following figures depict the distribution of temperature and nitric oxide concentration in the combustion chamber, which occurred for the analyzed ignition advanced angles. Moreover, courses of pressure, temperature, NO and CO_2 concentration (averaged values for the volume of combustion chamber) in function of crank angle are depicted. The temperature distribution is presented at crank angle in TDC. The NO distribution is presented at crank angle corresponding with the maximal concentration of this compound.

The temperature distribution as well as pressure courses (averaged values for the volume of combustion chamber) in function of crank angle are depicted in Fig. 2 – Fig. 4.

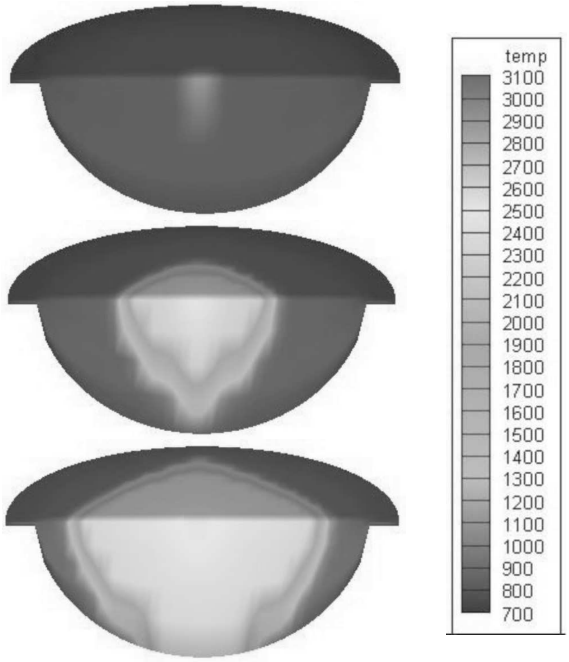

Fig. 2. Temperature distribution for three example ignition advance angles 2°CA, 10°CA, 16°CA before TDC

Fig. 2 reveals that the combustion process was intensified by increasing the ignition advance angle value. Greater portion of fuel was burnt at temperature above 2000 K. Such phenomenon is clearly seen in case of ignition advance angle equal 16°CA before TDC. In this case, the combustion process takes place in almost whole volume of the chamber.

Fig. 3 and 4 depict pressure and temperature courses (averaged values for the volume of combustion chamber) in function of crank angle.

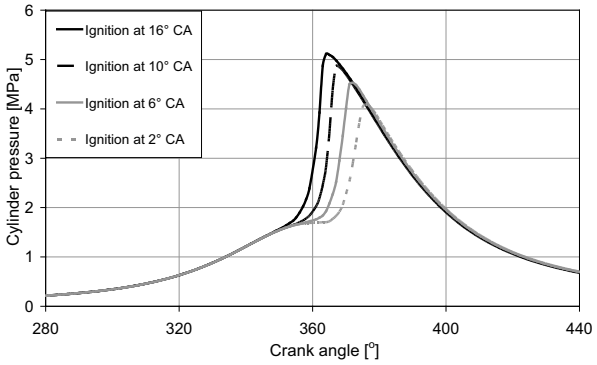

Fig. 3. In cylinder pressure courses for selected ignition advance angle values

In case of 2°CA ignition advance angle value, the pressure in the cylinder reaches its maximal value equal 4.1 MPa at 376°CA. The increase in the ignition advance angle to 16°CA before TDC causes the 24% increase in maximal pressure value.

The maximal pressure values occur earlier than in the configuration with 2°CA ignition advance angle value – the difference in crank angle are 12°CA. It proves that the combustion process was intensified for the configuration with earlier ignition. It is clearly seen on a chart depicting the

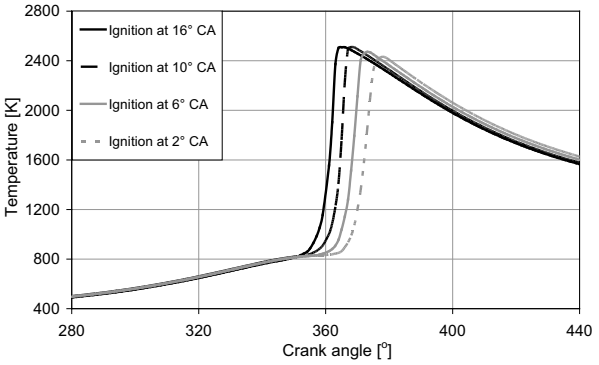

Fig. 4. In cylinder temperature courses for selected ignition advance angle values

pressure growth speed in the cylinder – Fig. 5. For case of 2°CA ignition advance angle value, this parameter reaches maximal value of 0.42 MPa/° at 372°CA. In case of 16°CA ignition advance angle value, $dp/d\varphi$ is two times bigger and reaches the value of 0.84 MPa/° at 361° CA.

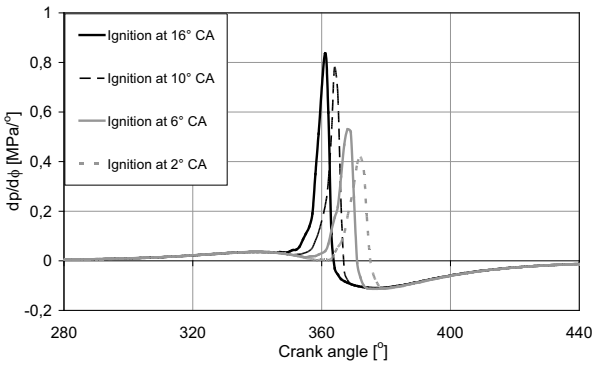

Fig. 5. Pressure increase courses in function of crank angle for selected ignition advance angle values

Taking into consideration the above mentioned data, it can be stated that configuration with more early ignition is not purposeful. The difference in maximal values of temperature (Fig. 4) is not significant. Although the acceleration of combustion process occurs, significant increase in pressure (Fig. 5) can lead to hard and noisy operation, which applies dynamic load to crankshaft and piston.

Increase the ignition advance angle value, causes increase in nitric oxide emission – Fig. 6 and 7.

Fig. 6 depicts the nitric oxide distribution in the combustion chamber for the three example ignition advance angles 2°CA, 10°CA, 16°CA before TDC. The pictures depict maximal values of nitric oxide concentration and which are prepared in the same scale. It can be noticed that increasing the ignition advance angle value significantly increases the NO concentration in the cylinder volume.

For 2°CA ignition advance angle value, the nitric oxide concentration (the averaged value for the volume of the combustion chamber – Fig. 7) reached its maximal value equal 2930 ppm at 394°CA. In case of 10°CA ignition advance angle value, the NO concentration increased by 65% up to 4850 ppm at 387°CA. For 16°CA ignition advance angle value, the NO concentration increased by 80% (5285 ppm) in comparison with case of 2°CA ignition advance angle.

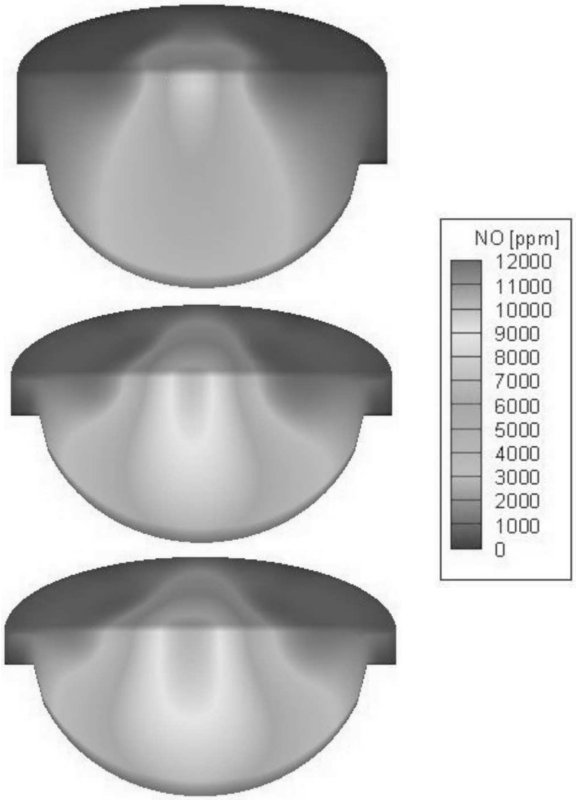

Fig. 6. NO distribution (actual maximum values at 46°, 28°, 25° CA after TDC) for three example ignition advance angles 2°CA, 10°CA, 16°CA before TDC

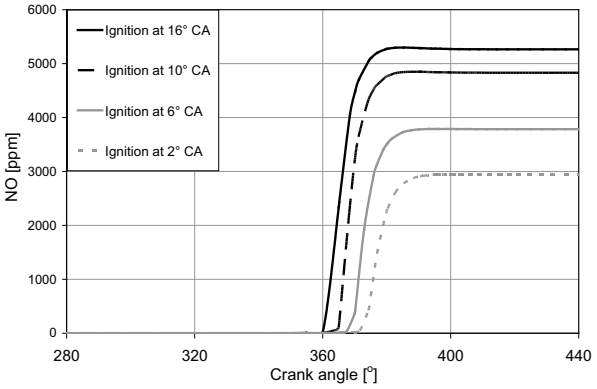

Fig. 7. Variations of NO concentration (mean values for cylinder volume) for selected ignition advance angle values

The above analysis proves, that increasing the ignition advance angle value to about 12°CA, 14°CA, 16°CA before TDC is not favourable. The pressure increase in the cylinder is too big, which can result in very hard engine operation and the nitric oxide emission increases significantly.

The chart depicted in Fig. 8. shows the variations of CO_2 concentration, which were occurred during modelled engine operation for all ignition advance angle values. The carbon dioxide emission values are mean values, calculated for the whole volume of cylinder. The maximal concentration of

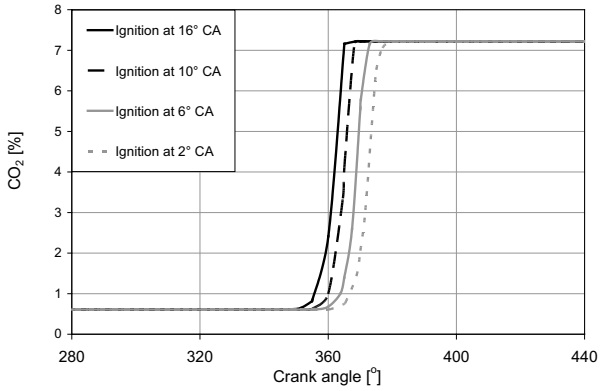

Fig. 8. Variations of CO_2 concentration (mean values for cylinder volume) for selected ignition advance angle values

this compound was 7,2% and was obtained at different crank angles depending on the value of ignition advance angle. With the increase of ignition angle, the maximal concentration of CO_2 was obtained faster.

The results of these tests were compared with those of a engine powered by a mixture of $\lambda = 1.2$ – Fig. 9-10. In this case ($\lambda = 1.2$) the optimal ignition advance angle was 2°CA before TDC.

The comparison shows that for the selected ignition advance angle much more preferred to use a leaner mixture. Although much smaller value of the pressure growth speed in this case, in the exhaust gas components is about 12% less CO_2 and up to almost 50% less nitrogen oxide.

CONCLUSIONS

The results of 3D modelling of methane combustion showed, that using earlier ignition advance angle caused very significant increase in NO emission, which gained even 80% for 16°CA ignition advance angle value. The difference in maximal values of temperature was insignificant. High values of pressure growth speed (maximal value of 0,83 MPa/°) can lead to noisy and hard engine operation.

The optimal value of ignition advance angle appears to be 6°CA before TDC. In this case model engine work parameters are proper and suitable to combustion lean gaseous mixture methane and air. The pressure in the cylinder reaches its maximal value equal 4.5 MPa at 372°CA and pressure increase is 0,53 MPa/°. Concentration of NO reaches its maximal value equal 3760 ppm at 387°CA and this is about 30% lower in comparison with case 16°CA ignition advance angle.

The results of numerical analysis can be used in stationary gaseous engines, operating at constant rotational speed and driving electric generators. Such engines can be fuelled with lean mixtures fuels containing methane and air.

REFERENCES

1. **Tutak W., Jamrozik A., Kociszewski A., Sosnowski M., 2006**: The influence of initial swirl profile on modelled piston engine work cycle parameters. XIV Ukrainian-

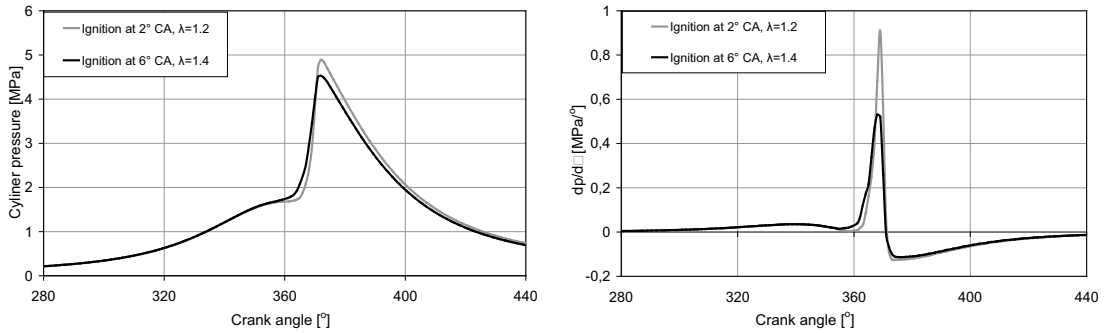

Fig. 9. In cylinder pressure and pressure increase courses in function of crank angle for optimal ignition advance angle values

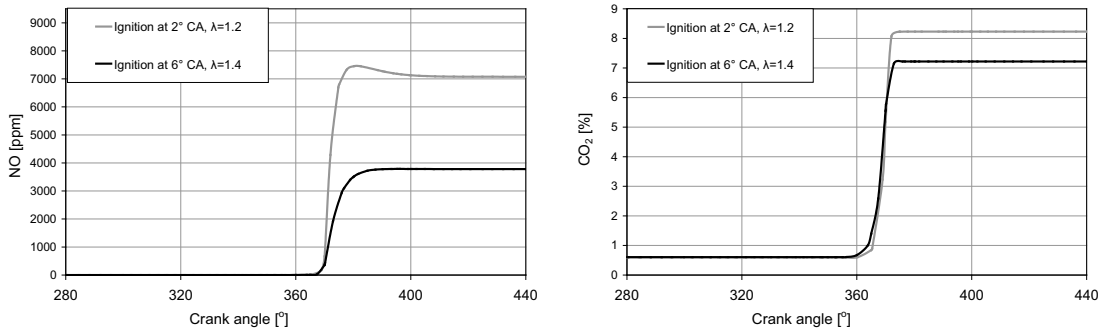

Fig. 10. Variations of NO and CO_2 concentration (mean values for cylinder volume) for optimal ignition advance angle values

-Polish Conference – CAD in Machinery Design Implementation and Educational Problems CADMD'2006, 118-121.
2. **Kociszewski A., Jamrozik A., Sosnowski M., Tutak W., 2006**: Numerical analysis of combustion in multi spark plug engine. XIV Ukrainian-Polish Conference – CAD in Machinery Design Implementation and Educational Problems CADMD'2006, 80-83.
3. **Jamrozik A., Kociszewski A., Sosnowski M., Tutak W., 2006**: Simulation of combustion in SI engine with prechamber. XIV Ukrainian-Polish Conference – CAD in Machinery Design Implementation and Educational Problems CADMD'2006, 66-69.
4. **Jamrozik A., Tutak W., Kociszewski A., Sosnowski M.M., 2006**: Numerical Analysis of Influence of Prechamber Geometry in IC Engine with Two-Stage Combustion System on Engine Work Cycle Parameters. Journal of KONES Powertrain and Transport, Vol 13, No 2, 133-142.
5. **Tutak W., Jamrozik A., Kociszewski A., Sosnowski M., 2007**: Numerical analysis of initial swirl profile influence on modelled piston engine work cycle parameters. Combustion Engines, Mixture Formation Ignition & Combustion, 2007-SC2, 401-407.
6. **Kociszewski A., Jamrozik A., Tutak W., Sosnowski M., 2007**: Simulation of combustion in multi spark plug engine in KIVA-3V. Combustion Engines, R.46 No. SC2, 212-219.
7. **Tutak W., 2008**: Thermal Cycle of Engine Modeling with Initial Swirl Proces Into Consideration. Combustion Engines, 1/2008 (132), 56-61.
8. **Kociszewski A., 2008**: Numerical analysis of spark plugs number influence on selected parameters of combustion in piston engine. Combustion Engines, No 1/2008 (132), 50-55.
9. **Jamrozik A., 2009**: Modelling of two-stage combustion process in SI engine with prechamber. MEMSTECH 2009 Perspective Technologies and Methods in MEMS Design, Proceedings of the Vth International Conference in MEMS Design, 13-16.
10. **Tutak W., 2009**: Modelling of flow processes in the combustion chamber of IC engine. MEMSTECH 2009 Perspective Technologies and Methods in MEMS Design, Proceedings of the Vth International Conference in MEMS Design, 45-48.
11. **Kociszewski A., 2009**: Three-dimensional modelling and experiment on combustion in multipoint spark ignition engine. MEMSTECH 2009 Perspective Technologies and Methods in MEMS Design, Proceedings of the Vth International Conference in MEMS Design, 20-23.
12. **Jamrozik A., Tutak W., 2010**: Modelling of combustion process in the gas test engine. MEMSTECH 2010 Perspective Technologies and Methods in MEMS Design, Proceedings of the VI-th International Conference in MEMS Design, 14-17.
13. **Tutak W., Jamrozik A., Kociszewski A., 2011**: Improved emission characteristics of SI test engine by EGR. MEMSTECH 2011 Perspective Technologies and Methods in MEMS Design, Proceedings of the VIIth International Conference in MEMS Design, 101-103.
14. **Jamrozik A., Tutak W., Kociszewski A., Sosnowski M., 2013**: Numerical simulation of two-stage combustion in SI engine with prechamber. Applied Mathematical Modelling, Volume 37, Issue 5, 2961-2982.
15. **Szwaja S., Jamrozik A., Tutak W., 2013**:A Two-Stage Combustion System for Burning Lean Gasoline Mixtures in a Stationary Spark Ignited Engine. Applied Energy, 105 (2013), 271-281.
16. **Jamrozik A., Tutak W., 2010**: Numerical analysis of some parameters of gas engine," Polish Academy of Science Branch in Lublin, TEKA, Commission of Motorization and Power Industry in Agriculture, Vol. X, 491-502.
17. **Tutak W., Jamrozik A., 2010**: Modelling of the thermal cycle of gas engine using AVL Fire Software. Combustion Engines, No 2/2010 (141), 105-113.
18. **Tutak W., 2011**: Modelling and analysis of some parameters of thermal cycle of IC engine with EGR. Combustion Engines, No 4/2011 (147). 43-49.
19. **Jamrozik A., Tutak W., 2012**: Application of numerical modeling to optimize the thermal cycle of the internal combustion engine. Scientific Research of the Institute of Mathematics and Computer Science, 1(11), 43-52.
20. **Tutak W., Jamrozik A., Gruca M., 2012**: CFD modeling of thermal cycle of supercharged compression ignition engine. Journal of Kones Powertrain and Transport, Vol. 19, No 1, 465-472.
21. **Jamrozik A., 2011**: Numerical Study of EGR Effects on the Combustion Process Parameters in HCCI Engines. Combustion Engines, No 4/2011 (147), 50-61.
22. **Tutak W., 2012**: An analysis of EGR impact on combustion process in the SI test engine. Combustion Engines, Vol 148, No 1/2012, 11-16.
23. **Kociszewski A., 2009**: Numerical modelling of combustion in SI engine fuelled with methane. COMBUSTION ENGINES, 4/2009 (139), 45-54.
24. **Kociszewski A.A., 2011**: Modelling of the thermal cycle of SI engine fuelled by liquid and gaseous fuel. Teka Commission of Motorization and Power Industry in Agriculture Polish Academy of Science Branch, Vol. XI, 109-117.
25. **Cupiał K., Kociszewski A., Jamrozik A., 2003**: Multipoint spark ignition engine operating on lean mixture. Teka Commission of Motorization and Power Industry in Agriculture Polish Academy of Science Branch, Vol. III, 70-78.
26. **Amsden A.A., "KIVA-3V, 1997**: A block-structured computer program for 3-D fluid flows with valves, chemical reactions, and fuel sprays. Los Alamos National Laboratory, Group T-3, March 1997.
27. **Rychter T., Teodorczyk A., 1990**: Mathematical modelling of work cycle piston engine. Polish Scientific Publishers, Warsaw 1990.
28. **Jamrozik A., 2006**: Modelling of nitric oxide formation process i combustion chamber of SI gas engine. VII-th International Scientific Conference GAS ENGINE 2006 – Design – Research – Development – Renewable Fuels.
29. **Tecplot Inc., 2006**: Tecplot 360 User's Manual. Bellevue.

OPTYMALIZACJA PARAMETRÓW PRACY SILNIKA GAZOWEGO ZI

Streszczenie. Wyniki analizy numerycznej spalania metanu w silniku ZI zostały przedstawione w artykule. Parametry pracy silnika zasilanego ubogimi mieszankami metanu $\alpha = 1{,}4$ dla kilku różnych kątów zapłonu zostały porównane. Wyniki tej analizy udowodniły, że przy kącie zapłonu 6° OWK parametry pracy silnika (ciśnienie, temperatura i szybkość wzrostu ciśnienia) są poprawne i optymalne. Jednocześnie, emisja gazu azotowego zmniejszyła się w porównaniu z wcześniejszymi wartościami kąta zapłonu.

Słowa kluczowe: Silniki SI, metan, modelowanie numeryczne, uboga mieszanka.

TEKA. COMMISSION OF MOTORIZATION AND ENERGETICS IN AGRICULTURE – 2013, Vol. 13, No. 2, 35–40

Force and work of cutting of sponge-fatty cake with oat flakes content

Elżbieta Kusińska, Agnieszka Starek

Department of Food Engineering and Machinery, University of Life Sciences in Lublin, Poland,
Doświadczalna 44, 20-280 Lublin, tel. 48 81 461 00 61, e-mail: elzbieta.kusinska@up.lublin.pl

Received May 9.2013; accepted June 14.2013

Summary. The processes of food processing are an important research instrument. The paper presents the results of study of force and work of cutting of sponge-fatty cake with the addition of oatmeal. The variable parameters in the experiment were the amount of oat flakes added (0, 5, 10, 15%), and knife wedge angle (2.5°, 7.5°, 12.5° and 17.5°). Additionally, sensory assessment was performed for the purpose of selection of the desired amount of oat flakes addition. Statistical analysis of the results showed a significant correlation of force and work of cutting on the amount of the additive and knife wedge angle. The cutting quality is affected by: the amount of the flakes additive and knife geometry. The most preferred energy and quality is achieved at the knife angle 2.5° and 7.5°, and the most unsuitable angle is 12.5° and 17.5°. The greatest force and the work occurred during the cutting of sponge-fatty cake with the addition of oatmeal in the amount of 15%, while the smallest – without the additive. The best cutting quality was obtained using the additive flakes in an amount not exceeding 10% of the knife with an angle of 2.5° and exacerbation of 7.5°.

Key words: cutting, sponge-fatty cake, oat flakes.

INTRODUCTION

Agrifood industry, which includes the production of bakery and confectionery as well biscuit making is a very important branch of the Polish industry, as food items and beverages account for about 17% of the Polish industrial production. One of the fastest growing sectors of the food industry's current production of confectionery [17].

When reaching for a cake we pay attention mainly to such characteristics as flavor, calories, freshness, appearance and quality [2]. The state of confectionery is influenced by the ingredients that are included in the recipe. Currently, there is a tendency for consumers to search for products containing (in addition to basic, traditional use) additives generally recognized for taste and health benefits, enabling the creation of products with new properties [7, 14]. Such criteria are met by oatmeal. Oats has as well-balanced amount of protein and soluble fiber, carbohydrates and fats, vitamins and minerals. Inclusion of oats in the diet is beneficial for both healthy people and diabetics [5, 12].

Knowledge of the effects of additives on the quality of the final product is useful not only to producers for the production of ready-mix cakes, but also cake manufacturers, who in addition to the quality of the product (the desired hardness or brittleness) can reduce the unhealthy factors, reducing the amount of sugar or fatty products [1, 16].

In order to determine the quality of the baked matter, sensory evaluation is usually performed. It consists in determining the batch uniformity, appearance, taste and smell, as well as the structure of the cake [9].

Currently, instrumental texture evaluation methods of the tested products are popular, including mechanical methods. They allow determination of mechanical parameters of pastries. Knowledge of these properties is essential for the development of new products and evaluation of the quality of finished products [4].

Fast development of production techniques in the confectionery industry allowed for the mechanization of virtually all the stages of production, including the cutting of cakes. The research on work of cutting boils down largely to the optimization of blade design features and parameters of the grinding process [3]. Cutting is the direct impact of the active material of the cutting tool on the cut material. The movement of the knife may be perpendicular or parallel to the cutting edge. Knives of different shapes are used for shredding the products. The most common are three types of knives: knives with a flat blade, with a straight continuous one, flat knives with a comb blade and knives with a scoop-shaped blade. The highest prevalence was found of flat knives with a blade angle [6, 13, 10, 11].

The cutting tests on confectionery products aimed at reducing the workload and a high efficiency of the cutting process while maintaining a good quality of cakes. However,

the efficiency of the grinding process is affected not only by the geometric features of cutting elements, but also the structure of the material to be shredded, which results in the quality of the portion dough [8].

OBJECTIVE AND SCOPE OF RESEARCH

The scope of the study comprised the development of the recipes and the baking of pastries, determination of the effect of the knife wedge angle on the force and work of the process of cutting cakes, and sensory assessment of the products, which allowed the selection of cakes of the highest quality and best cutting performance.

METHODS

The experimental material was four kinds of sponge-fatty cake obtained from wheat flour "Luksusowa" type 550 with 0, 5, 10 and 15% by the addition of instant oatmeal Melvit S.A. In each case, the weight of flour and oat flakes was 500 g, flakes were added in the natural entire form. Other dough ingredients were: 250 g of eggs, 350 g of sugar, 250 g of margarine Kasia, 200 g of 2% milk and 18 g of baking powder. The samples included cake with zero oatmeal. Baking pans were lined with the prepared cakes. The thickness of the dough was 50 ± 2 mm. Cakes were baked for 60 minutes at 160°C. Five cakes were made of each sample with oat addition. When the pastries cooled down, they were sealed in polyethylene bags and kept in a refrigerator at temperature of 6°C.

The cutting process was performed, which was conducted on texture analyzer type TA.XT. plus cooperating with the computer. In the study knives were used with the shapes of 2.5°, 7.5°, 12.5° and 17.5° angle. Approach angle, defined as the angle between a plane perpendicular to the direction of movement and the cutting edge of the knife was 0°. Speed during cutting was constant at 50 mm·min^{-1}. Laboratory tests were carried out in thirty repetitions on slices of cakes length 50 mm, width 40 mm and thickness of 20 mm (for each knife and for all types of cakes). The results of the measurement were in the form of graphs representing the relation between the cutting force and knife displacement, from which the values of the cutting force and work were determined (Fig. 1).

In the area A-B force increases from zero to a value that causes the compression of the material by the knife. In this area, the material is compacted at the threshold of the cutting process. At point C, there is a maximum cutting force, which gradually decreases to 0 (point D), which completes the process.

The cakes sensory assessment was conducted by the trained team of 10 people in accordance with the Polish Standard PN-A-74252 [15].

RESULTS

In order to investigate the effect of oatmeal addition on the process of cutting the sponge-fatty cake and its suitability for consumption, the force and cutting work for knives of various shapes were tested.

The results of measurements are presented in Fig. 2 and 3.

It was found out that the dough prepared with the addition of oatmeal was characterized by higher values of maximum force and work cutting than the dough without oats. The values of maximum force and work in case of the addition of flakes reached 15% and amounted to 5.05 N and 0.063 J (for knife wedge angle of 17.5°). And the lowest cutting force and work were recorded for the control, for the knife wedge angle of 2.5° – 2.58 N and 0.033 J.

The resulting standard deviations from the mean values of mechanical parameters (Fig. 2 and 3) indicate substantial

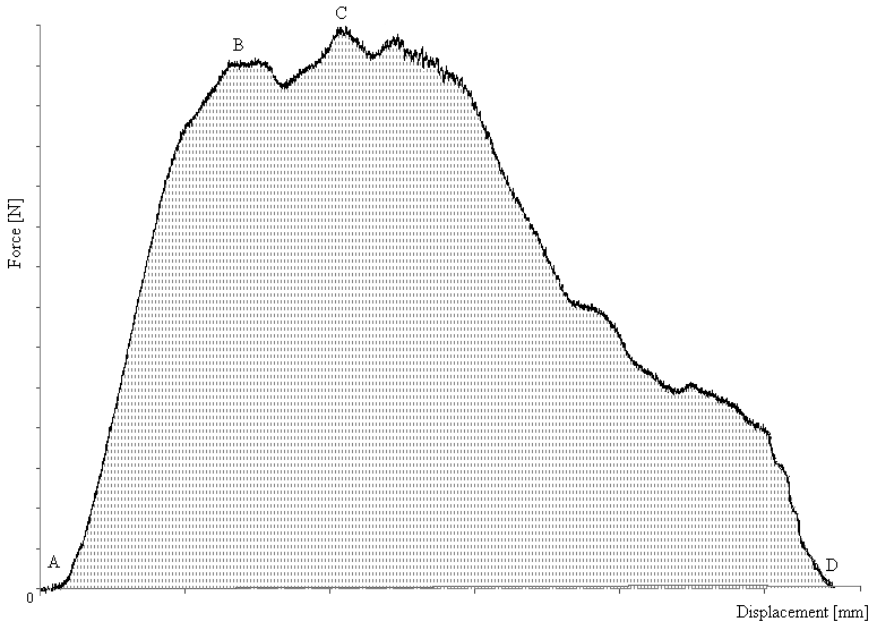

Fig. 1. Example of force-displacement relationship obtained during the cake cutting

heterogeneity of the tested products. They probably arise from their heterogeneous internal structure and surface after adding unminced oatmeal.

The relations presented in Figures 2 and 3 are described by equations (1) and (2):

$$F = 2{,}3057 + 0{,}0919k_z + 0{,}0766d, \quad (1)$$

$$R^2 = 0{,}883;\ \alpha \le 0{,}05,$$

$$W = 0{,}0291 + 1{,}09 \cdot d^2 \quad (2)$$

$$R^2 = 0{,}91;\ \alpha \le 0{,}05,$$

where:
F – cutting force [N],
W – cutting work [J],
k_z – knife wedge angle [deg],
d – addition of the oat flakes[%].

The results were subjected to two-way analysis of variance, which indicates that the cutting force has a significant impact (at the significance level $\alpha \le 0{,}05$) on the exacerbation of knife angle and the addition of oatmeal. Between research results there is a correlation between the independent variables at a high level. And the work of cutting is considerably affected by tightening the knife angle. The values of correlation coefficients calculated using a multiple regression analysis are shown in Table 1

Table 1. Correlation coefficients

Parameter	Knife wedge angle [deg]	Addition of the oat flakes [%]
Force [N]	0,916	0,885
Work [J]	0,772	-

During the testing of the impact of knife wedge angle and percentage content of oatmeal on the mechanical properties, attention should be paid to the behavior of crumb cake during the cutting process. For each type of knife and for different content of oatmeal the graph of force-displacement proceeds quite differently. The changes in graph's outline are shown in Figs. 4 and 5.

Observations carried out during the analysis of graphs can be summarized as follows: for all the studied pastry, the most appropriate wedge angle is that of 2.5° and 7.5°. For other knives with larger wedge angles the forces increase negatively.

During the cutting of crumb cake without the addition of oatmeal, we note a significant stress on the surface when the knife wedge going into the product, which causes a large deflection device and deformed end product. As a result, we get rough dough pieces with low quality.

For the added amount of 15%, the knife encounters the resistance of the material, which is due to an excessive amount of oatmeal. Cakes are damaged and mostly disrupted. The resulting pieces are baked at the intersection of the irregular structure and uneven thickness of the cut, causing losses in the material and reduced taste.

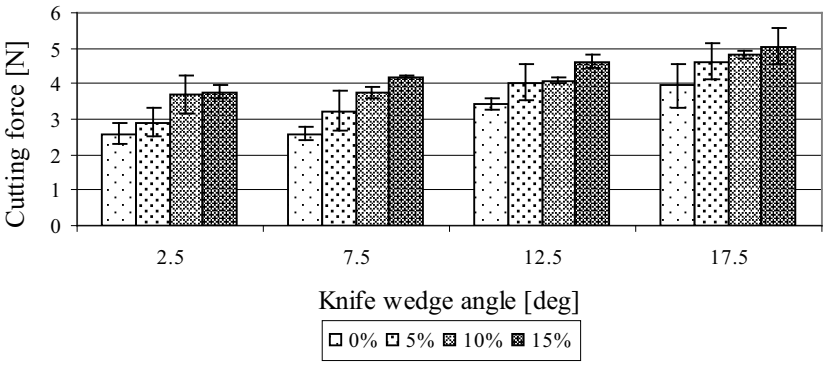

Fig. 2. Relation of cutting force of sponge-fatty cake with different addition of oatmeal to knife wedge angle

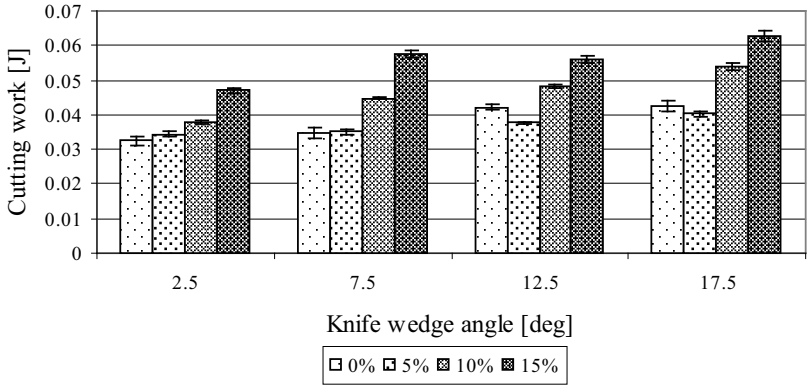

Fig. 3. Relation of cutting work of sponge-fatty cake with different addition of oatmeal to knife wedge angle

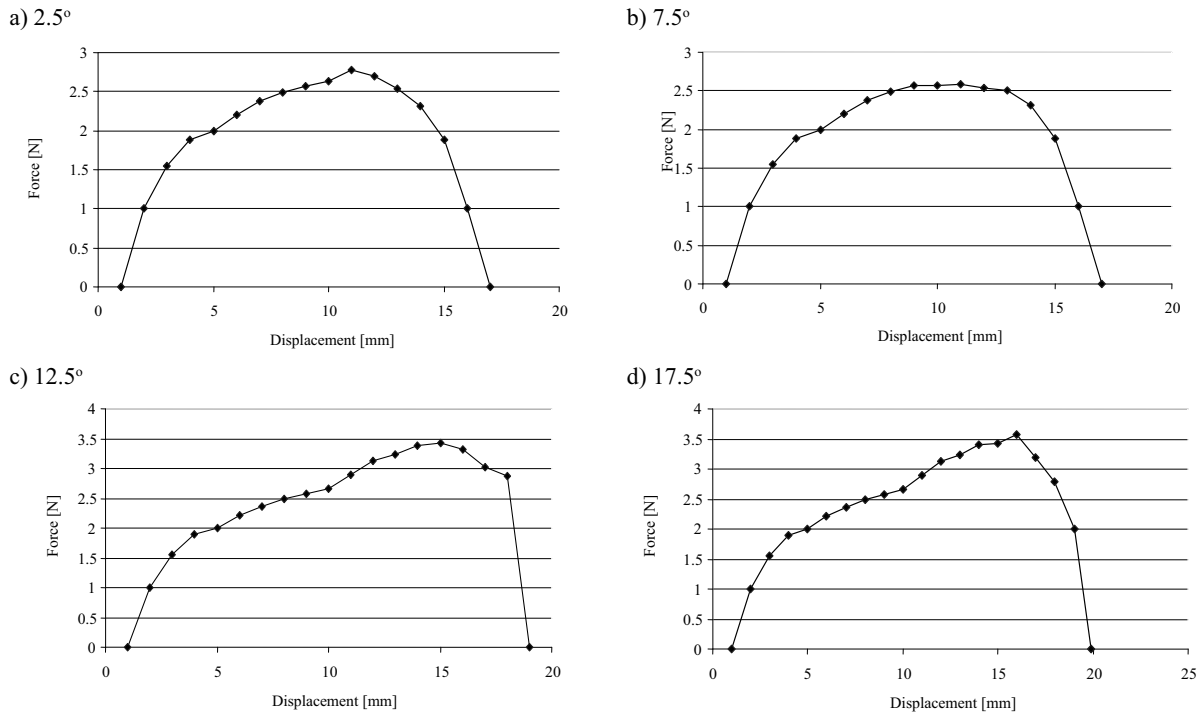

Fig. 4. Graphs proceedings of the force-displacement during the cutting of sponge-fatty cake with 0% addition of oatmeal for knives with wedge angle: a) 2.5°, b) 7.5°, c) 12.5°, d) 17.5°

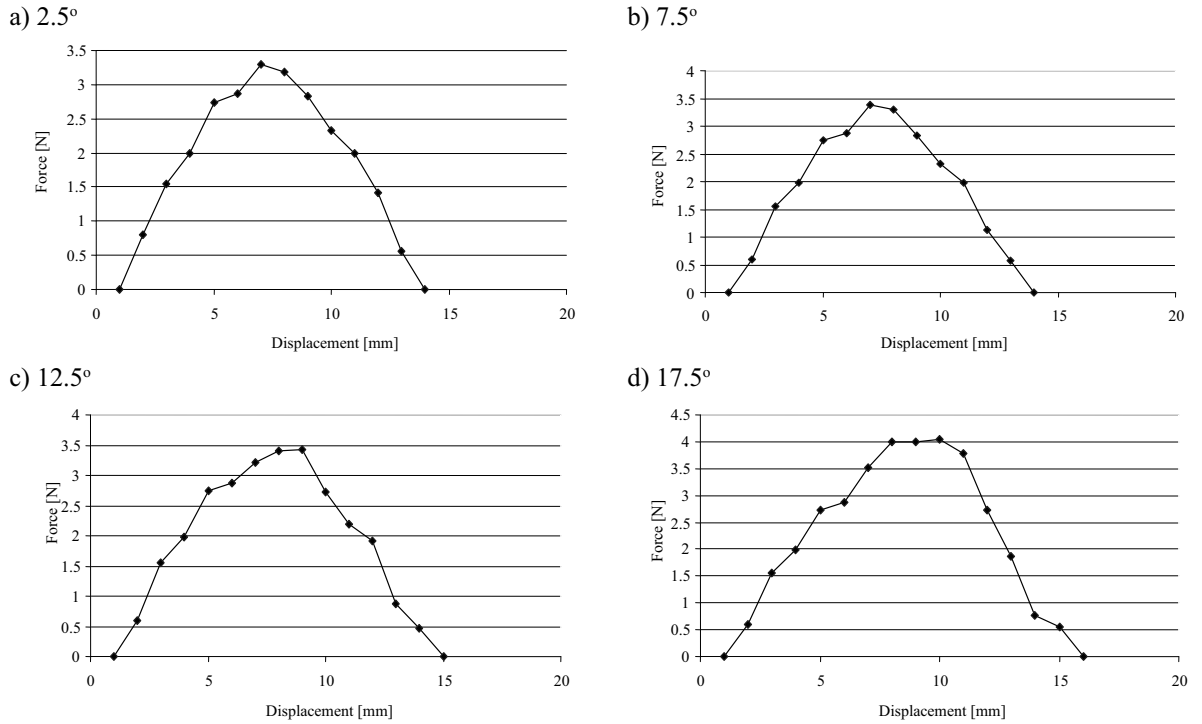

Fig. 5. Graphs proceedings of the force-displacement during cutting of sponge-fatty cake with 15% addition of oatmeal for knives with wedge angle: a) 2.5°, b) 7.5°, c) 12.5°, d) 17.5°

Depending on the course of the force for the addition of oatmeal at 5 and 10%, the displacement is steady and stable throughout the entire process of material distribution. Cakes are cut once and the area of intersection is fairly uniform. In this case, the dough pieces are precisely structured, have regular shape and the desired form stays without damage, as evidenced by organoleptic tests.

The results of sensory assessment of sponge-fatty cake carried out in accordance with PN-A-74252: 1998 indicate that the up to 10% addition of oatmeal to flour had a positive effect on the results of organoleptic assessment of cakes (very good flexibility and a mild taste and smell). Cakes made only from wheat flour also took the first level of quality (but they had slightly worse color of cover even with the

best taste and smell). However, the 15% share of oatmeal caused the baking quality deterioration (variations in shape, differences among the individual items).

CONCLUSIONS

1. With the increase in the knife wedge angle and addition of flakes, the force and work of cutting reach higher values.
2. The best quality of baked pieces is obtained using the additive flakes up to 10% for the knives with wedge angle of 2.5° and 7.5°.
3. The scoring shows that the best overall quality of the dough was achieved with the addition of flakes in the amount of 5 and 10%. It obtained 20 points out of the 20 possible and passed to the first class quality. Confectionery with the 15% share of flakes qualified to class II in accordance with the requirements.

REFERENCES

1. **Boobier W. J., Baker J. S. 2007**. Functional biscuits and coronary heart disease risk factors. British Food Journal, 3(109), 260-267.
2. **Borowy T., Kubiak M. 2010**. Tekstura wyróżnikiem jakości produktów piekarskich i cukierniczych. Cukiernictwo i Piekarstwo, 7-8(129), 33-36.
3. **Flizikowski J. 2006**. Globalny algorytm innowacji maszyn, Bydgoszcz, BTN-BKWoZ, ISBN 978-83-932977-0-2.
4. **Gibiński M., Gambuś H., Nowakowski K., Mickowska B., Pastuszka D., Augustyn G., Sabat R. 2010**. Wykorzystanie mąki owsianej – produktu ubocznego przy produkcji koncentratu z owsa – w piekarstwie. Żywność. Nauka. Technologia. Jakość, 3 (70), 56-75.
5. **Kobus Z., Guz T., Kusińska E., Nadulski R. 2011**. Influence of moisture and vertical pressure on airflow resistance through oat grain. Agricultural Engineering, 7(132), 29-35.
6. **Kowalik K., Sykut B., Marczak H., Opielak M. 2013**. A method of evaluating energy consumption of the cutting process based on the example of hard cheese. Eksploatacja i Niezawodność – Maintenance and Reliability, 15 (3), 241-244.
7. **Kowalski S., Lukasiewicz M., Juszczak L., Sikora M. 2011**. Charakterystyka teksturalna i sensoryczna mas cukierniczych otrzymanych na bazie miodu naturalnego i wybranych hydrokoloidów polisacharydowych. Żywność. Nauka. Technologia. Jakość, 3(76), 40-52.
8. **Kusińska E., Starek A., 2011**. Właściwości mechaniczne tekstury ciasta biszkoptowo-tłuszczowego. Inżynieria Rolnicza, 5(130), 157-164.
9. **Marzec A. Kowalska H., Gąsowski W. 2010**. Właściwości mechaniczne ciastek biszkoptowych o zróżnicowanej porowatości. Acta Agrophysica, 16(2), 359-368.
10. **Matuszewski M., Styp-Rekowski M. 2009**. Mikrocechy geometryczne elementów rozdrabniających. Inżynieria i Aparatura Chemiczna, 48(2), 94-95.
11. **Nadulski R., Strzałkowska K., Skwarcz J. 2010**. Wpływ kąta zaostrzenia noża na przebieg cięcia wybranych warzyw korzeniowych. Inżynieria Rolnicza, 7(125), 161-166.
12. **Otles S., Cagindi O. 2006**. Cereal based functional foods and nutraceuticals, Acta Scientiarum Polonorum. Technologia Alimentaria, 5(1), 107-112.
13. **Panasiewicz M., Mazur J., Sobczak P., Zawiślak K. 2012**. The analysis of the influence of initial processing of oat caryopses on the course and energy consumption of the flaking process. TEKA Komisji Motoryzacji i Energetyki Rolnictwa, 12 (1), 195-199.
14. **Piispa E., Alho-Lehto P. 2004**. Oat products digestibility studies and their nutritional information. Proceedings 7th International Oat Conference, Agrifood Research Reports 51. Peltonen-Sainio P., Topi-Hulmi M. (eds.). Finland, MTT Agrifood Research, ISBN 951-729-879-X.
15. PN-A-74252. 1998. Wyroby i półprodukty ciastkarskie. Metody badań.
16. **Rydzak L., Andrejko D. 2011**. Effect of different variants of pretreatment of wheat grain on the particle size distribution of flour and bran. TEKA Komisji Motoryzacji i Energetyki Rolnictwa, 11c, 283-290.
17. **Tajner-Czopek A., Kita A. 2005**. Analiza żywności – jakość produktów spożywczych. Wrocław, Wyd. Akademii Rolniczej we Wrocławiu, ISBN 83-89189-63-1.

SIŁA I PRACA CIĘCIA CIASTA BISZKOPTOWO-TŁUSZCZOWEGO Z DODATKIEM PŁATKÓW OWSIANYCH

Streszczenie. W procesach technologicznych przetwarzania żywności istotne znaczenie mają badania instrumentalne. W pracy przedstawiono wyniki pomiaru siły i pracy cięcia ciasta biszkoptowo-tłuszczowego z dodatkiem płatków owsianych. Parametrami zmiennymi w doświadczeniu były: ilość dodanych płatków owsianych (0, 5, 10, 15%) oraz kąt zaostrzenia noża (2,5°; 7,5°; 12,5° i 17,5°). Dodatkowo wykonano ocenę sensoryczną, która pozwoliła na dobór pożądanej ilości płatków. Analiza statystyczna wyników wykazała istotną zależność wartości siły i pracy cięcia od ilości użytego dodatku i kąta zaostrzenia noża. Na jakość cięcia wpływają: ilość zastosowanego dodatku płatków oraz geometria ostrza. Najkorzystniejszym energetycznie jak i jakościowo kątem zaostrzenia noża jest kąt 2,5° i 7,5°, a najbardziej nieodpowiednim 12,5° i 17,5°. Największa siła i praca wymagane są podczas cięcia ciasta biszkoptowo-tłuszczowego z dodatkiem płatków owsianych w ilości 15%, a najmniejsza – bez dodatku. Najlepszą jakość cięcia otrzymano przy zastosowaniu dodatku płatków w ilości nie przekraczającej 10% dla noży o kącie zaostrzenia 2,5° i 7,5°.

Słowa kluczowe: cięcie, ciasto biszkoptowo-tłuszczowe, płatki owsiane.

TEKA. COMMISSION OF MOTORIZATION AND ENERGETICS IN AGRICULTURE – 2013, Vol. 13, No. 2, 41–48

The representation of actions in probabilistic networks

Andrzej Kusz, Piotr Maksym, Jacek Skwarcz, Jerzy Grudziński

Department of Technology Fundamentals, University of Life Sciences in Lublin, Poland

Received May 9.2013; accepted June 14.2013

Summary. The method of modelling the problem of the agricultural production process management was shown in the article. The approach which assumes the set structure of the action network was proposed on the present stage of conceptualization. The essential element is correlating the duration of the activity with conditions and production resources which are accessible at present in comparison with methods of management applied nowadays. The introduced conception of the management model construction was based on the technology of the Bayesian networks.
Key words: agricultural production, planning problem modelling, the support of decision processes, Bayesian networks.

INTRODUCTION

Probabilistic networks are a useful system of knowledge representation in the case when you should openly code the factor of uncertainty and reasoning in the non-deterministic categories of cause-effects relationships [8, 19, 21]. Thus, they are a useful tool of modelling the predictability of technical objects behaviour [2, 3] and the representation of reliability knowledge both in practical formulation [4, 10] and for the needs of theoretical analyses [1, 24].

The agricultural productive process is a batch process in which the return of expenditure comes only after the process finishes and the uncertainty is its integral component and that is why the probabilistic methods are used to its modelling [13, 14, 15]. Nets are the useful tool of decision making process modelling in case of heterogeneous and uncertain information sources which enable making the uncertainty smaller in the decision making process in integrated agricultural production process [9, 16] as well as in modelling the reliability of complex bio-agri-technical systems [11].

The problem of the management of complex networks of actions is another area of the use of Bayesian network. The methods of the management well-known as Critical Path Method (CPM) and Project Evaluation and Review Technique (PERT), available nowadays, consist in the development of time structure of the process as the network of the activities leading to the realization of the assumed aim taking into consideration the duration of every activity [7, 20, 23]. The sequence of activities, each of which is conditioned by the realization of the previous one, creates so-called critical path marking the longest time of the task realization. In the case of CPM method it is assumed that the time of the realization of individual activities which compose the modelled activity network is determined. In PERT method it is assumed that the duration of activities have the β- distribution and the average value of the time of its realization and variance assuming the knowledge of the shortest time (optimistic), the longest (pessimistic) as well as the most probable is assigned for each activity. Then, on the base of the average values of realization times of individual operations the critical path is determined like in CPM method. Approximating the sum of random variables creating the critical path of the normal distribution of average value and variance equal the sum of the average times of the realization and the sum of variance of activities creating the critical path, the probability of the task realization in the set time can be determined.

Resigning from the methods introduced above and taking the model based on the Bayesian network is the alternative approach to the problem of modelling the action network. The essential element of the proposed approach is the possibility of taking into consideration the dependence between the realization time of the given action and the conditions of its realization in the model as well as accessible production resources. The problem of modelling the order relationship and time analyses for the needs of planning and providing documentation of complex action networks is shown in the paper.

THE AIM OF THE PAPER

The way of conceptualization of the problem of action network modelling in the agricultural productive process in

the language of Bayesian network was shown in the paper. On the present stage of construction of conception model it has been assumed that the action network has a fixed structure while the times of the realization of individual activities in the realized task have the random character which depends on conditions and presently accessible production resources. The essential element of the developed methodology is the paradigm being in accordance with the postulates of knowledge engineering which assumes the possibility of the use of machine learning methods for building the action network and the possible scenarios of functioning are based on the reasoning methods typical of Bayesian network [22].

THE CONCEPTUALIZATION OF ACTION PLANNING PROBLEM

The conceptualization process of action networks planning was shown on the example of the productive process of winter wheat [17]. It was assumed that there were two plant positions for the crop and the structure of the machine park was set. In case of some operations this structure enables, the configuration of various executive arrangements (aggregates) which were categorized according to the unitary efficiency [12]. Next the temporal relations between activities were determined as well as the structure of the

Table 1. The list of activities and the way of their coding in the Bayesian network

No.	Activity – Knot In BN	Preceding activities	Following activities	T
1	N01_Start	Lack	N02_Plough skimming_P1_1	0
2	N02_ Plough skimming_P1_1	N01_Start	N03_ Harrowing_P2_1 N04_ Harrowing_P1_1	15
3	N03_ Plough skimming_P2_1	N02_ Plough skimming_P1_1	N05_ Harrowing_P2_1	10
4	N04_ Harrowing_P1_1	N02_ Plough skimming_P1_1	N05_ Harrowing_P2_1 N06_ Pre-sow ploughing_P1_1	10
5	N05_ Harrowing_P2_1	N03_ Plough skimming_P2_1 N04_ Harrowing_P1_1	N08_ Harrowing_P2_2	12
6	N06_ Pre-sow ploughing_P1_1	N04_ Harrowing_P1_1	N07_ Harrowing_P1_2	12
7	N07_ Harrowing_P1_2	N06_ Pre-sow ploughing_P1_1 N08_ Harrowing_P2_2	N09_ NPK fertilizer sowing _P1_1	16
8	N08_ Harrowing_P2_2	N05_ Harrowing_P2_1	N07_ Harrowing_P1_2 N11_ PK fertilizer sowing _P2_1	10
9	N09_ NPK fertilizer sowing_P1_1	N07_ Harrowing_P1_2	N10_ Soil loosening and levelling-cultivation unit_P1_1	16
10	N10_ Soil loosening and levelling-cultivation unit_P1_1	N09_ NPK fertilizer sowing_P1_1	N14_ Seed sowing_P1_1	8
11	N11_PK fertilizer sowing_P2_1	N08_ Harrowing_P2_2	N12_ Winter ploughing_P2_1	16
12	N12_ Winter ploughing_P2_1	N11_ PK fertilizer sowing_P2_1	N13_ Harrowing_P2_3	23
13	N13_ Harrowing_P2_3	N12_ Winter ploughing_P2_1	N16_ N fertilizer sowing _P2_1	16
14	N14_ Seed sowing_P1_1	N10_ Soil loosening and levelling-cultivation unit_P1_1	N15_ N fertilizer sowing _P1_1	8
15	N15_ N fertilizer sowing_P1_1	N14_ Seed sowing_P1_1	N16_ N fertilizer sowing _P2_1 N17_ Cultivation harrowing_P1_1	16
16	N16_ N fertilizer sowing _P2_1	N13_ Harrowing_P2_3 N15_ N fertilizer sowing _P1_1	N18_ Soil loosening and levelling-cultivation unit_P2_1	8
17	N17_ Cultivation harrowing_P1_1	N15_ N fertilizer sowing _P1_1	N20_ Herbicide spraying_P1_1	9
18	N18_Soil loosening and levelling-cultivation unit_P2_1	N16_ N fertilizer sowing_P2_1	N19_ Seed sowing_P2_1	8
19	N19_ Seed sowing_P2_1	N18_ Soil loosening and levelling-cultivation unit_P2_1	N21_ Herbicide spraying_P2_1	8
20	N20_ Herbicide spraying_P1_1	N17_ Cultivation harrowing_P1_1	N21_ Herbicide spraying_P2_1 N22_ N fertilizer sowing _P1_2	7
21	N21_ Herbicide spraying_P2_1	N19_ Seed sowing_P2_1 N20_ Herbicide spraying_P1_1	N23_ N fertilizer sowing _P2_2	22
22	N22_ N fertilizer sowing _P1_2	N20_ Herbicide spraying_P1_1	N23_ N fertilizer sowing _P2_2 N24_ Seed harvest_P1_1	10
23	N23_ N fertilizer sowing _P2_2	N21_ Herbicide spraying_P2_1 N22_ N fertilizer sowing _P1_2	N26_ Seed harvest_P2_1	10
24	N24_ Seed harvest_P1_1	N22_ N fertilizer sowing _P1_2	N25_ Straw harvest_P1_1	14
25	N25_ Straw harvest_P1_1	N24_ Seed harvest_P1_1	N28_ Finish	14
26	N26_ Seed harvest_P2_1	N23_ N fertilizer sowing _P2_2	N27_ Straw harvest_P2_1	14
27	N27_ Straw harvest_P2_1	N26_ Seed harvest_P2_1	N28_ Finish	14
28	N28_ Finish	N25_ Straw harvest_P1_1 N27_ Straw harvest_P2_1	Lack	

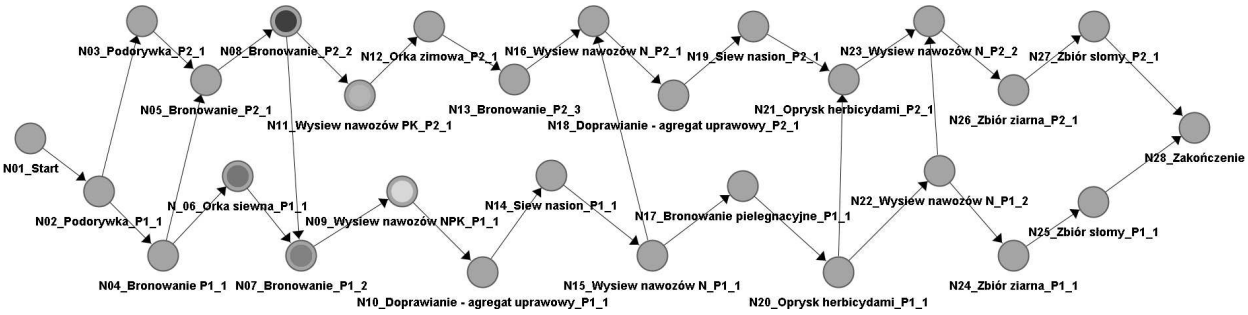

Fig. 1. The net representing the time structure of the modelled process

network assuming the deterministic structure of the productive task and the times of individual operations were determined. The obtained data were shown in Table 1. All activities composing the analysed productive task, the way of coding the activities in the Bayesian network, activities preceding given activity and the ones directly following it were shown in this table.

The graphic representation of the time structure of the modelled production process in the environment of the Bayesian network was shown in Fig. 1.

In this perspective the network knot represents the activity and directed bows describe temporal relations between activities. The basic difference between the conceptualization of the planning problem in the environment of the Microsoft Project and in networks is that Bayesian network knots representing individual operations are treated as complex objects (the network modules) having attributes represented by knots composing the elementary module. The graphic form of this conceptualization as well as the model of the single activity in Bayesian network were shown in Fig.2 [5].

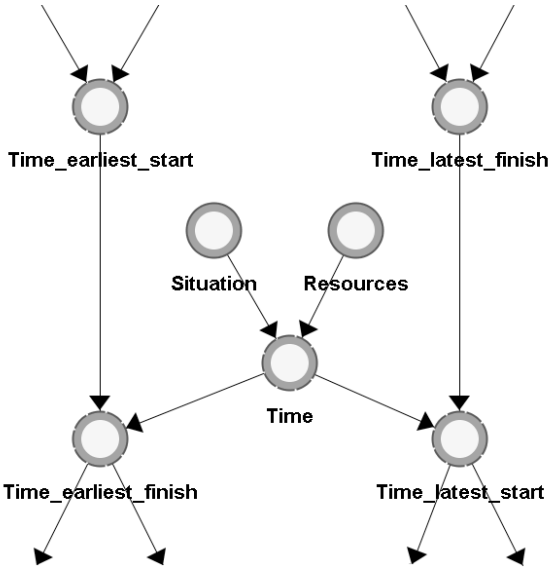

Fig. 2. The model of activities in Bayesian network

In this model the following notions were introduced – the earliest possible date of the beginning of the activity action T_{es}, the action duration T, the earliest possible date of the end the action T_{ef}, the latest date when the action has to finish T_{lf}, the latest date when the action has to start, resources R and the conditions of realization of activity S.

The knots corresponding to the notions shown above are at same time the knots of the Bayesian network representing discreet (R, S) or continuous (the remaining knots) random variables corresponding to the possible substantiation of notional models.

The network knots representing respectively the earliest possible date of the beginning of any activity (T_{es}) and the earliest possible date of the end of any activity (T_{ef}) are continuous random variables of the assigned distribution. For any activity j the values of these variables are calculated from the expression:

$$\forall_j Tes_j = \max_{i=1,2,\ldots n(j)} (Tef_i) = \max_{i=1,2,\ldots n(j)} (Tes_i + T_i),$$

$$Tef_j = (Tes_j + T_j),$$

Where:
T_{esj} – the earliest possible date of the beginning of activity j,
T_{efj} – the earliest possible date of the end of activity j,
T_{efi} – the earliest possible date of the end of activity i,
T_{esi} – the earliest possible date of the beginning of activity i,
T_j – duration of activity j,
T_i – duration of activity i,
i = 1,2 , n(j) – the set of activities immediately preceding activity j in the action network

In case of variables representing the latest dates of finishing (T_{lf}) and beginning (T_{ls}) their values for activity *i* are assigned according to expression:

$$\forall_i Tlf_i = \min_{j=1,2,\ldots m(i)} (Tls_j) = \min_{j=1,2,\ldots m(i)} (Tlf_j - T_j),$$

$$Tls_i = (Tlf_i - T_i),$$

Where:
T_{lfi} – the latest date of the end of activity i,
T_{lsj} – the latest date of the beginning of activity j,
T_{lfj} – the latest date of the end of activity j,
T_{lsi} – the latest date of the beginning of activity i,
T_i – the duration of activity i,
T_j – the duration of activity j,
j = 1, 2, n(i) – the set of activities being the consequents of the activity i in the action network.

The notion resources corresponds to Bayesian network knot representing discreet random variable R which values correspond to specific executive arrangements (aggregates). These arrangements are categorized according to unitary efficiency while the notion conditions of the realization of

the action corresponds to the network knot representing variable S which can take two values: the favourable conditions and the unfavourable conditions.

The notion activity duration corresponds to the knot of Bayesian network which represents continuous random variable of the log normal distribution. It was assumed that the parameters of this distribution were dependent on two variables: resources (Ra) and conditions (S). The principle was accepted that resources compensate the conditions, according to which the larger the resources (the efficiency of the aggregate) the lower the variance regardless of conditions (variable S) and vice versa. The average duration of the activity from T_{min} – maximum resources and favourable conditions to T_{max} – low resources and unfavourable conditions were also determined.

The topology of the Bayesian network the sub-network consisting of five modules representing activity 6 (pre-sow ploughing, field 1), 7 (harrowing, field 1), 8 (harrowing, field 2), 9 (NPK fertilizer sowing, field 1) and 11 (NPK fertilizer sowing, field 2) was shown in Fig. 3.

The typical mechanism of network functioning (the prediction of the decision results) is shown in Fig.4. In case A it is shown how the schedule of the probability changes over the set of the variable value. The earliest possible date of the end of the activity 08 T_{ef_08} (harrowing, field 2) in case when the time of the beginning of the activity (variable T_{es_08}) is known to an accuracy of probability distribution (the case A), or the value of this time is known (case B and C) and the activity is carried out with the use of the resources R1 in favourable (B) or unfavourable (C) conditions. The distribution of given activity duration was also shown in this picture. In case when the variable is known to an accuracy of probability distribution (soft evidence) our knowledge about terminal variable is blurred. For example (case A) the forecast earliest possible date of the end of the activity takes values: 43 with the probability of 0.25, 46.5 with probability of 0.55 and larger than 46.5 with the probability of 0.20. If the known time of the beginning of activity (hard evidence), e.g. T_{es_08}=33 (case B and C) the schedule of probability over the set of variable value T_{ef_08} undergoes sharpening and this variable can take two values – 43 with the probability of 0.66 and 46.5 with the probability of 0.34 if conditions are favourable and respectively 46.5 with the probability of 0.80 or large value with the probability of 0.20.

The mechanism of the diagnostic inference (the temporal projection backwards) accessible in network is useful in the situation when we want to determine conditions which have to be fulfilled to finish the task in the planned time and with the assumed level of the probability. The principles of applying this mode of inference were shown in Fig.5.

In all analysed examples it has been assumed that action 08 has to be finished in time 39.5 (i.e. it was assumed that variable T_{ef_08}= 39.5) with the probability of 0.61 and it has been assumed that the earliest possible date of the beginning of the activity 08 is known and equals 33 units (variable T_{es_08}= 33). In case A and B, we assume that we know the values of variable S (conditions), which takes the favourable values (case A) and unfavourable values (case B) and we ask about resources which should be used to realize the activities. The results of calculations show that in case of favourable conditions there is a chance of the prompt realization of the task even while using the resources of the lowest efficiency (R1) but with the probability of 0.14. In case of resources R2 this probability is much bigger and equals 0.37. Having resources R3, however we will carry out the task according to the plan with the probability of 0.49. However if conditions are unfavourable (the case B) the chances of meeting the deadline of the task realization exist only in the situation when we have resources R3 (the probability of 0.83) whereas practically it is not possible to fulfil the task having the resources R1 (the

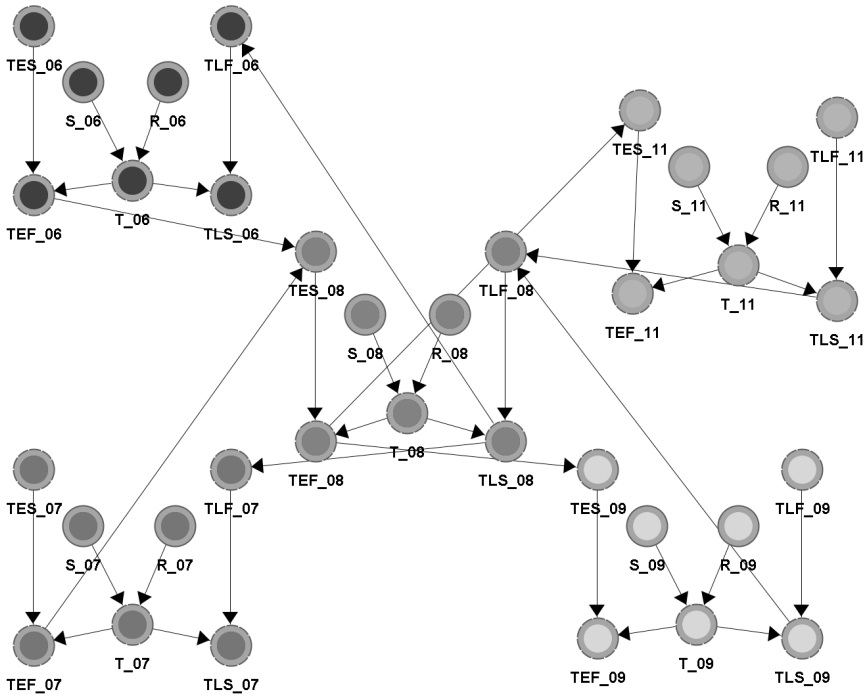

Fig. 3. The topology of the network representing chosen activities

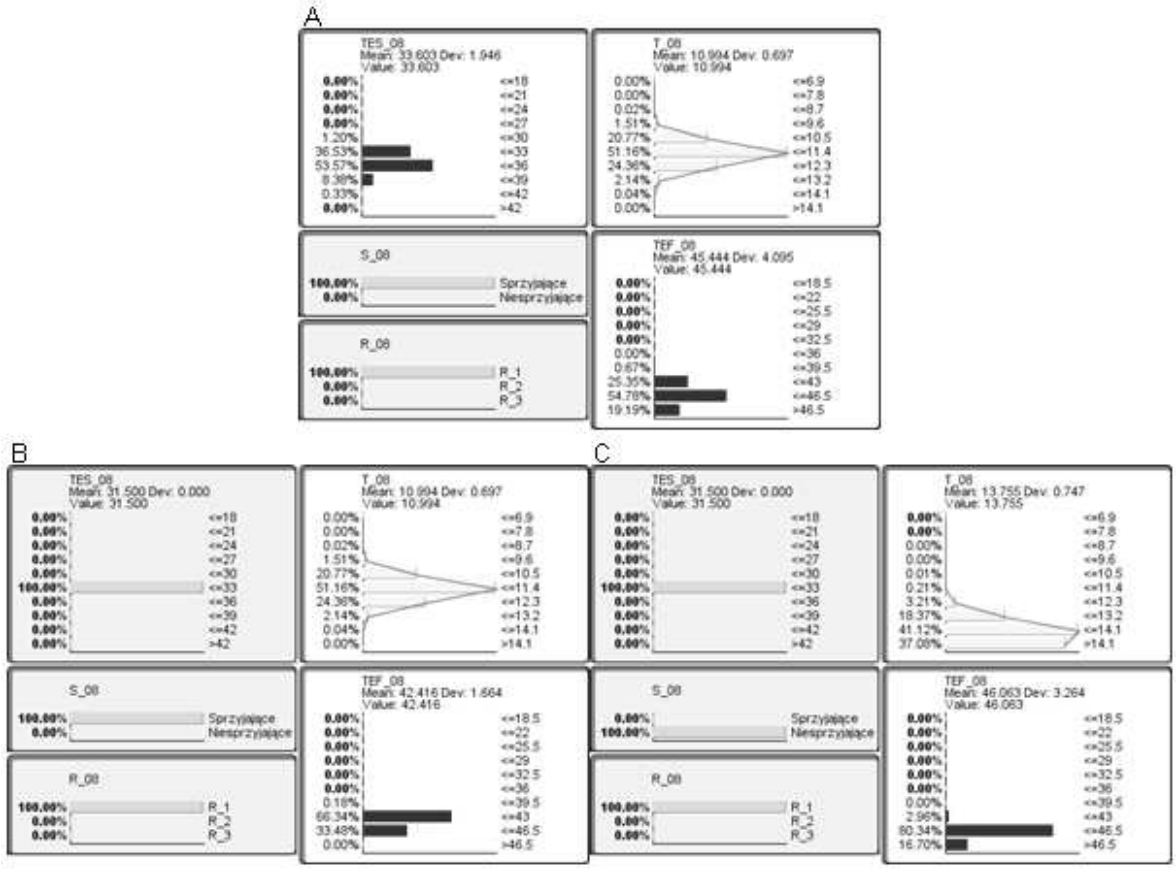

Fig. 4. Inference about the latest possible date of the end of the activity

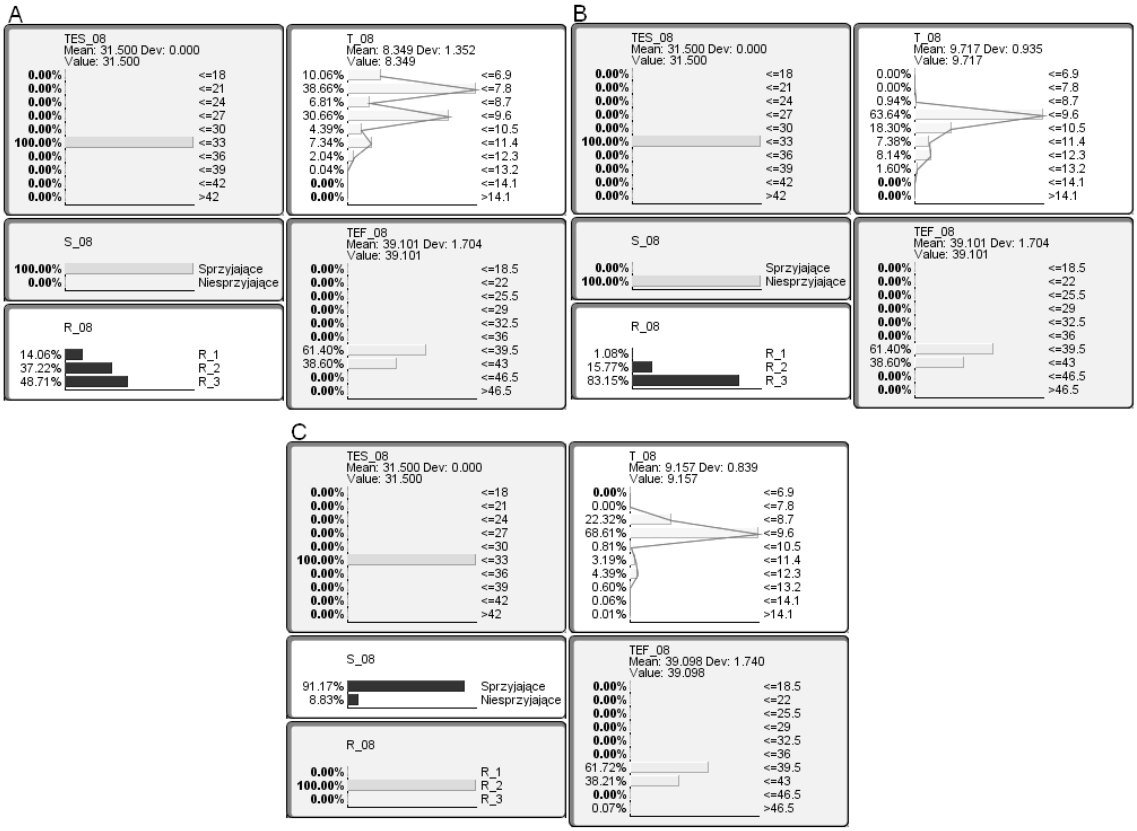

Fig. 5. Inference in case of the planned deadline with fixed probability

probability of 0.01). The possession of the resources R2 gives us little chance of meeting the deadline (probability 0.16).

In Fig. 5 C the situation which assumes that we have only one kind of the resources R2was shown. In this situation the planned realization of the task will be possible if the conditions of realizations are favourable (the probability of 0.91). However if unfavourable conditions occur there is little chance for meeting the deadline for activity realization which equals 0.09.

The scenarios of model functioning shown above can be analogically used for fixing the latest possible dates when the given activity has to start or finish. The information which is possible to obtain as the result of the model functioning has practical value and can be used to manage the action networks.

CONCLUSION

The introduced method of modelling the decision problems which is applied to the management of action networks can be a useful tool supporting the decision making process in case of planning and managing the agricultural production.

The introduced module representing the single activity which uses Bayesian networks enables conceptualization, specification and the analysis of the complex action networks in non-deterministic conditions.

The easiness of any shaping of given activity duration depending on accessible resources and conditions of activity realization causes that planned modelling method of complex action networks can have great practical significance on designing, monitoring and analysis stages in case of some threats and as well as on the stage of providing documentation of real action networks.

Built–in mechanisms of automatic inference enable simulation testing of possible situational variants, which is especially important at the stage of realization of complex actions in case of different threats which make it impossible to keep to a schedule. What is more, the learning mechanisms [6] ensure the easiness of model adaptation to changing conditions of its functioning on the base of empirical data.

The essential element of further model modification is the extension of principles of resources availability taking into consideration the costs connected with the realization of given activities.

REFERENCES

1. **Barlow RE. 1988**. Using influence diagrams. In: Clarotti CA, Lindley DV, editors. Accelerated life testing and experts' opinions in reliability. 145–57.
2. **Bartnik G., Kalbarczyk G. and Marciniak A. W. 2011**. Application of the operational reliability model to the risk analysis in medical device production. TEKA Vol. XIC, 2011, ISSN 1641-7739. 366-370.
3. **Bartnik G., Kusz A. and Marciniak A. 2006**. Dynamiczne sieci bayesowskie w modelowaniu procesu eksploatacji obiektów technicznych. Inżynieria Wiedzy i Systemy Ekspertowe, t. II, Oficyna Wydawnicza Politechniki Wrocławskiej. 201-208.
4. **Bartnik G. and Marciniak A. W. 2011**. Operational reliability model of the production Line. TEKA Vol. XIC. ISSN 1641-7739. 361-365.
5. Dokumentacja programu BayesiaLab. [dostęp 10.06.2012]. Dostępny w internecie http://www.bayesia .com
6. **Doguc O. and Ramirez-Marquez J.E. 2009**. A generic method for estimating system reliability using Bayesian networks. Reliability Engineering and System Safety, 94. 542-550.
7. **Fabrycky W.J., Ghare P.M. and Torgersen P.E. 1972**. Industrial Operations Research, Prentice-Hall, Imc., Englewood Cliffs, New Jersey.
8. **Halpern J., Y. 2005**. Reasoning about uncertainty. The MIT Press Cambridge, Massachusetts, London.
9. **Hołaj H., Kusz A., Maksym P. and Marciniak A. W. 2011**. Modelowanie problemów decyzyjnych w integrowanym systemie produkcji rolniczej. Inżynieria Rolnicza. Nr 6 (131). 53-60
10. **Kusz A., Maksym P. and Marciniak A. W. 2011**. Bayesian networks as knowledge representation system in domain of reliability engineering, TEKA Vol. XIC, ISSN 1641-7739. 173-180.
11. **Kusz A. and Marciniak A.W. 2010**. Modelowanie niezawodności złożonych systemów bioagrotechnicznych Inżynieria Rolnicza, z. 5 (114). 147-154.
12. **Lorencowicz E. 2007**. Poradnik użytkownika techniki rolniczej w tabelach. Agencja Promocji Rolnictwa i Agrobiznesu, Bydgoszcz.
13. **Maksym P., Marciniak A. W. and Kostecki R. 2006**. Zastosowanie sieci bayesowskich do modelowania rolniczego procesu produkcyjnego. Inżynieria Rolnicza. Nr 12 (87). 321-330.
14. **Maksym P., Marciniak A. W. and Kusz A. 2011**. Modelowanie syntezy działań ochronnych w rolniczym procesie produkcyjnym. Inżynieria Rolnicza. Nr 4 (129). 213-220
15. **Marciniak A. 2005**. Projektowanie systemu reprezentacji wiedzy o rolniczym procesie produkcyjnym. Rozprawy naukowe Akademii Rolniczej w Lublinie, Wydział Inżynierii Produkcji, zeszyt 298.
16. **Marciniak A., Maksym P.**: Model wspomagania działań interwencyjnych w
17. **Mrówczyński M. Korbas M., Szczepaniak W. and Paradowski A. 2011**. Zeszyt Technologiczny. Pszenica ozima, jęczmień jary 2011. Agrosan. s. 17-19, 42-43, 49-52
18. **Murphy K. P. Dynamic Bayesian Networks. 2002**. http://www.ai.mit.edu/~murphyk.
19. **Oniśko A., Marek J. Druzdzel M. J. and Wasyluk H. 2001**. Learning Bayesian network parameters from small data sets: Application of noisy-or gates. International Journal of Approximate Reasoning, 27(2). 165–182.
20. **Naiden N.V.R., Babu K.M., and Rajenda G. 2007**. Operations Research. I.K. International Publishing House. Put Ltd.
21. **Pearl J. 1986**. Fusion, Propagation, and Structuring in Belief Networks. Artificial Intelligence 29(3), 241-288.
22. **Pearl J. 1988**. Probabilistic Reasoning in Intelligent Systems: Network of Plausible Inference. Morgan Kaufmann.
23. **Ponneerselvan R. 2006**. Operations Research. Prentice-Hall of India, new Delhi.

24. **Tchangani A.P. 2001**. Reliability analysis using Bayesian networks. Stud. Inform. Control 2001;10(3).181–188.

REPREZENTACJA DZIAŁAŃ W SIECIACH PROBABILISTYCZNYCH

Streszczenie. W artykule przedstawiono metodę modelowania problemu zarządzania rolniczym procesem produkcyjnym. Na obecnym etapie konceptualizacji zaproponowano podejście, które zakłada zadaną strukturę sieci zadań. Istotnym elementem, w porównaniu do obecnie stosowanych metod zarządzania jest skorelowanie czasu trwania czynności od warunków i aktualnie dostępnych zasobów produkcyjnych. Przedstawioną koncepcję budowy modelu zarządzania oparto na technologii sieci bayesowskich.

Słowa kluczowe: produkcja rolnicza, modelowanie problemu planowania, wspomaganie procesów decyzyjnych, sieci bayesowskie.

TEKA. COMMISSION OF MOTORIZATION AND ENERGETICS IN AGRICULTURE – 2013, Vol. 13, No. 2, 49–52

The simplified method of determining internal volume of bean pods

Piotr Kuźniar

Department of Engineering in Agricultural Food Production, University of Rzeszów, Zelwerowicza 4, 35-601 Rzeszów, Poland, e-mail: pkuzniar@univ.rzeszow.pl

Received June 25.2013; accepted June 28.2013

Summary. The study includes the results of research on developing a simplified method of determining air volume inside a pod. The research has been performed on bean pods cultivated for dry seeds of the varieties Narew, Nida, Warta and Wawelska. Ten methods of determining volume have been compared (pycnometric and nine simple models of a pod).

The volumes determined by the method 1 (pycnometer) and method 7 were the most approximate and they were not statistically significant between themselves. It may be stated that the proposed simple model of a pod measurement makes it easier to determine the air volume inside the pod.

Key words: bean pod, volume, measurement methods.

INTRODUCTION

In cultivation of leguminous plants, a significant problem is i.a. susceptibility to cracking their pods and falling seeds. Susceptibility to cracking bean pods is shown by falling seeds during harvesting as a result of action of the working sets of harvesting machines, mainly various devices of cutting and trimming plants, gatherers and landing nets [5, 9]. The tendency of pods to burst open is conditioned by the content and structure of fibre in pod walls and their seams, which is a variety-related feature and depends on meteorological conditions during vegetation [3, 6, 8, 10, 14, 17].

In order to test the influence of various determinants on the susceptibility to cracking fruits of this plant, it is necessary to develop a method allowing its precise measurement. One of the methods of the susceptibility of pods to cracking is a pressure method [16]. It relies on forcing, to the inside of the pod, by means of the injection needle, of compressed air and measurement of the pressure at which there is breaking of its stitches. The measurement of the susceptibility of pods to cracking is the calculation of energy of bean pod opening [12, 13], for which the knowledge of not only the cracking pressure (relatively easy to be measured) is required, but also of the air volume in the pod. The second factor, due to an irregular shape of this kind of fruit, relies on the difficul measurement. Strobel [2003] defines the volume of air in a pod is as a difference of approximate volume and the volume of its seed. The approximate volume of a pod is calculated as the volume of a cylinder with the height equal to its length and diameter being arithmetic mean of pod width and thickness in its medium part.

Precise volumes of bodies with irregular shapes may be determined by a pycnometer, however, it is time consuming and requires relatively great work effort arising from the necessity of performing measurements for the entire pod and then for seeds and shells.

The aim of the work was an attempt to develop simplified methods of developing air volume inside bean pods.

MATERIAL AND METHODS

The research was carried out in 2008-2010. The bean was cultivated in the experimental field of the Department of Engineering in Agricultural Food Production in Rzeszów. The research was conducted on pods of bean cultivated on dry seeds of varieties: Narew, Nida, Warta and Wawelska which were characterized by varied seed and pod size (Tab. 1). Pod dimensions were calculated using an electronic slide calliper with the accuracy of 0.01 mm. Length was measured from the beginning of stalk to the peak, and width and thickness in cutting plane of perpendicular to main axis of the fruit, leading through its centre.

Table 1. Pod characteristics (average values) of the tested bean varieties

Specification	Narew	Nida	Warta	Wawelska
Dimension of pods [mm]:				
Length	93,2 a	91,1 a	105,9 b	113,8 c
Width	10,1 b	10,2 b	9,8 a	10,9 c
Thickness	9,4 c	9,1 b	8,8 a	9,6 c
Number of seeds in pod	4,7 d	4,1 b	4,4 c	3,8 a

* different letters in line signify significant differences, as per LSD test (significance level of $\alpha = 0.05$)

The measurement of breaking pods was performed with the pressure method relying on forcing compressed air to a pod and measurement of pressure at the moment of breaking along stitches. The obtained value is the energy of bean pod opening. Thus the energy required to open a pod was calculated with the pressure method [11, 13, 16], which is based on tearing a pod by compressed air, from the relation:

$$E = \frac{3}{2} pV, \tag{1}$$

where:
E – energy of bean pods opening [J],
p – air pressure in the pod [Pa],
V – air volume inside the pod [m^3].

There has been a comparison of exact determination of air volume inside a pod by a pycnometeric method [2] and nine simplified methods (simple models of a pod). In the method 1, air volume in a pod was determined as a difference of total volume of a pod and volume of seeds inside and volume of its shells determined by a pycnometric method according to the formula:

$$V_a = V_p - V_s - V_c, \tag{2}$$

where:
V_a – volume of the air in a pod,
V_p – volume of pod,
V_s – volume of seeds in a pod,
V_c – volume of pod coats.

In order to avoid moistening the pods, which would influence the values of pressure needed for their opening, water has been replaced with the powder ''Dry Flo". This method allows for exact determination of pressure volume inside the pod, and at the same time determining the energy needed for its opening. It allows for proper differentiation of bean varieties due to the susceptibility of their pods to breaking and more exactly defining an influence of various factors on this property of pods. This manner of determining volume is very time and labour consuming. The obtained exact values of internal volume of pods filled by air were applied in developing a simple model of a pod, which allows determining air volume in a pod, and at the same time, defining the energy needed for its opening.

In the method 2, the volume of a pod is calculated as the volume of a cylinder with a height equal to its length and diameter being an arithmetic mean of pod width and thickness in its medium part:

$$V_{a2} = V_{cy} = 0{,}25\,\pi \cdot W \cdot T \cdot L, \tag{3}$$

where:
V_{a2} – volume of the air in a pod,
V_{cy} – volume of the cylinder,
W – width of the pod,
T – thickness of the pod,
L – length of the pod.

In the methods 3-9, air volume in the pod was calculated as the volume of a body which is complex in the central part of a cylinder ended with two cones:

$$V_{a3\text{-}9} = 2V_{co} + V_{cy} = \pi \cdot W \cdot T\,(0{,}17H_{co} + 0{,}25H_{cy}), \tag{4}$$

where:
$V_{a3\text{-}9}$ – volume of the air in a pod,
V_{cy} – volume of the cylinder,
V_{co} – volume of the cone,
H_{cy} – height of the cylinder,
H_{co} – height of the cone,
W – width of the pod,
T – thickness of the pod.

The section of the cylinder and the base of cones constituted an ellipsis as in the method 2. In the method 10, air volume in a pod was calculated as the volume of the body made of two cones connected by bases with a shape of an ellipsis:

$$V_{a10} = 2V_{co} = 0{,}17\,\pi \cdot W \cdot T \cdot H_{co}, \tag{5}$$

where:
V_{a10} – volume of the air in a pod,
V_{co} – volume of the cone,
H_{co} – height of the cone,
W – width of the pod,
T – thickness of the pod.

The heights of a cylinder and cones for these methods 3-10 are included in Table 2.

Table 2. Height of the cylinder and cone in models of bean pods in the methods 3-10 (L – length of pod)

Method	Height of the cylinder H_{cy}	Height of the cone H_{co}
3	0,75 L	0,125 L
4	0,5 L	0,25 L
5	0,4 L	0,3 L
6	0,3 L	0,35 L
7	0,25 L	0,375 L
8	0,2 L	0,4 L
9	0,1 L	0,45 L
10	0	0,5 L

The obtained results were statistically analyzed [1, 4, 7, 15] with Statistica 9 program, including variance analysis and LSD significance test.

RESULTS

On the basis of the variance analysis, significant differentiation of air volume values inside the pod were confirmed for the applied methods of determination. For the tested varieties, air volume in bean pods was determined with the method 7:

$$V_{a7} = 0{,}125 \cdot \pi \cdot W \cdot T \cdot L. \quad (6)$$

that was the most approximate for the one determined precisely by means of the method 1 (pycnometric), which was confirmed by the test NIR indicating the lack of significant differences between the values of the described feature determined by these methods (Tab.3). The variety of Nida constituted an exception, for which the most approximate air volume determined by the pycnometric methods was the volume determined by the method 6:

$$V_{a6} = 0{,}133 \cdot \pi \cdot W \cdot T \cdot L. \quad (7)$$

Air volumes determined by the method 6 were higher and by the method 8 lower than the ones determined with methods 1 and 7, however, there were not statistically significant differences.

Table 3. The air volume [cm^3] in the pods of tested bean varieties for the applied of methods of their determination

Methods	Varieties				Average
	Narew	Nida	Warta	Wawelska	
1	3,35 cd I	3,49 c I	3,57 cd I	4,52 cd II	3,73 cd
2	6,93 h I II	6,68 g I	7,18 h II	9,36 h III	7,52 h
3	5,78 g I	5,51 f I	5,99 g I	7,80 g II	6,27 g
4	4,62 f I	4,41 e I	4,79 f I	6,24 f II	5,01 f
5	4,16 e I	3,97 d I	4,31 e I	5,61 e II	4,51 e
6	3,69 d I	3,52 c I	3,82 d I	4,98 d II	4,00 d
7	3,46 cd I	3,30 c I	3,59 cd I	4,68 cd II	3,76 cd
8	3,25c I	3,09 c I	3,36 c I	4,38 c II	3,52 c
9	2,77 b I	2,64 b I	2,87 b I	3,74 b II	3,01 b
10	2,31 a I	2,20 a I	2,39 a I	3,12 a II	2,51 a

*different letters in columns and Roman numerals in line signify significant differences, as per LSD test (significance level of $\alpha = 0.05$)

The conducted analysis by means of the test NIR (Tab. 3) indicated that due to the air volume in a bean pod determined by the method 1, the variety of Wawelska was statistically different from others. The same differentiation between the varieties was obtained by other methods, apart from the method 2, which additionally significantly differentiated the varieties of Nida and Warta.

To sum up, it must be confirmed that the method 7 allows, in a simplified manner, to determine the air volume in bean pods.

CONCLUSIONS

1. Air volume inside the pod significantly depended on the variety and the methods of determination.
2. The most approximate air volumes in the analysed pods of bean varieties to the ones determined precisely by the method 1 (pycnometric) was calculated by the method 7.
3. Air volumes determined by the method 6 were higher and by the method 8 lower than the ones determined with methods 1 and 7, however, there were not statistically significant differences.

REFERENCES

1. **Burski Z., Tarasińska J., Sadkević R. 2003**: The methodological aspects of using multifactoral analysis of variance in the examination of exploitation of engine sets. TEKA Komisji Motoryzacji i Energetyki Rolnictwa Polskiej Akademii Nauk Oddział w Lublinie, 3, 45-54
2. **Diehl K.C., Garwood V.A., Haugh C.G. 1988**: Volume measurement using the air-comparison pycnometer. Trans. ASAE, 1, 284-287.
3. **Dorna H., Duczmal K. W. 1994**: Influence of climatic conditions on the formation of the fibers in the seams of the bean pods *Phaseolus vulgaris L.* (in Polish). I Ogóln. Konf. Nak. Strączkowe Rośliny Białkowe. FASOLA, Lublin 25.11.1994, 135-138.
4. **Dziki D., Tomiło J., Różyło R., Laskowski J., Gawlik-Dziki U. 2012**: Influence of moisture content on the mechanical properties and grinding energy requirements of dried quince (Cydonia Oblonga Miller). TEKA Commission Of Motorization And Energetics In Agriculture, 12(2), 35-39.
5. **Furtak J., Zaliwski A. 1986**: Studies on the mechanical harvest of seeds (in Polish). Roczniki. Nauk Roln, ser. Technika Rolnicza, 2, 127-140.
6. **Hejnowicz Z. 1985**: Anatomy and vascular plants histogeneza (in Polish). PWN, Warszawa.
7. **Krzykowski A., Dziki D., Polak R., Rudy S. 2012**: Influence of heating plates temperature on freeze drying energy requirements and quality of dried vegetables. TEKA Commission Of Motorization And Energetics In Agriculture, 12(2), 129-132.
8. **Kuźniar P., Strobel W. 2000**: Determine the effect of thickness sclerenchyma bean pods on their susceptibility to cracking (in Polish). Acta Agrophysica, 37, 113-117.
9. **Kuźniar P., Sosnowski S. 2000**: Attempt to determine bean-pod susceptibility to cracking. International Agrophysics, 14, 197-201.
10. **Kuźniar P., Sosnowski S. 2003a**: Susceptibility of bean pods on cracking and losses of seeds during mechanical harvest (in Polish). Acta Agrophysica, 2(1), 113-118.
11. **Kuźniar P., Sosnowski S. 2003b**: Influence of moisture of bean pods and repeated moistening on force required for their opening (in Polish). Acta Agrophysica, 2(1), 119-126.
12. **Kuźniar P., Sosnowski S. 2006**: Energy necessary to open bean pods in various nitrogen fertilization levels.

TEKA Commission of Motorization and Power Industry in Agriculture. VI A, 123-127.
13. **Kuźniar P. 2012**: Energy of bean pods opening with phosphorous fertilization. TEKA Commission of Motorization and Energetics in Agriculture. 12(1), 131-134.
14. **Moś M. 1983**. Variability of morphological and anatomical features of the pod, its impact on the propensity to crack and seed yield of birdsfoot ordinary *Lotus corniculatus L.* (in Polish). Zesz. Probl. Post. Nauk Roln., 258, 197-203.
15. **Strobel W. 2003**: Comparison of the physical characteristics of pods of different lupine species (in Polish). Zeszyty Problemowe Postępów Nauk Rolniczych, 495, 73-80.
16. **Szwed G., Tys J., Strobel W. 1999**: Pressurized methods for grading the vulnerability of pods splitting. International Agrophysics, 13, 391-395.
17. **Tomaszewska Z. 1954**: Initial studies on the anatomy of pods of lupine (in Polish). Acta Agrobotanica, 2, 151-171.

UPROSZCZONA METODA WYZNACZANIA OBJĘTOŚCI WEWNĘTRZNEJ STRĄKÓW FASOLI

Streszczenie. Praca zawiera wyniki badań nad opracowaniem uproszczonej metody wyznaczania objętości powietrza wewnątrz strąka. Badania wykonano na strąkach fasoli uprawianej na suche nasiona odmian Narew, Nida, Warta i Wawelska. Porównano dziesięć metod wyznaczania objętości (piknometryczną i dziewięć prostych modeli strąka).

Objętości wyznaczone metodą 1 (piknometrem) i metodą 7 były najbardziej zbliżone i nie różniły się miedzy sobą statystycznie istotnie. Można więc uznać, że zaproponowany w tej metodzie prosty model strąka ułatwia wyznaczenie objętości powietrza w nim zawartego.
Słowa kluczowe: strąk fasoli, objętość, metody wyznaczania.

Scientific paper financed from the funds for science in the years 2007-2010 developed as part of research project N N310 2242 33

TEKA. COMMISSION OF MOTORIZATION AND ENERGETICS IN AGRICULTURE – 2013, Vol. 13, No. 2, 53–58

Energy of bean pod opening and strength properties of selected elements of their structure

Piotr Kuźniar, Józef Gorzelany

Department of Engineering in Agricultural Food Production, University of Rzeszów,
Zelwerowicza 4, 35-601 Rzeszów, Poland, e-mail: pkuzniar@univ.rzeszow.pl

Received May 18.2013; accepted June 28.2013

Summary. The study presents the correlations of bean pod opening energy in the varieties Narew, Nida, Warta and Wawelska with their geometric features and strength properties of selected elements of their structure. It has been confirmed that the pods which are more susceptible to cracking are those with a flatter section (wider and thinner), lower thickness of fibre and parenchyma layers as well as lower ration of the thickness of parenchyma and the fibre layer undergoing less deformations and more resistant to tearing, whose sclerenchymatous connections of the dorsal seam are more resistant to tearing and the abdominal seam are less resistant.

Key words: bean pod, elements of construction, strength properties, energy of pod opening.

INTRODUCTION

One of the unfavourable features of legumes is their susceptibility to cracking their pods and seeds falling out before and after harvesting [6, 12, 18, 19].

Susceptibility of pods to cracking is a variety feature and is conditioned by their anatomic and morphological structure. The main feature allowing the breaking of the pod is the structure of its endocarpium in which there is a layer of fibres constructed from strongly thickened sclerenchymatous cells located diagonally to the axis of the fruit. As a result of various location of micro fibrils in cellular walls, during drying they shrink in various directions and there is the breaking of the pod along with the ventral and dorsal suture. The most significant of the elements of the internal structure of the pods are the content and structure of the fibre in vascular bundles and walls of their shells. [3, 5, 9, 11, 24].

The susceptibility to cracking is also conditioned by their shape in the layer of the transverse section [10, 21].

The aim of the work was to determine the geometric features and strength properties of selected elements of the structure of the pod and comparing them with the susceptibility to cracking of these fruits whose opening energy is measured and determined by the pressure method.

MATERIAL AND METHODS

The research was carried out in 2008-2010. Bean was cultivated in the experimental field of the Department of Engineering in Agricultural Food Production in Rzeszów. The research was conducted on pods of bean cultivated on dry seeds of the varieties: Narew, Nida, Warta and Wawelska, which were characterized by varied seed and pod sizes (Tab. 1).

Pod dimensions were calculated using an electronic slide calliper with the accuracy of 0.01 mm. Length was measured from the beginning of stalk to the peak, and width and thickness in cutting plane of perpendicular to main axis of the fruit, leading through its centre. Thickness and width of the fibre layer and seam bundles were measured using an electronic dial gauge with the accuracy of 0.001 mm. Surface of cross section of the analyzed pod structure elements was calculated as a product of width and thickness.

The shape factor, s_f, was determined as the ratio of pod width to its thickness:

$$s_f = \frac{d}{e}, \tag{1}$$

where:
s_f – shape factor,
d – pod width [mm],
e – pod thickness [mm].

Strength research covers such pod structure elements as:
– fibre layer,
– seam sclerenchyma bundles; abdominal and dorsal

The research was conducted with the use of the testing machine ZWICK with which for the above mentioned pod the following structure elements were determined: critical stress, modulus of elasticity (Young's modulus) and deformation [2, 4, 7, 8, 22]. In order to separate fibre layer and seam sclerenchyma bundles from the other tissues, bundles were placed for 15 minutes in boiling water. Parenchyma tissues macerated in this way were removed (scraped off) with a blunt side of a scalpel so as to not damage sclerenchyma [11]. For the purpose of resistance tests ca 2 mm straps were cut from a fibre layer parallel to the direction of fibre location.

Energy required to open a pod was calculated with the pressure method which is based on bursting a pod by compressed air [15, 21]. Air volume in a pod was determined with modified pictometric method [13, 14].

Measurements were conducted on 80 pods for each of the tested varieties with their humidity within the range of 12.4-13.8%.

The result was statistically analyzed with Statistica 9 program, with which the variance analysis and LSD significance test were carried out [1].

RESULTS

The least susceptible to cracking (Fig.1) were pods of the Narew variety, which needed the energy of opening amounting to 258.1 mJ, on average. The greatest susceptibility occurred in the pods of Nida variety, which opened at the energy of 125,1 mJ, on average. The performed test LSD indicated that due to the average values of pod opening energy, all the tested bean varieties were significantly statistically different.

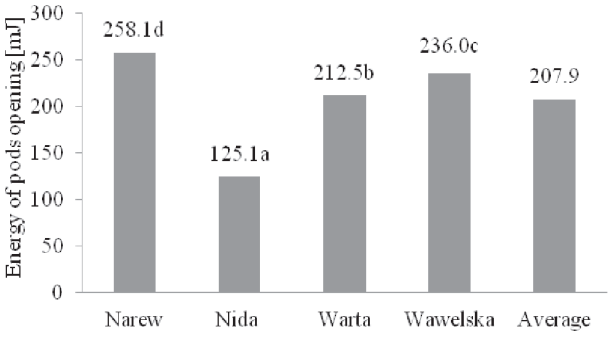

Fig. 1. Energy of pods opening on bean varieties
*different letters signify significant differences for the significance level α = 0.05

The pods of Wawelska variety (Tab.1) were statistically significantly the longest (118.6mm), Nida the widest (10.4mm) and with the greatest shape factor (1.28) and Narew the thickest (8.9mm). The shortest pods (96.8mm) were the Nida and the narrowest (9.7mm) and the thinnest (7.9 mm) were the Warta. The lowest shape factor (1.14) was found for the Narew variety.

Table 1. Geometric characteristics of bean pods and their correlation coefficient with pods opening energy

Specification	Dimension of pods [mm]			Shape factor of pod
	Length	Width	Thickness	
Narew	101.7b	10.2b	8.9b	1.14a
Nida	96.8a	10.4b	8.1a	1.28d
Warta	113.2c	9.7a	7.9a	1.24c
Wawelska	118.6d	10.2b	8.6b	1.19b
Correlation coefficients with energy of opening the pods	0.5335	-0.3302	0.6505	-0.9256

* different letters in column signify significant differences, as per LSD test (significance level of α = 0.05)

The energy of bean pod opening was highly and positively correlated with the length (0.5335) and thickness (0.6505) of pods and negatively, on average, with their width (-0.3302) and almost fully with the shape index (-0.9256). It means that the bean varieties whose pods are longer, narrower, thicker and with a less flat transverse section are more resistant to breaking. This regularity is confirmed in the conclusions of Szwed et. al. [20, 21], namely, that pods with greater convexity are easier to be opened as the lower curvature radius causes an increase of the arm of the moment of pod shell bending in the perpendicular plane towards the direction of the location of fibres on the parchment layer. It shall be assumed that the susceptibility to cracking pods in the analysed varieties, is conditioned by other features [13].

Table 2. Average values sclerenchematic of bundles abdominal (A) and dorsal (D) seam on bean pods and their correlation coefficient with pods opening energy

Specification	Seam bundles	Narew	Nida	Warta	Wawelska	Correlation coefficients
Thickness [μm]	A	178.4b	189.3bc	157.6a	194.2c	-0.1952
	D	172.7ab	181.1b	160.0a	204.5c	0.0425
Width [μm]	A	706.5cII	628.3bII	571.9aII	652.9bII	0.4458
	D	616.8bI	584.9bI	531.7aI	587.5bI	0.2307
Surface of cross section [mm^2]	A	0.129bII	0.120b	0.092a	0.128b	0.1810
	D	0.108bI	0.107b	0.087a	0.122c	0.1509
Width/ Thickness	B	4.24bII	3.57a	3.88a	3.60aII	0.6589
	G	3.79bI	3.44b	3.54b	3.02aI	0.1108

* different letters in line and Roman numerals in column signify significant differences, as per LSD test (significance level of α = 0.05)

Analysing the results included in Table 2, it must be confirmed that the bundles of the abdominal seam were characterised by greater dimensions, section area and the ratio of width and thickness than the bundles of the dorsal seam, except for the varieties of Warta and Wawelska, in which the bundle of the dorsal seam was thicker. Statistically significantly wider were the bundles of the abdominal seam in all of the tested varieties. However, significantly, the greatest transverse sec-

tion area of the abdominal suture bundle was characteristic of the pods of Narew variety, and the ratio of the width and thickness of bundles of the abdominal seam was significantly greater than in the varieties of Narew and Wawelska. With exception of the bundle width of the dorsal seam, the greatest dimensions and transverse section area were in the pods of Narew and lower in the pods of Warta varieties.

The bundles of the dorsal seam (Tab. 3) had a significantly greater damaging pressure, deformation and conventional module of elasticity from the bundles of the abdominal seam, except for the Wawelska variety in which an insignificantly greater value characterised the module of elasticity of the bundle of the abdominal seam. The sclerenchymatous bundles of the abdominal seam had the greatest resistance to tearing and deformations in the Warta pods, however, the greatest module of pod elasticity belonged to the Wawelska variety. The lowest stress, deformation and module occurred in the bundles of the abdominal seam in the Nida pods. The lowest stress and module for the bundles of the dorsal seam were noted in the pods of Warta and deformation in the variety of Narew. For the bundles of the dorsal seam, the greatest stress and module were noted in the pods of Warta and deformation in the variety of Narew, and the module of elasticity in the variety of Narew.

Table 3. Strength properties of sclerenchematic bundles abdominal (A) and dorsal (D) seam on bean pods and correlation coefficients of the energy pod opening

Specification	Seam bundles	Narew	Nida	Warta	Wawelska	Correlation coefficients
Critical stress [MPa]	A	84.95I	59.04I	105.57	90.03I	0.7049
	D	113.86II	121.02II	112.51	125.66II	-0.2476
Deformation [%]	A	5.52	4.99	6.69	5.35	0.3460
	D	6.49	7.96	7.75	7.46	-0.7811
Modulus of elasticity [MPa]	A	1875.8	1535.6	1715.3	1979.8	0.8951
	D	1977.0	1712.2	1600.9	1864.5	0.5887

*different letters in line and Roman numerals in columns signify significant differences, as per LSD test (significance level of $\alpha = 0.05$)

The energy of bean pod opening was positively correlated with the strength parameters of the abdominal seam bundles, however, much higher with the damaging stress and conventional module of elasticity and with deformation on average. It means that the varieties of beans whose bundles of sclerenchymatous abdominal seam are characterised with greater values of the analysed strength parameters need a greater energy of opening, i.e. they are less susceptible to breaking. The correlation indexes of the energy of opening with the damaging pressure and deformation of the bundles of the dorsal seam were negative, however, along with the module of elasticity, they were positive. The obtained values of correlation indicate that for the opening pods whose sclerenchymatous bundles of the dorsal seam are less resistant to tearing and undergo less deformations and are characterised with a greater module of elasticity, greater energy is needed.

The greatest thickness of the shell (282.4μm), parenchyma (183.1μm) and fibre layers (80.8μm) as well as the greatest ration of parenchyma thickness and layer of fibres (1.85) was noted in the pods of the variety of Wawelska (Tab.4). The thinnest shells (172.6μm), parenchyma (104μm), fibre layer (67.7μm) and the ratio of parenchyma thickness and layer of the fibres were characteristic of the pods of Nida. The pods opening energy was correlated very highly with the thickness of shell, parenchyma, and layer of fibres along with the ratio of parenchyma thickness and fibre layer.

Table 4. Average values thickness of fibre layer, shell pods and the ratio of parenchyma thickness and fibre layer, and correlation coefficients of the energy pod opening

Specification	Thickness [μm]			Ratio of parenchyma thickness and fibre layer
	Shell pods	Fibre layer	parenchyma	
Narew	232.6b	84.9b	147.7b	1.74c
Nida	172.6a	67.7a	104.9a	1.55a
Warta	187.5a	71.3a	116.2a	1.63b
Wawelska	282.4b	99.1c	183.3c	1.85d
Average	218.8	80.8	138.1	1.69
Correlation coefficients	0.7121	0.7045	0.7150	0.8018

* different letters in column signify significant differences, as per LSD test (significance level of $\alpha = 0.05$)

A positive correlation of the energy of bean pod opening of the examined bean varieties with the thickness of the fibre layer indicates that the thicker it is, the more difficult it is to open pods. However, the easiest opening of pods with a thicker layer of fibres was confirmed in the research on lupine pods [16, 24, 25] and lotus corniculatu, and siliqua. It may mean that the susceptibility to breaking in the pods of the tested varieties of beans are also determined by other features e.g. structure of cells – the more delicate and thinner walls, the weaker the cracking [25]. The very high correlation of opening energy with the thickness of parenchyma and the relation of the parenchyma thickness and fibre layers confirm the conclusions of the aforementioned researchers that the thicker is the part of the pod shell in relation to the fibre layer, the less susceptible fruits are to cracking.

The fibre layer of bean pods of Wawelska had the greatest resistance to tearing (170.3MPa) and deformations (8.2%). In the pods of Warta, however, the greatest module of pod elasticity was found (2296.9MPa). The lowest values of the determined strength parameters of the fibre layer were noted in the pods of Narew variety (damaging stress 119.18MPa, elongation by 6.13% and the module of elasticity 1958.75MPa).

The energy of bean pod opening was highly correlated with the stress damaging the layer of fibre and, on average, with their deformation and the module of elasticity. It may be confirmed that less susceptible to cracking are those pods whose fibre layer is determined by greater values of strength parameters.

Table 5. Strength properties of fibre layer bean pods and correlation coefficients of the pods opening energy

Varieties	Critical stress [MPa]	Deformation [%]	Modulus of elasticity [MPa]
Narew	127.9ab	6.28a	2040.5a
Nida	119.2a	6.13a	1958.8a
Warta	145.0b	6.35a	2296.9b
Wawelska	170.3c	8.20b	2078.8ab
Average	140.6	6.74	2093.8
Correlation coefficients	0.5052	0.3912	0.3575

* different letters in column signify significant differences, as per LSD test (significance level of $\alpha = 0.05$)

CONCLUSIONS

1. The pods which are the least susceptible to cracking are in the variety of Narew. They require significantly greater opening energy amounting to 258.1mJ. The most susceptible to cracking were the pods of Nida variety, where the necessary energy amounted to 125.1mJ.
1. The energy of bean pod opening was highly and positively correlated with the length (0.5335) and thickness (0.6505) of pods and negatively, on average, with their width (-0.3302) and almost fully with the shape index (-0.9256). It means that the bean varieties, whose pods are longer, narrower, thicker and with a less flat transverse section are more resistant to cracking.
2. The bundles of the abdominal suture were characterised by greater dimensions, section area and the ratio of width and thickness than the bundles of the dorsal seam, except for the varieties of Warta and Wawelska, in which the bundle of the dorsal seam was slightly thicker.
3. The bundles of the dorsal seam had a significantly greater damaging pressure, deformation and conventional module of elasticity than the bundles of the abdominal seam, except for the variety of Wawelska in which an insignificantly greater value was observed in the module of elasticity of the bundle of the abdominal seam.
4. For the pods of bean varieties whose sclerenchymatous bundles of the abdominal seam had greater values of the analysed strength parameters, whose sclerenchymatous bundles of the dorsal seam were less resistant to tearing and underwent fewer deformations and were characterised by a greater module of elasticity, greater energy was needed.
5. The pods with a thicker fibre layer, shell and parenchyma along with the greater ratio of parenchyma and layer of the fibres, required greater energy of opening.
6. The fibre layer of bean pods of Wawelska had the highest resistance to tearing (170.3MPa) and deformations (8.2%). In the pods of Warta, however, the greatest module of pod elasticity was found (2296.9MPa). The lowest values of the determined strength parameters of the fibre layer were noted in the pods of Narew variety: damaging stress 119.18MPa, elongation by 6.13% and the module of elasticity 1958.75MPa.
7. The energy of bean pod opening was highly correlated with the stress damaging the layer of fibre and, on average, with their deformation and the module of elasticity, i.e the pods whose fibre layer was characterised by greater values of strength parameters were less susceptible to cracking.

REFERENCES

1. **Burski Z., Tarasińska J., Sadkević R. 2003**: The methodological aspects of using multifactoral analysis of variance in the examination of exploitation of engine sets. TEKA Komisji Motoryzacji i Energetyki Rolnictwa Polskiej Akademii Nauk Oddział w Lublinie, 3, 45-54
2. **Ciupak A., GładyszewskaB., Dziki D. 2012**: Change in strength of tomato fruit skin during ripening process. TEKA. Commission Of Motorization And Energetics In Agriculture, 12(2), 13-18.
3. **Dorna H., Duczmal K. W. 1994**: Influence of climatic conditions on the formation of the fibers in the seams of the bean pods *Phaseolus vulgaris* L. (in Polish). I Ogóln. Konf. Nak. Strączkowe Rośliny Białkowe. FASOLA, Lublin 25.11.1994, 135-138.
4. **Dziki D., Laskowski J. 2006**: Influence of wheat grain mechanical properties on grinding energy requirements TEKA Kom. Mot. Energ. Roln., 6A, 45-52.
5. **Esau K. 1973**: Anatomy of plants (in Polish). PWRiL, Warszawa, 1973.
6. **Furtak J., Zaliwski A. 1986**: Studies on the mechanical harvest of seeds (in Polish). Roczniki. Nauk Rolniczych, ser. Technika Rolnicza, 2, 127-140.
7. **Gorzelany J., Puchalski C. 2010**: Mechanical properties of roots in selected sugar beet varieties (in Polish). Inżynieria Rolnicza. 1 (119), 199-204.
8. **Guz T. 2008**: Thermal quarantine of apples as a factor forming its mechanical properties. TEKA Komisji Motoryzacji i Energetyki Rolnictwa Polskiej Akademii Nauk Oddział w Lublinie, 8a, 52-62.
9. **Hejnowicz Z. 1985**: Anatomy and vascular plants histogeneza (in Polish). PWN, Warszawa.
10. **Kuźniar P., Sosnowski S. 2002**: Relation between the bean pod shape factor and force required for pod opening. International Agrophysics, 16(2), 129-132.
11. **Kuźniar P., Strobel W. 2000**: Determine the effect of thickness sclerenchyma bean pods on their susceptibility to cracking (in Polish). Acta Agrophysica, 37, 113-117.
12. **Kuźniar P., Sosnowski S. 2003**: Susceptibility of bean pods on cracking and losses of seeds during mechanical harvest (in Polish). Acta Agrophysica, 2(1), 113-118.
13. **Kuźniar P., Sosnowski S. 2007**: The attempt of measuring the air volume in bean pods. TEKA Commission of Motorization and Power Industry in Agriculture, 7A, 68-72
14. **Kuźniar P. 2008**: The energy of bean-pod opening and the method of determining air volume therein. MOTROL- Motoryzacja i Energetyka Rolnictwa. 10, 73-77.
15. **Kuźniar P. 2012**: Energy of bean pods opening with phosphorous fertilization. TEKA Commission of Motorization and Energetics in Agriculture. 12(1), 131-134.
16. **Moś M. 1983**: Variability of morphological and anatomical features of the pod, its impact on the propensity to crack and seed yield of birdsfoot ordinary *Lotus cor-*

niculatus L. (in Polish). Zeszyty Problemowe Postępów Nauk Rolniczych, 258, 197-203.
17. **Strobel W. 2003**: Comparison of the physical characteristics of pods of different lupine species (in Polish). Zeszyty Problemowe Postępów Nauk Rolniczych, 495, 73-80.
18. **Szot B., Tys J. 1979**: The reasons for shedding the oilseeds and legumes and methods of assessment of this phenomenon (in Polish). Problemy Agrofizyki, 29.
19. **Szot B., Tys J. 1987**: Test methods are the mechanical properties of rape siliques and stems (in Polish). Zeszyty Problemowe Postępów Nauk Rolniczych, 321, 193-202.
20. **Szwed G., Strobel W., Tys J. 1997**: The mechanisms governing the processes of cracking lupine pods (in Polish). Mat. Konf. Łubin we współczesnym rolnictwie, Olsztyn 25-27.06.1997,107-112.
21. **Szwed G., Tys J., Strobel W. 1999**: Pressurized methods for grading the vulnerability of pods splitting. International Agrophysics, 13, 391-395.
22. **Szymanek M., Sobczak P. 2009**: Some physical properties of spelt wheat seed. TEKA Komisji Motoryzacji i Energetyki Rolnictwa Polskiej Akademii Nauk Oddział w Lublinie, 9, 310-320.
23. **Tomaszewska Z. 1954**: Initial studies on the anatomy of pods of lupine (in Polish). Acta Agrobotanica, 2, 151-171.
24. **Tomaszewska Z. 1964**: Morphological studies and anatomical of siliques of several varieties of winter oilseed rape and turnip rape, and reasons and mechanism of their cracking (in Polish). Hodowla Roślin, Aklimatyzacja i Nasiennictwo, 2, 147-180.
25. **Tomaszewski Z. 1953**: Breeding of yellow lupine which pods do not crack and not fall off (in Polish). Acta Agrobotanica, 1, 89-104.

ENERGIA OTWARCIA STRĄKÓW FASOLI A WŁAŚCIWOŚCI WYTRZYMAŁOŚCIOWE WYBRANYCH ELEMENTÓW ICH BUDOWY

Streszczenie. Praca przedstawia analizę korelacji energii otwarcia strąków fasoli odmian Narew, Nida, Warta i Wawelska z ich cechami geometrycznymi oraz właściwościami wytrzymałościowymi wybranych elementów ich budowy. Stwierdzono, że bardziej podatne na pękanie są strąki; o bardziej płaskim przekroju (szersze i cieńsze); o mniejszej grubości warstwy włókien i parenchymy oraz mniejszym stosunku grubości parenchymy i warstwy włókien; których warstwa włókien ulega mniejszym odkształceniom i jest mniej wytrzymała na rozrywanie; których wiązki sklerenchymatyczne szwu grzbietowego są bardziej wytrzymałe na rozrywanie, a szwu brzusznego mniej.
Słowa kluczowe: strąk fasoli, elementy budowy, właściwości wytrzymałościowe, energia otwarcia.

Scientific paper financed from the funds for science in the years 2007-2010 developed as part of research project N N310 2242 33

TEKA. COMMISSION OF MOTORIZATION AND ENERGETICS IN AGRICULTURE – 2013, Vol. 13, No. 2, 59–62

Quality of raspberry combine harvesting depending on the selected working parameters

Norbert Leszczyński[1], Józef Kowalczuk[1], Janusz Zarajczyk[1], Adam Węgrzyn[1], Mariusz Szymanek[2], Wojciech Misztal[3]

[1]Department of Horticultural and Forest Machinery,
[2]Department of Agricultural Machines Sciences,
[3]Department of Agricultural Machines and Devices.
University of Life Sciences in Lublin, ul. Głęboka 28, 20-612 Lublin, Polska, e-mail: norbert.leszczynski@up.lublin.pl

Received April 10.2013; accepted June 28.2013

Summary. This paper presents the results of the research on the work quality of a tow-behind combine harvester Korvan 930 while picking Canby summer variety of raspberries cultivated on poles. The assumption was to determine the type and size of losses as well as the share of damaged fruits and impurities in the combine-harvested material.
Key words: raspberries, combine harvesting, losses, damaged fruits, impurities.

INTRODUCTION

On a vast majority of raspberry plantations in the world, the fruit are still harvested manually. Until not very long ago in fact, manual harvesting of raspberries was actually the only possible solution to apply. In Poland, due to constantly growing cost of labour and not enough of the labour force, and in connection with growing desire of producers to achieve better yields (especially in the period of peak purchasing prices), as of the beginning of this century first attempts at an automated raspberry harvest have repeatedly occurred [7, 8]. However, raspberry fruit are delicate and therefore susceptible to damage [1, 9, 12, 13, 15], and, what's more, they ripen non-simultaneously, which calls for the need of multiple harvests during one season, thus causing more risk of damage to the fruit. [14]. Even in case of vegetables resistant to damage, machine harvesting (which has been improved for the last several tens of years) still causes inevitable damages and losses of products [10]. A solution to the problem of having too much fruit damaged during the machine harvest is, apart from improving the construction of the machines, introduction of more damage-resistant fruit varieties [2-6].

AIM AND SUBJECT OF RESEARCH

The aim of the research was to determine the volume of losses and damages of the raspberry fruits as well as the amount of impurities in the harvested material generated during the automated harvest by means of a tow-behind combine-harvester Korvan 930 manufactured by an American company Oxbo. For the purpose of the research the harvester was aggregated with tractor Władimirec t 25. Examined was the suitability of the above harvester for picking summer variety of raspberry called Canby meant for cold storage.

Korvan 930 harvests fruits by shaking them off the bush (by means of 'fingers' of two vertical beaters and generally resembles the Polish combine harvester Natalia by Weremczuk company [7]. The difference is that the shell adjusting system designed to catch the falling fruits) does not have the rolls sliding on the shoots of bushes. Korvan 930 was designed to pick raspberries and put them in plastic boxes which were placed on the platforms next to inspection carriers attached on both sides of the harvester. The field examination of the harvester was carried out in a village called Kolonia Łubki close to the town of Opole Lubelskie on a 6-year old plantation of a Canby summer variety of raspberry cultivated on poles and linked by metal strings to which the raspberry shoots were attached in the direction opposite to the direction of picking. The research was conducted at the harvester working speed of 1.35 $km \cdot h^{-1}$ which was selected as the best for testing purposes and because it was the lowest speed possible to be achieved with the attached tractor. At higher tractor speeds, the operator of the whole aggregate had problems with leading the machine properly.

RESEARCH METHODOLOGY

While assessing the quality of combine harvester operation, methodology designed by Kowalczuk and Zarajczyk [7, 8] was used and modified. In order to determine the working conditions of the combine harvester, features of the raspberry plantation were examined and described. The

examination involved random measurement of: row spacing, row width, raspberry bush height, width of growing shoots (measured on the ground surface) and minimum height at which fruits were formed, all in one hundred repetitions. Apart from that a number of shoots on 1 meter sections was counted (in thirty repetitions). The raspberry yield (to be potentially harvested during one day) was determined on the measurement fields of 10 m in length, in six repetitions.

Prior to starting the assessment of the combine harvester working quality, its parameters were specified. The amplitude of beating cylinders was measured in the cylinder's axis while the frequency was determined by counting the multiplications of the cylinder inclinations within 10 seconds, all in thirty repetitions. The speed of the cooling fans and cooperating inspection carriers from over which impurities were sucked off, was determined on the basis of regulation knobs.

The quality of the combine raspberry harvest was assessed on previously appointed 10 m long measurement fields (in six repetitions). During tests, picked raspberries were taken to plastic boxes placed individually for every repetition to capture the picked fruit mass. Then the picked raspberries were segregated into: damaged and not damaged (serious damages visible with the naked eye), with and without stalks, and into green fruits and impurities. Then the ripe fruits were weighed. Apart from that, fruits dropped by the harvester were picked up manually from the measurement sections (before the test was started, the measurement sections were cleaned from previously fallen raspberry fruits). After that, shares of particular fractions in percentages were determined, compared to the whole fruit mass harvested. The fractions were weighed by means of Radwag WPT 30/CG and WTE2000p scales. Impurity percentages were calculated in relation to the mass of the entire sample picked by the harvester. Percentage of losses was calculated in relation to the total fruit mass collected by the harvester, lost and fallen from the previous harvest.

The research results were made subject to a statistical analysis by means of the Excel spreadsheet. The CV variability ratio was calculated:

$$CV = \frac{\delta}{n} \cdot 100\% ,$$

where:
d – standard deviation,
n – mean value.

Destructive changes in fruits were determined based on the observation of raspberry juice leakages, in accordance with the methodology adopted by Kuczyński and Rybczyński [9].

RESULTS AND DISCUSSION

The results of the measurement of the raspberry plantation characteristics, on which tests of combine harvester Korvan 930 were carried out, were summarised in Table 1.

Table 1. Characteristics of the raspberry plantation of Canby variety

Specification	Measurement unit	Average results	Variability ratio, %
Row spacing	cm	316,0	2,1
Distances between bushes in a row	cm	30,0	5,4
Width of growing shoots	cm	31,1	7,3
Number of shoots per 1 linear metre	shoots	29,3	23,4
Height of raspberry plants	cm	176,3	11,0
Row width	cm	102,3	8,6
Minimum height at which fruits are formed	cm	35,0	28,5
Average weight of 100 fruits	g	271,7	0,8
Fruit mass volume	$g \cdot (250\ cm)^{-3}$	106,6	7,0
Raspberry potential yield	$kg \cdot ha^{-1}$	643,8	7,16

Raspberries were seeded in rows spaced at 316 cm and the distance between the bushes in a row was 30 cm. On 1 linear metre 29.3 shoots grew. Plants formed a lane 176.3 cm high and 102.3 cm wide, and the lowest fruits were formed at the height of 35.0 cm. The average weight of 100 fruits was 271.7g and their mass volume 106.58g $(250\ cm)^{-3}$. The potential yield was 643.8 $kg \cdot ha^{-1}$.

Work parameters of combine harvester Korvan 930 were presented in Table 2.

Table 2. Work parameters of combine harvester Korvan 930

Specification	Measurement unit	Average results	Variability ratio, %
Shaking amplitude	cm	4,0	35,4
Frequency of shaking	Hz	4,6	0,1
Fan speed	6 on scale 0-10		
Speed of inspection carriers	0 on scale 0-10		

Research results related to the assessment of work quality of combine harvester Korvan 930 while harvesting Canby variety raspberries were presented on charts 1 and 2.

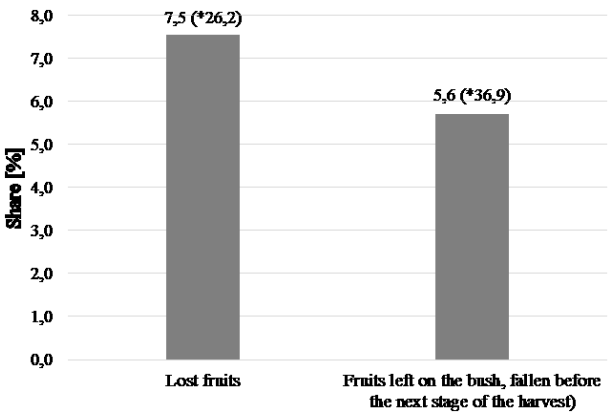

* variability ratio

Fig. 1. Losses occurring while harvesting Canby variety raspberries by means of combine harvester Korvan 930

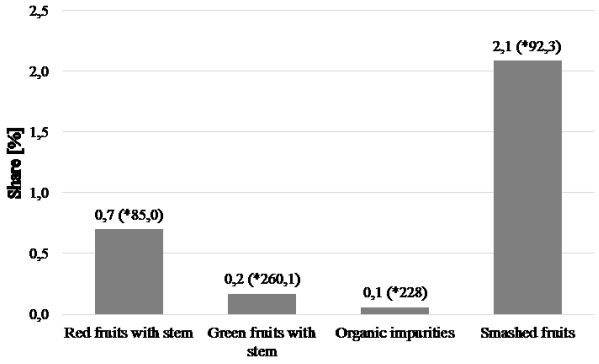

* variability ratio

Fig. 2. Damages and impurities occurring while harvesting Canby variety raspberries by means of combine harvester Korvan 930

Tests showed significant share of lost fruits of which majority i.e. 7,5% were fruits dropped out by the harvester at the junction of the adjusting system. The shells of the adjusting system could not touch each other due to significant width of the growing shoots (31.1 cm). Although we could have plantations with tighter rows and thus reduce the rate of the dropped out fruits but they would produce lower yields per hectare and in consequence be less profitable. Lost fruits were also ripe fruits left on the bushes and fallen before the next stage of the harvest – there were 5.7% of those. In reference to the results achieved by Rabcewicz [11] the amount of the losses can be decreased by increasing the frequency of shaking but such a technique would also cause the increase of damaged fruits, unwelcome by the cold storage industry.

The collected material was only very little contaminated with impurities such as stems (0.7%), green fruits (0.2%) and minute organic impurities (0.1%). These impurities can be eliminated entirely by having two workers remove them manually, each one at each inspection carrier on the harvester.

Combine harvester Korvan 930 also caused mechanical damages to the fruits. 2.4% of them were smashed. However, no destructive changes of the fruits were observed.

CONCLUSIONS

1. During combine harvesting of Canby variety raspberries by means of Korvan 930 two types of losses were observed: the machine lost/dropped 7.5% of fruits and did not properly pick all ripe fruits leaving 5.7% on the bushes.
2. Combine-harvested fruits were contaminated very little, i.e. there were only 0.7% of fruits with stem, 0.2% of green fruits and 0.1 of organic impurities%.
3. Fruit damages were 2.1%.
4. Tow-behind combine harvester Korvan 930 of Oxbo company may in friendly conditions be successfully used to harvest Canby variety raspberries meant for cold storage.

REFERENCES

1. **Barritt B.H., Torre L.C., Pepin H.S., Daubeny H.A. 1980.** Fruit firmness measurement in red raspberry. Horticultural Science, 15(1), 38-39.
2. **Chen P., Tang S., Chen S. 1985.** Instrument for testing the response of fruits to impact. ASAE, 85-3587.
3. **Delwiche M.J., Tang S., Mehlschau J. 1989.** An impact force response fruit firmness sorter. Transaction of the ASAE, 32(1), 321-326.
4. **Gołacki K., Rowiński P. 2006.** Dynamiczne metody pomiaru własności mechanicznych owoców i warzyw [Dynamic methods of measuring mechanical properties of fruits and vegetables]. Acta Agrophysica, 8(1), 69-82.
5. **Haffner K., Rosenfeld J.H., Skrede G., Wang L. 2002.** Quality of red raspberry *Rubus idaeus* L. cultivars after storage in controlled and normal atmospheres. Postharvest Biology and Technology, 24, 279-289.
6. **Heiberg N. 1988.** Fresh fruit quality evaluation for red raspberry. Norwegian Journal of Agricultural Sciences, 2(2), 73-78.
7. **Kowalczuk J., Zarajczyk J., Leszczyński N. 2008.** Analiza jakości zbioru malin kombajnem „Natalia" firmy Weremczuk. Inżynieria Rolnicza [Analysis of the quality of harvesting raspberries by means of "Natalia" combine harvester by Weremczuk company], 2(100), 89-93.
8. **Kowalczuk J., Zarajczyk J. 2008.** Influence of working parameters of the "Natalia" harwester manufactured by the Weremczuk company on the harvest quality of red raspberries. Teka Komisji Motoryzacji i Energetyki Rolnictwa, 8, 100-104.
9. **Kuczyński A.P., Rybczyński R. 2004.** Pomiar odporności mechanicznej owoców maliny w teście pełzania [Measurement of mechanical resistance of raspberry fruits in the creeping test]. Acta Agrophysica, 4(3), 707-713.
10. **Leszczyński N. 2011.** The influence of working parameters of a carrot harvester on carrot root damage. Usage and reliability, 1, 22-28.
11. **Rabcewicz J., Danek J. 2010.** Evaluation of mechanical harvest quality of primocane raspberries. Journal of Fruit and Ornamental Plant Research, 18(2), 239-248
12. **Rybczyński R., Dobrzański B., Wieniarska J. 2001.** Właściwości mechaniczne owoców maliny [Mechanical properties of raspberry fruits]. Acta Agrophysica, 45, 167-175.
13. **Rybczyński R., Krawiec P. 2010.** Efektywność ferdygacją w malinach odmian powtarzających [Effectiveness of fertilisation in case of repetitive raspberries]. Acta Agrophysica, 16(2), 347-358.
14. **Salamon Z., Wawrzyńczak P., Rabcewicz J. 1997.** Maszynowy zbiór owoców z krzewów jagodowych. Problemy Inżynierii Rolniczej [Machine harvesting of berry bush fruits. Agricultural engineering problems], 1, 61-68.
15. **Sjulin T.M., Robbins J.A. 1987.** Effects of maturity, harvest date, and storage time on postharvest quality of red raspberry fruit. American Society for Horticultural Science, 3(112), 481-487.

JAKOŚĆ KOMBAJNOWEGO ZBIORU MALIN W ZALEŻNOŚCI OD WYBRANYCH PARAMETRÓW ROBOCZYCH

Streszczenie. Przedstawiono wyniki badań dotyczące jakości pracy przyczepianego kombajnu Korvan 930, przy zbiorze letniej maliny odmiany Canby, prowadzonej na podporach. Określano rodzaj i wielkość strat owoców oraz udział uszkodzonych owoców i zanieczyszczeń w materiale zebranym kombajnem.

Słowa kluczowe: maliny, zbiór kombajnowy, straty, uszkodzenia owoców, zanieczyszczenia.

TEKA. COMMISSION OF MOTORIZATION AND ENERGETICS IN AGRICULTURE – 2013, Vol. 13, No. 2, 63–66

Energy consumption during corn starch extrusion-cooking

Marcin Mitrus, Maciej Combrzyński

Department of Food Process Engineering, Faculty of Production Engineering,
University of Life Sciences, Doświadczalna 44, 20-280 Lublin, Poland, marcin.mitrus@up.lublin.pl

Received May 25.2013; accepted June 28.2013

Summary. This paper presents the results of energy consumption measurements during extrusion-cooking of corn starch. The extrusion-cooking process was performed using a single screw extruder with L/D = 16 at variable screw speed ranging from 60 to 120 rpm. Native corn starch of varying humidity was used as the raw material. Changes in energy consumption depending on the moisture content, processing temperature, screw speed were measured during testing. Higher screw rpm increased specific mechanical energy. Corn starch with higher moisture content caused a decrease in energy consumption during the extrusion-cooking process. Processing temperature had no important effect on SME changes.
Key words: extrusion-cooking, corn starch, energy consumption.

INTRODUCTION

Extrusion-cooking technology is now one of the modernest grain processing technologies [1, 2, 9]. Currently, extrusion-cooking as a method is used for the manufacture of many food, feed and agrochemical products, ranging from the thermoplastic starch to pasta and aqua feed [10, 12, 13]. Wheat, corn and rice belong to one of the most often applied raw materials in the extrusion-cooking [3, 6].

Native starch has different industrial applications, however, due to many disadvantages (e.g. insolubility in cold water), its use is limited. Disadvantages of native starch can be reduced or even eliminated through its modification by various methods. The simplest method of physical modification of starch is thermal or pressure-thermal treatment. Humidity, temperature, pressure and mechanical shear – under the influence of these factors starch and protein components are plasticized and cooked during the extrusion-cooking, followed by rapid evaporation of the water when extrudates are leaving machine. This leads to further changes in the physical properties of the obtained products. Extrudates can be finished or semi-finished products and are characterized by new, chemical and dietary physical properties [8, 13].

The properties of the extrudates may be affected by many factors related to selecting various parameters of the extrusion-cooking process [5, 7, 14]. These include raw material processing time in the extruder, the intensity of shear stress during extrusion-cooking and the amount of energy supplied to the device [15, 16].

During extrusion-cooking, the primary source of thermal energy is the energy caused by friction forces and therefore derived from the conversion of mechanical energy into heat energy in the processed material. The process, despite popular opinions, is associated with a relatively low expenditure of energy [11]. The single screw extruder-cooker requires energy input in the range of 0.1 to 0.2 kWh (excluding energy required to prepare the raw material).

MATERIALS AND METHODS

Corn starch Meritena 100 type produced by T&L (Slovakia) was used. During our investigations the 4 levels of moisture content of raw material (17, 20, 25 and 30%) were used by mixing with sufficient amount of water. The obtained samples were stored for 24h in air tight polyethylene bags at room temperature to make the whole sample material homogeneous.

Extrusion-cooking of potato starch was carried out using a modified single screw extrusion-cooker TS-45 (Polish design) with L / D = 16. The die with one opening of 3 mm diameter was used. Processing was carried at different temperatures (100, 120 and 140 °C) and a variable speed of the screw (60, 80, 100, 120 rpm).

The extruder output was measured as a mass of the extrudate produced during 10 minutes; measurements were performed in 6 replications.

Power consumption measurement was performed with a standard method using wattmeter connected to the extruder

electric panel [4, 5, 7, 10]. The obtained results were converted to an index of specific mechanical energy consumption (SME) after the following formula:

$$SME = \frac{n \cdot P \cdot O}{n_m \cdot Q} \ [kWhkg^{-1}], \quad (1)$$

where:
n – screw rotations [min^{-1}],
n_m – maximal screw rotations [min^{-1}],
P – power [kW],
O – engine loading [%],
Q – extruder output [kgh^{-1}].

RESULTS

Extrusion-cooking of the corn starch was characterised by good efficiency, ranging between 10.8 kgh^{-1} and 26.6 kgh^{-1}, depending on the applied process parameters. Changes in the extruder output depended mainly on the screw speed and starch moisture content, less on the process temperature.

Measurements have shown that the increase of the screw speed increased the efficiency of the extrusion-cooking (Fig. 1). This effect was observed in the whole range of applied temperatures.

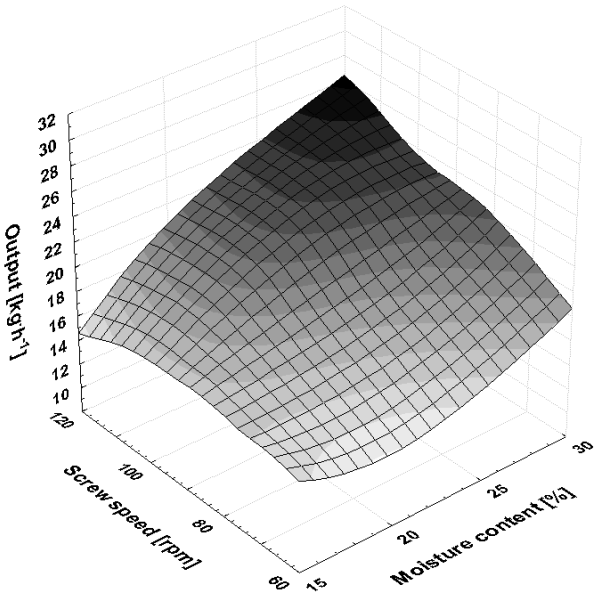

Fig. 1. Changes in the process output during corn starch extrusion-cooking at 100 °C

The extrusion-cooking of the corn starch with 17% of moisture content was hampered, especially at temperature of 140 °C. It was manifested by uneven flow of the material through the extrusion-cooker. During processing at all used temperatures, an increase of the process efficiency with increase of starch moisture content was observed.

Generally, extrusion-cooking of the corn starch was characterised by low energy consumption (SME) within a range 0,08-0,29 $kWhkg^{-1}$ (288-1044 $kJkg^{-1}$). Changes in SME depended mainly on the extruder screw speed and starch moisture content, less on process temperature.

A significant impact of the screw speed on the SME changes during corn starch processing was observed. The screw rotational speed increase caused a rise in mechanical energy consumption, independently of the process temperature (Fig. 2 and 3).

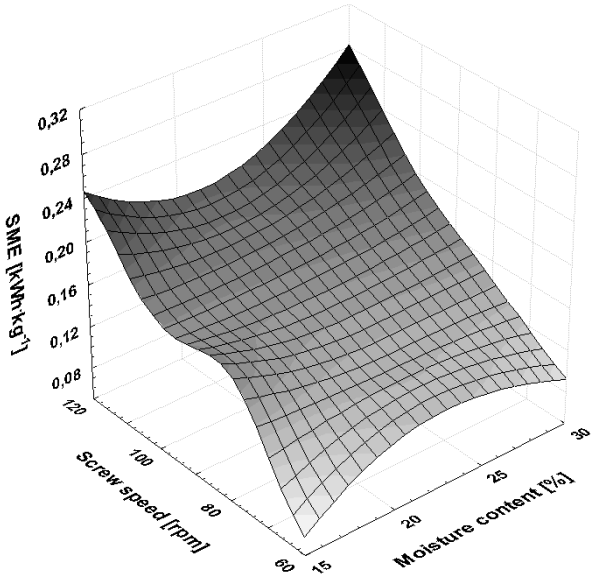

Fig. 2. SME changes during corn starch extrusion-cooking at 120°C

At a higher temperature, the influence of moisture content in the raw material on the process energy consumption was inconclusive. During the extrusion-cooking at 120 and 140 °C conducted with low screw speed range (60 and 80 rpm), the influence of moisture content on SME was neutral. The increase of energy consumption with raw material moisture content growth was only observed for a high screw speed range (100-120rpm).

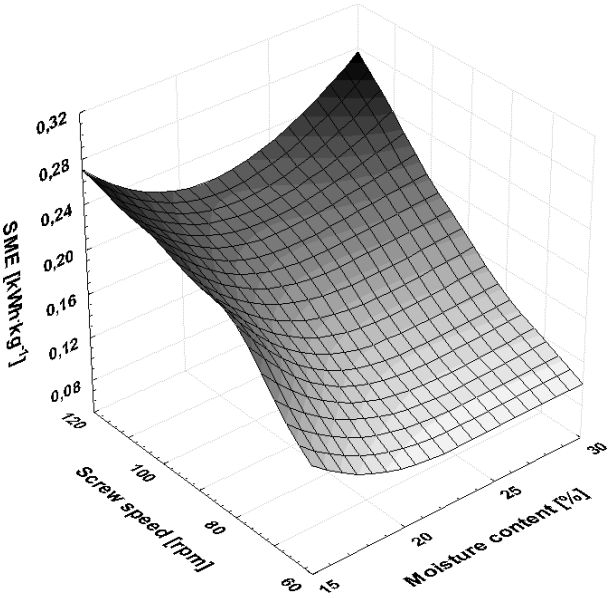

Fig. 3. SME changes during corn starch extrusion-cooking at 140°C

Generally, it can be stated that the temperature of extrusion-cooking had no significant effect on the energy consumption changes.

CONCLUSIONS

Extrusion-cooking of corn starch is characterized by relatively low specific mechanical energy consumption, ranging from 288 to 1044 $kJkg^{-1}$ (0,08-0,29 $kWhkg^{-1}$). A significant impact on the SME was exerted by the screw speed and moisture content of the raw material. The process temperature had a neutral impact on energy consumption changes.

REFERENCES

1. **Borowy T., Kubiak M. S. 2008.** Opakowania biodegradowalne alternatywą dla opakowań z tworzyw sztucznych. Gospodarka Mięsna, 5, 18-20.
2. **Ekielski A., Majewski Z., Żelaziński T. 2008.** Wpływ składu mieszanki na gęstość i rozpuszczalność ekstrudatu kukurydziano-gryczanego. Inżynieria Rolnicza, Nr 1 (99), 93-97
3. **Frame N.D. (edit.). 1994.** Technology of extrusion cooking. Chapman & Hall, New York. 73-79.
4. **Janssen L.P.B.M, Moscicki L. (ed.). 2009.** Thermoplastic Starch. WILEY-VCH Verlag & Co.KGaA, Weinheim, Germany.
5. **Janssen L.P.B.M, Mościcki L., Mitrus M. 2002.** Energy aspects in food extrusion. International Agrophysics, 16, 191-195.
6. **Jurga R. 1985.** Przetwórstwo zbóż. Część 3. Wydawnictwa Szkolne i Pedagogiczne. Warszawa.
7. **Levin L. 1997.** More on extruder balance. Cereals Foods Worlds, 42, 22.
8. **Mercier C., Linko P, Harper J.M. 1998.** Extrusion Cooking. AACC, Minnesota, USA, ISBN 913250678.
9. **Mitrus M., Wójtowicz A., Oniszczuk T., Mościcki L. 2012.** Rheological properties of extrusion-cooked starch suspension. Teka Commision of Motorization and Energetics in Agriculture, Vol. 12, No. 1, 143-147.
10. **Moscicki L. (ed.). 2011.** Extrusion-Cooking Techniques. WILEY-VCH Verlag & Co.KGaA, Weinheim, Germany.
11. **Mościcki L. 2002.** Engineering and energy aspects of baro-thermal processing in feed industry. Teka Commision of Motorization and Energetics in Agriculture, Vol. II, 129-135.
12. **Mościcki L., Mitrus M., Wójtowicz A. 2007.** Technika ekstruzji w przemyśle rolno-spożywczym. Warszawa, PWRiL, ISBN 9788309010272.
13. **Oniszczuk T., Mościcki L. 2009.** Physical properties and energy consumption of the manufacture of extrusion-cooked carp feed enriched with Echinacea. Teka Commision of Motorization and Energetics in Agriculture, Vol. IX, 181-191.
14. **Wójtowicz A. 2012.** Influence of process conditions on selected texture properties of precooked buckwheat pasta. Teka Commision of Motorization and Energetics in Agriculture, Vol. 12, No. 1, 315-322.
15. **Wójtowicz A., Kolasa A., Mościcki L. 2013.** The influence of buckwheat addition on physical properties, texture and sensory of extruded corn snacks. Pol. J. Food Nutr. Sci., Vol. 63, No. 1.
16. **Wójtowicz A., Mościcki L., Mitrus M., Oniszczuk T. 2010.** Wpływ konfiguracji układu plastyfikującego na wybrane cechy ekstrudowanych makaronów pełnoziarnistych. Inżynieria Rolnicza, Nr 4 (122), 291-297

ENERGOCHŁONNOŚĆ PROCESU EKSTRUZJI SKROBII KUKURYDZIANEJ

Streszczenie. W pracy przedstawiono wyniki pomiarów energochłonności procesu ekstruzji skrobi kukurydzianej. Proces ekstruzji przeprowadzono na ekstruderze jednoślimakowym o L/D=16 przy zmiennych obrotach ślimaka w zakresie 60 – 120 obr×min-1. W badaniach zastosowano skrobię kukurydzianą o zróżnicowanej wilgotności. W trakcie prowadzonych badań odnotowano zmiany energochłonności procesu ekstruzji w zależności od wilgotności surowca, obrotów ślimaka ekstrudera i temperatury obróbki. Wzrost prędkości obrotowej ślimaka ekstrudera przyczyniał się do wzrostu energochłonność procesu ekstruzji. Zastosowanie skrobi kukurydzianej o wyższej wilgotności skutkowało obniżeniem energochłonności procesu ekstruzji. Temperatura procesu nie miała istotnego wpływu na zmiany SME podczas przetwarzania skrobi kukurydzianej.

Słowa kluczowe: ekstruzja, skrobia kukurydziana, energochłonność.

TEKA. COMMISSION OF MOTORIZATION AND ENERGETICS IN AGRICULTURE – 2013, Vol. 13, No. 2, 67–72

Selection of decisive variables for the construction of typical end user power demand profiles

Krzysztof Nęcka

Department of Power Engineering and Agricultural Processes Automation, Agricultural University of Cracow
Balicka Str. 116B, 30-149 Kraków, Poland, e-mail: krzysztof.necka@ur.krakow.pl

Received May 16.2013; accepted June 28.2013

Summary. This study provides a description of the impact of critical variables of various grouping methods on the quality of the developed hourly power demand schedule. The adequacy of various indicators reflecting the course of power consumption was checked against the appropriate classification of daily load profiles in the clustering process. According to the performed simulations, the lowest MAPE and ΔESR error values of 14,01% and 12,65% were achieved with the EM concentration analysis algorithm and the following variables: daily peak and average daily load of electric power, shape coefficient, interval, variance, daily load variation rate and production output quantity. Furthermore, it was observed that within the data clustering performed on basis of the EM algorithm more homogeneous groups of week days were obtained, provided that the input variables had been standardised.

Key words: concentration analysis,load profile, load variation rates, short-term forecast.

INTRODUCTION

As of 1st July 2007 all end recipients, that is customers purchasing electricity for own needs, are entitled to freely choose the electricity supplier [13]. Since the freeing of the electricity prices until the end of October 2012 over 61 500 of industrial and commercial customers and almost 64 thousand households have used the right to change the electricity provider [18]. Customers who have exercised this right may become schedule-based recipients, provided that they are equipped with a measurement and billing system, with a possibility to register the real hourly power consumption values [8]. In such case they are obliged to develop a commercial consumption schedule which specifies the amounts of power demand in the specific hours of day and night '*n*'. This schedule must be submitted in a format determined in the power supplies contract to the distribution system on the day '*n*-1' before 7.30 am. It is mainly the quality of the developed load schedule which determines whether instead of expected profit additional expenses will be incurred due to the necessity to make additional deals in the power balancing market [12]. On the day '*n*+1' a clearance of differences generated by the real consumption diverging from the ordered power in the specific hours of the '*n*' day is performed. Such clearance is carried out on basis of dynamically changing prices of electric power on the balance market in the specific hours of the '*n*' day.

As an alternative for acting as a schedule-based customer within the SMEs sector, and in order to lower the electricity costs, it is possible to remain a tariff customer and renegotiate the so-far terms of contract, together with the re-selection of power demand and tariff group [14, 16]. While negotiating the unit price of electric power with the current or new supplier it is advantageous to have an own hourly power demand profile which enables the customer to reduce the balance difference against the allocated standard power consumption profile.

The knowledge of the typical hourly power demand profiles of end customers is thus essential both from the point of view of power suppliers and customers [20, 22]. Currently, as electricity is regarded as merchandise, the appropriate classification of daily load profiles and their effective analysis gains high economic and technical importance. The developed power demand profiles may be used by the end user among other for the creation of a commercial operating schedule and the selection of an optimal tariff group. On the other hand, power distribution companies use the load curves in order to formulate their pricing strategies, develop tariffs and undertake measures for the improvement of efficiency of their distribution grids.

After the emerging of microprocessor devices for constant measurement and recording of power consumption, the access to data required for the construction of typical hourly power demand profiles has become very simple. Extensive databases are thus available, but the question arises how to obtain the greatest possible amount of information to

construct an optimal hourly load profile out of such a great collection of power demand variation data.

The purpose of this study is to determine an optimum set of decisive variables for the determination of typical hourly power demand profiles of end users generating the lowest total amount energy subject to clearance on the balancing market.

MATERIAL AND METHOD

The objective of this study was accomplished on basis of own research in a medium-size family company established in 1990. The company runs a modern poultry slaughterhouse with a cold store in the Małopolskie voivodeship. The main scope of its business is slaughter and sales of poultry in the national market, as well as Slovakia and Ukraine.

The study goal was achieved on basis of own research results of 24-hour measurements and automatic recording of average active power load and power consumption at 15-minute intervals, carried out for one year by means of a specialist AS-3 Plus grid parameter analyser manufactured by the Twelve Electric company from Warsaw. The measurement results were then compiled into one-hour time intervals and saved in a worksheet as a database. Each record of the created database included also information on the date and hour of the specific power consumption and the number of production output quantity of a given day. The collected data provided the basis to determine the indicators depicting the daily fluctuation of load and develop the daily load profiles.

In order to create homogeneous day groups of the greatest hourly power consumption match rate, the adequacy of the *k*-average grouping method and EM method was checked, with the application of various distance measures between clusters.

The quality evaluation of developed load profiles was performed by (*APE*) with the use of differences between the forecast hourly power demand determined on their basis and the real consumption, with the consideration of the value of relative forecast tolerance (APE), average relative forecast tolerance (*MAPE)* and percentage share of balance power in the total power consumption (Δ*ESR*):

$$APE = \frac{\left|E_t - E_t^p\right|}{E_t} \cdot 100, \tag{1}$$

$$MAPE = \frac{1}{n} \cdot \sum_{t=1}^{n} \frac{\left|E_t - E_t^p\right|}{E_t} \cdot 100, \tag{2}$$

$$\Delta ESR_t = \frac{\sum_{t=1}^{n} \left|E_t - E_t^p\right|}{E_c} \cdot 100, \tag{3}$$

where:
E_t – real electric power consumption in t hour,
E_t^p – forecast electric power consumption in t hour,
E_c – real electric power consumption in the examined period,
n – number of monitoring hours.

RESEARCH RESULTS

In the first stage of research, one common load profile of all days of the year was developed on basis of raw data. As the next step, the number of developed profiles was increased for an ever narrower number of days, taking into account calendar days, that is month name, type of day (working or holiday) and day name. In the last stage it was assumed that on the day preceding the planned electricity supplies, that is day *n-1*, the facility would inform the seller whether slaughtering of poultry was planned on day *n*, without providing the production output quantity. The quality evaluation results of the specific profiles are presented in Table 1.

According to the performed analyses, the development of a single common hourly profile of power consumption for all days of the year will have an average value of relative forecast tolerance of 40%, while the share of power to be cleared on the balancing market will amount to 30% of total power consumption. As expected, the calendar data improved the quality of developed typical profile models. On basis of these information the lowest values of indicators reflecting the quality of the hourly power demand schedule were obtained by constructing separate load schedules for working days and holidays, regardless of the specific months of the year. For the analysed load profiles, the value of the MAPE tolerance ranged from 20,79% to 24,25%. On the other hand,

Table 1. Quality of daily load profile developed with the consideration of the calendar

Type of schedule	*MAPE* [%]	Δ*ESR* [%]
Common schedule for all days of the year	39,75	31,51
Separate load schedules for working days and holidays	24,25	20,69
Separate load schedules for working days and holidays, taking into account whether slaughter activities were planned on a given day	22,80	19,90
Separate load schedules for working days, Saturdays, Sundays and holidays	22,91	19,80
Separate load schedules for the specific days of the week	22,63	19,57
Separate load schedules for working days and Saturdays, Sundays and holidays, taking into account whether slaughter activities were planned on a given day	21,66	19,42
Separate load schedules for working days and holidays in the summer, winter and spring-autumn	22,67	19,33
Separate load schedules for working days and holidays in the specific months	20,79	17,78
Separate load schedules for working days and holidays in the specific months, taking into account whether slaughter activities were planned on a given day	18,13	15,38

the share of energy to be cleared in the balancing market amounted to 17,78%-20,69% of total power consumption in the facility. Thanks to the use of information whether on a given day poultry slaughtering activities were to be carried out, it was possible to lower the values of indicators evaluating the quality of estimate profiles approximately by further 2%. The reason why the quality of performed hourly consumption forecast has improved was the correct classification of the specific day types into the groups of working days and holidays. Poultry slaughtering was not performed on every working day and also there were holidays on which slaughtering-related processes were running.

Nevertheless, all the so-far developed typical hourly power consumption profiles were highly erroneous. Their main reasons include changes of load profile for working days depending on the production output quantity and the occurrence of days with modified production technology. The first variable can be quite easily considered while developing the load curves, as daily production records were maintained in the facility. The information on switching between the production of whole or portioned poultry meat were unfortunately not recorded.

In the next stage of research the determination of typical days was performed, so that the respectively developed daily load curves would allow to determine hourly power demand forecasts generating smaller amounts of power proportion to be cleared in the balancing market. The results of this research will also be used to identify the days with the corresponding production process.

In order to create typical load profiles, the most effective indicators reflecting the daily load variation were searched for out of the ones described in the literature [1, 2, 3, 4, 5, 9, 10, 11, 17, 19]. Due to the great number of available indicators, their preliminary selection was performed on basis of their importance, variability and mutual correlation strength.

The importance analyses of the specific indicators was performed on basis of convexity of the cumulative distribution function. Examination of convexity of the empiric cumulative distribution function was performed according to the following algorithm [15]:

a) specific load variation indicators $X_j (j = 1, 2,...,m)$ were subjected to normalisation according to formula 4, as a result of which vectors were obtained with feature values contained within <0,1>:

$$x_{ij} := \frac{x_{ij} - \min\limits_{i} x_{ij}}{\max\limits_{i} x_{ij} - \min\limits_{i} x_{ij}}, \quad i = 1,2,...,n; \; j = 1,2,...,p, \tag{4}$$

b) transformed values of the specific features were sorted ascending and a median was determined:

$$M_{ej} = \frac{x_{ij\left(\frac{n}{2}\right)} + x_{ij\left(\frac{n}{2}+1\right)}}{2}, \tag{5}$$

c) value of the t_j indicator was found:

$$t_j = 1 - \sum_{(i:x_{ij} \le o,5)} w_{ij}, \qquad \text{j} = 1,2,..., \text{p}, \tag{6}$$

where:

$$w_{ij} = \frac{1}{n}.$$

Evaluation of importance of the specific indicators performed on basis of value t_j. This parameter may be regarded as an inhibitor, as together with its growth the feature importance falls. For further analyses, only such load variation rates were selected in case of which t_j was lower than the adopted threshold value of 05.

In order to evaluate the variation of the specific indicators, the ε variation rate was used, calculated with the relationship (7) and it was required that the features are more changeable than the arbitrarily adopted value of ε=20% [15]:

$$\varepsilon_j = \frac{s_j}{X_{jsr}}, \tag{7}$$

where:
S_j – standard deviation of the load fluctuation rate,
$X_{jśr}$ – average value of the load fluctuation rate.

In order to eliminate unfavourable phenomena occurring in case of common varying of coefficients, it was required that the linear correlation power between the specific indicators reflecting the load variation used for the development of a typical load profile had to be lower than 0,8.

As the presented requirements for the development of typical hourly power demand profiles are met, the following indicators were selected:

daily power consumption: $$A_d = \int_{i=1}^{T_d} P_i dt, \tag{8}$$

daily peak load: P_{ds},
daily average load P_{dsr},
peak load hour: t_{ps},

unevenness indicator of daily power demand: $$m_o = \frac{P_{do}}{P_{ds}}, \tag{9}$$

daily peak compensation grade: $$l_{ds} = \frac{P_{ds}}{P_{dsr}}, \tag{10}$$

daily load shape coefficient: $$k = \frac{P_{srkw}}{P_{dsr}},$$

daily load interval: $$R = P_{ds} - P_{do},$$

daily load variance: $$s^2 = \frac{1}{24}\sum_{i=1}^{24}\left|P_i^2 - P_{dsr}{}^2\right|, \tag{11}$$

standard deviation of daily load: $$s = \sqrt{s^2},$$

average deviation of daily load: $$d = \frac{1}{24}\sum_{i=1}^{24}\left|P_i - P_{dsr}\right|, \tag{12}$$

fluctuation rate of daily load: $$V = \frac{s}{P_{dsr}},$$

daily load median: $$M_e = \frac{P_{\left(\frac{n}{2}\right)} + P_{\left(\frac{n}{2}+1\right)}}{2}, \tag{13}$$

geometrical average of daily load:

$$G_e = (P_1 \cdot P_2 \cdot ... \cdot P_{24})^{\frac{1}{24}}, \quad (14)$$

average harmonious daily load:

$$H = \frac{24}{\sum_{i=1}^{24} \frac{1}{P_i}}, \quad (15)$$

where:
P_i, P_j - load in hour i (j),
i, j = 1, 2, ..., 24,
T_d = 24 hours.

Due to the fact that many coefficients depicting the load fluctuation fulfilled the requirements during the cluster analysis performed in the *Statistica 10.0* application, attempts were made to determine the most effective indicators by means of the „*Selection of variables and analysis of causes*" module available in the programme. The cluster analyses were performed with the *k*-average method and EM method, belonging to the non-hierarchical category. The classic algorithm of *k*-averages was popularised by Hartigan [6, 7]. The essential idea of this algorithm is to assign an observation of a set number of *k*-clusters in such a manner that a minimum internal differentiation and maximum inter-group differentiation is achieved. During the cluster analysis performed with *k*-averages also the influence of the following observation distance measures was examined:

– Euclidean – distance $(x, y) = \sum_{i=1}^{n} \sqrt{(x_i - y_i)^2}$,

– city (Manhattan, City block) – distance:

$$(x, y) = \sum_{i=1}^{n} |x_i - y_i|,$$

– Chebyshev – distance $(x, y) = maksimum|x_i - y_i|$.

The EM method algorithm for cluster analysis was described in detail by Witten and Frank [21]. Its basic idea relies on the determination of the probability density function for the specific variables. Then, the average value is determined, together with standard deviation for each created cluster, so that the reliability of observed distribution is maximised. In the EM method, the distances between clusters are calculated with the Euclidean measure.

In the specific analyses the optimum cluster quantity was determined on basis of a crosscheck multiplied with *v*. This method consists of dividing data into random-selected v-separable parts. In the next step, an analysis for the preliminarily adopted *k* value is performed in order to find a prediction for *v*-of this data group by using for this purpose *v-1* of a part of data as reference cases. As we know the dependent variable data in the data cluster for which the prediction was made, the prediction tolerance can be calculated. The accuracy rate is counted as a percentage of properly classified cases. Then the entire procedure is repeated for all *v* data segments. At the end of the cycle the errors are averaged and model quality measures are determined. The above procedure is repeated for various *k* values. As an optimum number of clusters *k* value was adopted with regard to which the best model quality was obtained.

Table 2. Quality description of a daily load profile developed on basis of power demand fluctuation indicator cluster analysis

Grouping method	Input variable, formula no.	Cluster interval	Number of clusters	*MAPE* [%]	Δ*ESR* [%]
k-average algorithm	8-24	Euclidean	5	17,34	14,73
k-average algorithm	8-24 after standardisation	Euclidean	5	17,34	14,73
k-average algorithm	9,16,23,24	Euclidean	5	18,43	15,68
k-average algorithm	24	Euclidean	9	19,93	16,16
k-average algorithm	9,10,14–16,19, 23, 24	Euclidean	5	17,47	14,8
k-average algorithm	8-24	Manhattan	5	21,39	17,3
k-average algorithm	8-24 after standardisation	Manhattan	5	17,28	14,72
k-average algorithm	9,16,23,24	Manhattan	6	18,04	15,12
k-average algorithm	24	Manhattan	9	18,61	15,04
***k*-average algorithm**	8-10,14-16, 19, 23, 24	Manhattan	5	16,11	14,1
k-average algorithm	8-10,14-16, 19, 23, 24 after standardisation	Manhattan	5	18,31	15,29
k-average algorithm	8-24	Chebyshev	5	18,19	15,16
k-average algorithm	8-24 after standardisation	Chebyshev	5	18,19	15,16
k-average algorithm	9,16,23,24	Chebyshev	5	18,48	15,55
k-average algorithm	24	Chebyshev	9	18,61	15,04
k-average algorithm	9,10,14-16,19,23, 24	Chebyshev	5	17,19	14,68
EM algorithm	8-24	Euclidean	3	19,4	16,13
EM algorithm	8-24 after standardisation	Euclidean	5	16,02	14,16
EM algorithm	9,10,17,23,24	Euclidean	2	21,36	17,64
EM algorithm	13,14,21-23 after standardisation	Euclidean	5	15,18	13,58
EM algorithm	24	Euclidean	1	39,74	31,51
EM algorithm	21 after standardisation	Euclidean	2	26,23	21,49
EM algorithm	8-10, 14 -16, 23, 24	Euclidean	3	19,88	16,52
***EM* algorithm**	8-10,13,14,19-23 after standardisation	Euclidean	7	14,01	12,65

In table 2, the error values of hourly power demand forecast errors are listed, as obtained on basis of various indicator combinations depicting the power demand and various distance measures between the observations.

By using indicators depicting the fluctuation of load for the purpose of determining days with a similar load profile, both the average relative percentage tolerance and the power cleared on the balancing market was reduced. By using the *k*-average algorithm for analysing purposes the lowest MAPE and Δ*ESR* error values of 14,01% and 12,65% were achieved by using the following indicators for the development of typical daily load profiles: daily peak and average daily load of electric power, shape coefficient, intervals, variance, daily load variation rate and production output quantity. Also an over 1% error rate reduction was observed in case of analyses where the clusters observation interval was Manhattan.

The same set of variables in the cluster analysis with the EM method has allowed to obtain load profiles that were less consistent with real data, while forecasts created on their basis generated higher amounts of power to be balanced out. It was however noticed that for the EM algorithm one can achieve much more homogeneous week day clusters, and therefore develop load profiles which may generate forecasts involving a relatively small error risk (*MAPE* = 14,01%, Δ*ESR* = 12,65%), provided that the input data are standardised. The desired impact of standardisation of exogenous variables on the quality of hourly power demand forecasts was not clearly stated for the *k*-average algorithm.

CONCLUSIONS

According to the performed analyses, the development of a single common hourly profile of power demand for all days of the year will have an average value of relative forecast tolerance of 40%, while the share of power to be cleared on the balancing market will amount to 30% of total power consumption.

Thanks to the use of calendar data for the development of typical profiles, the *MAPE* tolerance was reduced below 25%. On the other hand, the share of energy to be cleared in the balancing market remained below 21% of total power consumption in the facility. Furthermore, thanks to the use of information whether on a given day poultry slaughtering activities were to be carried out (without information on their extent), it was possible to lower the values of indicators evaluating the quality of estimate profiles approximately by further 2%.

By using indicators depicting the fluctuation of load for the purpose of determining days with a similar load profile, both the average relative percentage tolerance and the power cleared on the balancing market was reduced. Within the performed research the lowest MAPE and Δ*ESR* error values of 14,01% and 12,65% were achieved with the EM concentration analysis algorithm and the following variables: daily peak and average daily load of electric power, shape coefficient, interval, variation, daily load fluctuation rate and production output quantity. The obtained tolerance (error) level will act as a point of reference while developing hourly power demand forecasts both for conventional and alternative models.

REFERENCES

1. **Bieliński W. 1998:** Typowe wykresy obciążeń elektroenergetycznych wybranych odbiorców. Materiały V Konferencji Naukowo-Technicznej „Rynek energii elektrycznej REE'98". Nałęczów. 307-314.
2. **Chojnacki A. Ł. 2008**: Zmienność obciążeń w układach sieciowych SN zasilających odbiorców komunalnych na terenach miejskich oraz wiejskich. V Ogólnopolska Konferencja Naukowa PTETiS „Modelowanie i Symulacja". Kościelisko 23-27 czerwca. 125-128.
3. **Chojnacki A. Ł. 2009**: Analiza dobowej, tygodniowej i rocznej zmienności obciążeń elektroenergetycznych w sieciach miejskich oraz wiejskich. Przegląd elektrotechniczny. Nr 06. 9-12.
4. **Derecka M., Bieliński W. 2002:** Nowe charakterystyki zmienności mocy pobieranej przez odbiorców. Materiały VI Konferencji Naukowej „Prognozowanie w elektroenergetyce PE'2002". Częstochowa. 39-47.
5. **Dudek G. 2004:** Wybrane metody analizy szeregów czasowych obciążeń elektroenergetycznych. Materiały VII Konferencji Naukowej „Prognozowanie w elektroenergetyce PE'2004". Częstochowa. 116-125.
6. **Hartigan J. A. 1975:** Clustering Algorithms**,** New York: John Wiley & Sons.
7. **Hartigan J. A., Wong M. A. 1978:** Algorithm 136. A *k*-means clustering algorithm. Applied Statistics. *28*. 100.
8. Instrukcja Ruchu i eksploatacji sieci dystrybucyjnej. Enion Grupa TAURON
9. **Kaźmierczyk A., Chojnacki A. Ł. 2011:** Analiza dobowej i tygodniowej zmienności obciążeń mocą czynną i bierną elektroenergetycznych sieci dystrybucyjnych SN, miejskich oraz terenowych. Energetyka. Nr 1. 29-37.
10. **Łyp J. 2003:** Metodyka analizy i prognozy obciążeń elektroenergetycznych systemów lokalnych. Rozdział w książce pt. „Zastosowania metod statystycznych w badaniach naukowych II". StatSoft. Kraków. 91-104.
11. **Łyp J., Kurach M. 2011:** Problematyka prognozowania sezonowej zmienności obciążeń szczytowych krajowego systemu elektroenergetycznego. Rynek Energii. Nr 1(92). 97-100.
12. **Majchrzak H, Mroziński A., Pozniak R. 2005:** Wpływ funkcjonowania rynku bilansującego na koszty ponoszone przez uczestników rynku energii elektrycznej. Energetyka. Nr 6. 376-380.
13. Ustawa z dnia 10 kwietnia 1997 r. Prawo energetyczne. Dz.U. z 1997 r. nr 54 poz. 348 wraz z późniejszymi zmianami.
14. **Nęcka K. 2012:** Analiza efektywności zmiany grupy taryfowej na przykładzie oczyszczalni ścieków. Inżynieria Rolnicza. Nr 2 (136). 257-266.
15. **Ostasiewicz W. (red). 1999:** Statystyczne metody analizy danych. Wydawnictwo Akademii Ekonomicznej we Wrocławiu.

16. **Połecki Z., Michalak G. 2012:** Minimalizacja kosztów zakupu energii elektrycznej odbiorcy przemysłowego. Materiały konferencyjne VIII Konferencja Naukowo-Techniczna Optymalizacja w Elektroenergetyce.
17. **Popławski T. 2005:** Problematyka analizy zmienności i prognoz obciążeń w systemach elektroenergetycznych w warunkach transformacji rynku. Rozdział w Monografii: Metody i systemy komputerowe w automatyce i elektrotechnice. ISBN 83-7193-288-X. Wydawnictwo Politechniki Częstochowskiej. Częstochowa. 144-149.
18. Raport Urzędu Regulacji Energetyki styczeń 2013. [online]. [dostęp 27-03-2013]. Dostępny w Internecie: http://optimalenergy.pl/blog/aktualnosci/raport-urzedu-regulacji-energetyki-styczen.
19. **Trojanowska M. 2010:** Analysis of the power and electricity demand in the dairy plant. Journal of Research and Applications in Agricultural Engineering. Vol. 55(2). 113-116.
20. **Trojanowska M., Nęcka K. 2009:** Determination of typical electric power loads for rural end users. TEKA Komisji Motoryzacji i Energetyki Rolnictwa Vol. IX. Lublin. 357-363.
21. **Witten I. H., Frank E. 2000:** Data Mining: Practical Machine Learning Tools and Techniques. New York: Morgan Kaufmann.
22. **Zalewski W. 2010:** Statystyczna analiza zmienności obciążeń w sieciach rozdzielczych. Economy and Management. Nr 4. 206-213.

DOBÓR ZMIENNYCH DECYZYJNYCH DO BUDOWY CHARAKTERYSTYCZNYCH PROFILI ZAPOTRZEBOWANIA ODBIORCÓW KOŃCOWYCH NA MOC I ENERGIĘ ELEKTRYCZNĄ

Streszczenie. W pracy przedstawiono wpływ zmiennych decyzyjnych oraz różnych metod grupowania na jakość opracowanego grafiku godzinowego zapotrzebowania na energię elektryczną. Sprawdzono przydatność różnorodnych wskaźników opisujących zmienność zużycia energii elektrycznej do właściwej klasyfikacji dobowych profili obciążenia podczas tworzenia skupień. Z wykonanych symulacji wynika, że najniższe wartości błędów MAPE i ΔESR o wartościach 14,01% i 12,65% uzyskano wykorzystując do analizy skupień algorytm EM i następujące zmienne: dobowe obciążenie szczytowe oraz średnie, dobowe zużycie energii elektrycznej, współczynnik kształtu, rozstęp, wariancję, współczynnik zmienności obciążenia dobowego oraz czystą ilość sztuk produkcji. Ponadto zaobserwowano, że w analizie skupień wykonywanej w oparciu o algorytm EM uzyskano bardziej jednorodne grupy dni tygodnia pod warunkiem, że zmienne wejściowe zostały poddane standaryzacji.
Słowa kluczowe: analiza skupień, profil obciążenia, prognoza krótkoterminowa, wskaźniki zmienności obciążenia.

TEKA. COMMISSION OF MOTORIZATION AND ENERGETICS IN AGRICULTURE – 2013, Vol. 13, No. 2, 73–78

The evaluation of the power consumption of the pellets production process from the plant materials

Sławomir Obidziński

Department of Agricultural and Food Techniques, Faculty of Mechanical Engineering, Bialystok University of Technology, 45C Wiejska Street, 15-351 Bialystok, Poland,
tel. +48 0857469282, fax: +48 0857469210, e-mail: obislaw@pb.edu.pl

Received April 5.2013; accepted June 28.2013

Summary. In the paper presents the results of a research on the influence of potato pulp content (15, 20 and 25%) in a mixture with buckwheat hulls and the variable mass flow rate of the mixture (50, 75 and 100 kg·h^{-1}) on the energy consumption of the pelletisation process and on the moisture content of the obtained pellets. On the basis of the research results it was established that the addition of potato pulp to pelletised buckwheat hulls caused a significant reduction in the power consumption of the pellet mill at each of the tested mass flow rates of the flow of the mixture through the working system of the pellet mill and increase of the moisture content of the densified mixture and the pellets produced from this mixture.
Key words: potato pulp, buckwheat hulls, energy consumption, moisture content of pellets.

1. INTRODUCTION

Due to the requirement addressing the reduction of carbon dioxide emission into the atmosphere, universally respected in the recent years, the use of biomass as a raw material in the production of electric energy and heat, including waste biomass from the agriculture and food industry, has become more and more common. Due to the increase in prices and the increasingly more limited accessibility of wood sawdust on the market, as reported by Stolarski, Kwiatkowski [23], there is an growing interest in the use of other natural raw materials for the production of pelletised biofuels, e.g. sunflower, coffee, oats, and many other types of post-production waste [21, 22], including those from the agriculture and food industry [3, 24, 14].

One of the types of waste raw materials obtained from processing buckwheat into groats are by-products such as contaminants, hulls, or shredded buckwheat grains, mixed with particles of broken hulls, commonly known as buckwheat bran. Buckwheat hulls have multiple uses: due to their therapeutic properties they are sold as pillow filler material for therapeutic pillows, quilts or mattresses [23]. Despite the low nutritional value, and owing to the high content of phenols of strong antioxidant properties, they can serve as a source for obtaining these compounds [23]. They can be used as a fodder additive, which allows it to be stored for longer periods of time [2]. They are also used as a raw material for creating composts and substrata for horticulture; as bedding for domestic animals; and as filler for packing fruit and fragile goods [23]. In practice, however, as claimed by Stolarski and Kwiatkowski [23], buckwheat hulls are most commonly treated a waste material, and buckwheat processing plants are seeking realistic possibilities of their utilization.

Stolarski, Kwiatkowski [23] claims that the calorific value of by-products of buckwheat processing, as well as the pellets produced from them, is similar to the calorific value of pellets from pine sawdust or pellets from the common osier. The content of sulphur in buckwheat hulls is very small, therefore, combustion of fuels produced from them causes only a negligible pollution to the environment, which is obviously a significant aspect as far as environmental protection is concerned. According to Borkowska and Robaszewska [1], the advantages of briquettes obtained from buckwheat hulls are similar to those of wood briquettes, and their calorific value is higher than the calorific value of firewood.

An undeniable drawback of buckwheat hulls, however, is their small bulk mass, which makes transport difficult; hence, processing the hulls in the plant where they are produced is the most beneficial solution. In addition, unshredded buckwheat hulls are a material characterized by a low susceptibility to densification, which is confirmed by the author's own research as well as the experiments of Ekofrisa [6], a company that produces pellets from buckwheat hulls. The research allowed to conclude that the production of pellets from buckwheat hulls is more complicated than the produc-

tion from typical biomass material e.g. sawdust, because buckwheat hulls have no binding material. Therefore, hulls are ground into dust and compressed with steam. Due to this, in order to increase the susceptibility of buckwheat hulls to densification and improve the conditions for carrying out the process, a binder material needs to be added to them during the pelletisation process. Potato pulp, which mainly consists of raw fiber, starch remnants and mineral compounds, and is a post-production waste material created during the production of potato starch, can serve as such a material.

According to many researchers the introduction binder additives or another type of biomass waste causes an increase of the kinetic durability of the obtained pellets and a reduction of the power consumption of the pelletisation process [4, 5, 7, 17, 18, 19, 20].

Mediavilla et al. [9] pelletized different mixtures of vine shoots and cork in a commercial pellet mill, using a 20 mm compression flat die. They discovered that with the addition of industrial cork residue to vine shoots less energy was demanded. Other Mediavilla et al. [10] work show that maize starch or lignosulphonate addition (in dosages of 2.5, 5.0 and 7.0 wt.% (d.b.) of dry additive) increased the process stability and decreased the specific energy demand during the pelletisation process of poplar. Kaliyan and Morey [7] also confirmed that addition of lignosulphonate as a binder during pelletisation process improves pellets physical quality and decreases energy demand. According to Kulig and Laskowski [8], total energy consumption of pelleting is affected mostly by the chemical composition of the processed raw materials. Niedziółka et al. [11] claims that the value of power consumption during the densification process is considerably affected by contents of particular elements in plant mixes used for pelleting. Increase of ground wheat and sawdust in plant mixes results in an increase of power consumption from 14 to 34% compared to the power consumed for mixes with lower contents of these elements. Stahl and Berghel [20] concluded, on the other hand, that as the content of turnip waste obtained in the process of making turnip oil in the densified mixture with sawdust was increasing, the energy consumption of the pelletisation process, as well as the mechanical strength and density of the obtained pellets, were decreasing.

The purpose of the paper was to determine the influence of the addition of potato pulp to buckwheat hulls and the variable mass flow rate of the flow of the mixture through the working system of the pellet mill on the power consumption of the process and on the kinetic durability of the obtained pellets.

2. RESEARCH METHODS

This paper presents the results of a research study on the process of pelletisation of a mixture of post-production waste: buckwheat hulls, which were post-production waste created during the production of buckwheat groats in Podlaskie Zakłady Zbożowe S.A. in Białystok, and potato pulp, which was a remnant of washing out starch from potatoes in PEPEES S.A in Łomża.

The moisture content of the raw materials (buckwheat hulls, potato pulp and the prepared mixtures of buckwheat hulls and pulp) before the densification process was determined pursuant to PN-76/R-64752 using a WPE 300S moisture balance with an accuracy of 0.01%, according to the methods presented in [12, 15]. Each time the moisture content of five samples was determined. For the purpose of the measurements, samples with a mass of 5 g were taken and dried in a temperature of 105°C until the indications of the moisture balance remained unchanged in three consecutive readouts in 15s intervals. The mean of the obtained values was adopted as the end result of the determination of the moisture content.

The tests of the pelletisation process of the mixture of buckwheat hulls with potato pulp were carried out on a SS-4 test stand (fig. 1), whose main component was a P-300 pellet mill with a "flat matrix – densification rolls" working system.

The pellet mill (1) was driven by the electric motor 2, whose torque was transmitted through a bevel gear to the shaft on which a flat rotating matrix was mounted; the matrix worked with a stationary system of two bearing-supported densification rolls that force the densified material through the matrix openings. Feeding the densified raw material evenly to the working system of the pellet mill 1 was possible owing to the vibrating feeder 5, passing the material to the working system of the pellet mill through the inlet 3. The pellets left the working system through the outlet 4. The SS-4 stand was equipped with a universal meter 6 for measuring the electric power demand of the device, and a Spider 8 recorder 7 connected to the computer 8. Signals from the universal meter 6 were transmitted to the Spider 8 recorder 7 in the form of binary files which were further processed using the Microsoft Excel and Statistica 10.0PL software.

In the course of the tests carried out on the SS-4 stand, the influence of potato pulp content (z_w=15 %, 20 % and 25 %) in a mixture with buckwheat hulls and the mass flow rate of the flow of the mixture through the working system of the pellet mill (50, 75 and 100 $kg \cdot h^{-1}$) on the electric power consumption of the engine driving the pellet mill, as well as on the kinetic durability of the obtained pellets were determined.

The tests of the densification of the mixture of buckwheat hulls with potato pulp in the working system of the pellet mill, were conducted for the working gap between the densification roll and the matrix of h_r=0.4 mm and a rotational speed of the matrix of n_m=280 rpm. The diameter of the openings in the matrix used in the tests was d_o=8 mm, while their length was l_o=28 mm.

Designating the humidity of the materials, mixture and obtained pellets was performed pursuant to PN-76/R-64752 with the use of a WPE 300S scale-dryer exact to 0.01%. Each time, the humidity of five samples was determined. In the measurement, samples weighing 5g each were taken and dried at the temperature of 105°C until three consecutive readings of the scale-dryer at intervals of 15s remained unchanged. The mean values obtained as a result of this procedure were adopted as the final result of determining the humidity.

a)

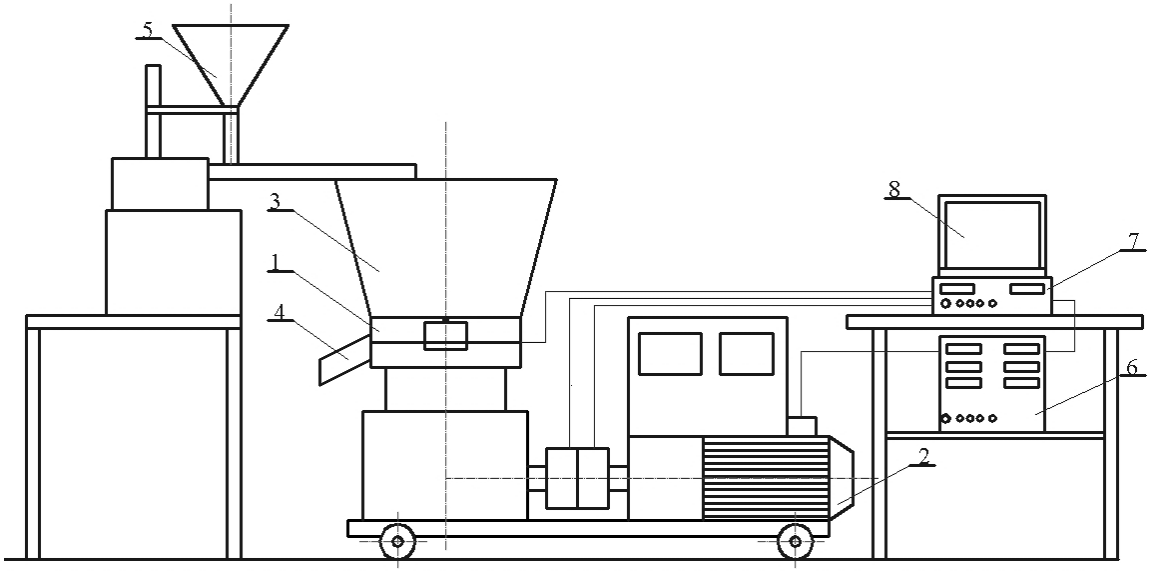

b)

Fig. 1. The SS-4 stand: a) schema of the stand: 1 – working system of the peletizer with the flat matrix, 2 – electric engine driving the peletizer, 3 – cover up the material, 4 – pour out of the pellets, 5 – vibratory feeder, 6 – universal measure to the measurement of the power consumption, 7 – record- keeper Spider 8, 8 – the PC computer, b) the view of the stand

RESEARCH RESULTS

Fig. 2 shows the results of the tests of the influence of the content of potato pulp in a mixture with buckwheat hulls and the influence of the mass flow rate of the flow of the mixture through the working system of the pellet mill on the power consumption of the pellet mill.

The obtained test results (fig. 2) allowed to conclude that increasing the content of potato pulp in a mixture with buckwheat hulls from 15 to 25 % caused a significant reduction of the power consumption of the pellet mill, by approx. 35 % at a mass flow rate of the flow of the mixture through the working system of the pellet mill of 50 kg·h^{-1} (from 2.08 to 1.35 kW); by approx. 35% at a mass flow rate of the mixture of 75 kg·h^{-1} (from 2.73 to 1.78 kW); and by approx. 51 % at a mass flow rate of the mixture of 100 kg·h^{-1} (from 4.26 to 2.07 kW).

The achieved reduction of the power consumption of the pellet mill is caused mainly by the significant increase of the moisture content of the mixture resulting from the increased potato pulp content, from 15 to 25 % (fig. 3).

On the basis of the conducted research of the moisture content of the buckwheat hulls and of a mixture of buckwheat hulls and pulp prior to the pelletisation process it

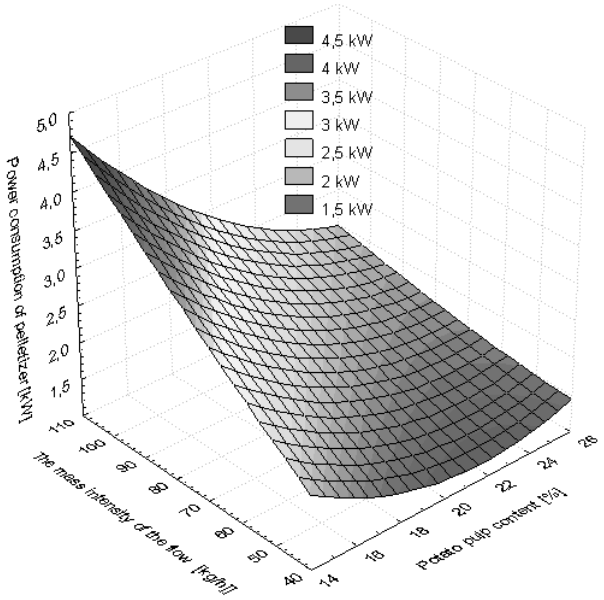

Fig. 2. Correlation between the power consumption of the pellet mill, the content of potato pulp in a mixture with buckwheat hulls and the mass flow rate of the flow of the mixture through the working system of the pellet mill

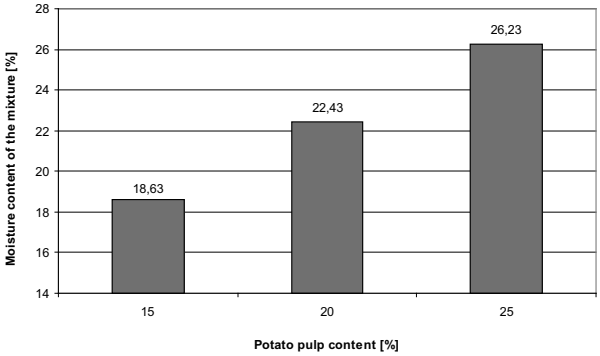

Fig. 3. Correlation between the moisture content of the mixture of buckwheat hulls with potato pulp and the potato pulp content in the mixture

was concluded that the moisture content of the mixture is increasing as the content of pulp in the mixture is increasing.

Buckwheat hulls have a low moisture content of approx. 9.2 %. Pelletisation of hulls of such a low moisture content yields unsatisfactory results. In order to increase their susceptibility to densification and to obtain high density pellets, they need to be shredded, their moisture content needs to be increased prior to the pelletisation process or a binder additive needs to be used. Potato pulp can serve as such an additive, as shown in the author's previous research [12, 13, 15].

The moisture content of the buckwheat hulls mixture increased from 18.63 % (at a 15 % pulp content in the densified mixture) to 26.23 % (at a 25 % pulp content in the densified mixture). Increasing the pulp content in the densified mixture resulted in obtaining bigger and bigger amounts of binder (in the form of a sticky liquid produced from starch and moisture) during the pelletisation process. The increasing content of the produced binder had the effect of "lubrication" of the surface of the openings in the pellet mill matrix, and of reduction of resistance to forcing through the openings. This, in turn, caused a reduction of the power consumption of the pellet mill. This is confirmed by other research of the author, conducted for a mixture of oat bran and potato pulp [16].

The obtained test results (fig. 2) allowed to conclude that increasing the mass flow rate of the flow of the mixture through the working system of the pellet mill from 50 to 100 kg·h^{-1} caused an increase of the power consumption of the pellet mill. At a pulp content in the mixture of 15 %, the increase of the power consumption of the pellet mill was approx. 105% (from 2.08 to 4.26 kW); at a pulp content in the mixture of 20%, the increase of the power consumption of the pellet mill was approx. 49% (from 1.58 to 2.36 kW); whereas at a 25% pulp content in the mixture the increase of the power consumption of the pellet mill was approx. 53% (from 1.35 to 2.07 kW).

The observed increase in the power consumption of the pellet mill at an increasing mass flow rate of the flow of the mixture through the working system of the pellet mill is caused by the fact that as the amount of mixture fed to the working system of the pellet mill is increasing, the amount of material densified in a single densification cycle is also increasing (the thickness of the layer of material pumped into the matrix openings in a single densification cycle is increasing). The increased thickness of the layer in a single densification cycle translates into an increase of the resistance to forcing through the openings and, consequently, an increase of the power consumption of the pellet mill.

The influence of the pulp content z_w in a mixture with buckwheat hulls and the mass flow rate of the flow of the mixture through the working system Q_s on the power consumption of the pellet mill N_g obtained during the densification of a mixture of buckwheat hulls and potato pulp in a "flat matrix – densification rolls" working system was described by the following equation:

$$N_g = 4.62 - 0.46z_w + 0.067Q_s + 0.013z_w^2 - 0.003\, z_w\, Q_s + 5.87\times10^{-5}Q_s^2 \ \text{[kW]}, \quad (1)$$

where:
z_w – pulp content in a mixture with buckwheat hulls [%],
Q_s – mass flow rate of the densified mixture [kg·h^{-1}].

Fig. 4 shows the results of the tests of the influence of potato pulp content in a mixture with buckwheat hulls and the mass flow rate of the flow of the mixture through the working system of the pellet mill on changes in moisture content of the obtained pellets.

On the basis of the performed tests (fig. 4), it can be concluded that increasing the pulp content in a mixture with buckwheat hulls from 15 to 25 % caused a significant increase of the moisture content of the pellets, determined immediately after the densification process.

The obtained increase of the water activity and the moisture content of the pellets as the pulp content increased in a mixture with buckwheat hulls was increasing from 15 to 25 % was caused by the moisture content of the mixture increasing as the pulp content in a mixture with buckwheat hulls was increasing (fig. 3).

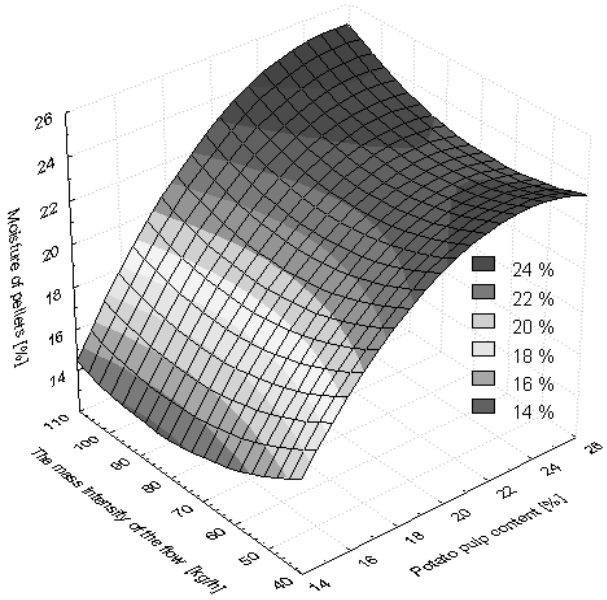

Fig. 4. The influence of potato pulp content in a mixture with buckwheat hulls and the mass flow rate of the flow of the mixture through the working system of the pellet mill on the moisture content of the pellets

The obtained test results (fig. 4) also allowed to conclude that increasing the mass flow rate of the flow of the mixture through the working system of the pellet mill from 50 to 100 $kg \cdot h^{-1}$ caused a slight reduction of the moisture content of the obtained pellets. The highest reduction of the moisture content of the obtained pellets as the mass flow rate of the flow of the mixture through the working system of the pellet mill was increasing from 50 to 100 $kg \cdot h^{-1}$ was recorded at a 15 % pulp content in the mixture – a reduction of the moisture content of the obtained pellets by approx. 7%.

The pelletisation process caused a reduction of the moisture content (fig. 4), in comparison with the moisture content prior to the densification process (fig. 3).

CONCLUSIONS

1. Increasing the potato pulp content in a mixture with buckwheat hulls from 15 to 25 % caused a significant reduction in the power consumption of the pellet mill at each of the tested mass flow rates of the flow of the mixture through the working system of the pellet mill.
2. Increasing the mass flow rate of the flow of the mixture through the working system of the pellet mill from 50 to 100 $kg \cdot h^{-1}$ caused a significant increase of the power consumption of the pellet mill, at each of the tested pulp contents in a mixture with buckwheat hulls. The highest increase, by approx. 105 % (from 2.08 to 4.26 kW), was recorded at a pulp content in the mixture of 15 %.
3. The pelletisation process influenced the reduction of the moisture content of the densified mixture. The value of the reduction of the moisture content was decreasing as the pulp content in the densified mixture was increasing.

REFERENCES

1. **Borkowska B., Robaszewska A., 2012**. Use of buckwheat grain in various industry branches. Science Excercises of The Sea Academy in Gdynia, No. 73, 43-55. [in Polish].
2. **Chachułowa J., (editor). 1999**. Fodders. SGGW Publication, Warsaw. [in Polish].
3. **Chou C.S., Lin S.H.,. Lu W.C. 2009**. Preparation and characterization of solid biomass fuel made from rice straw and rice bran. Fuel Processing Technology, 90(2009), 980-987.
4. **Finney K.N., Sharifi V.N., Swithenbank J., 2009**. Fuel pelletisation with a binder: Part I – Identification of a suitable binder for spent mushroom compost – coal tailing pellets, Energy & Fuels 23 (2009) 3195-3202.
5. **Hejft R., 2002.** The pressure agglomeration of vegetable materials. The Library of Exploitation Problems, ITE Radom. [in Polish].
6. **Janušonis V., Erlickyt-Marčiukaitien R., Marčiukaitis M., 2009**. Biomass fuel use in Ekofrisa, Lithuania. EUBIONET III – EE/07/777/SI2.499477.
7. **Kaliyan N., Morey R.V., 2009**. Factors affecting strength and durability of densified biomass products, Biomass Bioenerg. 33 (2009) 337-359.
8. **Kulig R., Laskowski J., 2008**. Energy requirements for pelleting of chosen feed materials with relation to the material coarseness. TEKA Kom. Mot. Energ. Roln., 8, 115-120.
9. **Mediavilla I., Fernández M.J., Esteban L.S., 2009**. Optimization of pelletisation and combustion in a boiler of 17.5 kWth for vine shoots and industrial cork residue, Fuel Processing Technology. 90 (2009) 621-628.
10. **Mediavilla I., Esteban L.S., Fernández M.J., 2012**. Optimisation of pelletisation conditions for poplar energy crop. Fuel Processing Technology 104 (2012), 7-15.
11. **Niedziolka I., Szymanek M., Zuchniarz A., Zawiślak K., 2008**. Characteristics of pellets produced from selected plants mixes. TEKA Kom. Mot. Energ. Roln. – OL PAN, 2008, Vol. 8, 157-162.
12. **Obidzinski S., 2012**. Analysis of usability of potato pulp as solid fuel. Fuel Processing Technology. Fuel Processing Technology 94(2012) 67-74.
13. **Obidzinski S., 2012a**. Fuel and fodder pellets and his production technology. The patents application, P.398399, 12.03.2012r. Polish Patent Office, Warsaw. [in Polish].
14. **Obidzinski S., 2012b** Pelletization process of post-production plant waste. International Agrophisics. Vol. 26(3), 279-284.
15. **Obidzinski S., 2013**. The evaluation of the producing process of the fuel pellets from the oat bran with potato pulp content. Acta Agrophysica, Vol. 20(2), 2013, 389-402. [in Polish].
16. **Obidziński S., Hejft R., 2013**. The pelletting of the plant wastes in the working system of the pelletizer. Journal of Research and Applications in Agricultural Engineering, **Vol. 58**(1), 133-138. [in Polish].

17. Ohman M, Boman C, Hedman H, Eklund R., 2006. Residential combustion performance of pelletized hydrolysis residue from lignocellulosic ethanol production. Energy Fuels 20, 298-304.
18. **Sokhansanj, S., Mani S., Bi X., Zaini P., Tabil L., 2005**. Binderless pelletization of biomass. Presented at the ASAE Annual International Meeting, July 17-20, 2005, Tampa, FL. ASAE Paper No. 056061. ASAE, 2950 Niles Road, St. Joseph, MI 49085-9659 USA.
19. **Sotannde O.A., Oluyege A.O., Abah G.B., 2010**. Physical and combustion properties of charcoal briquettes from neem wood residues. International Agrophisics, 24, 189-194.
20. **Stahl M., Berghel J., 2011**. Energy efficient pilot-scale production of wood fuel pellets made from a raw material mix including sawdust and rapeseed cake. Biomass and Bioenergy 35 (2011), 4849-4854.
21. **Stolarski M., 2006**. Utilization of the biomass to the pelet production. Clean Energy, 6(56): 28-29. [in Polish].
22. **Stolarski M., Szczukowski S., 2007**. The variety of materials to the pelet production Clean Energy, 6(68), 42-43. [in Polish].
23. **Stolarski M., Kwiatkowski J., 2009**. Remains from processing buckwheat nuts into groats as fuel. Pulawy Diary, Exercise 149, 73-80. Puławy. [in Polish].
24. **Shaw M., 2008**. Feedstock and process variables influencing biomass densification. A Thesis. Department of Agricultural and Bioresource Engineering, University of Saskatchewan. Saskatoon, Saskatchewan, Canada.
25. **Wach E., 2005**. The wood pellets properties. Clean Energy, 6/2005 (44). [in Polish].

OCENA ZAPOTRZEBOWANIA NA MOC W PROCESIE PELLETOWANIA ODPADOWYCH MATERIAŁÓW ROŚLINNYCH

Streszczenie. W pracy przedstawiono wyniki badań wpływu zawartości wycierki ziemniaczanej (15, 20 i 25%) w mieszaninie z łuską gryki oraz warunków prowadzenia procesu granulowania (zmiennego masowego natężenia przepływu mieszanki: 50, 75 i 100 kg•h^{-1}) na energochłonność procesu granulowania oraz na wilgotność otrzymanego granulatu. W wyniku badań stwierdzono, że dodatek wycierki ziemniaczanej spowodował znaczny spadek zapotrzebowania granulatora na moc przy każdym z badanych masowych natężeń przepływu mieszanki przez układ roboczy granulatora oraz istotny wzrost wilgotności zagęszczanych mieszanek oraz pelletu wytworzonego z tych mieszanek.

Słowa kluczowe: wycierka ziemniaczana, łuska gryki, zapotrzebowanie na moc, wilgotność granulatu.

Research carried out within the framework of independent research MNiSzW Nr N N504488239.

TEKA. COMMISSION OF MOTORIZATION AND ENERGETICS IN AGRICULTURE – 2013, Vol. 13, No. 2, 79–82

The efficiency of the supplementary light sources applied in the signaling systems of car vehicles

Marek Ścibisz, Jacek Skwarcz

University of Life Sciences in Lublin, Department of Technology Fundamentals

Received May 15.2013; accepted June 28.2013

Summary. The analysis of the light effectiveness of the chosen LED type electric sources used in motorization was shown in the article. The test stand and the test methodology were described. The evaluation of the influence of LED type bulb and the way of its fixing on the efficiency of generating the luminous flux was made on the basis of carried out measurements.
Key words: car lighting, LED bulbs, light effectiveness.

INTRODUCTION

Certifying a car vehicle fit for use needs meeting many technical requirements [9]. One of the basic ones is the efficiency of lighting elements, both the lighting of road (road lights, passing lights, fog lights, reverse lights) and signalling (indicators, stop lights, parking lights). The use of LED type light sources in new constructions of vehicles encourages the owners of older vehicles to search for this type of new light sources and their use in their vehicles. Therefore the range of LED construction were launched on the market [6, 10, 14, 15, 16]. They were recommended as the replacements for traditional bulbs. Unfortunately LED type light devices are fixed in lighting fittings which were certified for incandescent lighting, thus the vehicles which lighting doesn't meet standards can be often met on roads (e.g. the inequality of lighting of the observed surface). It made the authors carry out test allowing to determine the basic parameters of the lighting of the chosen sources of the incandescent light and LED type lighting which can be used in car vehicles.

CAR LIGHT SOURCES

Electric lights sources used in car vehicles can be divided on the basis of the working principle into incandescent lamps and discharge lamps [8]. The construction of these lamps is shown in Fig. 1.

Fig. 1 Car light sources [2]: a. incandescent lamp; b. discharge lamp

In the first group the working principle is based on the flow of current through a conductor. The second group uses the electric discharge in gases. The incandescent lamp emits the light as the result of the heating of the heating element (filament) [12]. The quantity of the emitted light stream and its colour depend on the temperature of the filament. It is proportional to the intensity of the flowing current. Supply voltage and the resistance of the filament influence the value of intensity [1].

The discharge lamp emits the light in the result of the electric discharge in the arc tube. The change of the spectrum of light radiation is obtained by changing the gas which arc tube is filled with [17]. Xenon is popular gas at present. Unfortunately these sources of the light require the additional converter raising the supply voltage. The LED light-emitting diode – the new kind of the light source does not have this inconvenience. The visible radiation comes into being in the result of the recombination of electric charges coming through the p-n joint [4]. The schematic principle of the operation of LED was shown in Fig. 2.

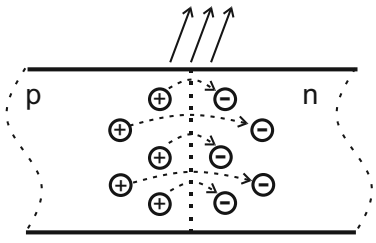

Fig. 2. The schematic principle of operation of light-emitting diode [own study]

In the result of the connection of the electron with "the hole" there is the excess of energy in the p-n joint which is emitted as the electromagnetic radiation [5]. The frequency of the wave, that is the colour of the light, depend on the composition of the base material of the semi-conductive element [13]. The intensity of radiation however depends on the intensity of the electric current coming through the p-n joint [7].

THE TEST STAND

Measurements were carried out with the use of the test stand made in the Department of Technology Fundamentals in Lublin (Fig. 3). The darkroom (1) was used for the test and the investigated sources of light (2) were placed inside. Light source were connected to the controllable feeder of direct current (3). The source of light lit up the measuring screen (4), on the surface of which the illumination was measured with the luxmeter.

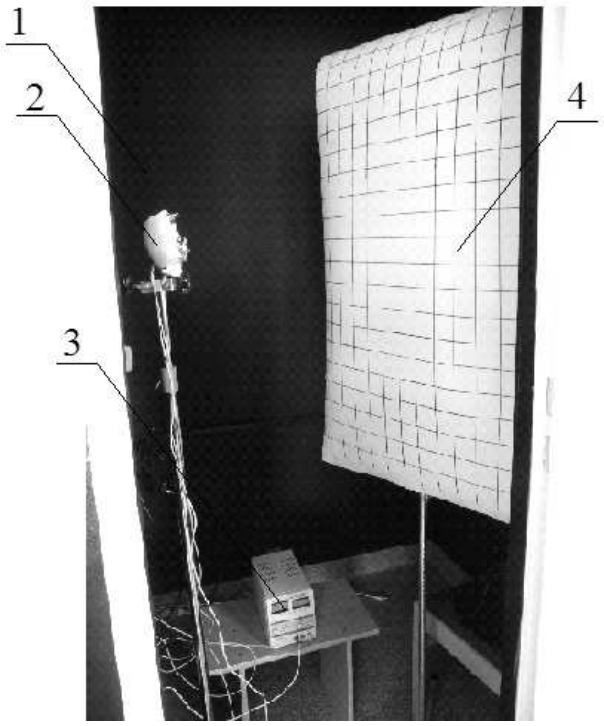

Fig. 3. The test stand for the investigation of the car light sources [own study]: 1- the darkroom; 2 – the lighting fitting of the light source ; 3 – DC feeder; 4 – the measuring screen

The light sources with the type P21W fixing handle were used for the tests. The bulbs of this type are used e.g. in fog lights . R21W bulb, R5W bulb and LED lighting with 5, 9, 12 and 19 light-emitting diodes were used to the test (Fig.4).

The light sources mentioned above were installed in the lighting fitting of rear fog lights (Fig. 5) with the central fixing and side fixing of the light source.

The light bulbs were added to the controllable feeder of the direct current, enabling the control and the measurement of the voltage and the measurement of the intensity of the supply current.

Fig. 4. Light sources used in tests [L11]: BA15s – R21; b. BA15d – R5; c. BA15s – 5LED; d. BA15s – 9LED; e. BA15s – 12LED; f. BA15s – 19LED

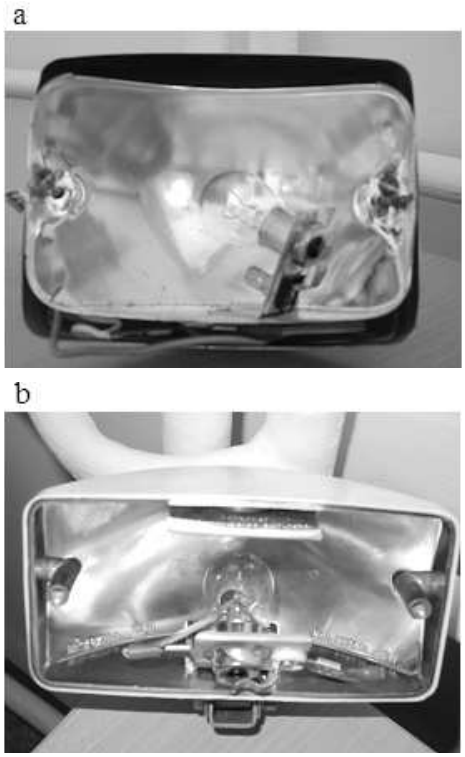

Fig. 5. The lighting fittings used in the test [own study]: a. the central fixing of the light source; b. the side fixing of the light source

THE TEST METHODOLOGY

In order to avoid the influence from outside the test stand was placed in the darkened room. Lighting fittings were fixed to the tripod allowing the control of the fixing height. Light sources were connected to DC feeder. They were supplied with two voltages 12 V and 14,6 V. It corresponds respectively to the voltage of the charged battery and the charging voltage developing when the vehicle engine is running. The feeder makes it possible to read the supply voltage $\boldsymbol{U}$ as well as the consumed current $\boldsymbol{I}$. The lighting of the surface was observed on the measuring screen placed in the distance of 1.5 m from the light source. The surface of the screen was divided into 50mm x 50mm squares.

Each square had attributed coordinates, in order to obtain the explicitness and the repeatability of the position of the measuring points. 80 readings of the value of the lighting intensity were made in every measuring series, placing the sensor of the Elbro ELX2111 Light Meter illuminometer on the marked areas of the screen. The results of measurements were shown in the tables of the spreadsheet (table No. 1). The obtained results of the measurements of the lighting intensity ***E*** were converted into the light stream ***f*** on the basis of the dependence:

$$\phi = \sum_{i=1}^{80} E_i \; S\,[lm], \tag{1}$$

where:
E_i – lighting intensity in measuring point ***i***, lx,
S – the surface of the unitary measuring area, m^2.

The measured value of the supply voltage U and the value of the current intensity I make it possible to calculate the power of the light source:

$$P = U \cdot I\,[\mathrm{W}]. \tag{2}$$

The parameters calculated on the basis of the dependence (1) and (2) enable the calculation of the light effectiveness of the tested light source [8]:

$$\eta = \frac{\phi}{P}\;[lm/W]. \tag{3}$$

THE TEST RESULTS

The measurements were carried out to determine the illumination in given points of the measuring screen. The results of measurements for R5W bulb supplied with the voltage of 14.6 V being the reference to further tests were shown in Table 1.

On the basis of carried out tests the value of the power of the lighting source, the light stream and the light effectiveness were calculated. The overall results of calculations were shown in Table 2.

Table 1. The distribution of the illumination of the measuring screen lighted with the R5W bulb supplied with the voltage of 14.6V centrally installed in the lighting fitting

143	65	38	20	17	20	41	57	74	30
118	62	46	25	17	23	42	60	95	38
77	37	24	20	18	22	30	64	73	59
89	52	21	19	18	20	24	42	72	43
84	36	22	18	17	20	27	50	81	46
34	35	33	27	23	26	33	36	98	38
20	24	28	28	26	28	28	26	43	26
9	11	13	17	17	18	17	16	15	10

Table 2. The electric power, the light stream and the light effectiveness of studied light sources.

The type of lighting	Bulb fixing	Power, W	The light stream ϕ, lm	The light effectiveness E, lm/W
R5W	central	5.8	7.6	1.3
	side	5.7	13.2	2.3
R21W	central	28.3	97.3	3.4
	side	28.2	199.5	7.1
5LED	central	0.4	4.6	10.5
	side	0.4	6.5	14.8
9LED	central	0.6	4.5	7.8
	side	0.6	7.1	12.1
12LED	central	0.8	6.8	8.5
	side	0.9	15.0	17.1
19LED	central	1.8	5.4	3.1
	side	1.8	12.0	6.9

The preliminary analysis of the received test results showed that LED type light source can replace only the bulb of R5W type as far as the light stream is concerned. Thus the further lists do not contain calculations for the R21W bulb.

The basic parameter enabling the exchange of light elements is the light stream emitted by them. The list of values of light streams emitted by various light sources with the voltage supply of 14.6 V and for two ways of fixing the bulb in the lighting fitting (central and side) was shown Fig. 6.

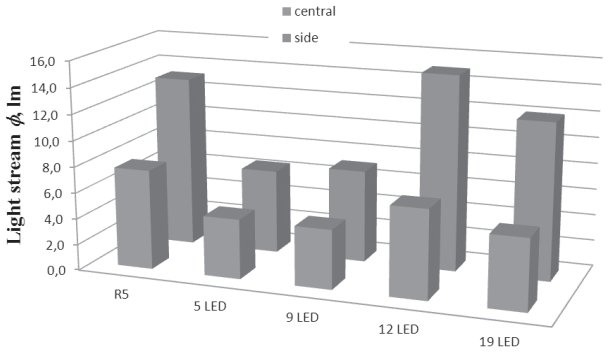

Fig. 6. The comparison of light streams emitted by studied light sources

The comparison of light streams reaching the measuring screen lets us state that 12LED can be the equivalent of the R5W bulb. It has the comparable value with the central fixing in the lighting fitting (7.6 lm and 6.8 lm, i.e. approximately 10% less) and higher with the side fixing (13.2 lm and 15.0 lm, i.e. approximately 13.6% more). The remaining diode light sources however generate the smaller light stream. 19LED has the stream lower by approximately 30% with the central fixing and by approximately 9% with the side fixing. In 9LED the fall of the stream is approximately as much as 41% with the central fixing and approximately 46% with the side fixing. 5LED however is characterized by respectively approximately 39% and 51% lower value of the stream.

The basic advantage of LED type light sources is their high light effectiveness, that is the quantity of the light stream received from 1 watt of the electric power. Thus it

was the next parameter which was the subject of the analysis. The comparison of light effectiveness of the studied light sources was shown in Fig. 7.

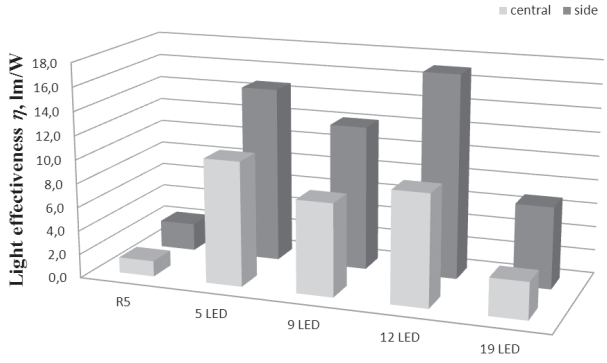

Fig. 7. The comparison of light effectiveness of the studied light sources.

On the basis of the analysis of the of calculations it can be concluded that light effectiveness was higher for every studied light source with side fixing. The diode with 12 light elements (12LED) had the highest light effectiveness. It equalled 17.1 lm/W. The diode with 5 elements (5 LED) had the effectiveness lower by 14 % (14.8 lm/W), the diode with 9 elements (9 LED) had the effectiveness lower by 30% (12.1 lm/W) and the one with 19 elements (19 LED) had the effectiveness lower by 60% (6,9 lm/W). The R5W bulb had the lowest efficiency. Its light effectiveness equalled 2.3 lm/W which was approximately 13% of the maximum effectiveness.

With the central fixing the values of light effectiveness were ranked in the same way as in the side fixing. Their values however were lower by approximately 50% for 12 LED, 30% for 5 LED, 35% for 9 LED and 55% for 19 LED.

CONCLUSIONS

Lighting fittings of car lights used nowadays are designed to use heat or discharge light sources. The use of LED sources in these fittings makes it impossible to use the produced light fully, because of different ways of radiation distribution. The light sources of the LED type emit the directed radiation while the heat sources send the light in all directions.

Large light effectiveness is characteristic of the LED type sources so they becoming more and more popular substitutes of traditional bulbs.

The tests show that these substitutes can only be used in the fittings for fixing light sources used for lighting the elements of the vehicle e.g. the lighting of registration boards or the lighting of the interior. Because the requirements for signalling light such as positional lights or rear fog lights are higher LED with larger number of light elements should be chosen. In our tests it was possible to replace the R5W bulb with 12LED or 19LED diode. The smaller number of elements did not fulfil the condition of the equivalence of the light stream.

However, the large efficiency of the lights of the LED type should lead to development of the new constructional solutions of the lighting fittings adapted to the use of this new light source.

REFERENCES

1. **Bolkowski St. 2013**. Elektrotechnika. WSiP. Warszawa. ISBN: 978-83-02-09397-5, 64
2. **Bosma. 2009**. Bosma – Lamps & Leds. Katalog
3. **Bosma. 2012**. Bosma – for better life. Automotive solutions. Katalog
4. **Chochowski A. 2009**. Podstawy elektrotechniki i elektroniki dla elektryków – cz.2. WSiP. Warszawa. ISBN:978-83-02-08783-7, 60
5. **Chwaleba A., Moeschke B., Płoszajski G. 2008**. Elektronika. WSiP. Warszawa. ISBN:978-83-02-10118-2124
6. **Hella 2013**. Led Technology. http://www.hella.com/hella-pl/129.html?rdeLocaleAttr=pl
7. **Horowitz P., Hill W. 2003**. Sztuka elektroniki. WKŁ. Warszawa. ISBN: 978-83-206-1128-1, 17
8. **Majka K. 1989**. „Elektryfikacja rolnictwa" PWRiL Warszawa ISBN: 83-09-01330-2, 256-269
9. **Ocioszyński J. 2010**. Elektrotechnika i elektronika pojazdów samochodowych. WSiP. Warszawa. ISBN:978-83-02-08141-5, 157-160
10. **Osram 2013**. Osram Led Highlights in motion. http://www.osram.com/osram_com/microsites/amled/amled_microsite_flash_swfobject_com.jsp
11. **Oziemblewski P. 2006**. Technika świetlna od podstaw. http://luxon.pl/PDF/ technika%20swietlna%20od%20podstaw.pdf, 18
12. **Philips. 1995**. Philips Lighting Poland. Informacje o produkcie. Katalog
13. **Praca zbiorowa. 2009**. Elektrotechnika i elektronika dla nieelektryków. WNT. Warszawa. ISBN: 978-83-204-3587-0, 154-5
14. **Polit R. 2012**. Światła do jazdy dziennej – uważaj co instalujesz klientowi. Auto Moto Serwis nr 10, 20-21
15. **Rudek Z. 2012**. Światła do jazdy dziennej, Serwis motoryzacyjny nr 5, 36-37
16. **Ścibisz M., Skwarcz J. 2011**. The effectiveness of lihting of henhouse stands with the use of modern light sources. TEKA Kom. Mot. i Energ. Roln. – OL PAN. Lublin. T.XIc, 385-392
17. Philips Catalogue on line. http://www.ecat.lighting.philips.com

EFEKTYWNOŚĆ ZASTĘPCZYCH ŹRÓDEŁ ŚWIATŁA STOSOWANYCH W UKŁADACH SYGNALIZACJI POJAZDÓW SAMOCHODOWYCH

Streszczenie. W artykule przedstawiono analizę skuteczności świetlnej wybranych elektrycznych źródeł światła typu LED stosowanych w motoryzacji. Opisano stanowisko badawcze i metodykę badań. Na podstawie przeprowadzonych pomiarów dokonano oceny wpływu typu żarówki LED oraz sposobu jej mocowania na efektywność wytwarzania strumienia świetlnego.
Słowa kluczowe: oświetlenie samochodowe, żarówki LED, skuteczność świetlna.

TEKA. COMMISSION OF MOTORIZATION AND ENERGETICS IN AGRICULTURE – 2013, Vol. 13, No. 2, 83–86

The effect of thermal processing on changes in the texture of green peas

Beata Ślaska-Grzywna[1], Dariusz Andrejko[1], Halina Pawlak[2]

[1]Department of Biological Bases of Food and Feed Technologies
[2]Department of Technology Fundamentals
University of Life Sciences in Lublin

Received April 10.2013; accepted June 28.2013

Summary. The study analyzed the effect of thermal processing on changes in the structure of green peas, which was then compared with the texture of canned peas. Thermal processing was done by means of the traditional method (boiling) and in a steam convection oven with different processing parameters. The time of processing and the amount of steam had a significant influence on changes of parameters such as: hardness, elasticity, cohesiveness, gumminess and chewiness. While comparing the values of distinguishing features of canned green peas, it was observed that they were similar to the values obtained for frozen peas after the process of boiling.
Key words: thermal processing, texture, green peas.

INTRODUCTION

The common pea (*Pisum sativum* L.) is a species of leguminous annuals from the Fabaceae. *Pisum sativum* has been known for a few thousands of years, which is confirmed by archaeological findings from the early Neolithic Age (6,000 BC). On the area of Poland the pea was known in the 6th century BC, and the evidence was found in Biskupin settlement. The first information on its cultivation comes from the middle of the 19th century, yet it did not become cultivated on a wide scale until after the 1st World War [1, 2, 3, 11].

As regards its nutritional value and organoleptic properties, grean peas are one of the most valuable food products. It contains a lot of protein, B vitamins, nicotinic acid, panthotenic acid and folic acid, little vitamin C, yet quite a few minerals: potassium, calcium, iron, manganese, phosphorus, sodium, copper, chlorine and iodine [7].

Regarding the structure of the pod, two botanic pea varieties can be distinguished: snow pea (*Pisum sativum* L. *var saccharatum* Ser.) which can be eaten as a whole as it does not have fibrous layer in the inner pod, and scaly pea (*Pisum sativum* L. *var pachylobum* Beck.) with its pods having a "parchment" layer and we can eat its unripe green seeds. As far as the way we make use of it is concerned, we can distinguish pea harvested when still green, that is harvesting mature succulent pods in the state of the so-called milk maturity, filled with green seeds of varied intensity, from dark green to pastel green, and pea harvested dry, that is harvesting dried pods with hardened seeds inside [7, 9, 11, 13, 15].

Green peas are cultivated primarily as an edible plant meant almost exclusively for food processing industry. In food processing fresh seeds are preserved by freezing or canning, and the procedure must take place during the quickest possible time following harvesting. Pea seeds meant for sales i.e. direct consumption or processing should fulfill a number of requirements regarding their organoleptic assessment. The pea should look clean, intact, healthy, well-shaped, the diameter of the seeds must be at least five millimeters. It should be green or yellow, with natural and specific smell [5, 8, 12, 14, 15]. Thus, the aim of the study was to determine the range of modifications: hardness, elasticity, cohesiveness, gumminess and chewiness of frozen green peas, resulting from thermal processing. The results were compared with the data obtained for canned peas [4, 6, 10].

MATERIALS AND METHODS

The research material was provided by canned and frozen green peas made by Bonduelle.

Prior to analyses, frozen pea seeds were calibrated in order to make them homogenous regarding their size. The material prepared in this way was next subject to thermal processing. Each research sample consisted of 15 seedlings of similar mass and size. In the case of canned peas, the seedlings were separated from the sauce.

The seedlings of frozen peas were thermally processed by boiling and heating in the steam convection oven. The thermal processes were done at different time spans, i.e. for 5, 10, 15, 20 and 25 minutes. Steam heating was performed in the XV 303G oven made by Unox, at the temperature

of 80° C and 100° C, with the 100% addition of steam in relation to the initial humidity in the oven's chamber.

Immediately after heating, the texture of warm seedlings (and canned seeds) was analyzed. The measurement of the compression force of individual seedlings was performed in the TA.XT plus texture meter co-operating with the computer. The material was double compressed, with the head moving at the speed of 50 mm·min^{-1}. The process of compression was performed at the constant deformation of the samples amounting to 50% of their height, while the time of the break between the series was 5 s. The measurements were done in 15 replications. The obtained measurements in the form of a fiber diagram in the system of two coordinates of force and time were used to determine the following parameters of the texture: hardness, elasticity, cohesiveness, gumminess and chewiness. After the analyses, the results of measuring the compressive force of the samples were statistically analysed (the analysis of regression and correlation) on the basis of Texture Exponent 32 and Microsoft Excel software.

RESULTS

Figures 1-5 present changes regarding five distinguishing features of the texture (hardness, elasticity, cohesiveness, gumminess and chewiness) of frozen green peas, resulting from thermal processing performed in different conditions. All the analyzed variables are presented in the function of heating time duration.

The hardness of frozen green peas depended both on the applied type of thermal processing and the duration of heating (Fig. 1). The lowest values were registered during boiling, while the highest ones during heating the material in the steam convection oven at the temperature of 80°C and with a 100% addition of steam. After 15 minutes of boiling the hardness of the peas was the lowest, amounting to 2.04 N. It should be noted that no statistically significant differences were observed in the hardness of green peas treated with different methods for 25 minutes. Generally, it should be concluded that heating the material for 5 to 15 minutes led to its reduced hardness, and prolonging the time of processing to 20 and 25 minutes did not result in lowering this value; on the contrary, a slight increase in the hardness of green peas was noted.

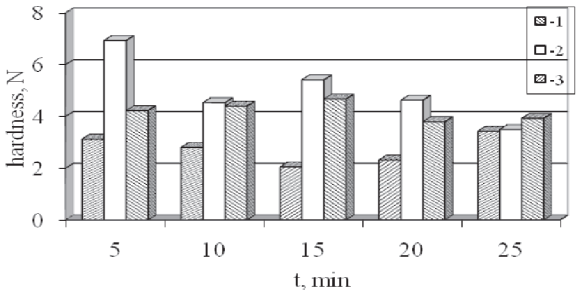

Fig. 1. Changes in the hardness of green peas, depending on the time of its heating with different methods.

1 – boiling, 2 – thermal treatment in steam convection oven at the temperature of 80°C and with a 100% addition of steam, 3 – thermal treatment in a steam convection oven at the temperature of 100°C and with a 100% addition of steam

Table 1. Regression equations and coefficients of determination, R^2, defining changes in the hardness (F) of green peas depending on the duration of heating (t) for the confidence interval of 0.05, 1 – boiling, 2 – thermal treatment in steam convection oven at the temperature of 80°C and with a 100% addition of steam, 3 – thermal treatment in a steam convection oven at the temperature of 100°C and with a 100% addition of steam

Type of treatment	Equation	R^2
1	$F(t) = 0.3\ t^2 - 1.7\ t + 4.7$	0.84
2	$F(t) = 0.06\ t^2 - 1.1\ t + 7.5$	0.71
3	$F(t) = -0.09\ t^2 + 0.4\ t + 3.9$	0.50

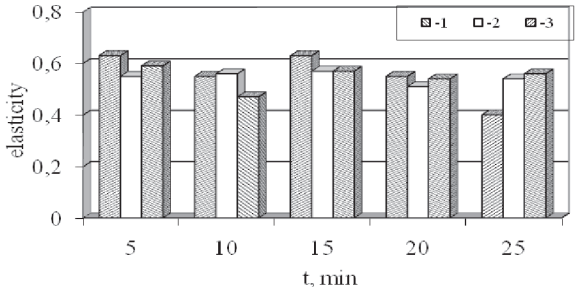

Fig. 2. Changes in the elasticity of green peas, depending on the time of its heating with different methods,

1 – boiling, 2 – thermal treatment in steam convection oven at the temperature of 80°C and with a 100% addition of steam, 3 – thermal treatment in a steam convection oven at the temperature of 100°C and with a 100% addition of steam

Table 2. Regression equations and coefficients of determination, R^2, defining changes in the elasticity (E) of green peas depending on the duration of heating (t) for the confidence interval of 0.05, 1 – boiling, 2 – thermal treatment in steam convection oven at the temperature of 80°C and with a 100% addition of steam, 3 – thermal treatment in a steam convection oven at the temperature of 100°C and with a 100% addition of steam

Type of treatment	Equation	R^2
1	$E(t) = -0.02\ t^2 + 0.08\ t + 0.5$	0.78
2	$E(t) = 0.007\ t^3 - 0.07\ t^2 + 0.2\ t + 0.4$	0.64
3	$E(t) = -0.01\ t^3 + 0.1\ t^2 - 0.4\ t + 0.9$	0.53

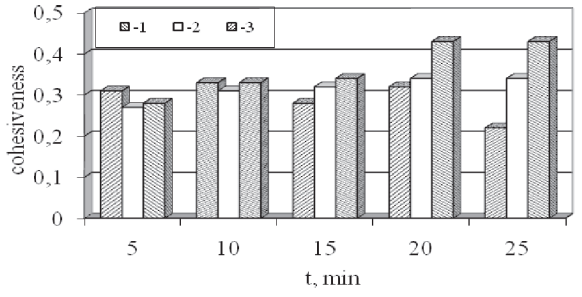

Fig. 3. Changes in the cohesiveness of green peas, depending on the time of its heating with different methods,

1 – boiling, 2 – thermal treatment in steam convection oven at the temperature of 80°C and with a 100% addition of steam, 3 – thermal treatment in a steam convection oven at the temperature of 100°C and with a 100% addition of steam

Table 3. Regression equations and coefficients of determination, R^2, defining changes in the cohesiveness (C) of green peas depending on the duration of heating (t) for the confidence interval of 0.05, 1 – boiling, 2 – thermal treatment in steam convection oven at the temperature of 80°C and with a 100% addition of steam, 3 – thermal treatment in a steam convection oven at the temperature of 100°C and with a 100% addition of steam

Type of treatment	Equation	R^2
1	$C(t) = -0.01\ t^2 + 0.05\ t + 0.3$	0.66
2	$C(t) = -0.005\ t^2 + 0.05\ t + 0.2$	0.98
3	$C(t) = -0.001\ t^2 + 0.05\ t + 0.2$	0.92

Neither of the thermal treatments affected significantly the elasticity or cohesiveness of green peas (Fig. 2 and 3). Only after 25-minute heating statistically significant differences were observed between the process applied and the cohesiveness: the lowest value was recorded after boiling, while the highest value occurred after heating in the steam convection oven at the temperature of 100°C and with a 100% addition of steam. Prolonging the duration of heating did not significantly affect the values of elasticity or cohesiveness.

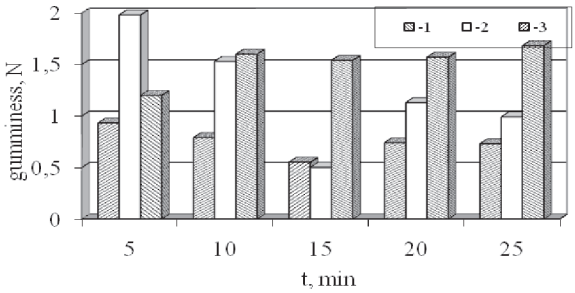

Fig. 4. Changes in the gumminess of green peas, depending on the time of its heating with different methods,
1 – boiling, 2 – thermal treatment in steam convection oven at the temperature of 80°C and with a 100% addition of steam, 3 – thermal treatment in a steam convection oven at the temperature of 100°C and with a 100% addition of steam

Table 4. Regression equations and coefficients of determination, R^2, defining changes in the gumminess (G) of green peas, depending on the duration of heating (t) for the confidence interval of 0.05, 1 – boiling, 2 – thermal treatment in steam convection oven at the temperature of 80°C and with a 100% addition of steam, 3 – thermal treatment in a steam convection oven at the temperature of 100°C and with a 100% addition of steam

Type of treatment	Equation	R^2
1	$G(t) = 0.05\ t^2 - 0.3\ t + 1.2$	0.73
2	$G(t) = 0.006\ t^2 - 0.3\ t + 2.2$	0.91
3	$G(t) = -0.04\ t^2 + 0.3\ t + 1.0$	0.76

Figure 4 presents changes in the gumminess of green peas, resulting from its heating in different conditions. The lowest values were noted during boiling; after 15 minutes of boiling the gumminess of green peas dropped to 0.55 N, reaching its minimum. Further boiling caused further increase in this value. After thermal treatment in the steam convection oven significantly higher values of gumminess were recorded, and a statistically significant effect of the temperature of the process on the measured value was observed.

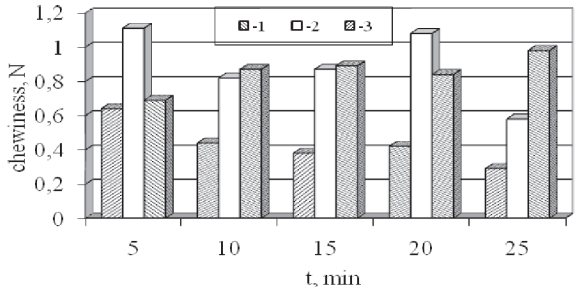

Fig. 5. Changes in the chewiness of green peas, depending on the time of its heating with different methods,
1 – boiling, 2 – thermal treatment in steam convection oven at the temperature of 80°C and with a 100% addition of steam, 3 – thermal treatment in a steam convection oven at the temperature of 100°C and with a 100% addition of steam

Table 5. Regression equations and coefficients of determination, R^2, defining changes in the chewiness (Z) of green peas depending on the duration of heating (t) for the confidence interval of 0.05, 1 – boiling, 2 – thermal treatment in steam convection oven at the temperature of 80°C and with a 100% addition of steam, 3 – thermal treatment in a steam convection oven at the temperature of 100°C and with a 100% addition of steam

Type of treatment	Equation	R^2
1	$Z(t) = 0.02\ t^2 - 0.2\ t + 0.8$	0.84
2	$Z(t) = -0.09\ t^3 + 0.8\ t^2 - 2.0\ t + 2.5$	0.96
3	$Z(t) = -0.01\ t^2 + 0.1\ t + 0.6$	0.72

Similarly to the case of gumminess, the lowest values of chewiness for green peas were noted after the process of boiling. After heating in the steam convection oven, the analyzed values were much (statistically significantly) higher in comparison to boiling. On the other hand, no significant effect of the temperature of heating in the steam convection oven was observed on the value of chewiness of green peas.

Changes of the distinguishing features measured for the texture of green peas caused by different methods of thermal treatment and presented in Figures 1-5 were described by means of regression equations where the time of treatment was adopted as the variable. These equations are valid for the time span of 5 to 25 minutes. The majority of dependencies were described with equations of the 2nd degree, and some of them with equations of the third degree, though we do realize that this presents merely an approximation of the expected changes.

Table 6. Texture parameters of canned green peas

Texture parameters	The arithmetic mean of measurements
Hardness [N]	2.64
Elasticity	0.44
Cohesiveness	0.21
Gumminess [N]	0.55
Chewiness [N]	0.25

Table 6 presents the values of the texture properties included in the research program involving canned green peas. While comparing the data quoted in Table 2 with those recorded after different thermal processes (Fig. 1-5), we can claim that they are similar to the values observed after the process of boiling. On this basis it should be concluded that the texture of canned green peas is very similar to the texture of green peas after 25-minute boiling.

CONCLUSIONS

1. The elasticity of boiled green peas and green peas treated in the steam convection oven does not reveal significant differences.
2. The values of hardness, cohesiveness, gumminess and chewiness of green peas cooked in a traditional way were lower when compared with green peas treated in the steam convection oven.
3. Changes in the texture properties of green peas resulting from thermal treatment can be described very accurately by means of regression equations of the second or third degree.
4. The texture properties of canned green peas are similar to the structural parameters of frozen green peas subjected to 25 minutes of boiling.

REFERENCES

1. **Balcerzak J., Legańska Z., 2000**: Warzywnictwo. Wyd. Hortpress, Warszawa.
2. **Biggs M., McVicar J., Flowerdew B., 2007**: Wielka księga warzyw, ziół i owoców. Dom Wydawniczy Bellona, Warszawa.
3. **Dobrakowska-Kopecka Z., Doruchowski R., Gapiński M., 1998**: Warzywnictwo. PWRiL, Warszawa.
4. Gładyszewska B., Ciupak A., 2011: A storage time influence on mechanical parameters of tomato fruit skin. TEKA Komisji Motoryzacji i Energetyki Rolnictwa PAN V/XI C, 64-73.
5. **Gołacki K., Kołodziej P., 2011**: Impact testing of biological material on the example of apple tissue. TEKA Komisji Motoryzacji i Energetyki Rolnictwa PAN V/XI C, 74-82.
6. **Guz T., 2008**: Thermal quarantine of apples as a factor forming its mechanical properties. TEKA Komisji Motoryzacji i Energetyki Rolnictwa PAN V/VIII A, 52- 62.
7. **Jasińska Z., Kotecki A., 2003**: Szczegółowa uprawa roślin. Tom II, cz. 5. Rośliny strączkowe. Wyd. Akademii Rolniczej we Wrocławiu, Wrocław.
8. **Jiménez-Monreal A.M., García-Diz L., Martínez--Tomé M., Mariscal M., Murcia M.A., 2009**: Influence of cooking methods on antioxidant activity of vegetables. J.of Food Science, Vol. 74, 3, H97-H103.
9. **Kołota E., Orłowski M., Biesiada A., 2007**: Warzywnictwo. Wyd. Uniwersytetu Przyrodniczego we Wrocławiu, Wrocław.
10. **Kuna-Broniowska I., Gładyszewska B., Ciupak A., 2011**: A comparison of mechanical parameters of tomato's skin greenhouse and soil-grown varieties. TEKA Komisji Motoryzacji i Energetyki Rolnictwa PAN V/XI C, 151-161.
11. **Orłowski M., Kołota E., 1999**: Uprawa warzyw. Wyd. BRASICA, Szczecin.
12. **Panasiewicz M., 2009**: An influence of kernel conditioning method on energy consumption during flaking process. TEKA Komisji Motoryzacji i Energetyki Rolnictwa PAN V/IX, 211-216.
13. **Polese J., 2009**: Uprawa fasoli i grochu. Wyd. RM, Warszawa.
14. **Ślaska-Grzywna B., 2010**: Changes in mechanical properties and microstructure of root of celery after thermal treatment. TEKA Komisji Motoryzacji i Energetyki Rolnictwa PAN V/X, 355-362.
15. **Świetlikowska K., 2006**: Surowce spożywcze pochodzenia roślinnego. Wyd. SGGW, Warszawa.

ZMIANY PARAMETRÓW TEKSTURY ZIELONEGO GROSZKU POD WPŁYWEM OBRÓBKI CIEPLNEJ

Streszczenie. W pracy badano wpływ obróbki cieplnej na zmiany tekstury zielonego groszku mrożonego i porównywano z teksturą groszku konserwowanego. Obróbkę cieplną prowadzono sposobem tradycyjnym (gotowanie w wodzie) i w piecu konwekcyjno-parowym przy różnych parametrach obróbki. Stwierdzono istotny wpływ czasu obróbki i ilości dodanej pary na zmiany takich wyróżników tekstury jak: twardość, sprężystość, kohezyjność, gumiastość i żujność. Porównując wartości wyróżników dla groszku konserwowanego stwierdzono, że są one zbliżone do wartości uzyskanych dla groszku mrożonego po procesie gotowania.
Słowa kluczowe: obróbka cieplna, tekstura, zielony groszek.

TEKA. COMMISSION OF MOTORIZATION AND ENERGETICS IN AGRICULTURE – 2013, Vol. 13, No. 2, 87–90

The effectiveness of paprika seeds germination in relation to the physical properties

Paweł Sobczak[1], Janusz Zarajczyk[2], Józef Kowalczuk[2], Kazimierz Zawiślak[1], Marian Panasiewicz[1], Jacek Mazur[1], Agnieszka Starek[1]

[1]Department of Food Engineering and Machinery, University of Life Sciences in Lublin, Poland, Doświadczalna 44, 20-280 Lublin, telefon: 48 81 461 00 61, e-mail: pawel.sobczak@up.lublin.pl
[2]Department of Horticulture Machinery and Tools, University of Life Sciences in Lublin, Poland

Received April 10.2013; accepted June 18.2013

Summary. The paper presents an assessment of the strength of paprika seeds germination, depending on their size. Three fractions of paprika seeds were assessed, i.e. seeds of the size range from 1 to 2 mm, next the range of 2 to 3.15 mm, and the fraction in the range above 3.15 mm. A control sample in the study were not calibrated paprika seeds. The germination strength was determined according to the PN-69/R65950 norm using paper as a substrate. 50 seeds from each fraction were used for the research. The strength of germination was determined in three replications. Paprika seeds germination depends on their size. Seeds in the range greater than 3.15 mm had the highest strength of germination of 80% after 14 days from sowing.
Key words: germination strength, paprika seeds, separation.

INTRODUCTION

For a long time the industry connected with seed processing, where seeds are used in herbalism, horticulture and market gardening, has been facing the problems related to seeds purification, separation and processing. It especially regards economic entities involved in export activities of these products. Each producer aims at achieving the highest quality of seeds on offer. A measurable indicator of quality of seeds on offer is their high strength of germination. Germination is defined as a complex of processes occurring in a seed, the result of which is the activation of a germ which consequently leads to the growth of a seedling. Cardinal thermal points are determined for the germination of a seed, i.e. the minimal, maximal and optimal temperature for the process, whereas the optimal temperature does not guarantee the highest germination capability. The value of cardinal points depends on the species of seeds and is connected with their origin [5, 9].

The germination strength of particular seeds depends on the thickness and hardness of the husk, as well as the presence of physiologically active substances on the husk, called growth regulators, which delay or halt the germination process. One of the methods for stimulating the seeds for germination is their scarification, that is abrasion of the seed coat in order to weaken it [2].

Some of the seeds may have different types of fungi on their surface, e.g. *Alternaria dauci* and *A. radicina,* which negatively influence the germination process [11]. The process which reduces the quantity of fungi on the surface of seeds is their treatment in different kinds of solutions [3].

In the food processing industry the process of separation is conducted for a wide range of materials, which include: cereal seeds, seeds of other plants, and fragmented herbs. The necessity to purify and separate tens of millions of tons of seeds representing four basic cereals and a various range of food materials clearly manifests the depth of this problem. The process of separation often involves several stages, e.g. cereal seeds are firstly separated in a harvester, secondly in machinery for purification, and part of seeds, later on, in different processes of technological processing [13, 14]. Taking into consideration the fact that separation processes involve seeds of, at least, a few hundred plant species (i.e. seeds of basic species and weeds), it is easy to understand the difficulties which accompany the process. Hence, a special care should be taken while selecting the machinery which executes the separation processes, and selecting optimal parameters for these processes which are adjusted to specific materials. That is why, the processes of separation and purification are often based on the use of aerodynamic properties, the shape of material or its surface structure in order to separate the required material [12, 15].

The most common method of separation in agriculture and the food industry is sieving. It is characteristic of high efficiency, accuracy of purification and a wide range of the applied material. On the basis of distribution curves of the purified material it can be concluded that it is possible to separate the material according to a particular property, as well as make an assessment of the loss volume in relation

to the separated impurities. Such research was carried out on seeds of selected carrot varieties [1] and other grain materials [4, 6, 7, 8]. The assessment of the purity of seeds was conducted with the use of complex separation, that is pneumatic-sieve separation. While applying only a sieve, the effect of purification was low. Generally, it may be stated that the use of a sieve of a bigger diameter of apertures results in an increase of material purity with a simultaneous increase of material loss. For the research seeds the best results were achieved while purifying the material in an aspiration canal, in which the velocity of the air stream was 2.0 $m \cdot s^{-1}$, and then sifting it through a sieve with oblong 1.6 mm wide apertures [10].

THE AIM AND SCOPE OF THE RESEARCH

The aim of the paper was to identify the effect of selected physical properties of paprika seeds on their germination strength. Assessed were three fractions of paprika seeds, i.e.: seeds within the size range from 1 mm to 2 mm, next the size range from 2 to 3.15 mm and fractions from the range above 3.15 mm. The control group in the research were not calibrated paprika seeds. For each assessed fraction of seeds their hardness was determined with the use of a texture analyser. The research was conducted in 30 replications.

RESEARCH METODOLOGY

The germination strength was determined according to the PN-69/R65950 norm using paper as a substrate. 50 seeds from each fraction were used for the research. The strength of germination was determined in three replications. The separation of paprika seeds was carried out with the use of a vibrating sieve separator AS 200 (Fig. 1), using sieves with oblong apertures with the following sizes: 0, 1, 2, 3, 15 mm.

Fig. 1. Vibrating laboratory sifter AS 200

RESULTS

Table 1 presents the research results of the germination strength of particular paprika seeds fractions.

Table 1. The strength of germination of particular seeds fractions

Fraction	Germination strength [%]	
	After 6 days	After 14 days
Above 3.15 mm	52	80
2-3.15 mm	32	56
1-2 mm	20	47
Seeds before calibration	32	59

While analysing individual research results of the germination strength it can be stated that an essential part is played by the size of seeds. With the increase of seed sizes, the germination strength also increases. Small seeds germinate much later and the number of seedlings is smaller compared to the seeds from the biggest fraction. Among seeds which did not undergo the process of calibration there is a vast discrepancy in the number of seedlings.

The paprika seeds provided by the producer are of various sizes. The size distribution of the analysed seeds is presented in Figure 2.

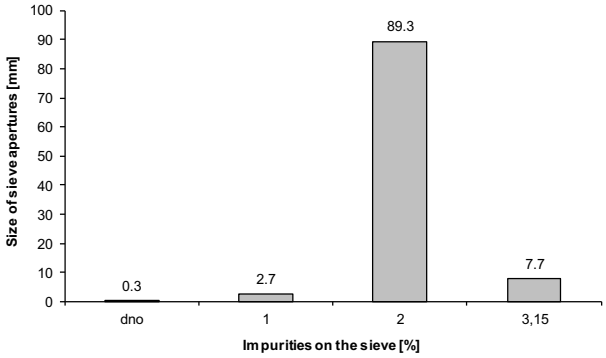

Fig. 2. The size distribution of paprika seeds

The biggest quantity (almost 90%) of paprika seeds belongs to the fraction from the range 2-3.15 mm. In the analysed material there is 7.7% of seeds from the fraction above 3.15 mm, while there is 2.7% of seeds from the smallest fraction. The remaining mass of the sample which is on the bottom of the separator are impurities.

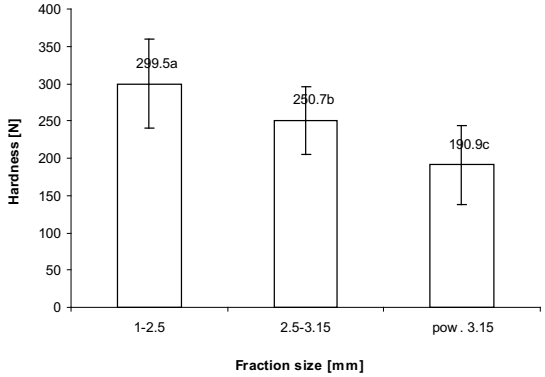

Fig. 3. The hardness of paprika seeds after separating into fractions

Table 2. The analysis of the variance of paprika seeds hardness in relations to the size at the level of significance a=0.05

Source of diversity	Degrees of freedom	Sums of squares	Average squares	The value of a testing function F	F_α	p
Fraction size	2	175762.1	87881.05	31.4177	3.11	$p<\alpha$
Error	85	237760.5	2797.182			

The hardest paprika seeds are in the range between 1 and 2.5 mm. Their hardness amounted to 300 N, with a relatively high discrepancy (standard deviation 59). The statistical analysis at the level of significance 0.05 proved fundamental differences in the hardness of paprika seeds from the range between 2.5-3.15 mm and seeds bigger than 3.15 mm. The hardness of seeds with the size above 3.15 mm was over 190 N.

CONCLUSIONS

On the basis of the conducted research the following conclusions were formulated:

1. The germination strength of paprika seeds depends on their size. The biggest seeds (above 3.15 mm) had the highest germination strength of 80% after 14 days following sowing.
2. Among seeds which did not undergo calibration there is a vast discrepancy of the germination strength value in the conducted research, which is caused by different sizes of seeds in the samples.
3. Approx 90% of paprika seeds are characteristic of size within the range 2 – 3.15 mm.
4. The hardness of paprika seeds depends on their size. Smaller seeds are characteristic of higher hardness.

REFERENCES

1. **Choszcz D., Jadwisieńczak K., Konopka S. 2008**. Efektywność czyszczenia nasion marchwi (*daucus carota L.).* Inżynieria Rolnicza, 9(107), 33-38.
2. **Domoradzki M., Korpal W., Weiner W. 2007.** Badania procesu mechanicznej skaryfikacji nasion. Inżynieria Rolnicza, 5(93), 97-106.
3. **Dorna H., Kaniewski R., Jarosz M., Banach J., Szopińska D. 2010.** Zdrowotność i kiełkowanie nasion marchwi traktowanych wyciągiem wodnym z konopii siewnych (*Cannabis Sativa L.*). Progress in Plant Protection. Postępy w Ochronie Roślin, 50(1), 373-377.
4. **Feder S., Kęska W., Włodarczyk K. 2008.** Pneumatyczne wspomaganie procesu przesiewania mieszanin ziarnistych na przesiewaczu płaskim. Inżynieria Rolnicza, 4 (102), 263-270.
5. **Gładyszewska B. 1998**. Ocena wpływu przedsiewnej laserowej biostymulacji nasion pomidorów na proces ich kiełkowania. Rozprawa doktorska. AR Lublin.
6. **Kęska W., Feder S., Włodarczyk K. 2005.** Wstępne wyniki badań nad pneumatyczną intensyfikacją procesu sortowania mieszanin ziarnistych na sicie wibracyjnym. Inżynieria Rolnicza, 3(63), 235-242.
7. **Komarnicki P., Banasiak J., Bieniek J. 2008.** Rozkład aerodynamicznych parametrów stanu równowagi procesowej czyszczenia ziarna. Inżynieria Rolnicza, 4(102), 389-396.
8. **Komarnicki P., Banasiak J., Bieniek J. 2008a**. Warunki równowagi procesowej czyszczenia masy zbożowej na powierzchni roboczej sita żaluzjowego. Inżynieria Rolnicza, 4(102), 397-404.
9. **Lityński M. 1982.** Biologiczne podstawy nasiennictwa. PWN, Warszawa.
10. **Mieszkalski L., Anders A. 1999.** Analiza parametrów separacji okrywy nasiennej z mieszaniny powstałej po obłuskaniu nasion rzepaku. Inżynieria Rolnicza, 2(8), 29-36.
11. **Nowicki B. 1995.** Patogeniczne grzyby zasiedlające nasiona marchwi. Acta Agrobotanica, 48(2), 49–57.
12. **Oszczak Z. 2006.** Optymalizacja parametrów pracy pneumatycznego separatora kaskadowego. Inżynieria Rolnicza, 7, 359-365.
13. **Panasiewicz M., Zawiślak K., Kusińska E., Sobczak P. 2008.** Purification and separation of loose material in a pneumatic system with vertical air stream. TEKA Commission of Motorization and Energetics in Agriculture, 8, 171-176.
14. **Pastushenko S., Tanaś W., Ogiyenko N. 2009.** Research on influence of cavitation process on clearing vegetables and melon seeds by hydro-pneumatic separator. TEKA Commission of Motorization and Energetics in Agriculture, 9, 223-230.
15. **Sobczak P. 2009.** Separacja w produkcji pasz przemysłowych. Pasze Przemysłowe, 3/4, 6-9.

EFEKTYWNOŚĆ KIEŁKOWANIA NASION PAPRYKI W ZALEŻNOŚCI OD ICH WŁAŚCIWOŚCI FIZYCZNYCH

Streszczenie. W pracy przedstawiono ocenę siły kiełkowania nasion papryki w zależności od ich wielkości. Ocenie poddano trzy frakcje nasion papryki, tj.: nasiona o wielkości z przedziału od 1 do 2mm, następnie z przedziału od 2 do 3,15 mm oraz frakcje z przedziału powyżej 3,15mm. Próbą kontrolną w badaniach były nasiona papryki nie kalibrowane. Siłę kiełkowania nasion wyznaczono wg normy PN-69/R65950 stosując jako podłoże bibułę. Do badań przeznaczono 50 nasion z każdej frakcji. Siłę kiełkowania oznaczono w 3 powtórzeniach. Siła kiełkowania nasion papryki zależy od ich wielkości. Nasiona największe powyżej 3,15 mm posiadały najwyższą siłę kiełkowania wynoszącą 80% po 14 dniach od wysiewu.
Słowa kluczowe: siła kiełkowania, nasiona papryki, separacja.

Badania finansowane ze środków KBN prowadzonych w latach 2011-2013 jako projekt badawczy nr NN 313757140.

TEKA. COMMISSION OF MOTORIZATION AND ENERGETICS IN AGRICULTURE – 2013, Vol. 13, No. 2, 91–96

Multi-criterion optimisation of photovoltaic systems for municipal facilities

Tomasz Szul, Jarosław Knaga, Krzysztof Nęcka

Krakow University of Agriculture, Faculty of Powering and Automation of Agricultural Processes
ul. Balicka 116B, 30-149 Kraków, Poland, e-mail: tomasz.szul@ur.krakow.pl

Received April 10.2013; accepted June 18.2013

Summary. This study provides a technical and economic analysis of a photovoltaic plant providing power supplies to a municipal waste water treatment plant. Power generation in a photovoltaic farm was considered in its two aspects, that is connected to the grid with an option of feeding power to the grid in case of overproduction and as an autonomous system which will generate power exclusively for the needs of the waste water treatment plant without the possibility of supplying power to the grid. On basis of the analysis it was concluded that the operation of the photovoltaic farm within the power grid is a better solution. In spite of small unit profit of the project, it brings about a positive environmental effect in form of reduction of CO_2 emission. In order to implement photovoltaic installations in its facilities, the municipality should apply for various subsidies due to the fact that only a subsidy covering above 50% of investment costs will guarantee a minimum profitability of such a project.

Key words: photovoltaic farm, technical and economic analysis of photovoltaic installations, waste water treatment plant, subsidies for renewable energy sources.

INTRODUCTION

Total capacity of commercial power plants in Poland amounted to 37,4 GW as per the end of 2012. 82% of them were power plants fired mainly with non-renewable resources, such as hard coal and brown coal. According to the Energy Regulatory Office [URE 2013], power capacity of renewable energy installations amounts to 4,4 GW, out of which 2,5 GW is made up by wind turbines, 0,96 GW by hydroelectric power stations and 0,82 GW by biomass-fired plants. Solar power stations are a novelty in this listing, as currently there are only nine photovoltaic farms operating in Poland, with a summed capacity of 0,0013 GW. In near future another four sites are planned to be commissioned which will increase the nationwide solar power output up to 0,0063 GW. The development of such installations is determined both by means of appropriate regulations [directive 2009], as well as environmental and economic aspects. Renewable energy sources do not emit any harmful pollution to the atmosphere, including the most burdensome CO_2. The necessity to reduce the emission of greenhouse gases provides a very strong impulse for the development of environment-friendly energy sources. This necessity is imposed on Poland under international obligations stipulated in the Kyoto protocol and the United Nations Framework Convention on climate change [4, 9]. As an additional stimulus for the development of renewable energy sources, the Ministry of Economy enacted a decree of 18th October 2012 which forces the power distribution companies to acquire power from renewable energy sources. According to the decree valid as of 1st January 2013, the percentage share of renewable energy sources in the Polish power system should increase regularly by one per cent from 12 in 2013 to 20% in 2021 [Decree 2012]. Apart from promoting major sites using renewable energy sources, works are currently being conducted on the creation of an efficient supporting system of renewable energy sources, as a development opportunity not only for local communities, but also local governments, as assumed among other in the act on power efficiency according to which the public sector should play a leading role in the promotion of energy savings and usage of renewable energy sources [Journal of Laws 2011]. Out of many available renewable energy sources, small photovoltaic installations attract ever larger interest of administrators of municipal buildings, as they may be used to cover their own power demand and to sell the excess of electric power [19]. The economic calculation is the essential criterion influencing the selection of a power system to be installed [16, 20]. In practice, an energy balance analysis cannot act as a decisive factor for the selection of a given type of installation. A potential user should assess both the technical and economic aspects of each of the considered systems and choose the most advantageous one from the perspective of its entire lifespan [1, 8, 13, 15].

The goal of this study is to deliver a technical and economic analysis of a photovoltaic plant providing power supplies to a municipal waste water treatment plant located in the South of Poland. The scope of research covers an operating analysis of a photovoltaic farm in its two aspects, that is connected to the grid with an option of feeding power to the grid in case of overproduction and as an autonomous system which will generate power exclusively for the needs of the waste water treatment plant without the possibility of submitting power to the grid.

SCOPE OF RESEARCH

The facility covered in this research is a municipal waste water treatment plant which is planned to be equipped with a photovoltaic farm in order to cover the electric power demand of the receivers located within the plant. The receivers include lamps, electric sockets for portable receivers and three-phase receivers. Asynchronous motors powering the waste water treatment process machinery will act as the main power receivers. The power demand of currently installed and operating receivers within the waste water treatment process amounts to 105,9 kW. The total power demand of electric power receivers amounts to 116,9 kW. As the assumed coincidence factor amounts to 0,41, peak power demand of the facility is 48,1 kW. After the commissioning of the second reactor, the planned power of installed receivers will grow to 182,7 kW, while their peak power will reach 75 kW. Real yearly consumption of electric power by all receivers operating in the waste water treatment plant at 150 [MWh].

TECHNICAL ANALYSIS

The following criteria were used for the calculation of active surface of photovoltaic modules:

1. Maximum photovoltaic farm power should not exceed the peak power subscribed with the power supplier, increased by the mean value of power demanded by electric devices installed at the waste water treatment plant.
2. Power generated by the PV farm should cover at least 90% of demand in the summer half of the year (April-September).
3. Points 1 and 2 should be fulfilled assuming that two reactors of the plant are operating; therefore, a growth of power consumption and power demand by electric devices of the waste water treatment plant by 62,26% was assumed.
4. The smallest photovoltaic farm to be considered in the analyses should meet the criterion 1 and 2 at current power and energy demand, that is operation of a single waste water treatment plant reactor.

On basis of the adopted criteria 1-4, and considering the limit values of solar radiation flux density, that is from 200 W/m2 up to 350 W/m2, three variants of photovoltaic module surface were adopted according to insolation value of 200 W/m^2 **W1**, 250 W/m^2 **W2**, 350 W/m^2 **W3**. The parameters and average costs of such installations are provided in table 1.

Table 1. Listing of photovoltaic plant parameters for three variants

Variant	W1	W2	W3
Mean power demand [W]	30000	30000	30000
Threshold flux density [W·m^2]	200	250	350
Efficiency rate	13,9	13,9	13,9
Required receiving module surface [m^2]	1100	860	620
Peak farm power [Wp]	153061	120000	85714
Maximum farm power [W]	137755	108000	77143
Cost of photovoltaic modules, PLN	1726531	1353600	966857
Installation cost (20% cost of cells), PLN	345306	270720	193371
Project costs, PLN	25000	25000	25000
Inverter, PLN	160000	160000	100000
Power connections and commissioning, PLN	69061	54144	38674
System maintenance and insurance	17265	13536	9669
Total installation cost kPLN	**2343**	**1877**	**1334**

After determining the power generation potential for such a selection modules, a further analysis of coverage of power demand of the waste water treatment plant could be performed. The conducted research considered a photovoltaic farm connected to the grid with an option of feeding power to the grid in case of overproduction and an autonomous system which will generate power exclusively for the needs of the waste water treatment plant without the possibility of submitting power to the grid. For the purpose of the analysis, a mean power output in a 25-year lifespan was adopted. Due to the planned commissioning of the second power plant reactor, the analysis of power demand was performed with the consideration of the forecast energy consumption after the extension. Within the calculations of the coverage rate, the decrease of efficiency rates of photovoltaic cells was considered along the lifespan. The estimated mean coverage of power demand of the waste water treatment plant within 25 years of lifespan amounts variant-specifically to 36-65% in case of a farm connected to grid, while in case of an autonomous solution, the coverage the plant's power demand will be confined within 16-27% depending on the adopted variant.

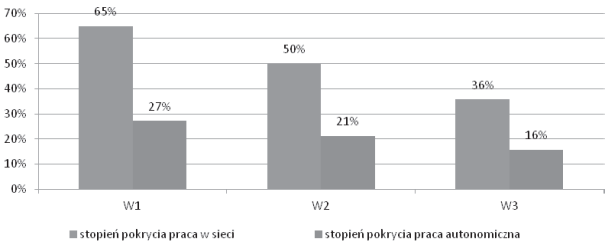

Fig. 1. Coverage of power demand of the waste water treatment plant in a lifespan perspective of 25 years.

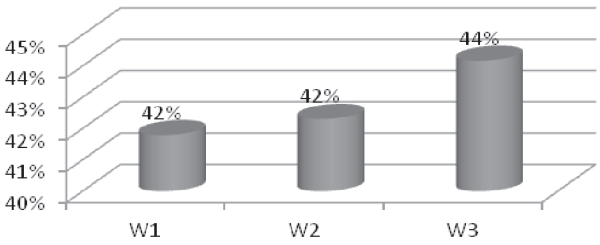

Fig. 2. Photovoltaic farm underload in autonomous operation

If the farm operates autonomously, 42-44% of power is lost due to the insufficient operating coherence of waste water treatment processes with the photovoltaic farm. As a solution for this problem, electric batteries could be used, however due to the high power storage costs amounting from 0,6 to 1,2 PLN per kWh [7] such option has not been considered in further research.

ECONOMIC ANALYSIS

The project economic efficiency analysis was performed on basis of the following economic factors [2, 5, 6]:

- simple payback period (SPBP),
- pay-back period (PBP),
- net present value (NPV),
- net present value ratio (NPVR),
- internal rate of return (IRR),
- dynamic generation cost (DGC).

The selection of a specific photovoltaic system of the waste water treatment plant should be based on objective criteria. Excess of effects over expenditures is regarded commonly as such a criterion. The technical and economic analysis was performed on basis of simple and complex evaluation methods of asset investments, based on discount rate and considering the currency value fluctuation in time, risk and inflation.

Simple pay-back time. Defined as the time necessary to retrieve the capital expenditures incurred for the delivery of the specific project:

$$SPBT = \frac{NI}{WRK} \text{ [years].}$$

Calculated from the commissioning of investment until the gross sum of benefits gained from the investment compensates the expenditures.

Pay-back period (PBP), that is the period in which discounted cash flows cover the incurred capital expenditures. Discounted pay-back period considers the changing value of the investment amount in time:

$$PBP = \frac{\ln\left[\frac{1}{1-\left(\frac{NI}{WRK}\right)\cdot i}\right]}{\ln(1+i)} \text{ [years].}$$

Net present value (NPV). Sum of all future income of the investment lifespan calculated per the current year and reduced by the incurred capital expenditures:

$$NPV = \sum_{n=1}^{n=t} \frac{WRK_n}{(1+i)^n} - NI \text{ [PLN].}$$

Net present value ratio (NPVR) captures the relation of project net value and the value of capital expenditures necessary to acquire NPV:

$$NPVR = \frac{NPV}{WRK} \text{ [PLN].}$$

NPVR is an auxiliary index allowing to select the investment option by comparing projects that are similar in terms of structure, capital expenditures, lifespan etc. In most cases, the following condition has to be met:

$$NPVR \rightarrow \max.$$

Internal rate of return (IRR). Calculated on basis of cash flow; it is such a discount rate value at which the net present value equals zero (5):

$$\sum_{n=1}^{n=t} \frac{WRK_n}{(1+IRR)^n} - NI = 0 \text{ [\%].}$$

Dynamic generation costs equals the price which enables the acquisition of discounted income equalling discounted costs. In other words, DGC shows the technical cost of acquisition of a unit of environmental effect [Rączka 2002]. This cost is indicated in PLN per unit of environmental effect. The lower the DGC value is, the higher the efficiency of the project:

$$DGC = p_{EE} = \frac{\sum_{t=0}^{t=n} \frac{KI_t + KE_t}{(1+i)^t}}{\sum_{t=0}^{t=n} \frac{EE_t}{(1+i)^t}}. \text{ [PLN/kgCO}_2\text{],}$$

where:

re – energy price growth rate,
n – 1..25 consecutive cost year (n=25 estimated number of installation lifespan years).
NI – capital expenditures [kPLN],
WRK – value of yearly benefits [kPLN],
KI_t – investment costs incurred in a given year – t,
KI_t – operating costs incurred in a given year – t,
i – discount rate (down to second decimal),
t – year, value from 0 to n, where 0 is the year of first costs and n the last year of system operation,
EE_t – environmental effect rate in physical units acquired in each year. Environmental effect to which p_{EE} price per physical unit is assigned (assuming that price is constant during the entire period covered by the analysis),
p_{EE} – price for physical unit of environmental effect.

The following components were used for the purpose of financial projection:

1. Sales revenues on ownership rights to power generation with a renewable energy source, so-called green certificates. Value of ownership rights in 2011 amounted on

average to 285 PLN/MWh and it is estimated to grow by 2-3% per year (2% in the analysis).
2. Costs avoided thanks to not purchased power. In the analysis, an electricity price growth of 4,5% was adopted (according to historical data from 2000-2010).
3. Operation and maintenance costs – in the calculations, a growth by 4% was assumed.

Table 2 provides a projection of yearly profit (value of yearly benefits) in kPLN gained thanks to the operation of the PV farm (mean value for a 25 year lifespan) according to the specific variants.

The following data were used to calculate the economic rates.

– capital expenditures in the installed photovoltaic farm (as in table no. 1) W1 – 2343 kPLN, W2 – 1877 kPLN, W3 – 1334 kPLN
– **Table 2.** Value of yearly benefits

Variant	W1 in grid	W2 in grid	W3 in grid	W1	W2	W3
kPLN	224,86	169,89	121,47	80,32	59,37	45,03

– discount rate 5,91%,
– project lifespan 25 years,
– in the calculation, three project funding levels were used: 100% of own funds, 50% subsidy and 75% subsidy from environmental funds.

In the calculations it was assumed that the provisions on the acquisition of green certificates will remain in power after 2012. The results of the performed economic analysis are specified in table 3.

While analysing the evaluation factors one can conclude that the operation of the photovoltaic farm within the power grid is a better solution, as confirmed by all rates. Out of grid-connected variants W1 is the best one, regardless of the subsidy value from funds supporting renewable energy sources. In case of smaller own funds, W3 is an alternative solution, as confirmed by IRR and PBP, which are the most advantageous in comparison to variant W2. The exemplary course of NPV rate as a function of installation lifespan is presented on the diagram (fig. 3 and 4). According to these diagrams (fig. 3 and 4), the operation of the photovoltaic farm as an autonomous facility will generate losses in each variant, as indicated by the negative NPV values and PBP return period exceeding project lifespan. A subsidy covering above 50% of investment costs will guarantee a minimum profitability of such a project.

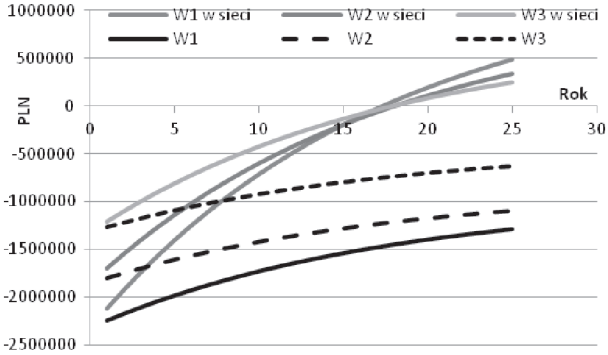

Fig. 3. Course of NPV rate in the operating period, assuming own project funding

Table 3. Values of profitability rates of the photovoltaic farm delivery

Variants of grid-connected installation				
Rate	Subsidy value	W1	W2	W3
NPV	Own funds	485,4 kPLN	342,3 kPLN	253,3 kPLN
	Subsidy 50%	1 756,5 kPLN	1 274 kPLN	915,2 kPLN
	Subsidy 75%	2 338 kPLN	1 756,9 kPLN	1 246,2 kPLN
IRR	Own funds	8,01%	7,77%	7,84%
	Subsidy 50%	19,23%	18,07%	18,20%
	Subsidy 75%	38,93%	36,71%	36,95%
SPBP	Own funds	10,7 years	10,9 years	10,8 years
	Subsidy 50%	5,1 years	5,4 years	5,4 years
	Subsidy 75%	2,6 years	2,7 years	2,7 years
PBP	Own funds	17,3 years	18,0 years	17,8 years
	Subsidy 50%	6,3 years	6,8 years	6,7 years
	Subsidy 75%	2,9 years	3,1 years	3,0 years
Autonomous variants				
NPV	Own funds	- 1 290,3 kPLN	- 1 097,9 kPLN	- 627,2 kPLN
	Subsidy 50%	- 127,3 kPLN	- 166,2 kPLN	34,6 kPLN
	Subsidy 75%	454,1 kPLN	299,6 kPLN	365,6 kPLN
IRR	Own funds	-	-	0,15%
	Subsidy 50%	4,73%	3,96%	6,45%
	Subsidy 75%	13,19%	11,99%	15,92%
SPBP	Own funds	29,0 years	31,4 years	24,5 years
	Subsidy 50%	14,5 years	15,7 years	12,3 years
	Subsidy 75%	7,2 years	7,8 years	6,1 years
PBP	Own funds	no capital return	no capital return	no capital return
	Subsidy 50%	exceeds 25	exceeds 25	22,4 years
	Subsidy 75%	9,7 years	10,9 years	7,8 years

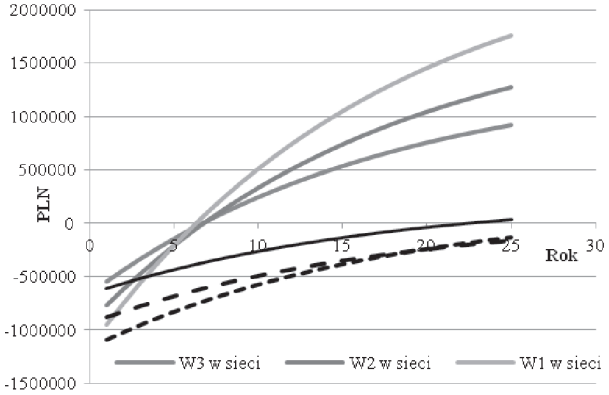

Fig. 4. Course of NPV rate in the operating period, assuming 50% subsidy from funds supporting renewable energy sources

Having analysed the project by means of NPVR and DGC rates one can state that power generated in photovoltaic farms connected to the grid, in spite of small unit investment profits (from 0,18 in variant W2 up to 0,21 PLN to variant W1), brings about a positive environmental effect in form of reduction of CO_2 emission (fig. 5). The environmental effect generation cost clearly distinguishes variant W1 (DGC=-0,4PLN/kgCO_2) from other variants (fig. 5).

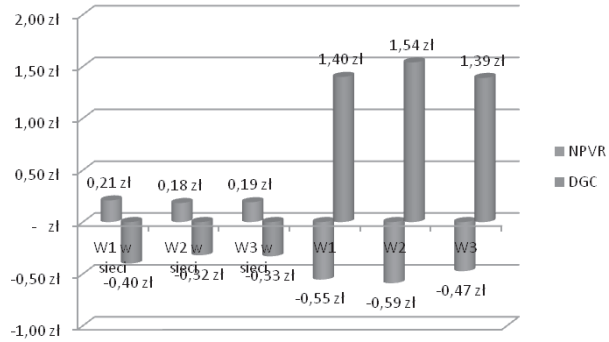

Fig. 5. NPVR rate and technical generation cost in case of own funding

Also in this case, if a municipality due to limited funds does not choose W1, it may choose W3 as an alternative. It is worth noting that complete own funding for autonomous operation is not efficient.

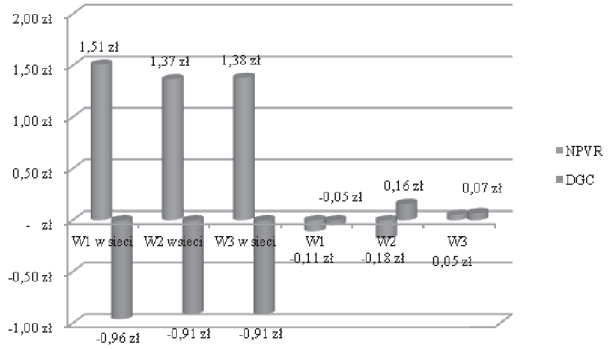

Fig. 6. NPVR rate and technical generation cost in case of 50% subsidy from funds supporting renewable energy sources

While analysing the diagram (fig. 6) one can notice that in spite of disadvantageous economic NPVR rates of the autonomous system regardless of the variant, in case of a 50% subsidy of renewable energy sources, the W1 variant is profitable from the environmental point of view (DGC < 0).

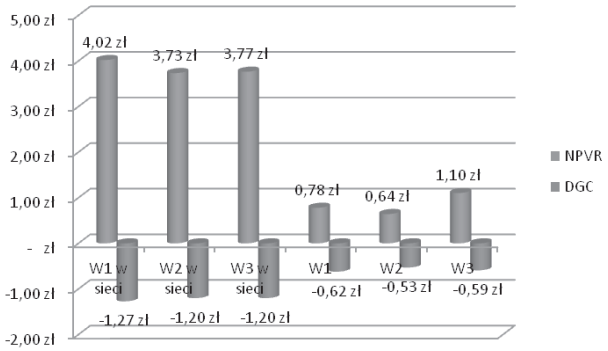

Fig. 7. NPVR rate and technical generation cost in case of 75% subsidy from funds supporting renewable energy sources

In case of subsidising 75% of project value, all variants are profitable for the municipality, while the best one is W1 in case of grid connection and W3 in case of autonomous operation (fig. 7). This variant generates the greatest benefits (NPVR=1.1PLN) compared to others, while it is only slightly worse (0.03PLN) in its environmental aspect than others.

CONCLUSIONS

1. While analysing the evaluation factors one can conclude that the operation of the photovoltaic farm within the power grid is a better solution, as confirmed by all rates. Out of grid-connected variants W1 is the best one, regardless of the subsidy value from funds supporting renewable energy sources. In case of smaller own funds, W3 is an alternative solution, as confirmed by IRR and PBP, which are the most advantageous in comparison to variant W2.
2. Having analysed the project by means of NPVR and DGC rates one can state that power generated in photovoltaic farms connected to the grid, in spite of small unit investment profits brings about a positive environmental effect in form of reduction of CO_2 emission. The environmental effect generation cost clearly distinguishes variant W1 (DGC=-0,4PLN/kgCO_2) from other variants. If a municipality due to limited funds does not choose W1, variant W3 is the best alternative. It is worth noting that complete own funding for autonomous operation is not efficient.
3. In case of subsidising 75% of project value, all variants are profitable for the municipality, while the best one is W1 in case of grid connection and W3 in case of autonomous operation. This variant generates the greatest benefits (NPVR) compared to others, while it is only slightly worse in terms of environmental aspect than others.

REFERENCES

1. **Bartnik R. 2008**. Rachunek efektywności techniczno-ekonomicznej w energetyce zawodowej. Oficyna Wydawnicza Politechniki Opolskiej. Opole.
2. **Bławat F. 2010**. Analiza Ekonomiczna. Wydawnictwo Politechniki Gdańskiej. Gdańsk.
3. Dziennik Ustaw z 2005 roku. Protokół z Kioto do Ramowej konwencji Narodów Zjednoczonych w sprawie zmian klimatu. Dz.U.05.203. 1684.
4. Dyrektywa Parlamentu Europejskiego i Rady 2009/28/WE z dnia 23 kwietnia 2009 roku w sprawie promowania stosowania energii ze źródeł odnawialnych zmieniająca i w następstwie uchylająca dyrektywy 2001/77/WE oraz 2003/30/WE.
5. **Jerzemowska M. (red.) 2006**. Analiza ekonomiczna w przedsiębiorstwie. PWE. Warszawa.
6. **Johnson H. 2000**. Ocena projektów inwestycyjnych. Maksymalizacja wartości przedsiębiorstwa. LIBER. Warszawa.
7. **Knaga J., Szul T. 2012**. Optimising the selection of batteries for photovoltaic applications. TEKA. Commission of Motorization and Energetics in Agriculture – 2012, Vol. 12, No. 1, 73–77.
8. **Laudyn D. 1999**. Rachunek ekonomiczny w elektroenergetyce. Oficyna Wydawnicza Politechniki Warszawskiej. Warszawa.
9. **Ministerstwo Gospodarki 2009**. Polityka energetyczna Polski do 2030 roku. Załącznik do uchwały 202/2009 Rady Ministrów z dnia 10 listopada 2009.
10. **Modzelewski A. 2010**. Wyzwania związane z inwestycjami w nowe moce wytwórcze Elektroenergetyka: współczesność i rozwój. Nr 2-3(4-5). Polskie Sieci Elektroenergetyczne Operator S.A. s. 38-45.
11. Ramowa Konwencja Narodów Zjednoczonych w sprawie Zmian Klimatu (UNFCCC), Rio de Janeiro, 1992.
12. **Rączka J. 2002**. Analiza efektywności kosztowej w oparciu o wskaźnik dynamicznego kosztu jednostkowego. TRANSFORM ADVICE PROGRAMME Investment in Environmental Infrastructure in Poland. NFOŚiGW. Warszawa.
13. **Rogowski W. 2004**. Rachunek efektywności przedsięwzięć inwestycyjnych. Oficyna Wydawnicza. Kraków.
14. Rozporządzenie Ministra Gospodarki z dnia 18 października 2012 r. „w sprawie szczegółowego zakresu obowiązków uzyskania i przedstawienia do umorzenia świadectw pochodzenia, uiszczenia opłaty zastępczej, zakupu energii elektrycznej i ciepła wytworzonych w odnawialnych źródłach energii oraz obowiązku potwierdzania danych dotyczących ilości energii elektrycznej wytworzonej w odnawialnym źródle energii", Dz.U. 2012 nr 0 poz. 1229
15. **Skorek J. 2002**. Ocena efektywności energetycznej i ekonomicznej gazowych układów ko generacyjnych małej mocy. Wydawnictwo Politechniki Śląskiej. Gliwice.
16. **Szul T. 2012**. Energetyczne wykorzystanie biogazu do produkcji energii elektrycznej i ciepła w skojarzeniu w średniej wielkości oczyszczalni ścieków. Część 2. Analiza ekonomiczna . Technika Rolnicza, Ogrodnicza, Leśna nr 2.
17. **Urząd Regulacji Energetyki. 2013**. Sprawozdanie Prezesa Urzędu Regulacji Energetyki w 2012 r. Warszawa.
18. Ustawa z dnia 15 kwietnia 2011 r. o efektywności energetycznej. Dz.U. z 2011 nr 94 poz. 551.
19. **Wiśniewski G (red.), Więcka A., Dziamski P., Kamińska M., Rosołek K., Santorska A. 2012**. Małoskalowe odnawialne źródła energii i mikroinstalacje. Instytut Energii Odnawialnej. Publikacja Fundacji im. Heinricha Böll. Warszawa.
20. **Wojciechowski H. 2010**, Efektywność techniczna i ekonomiczna rozproszonych i rozsianych układów wytwarzania energii, „Instal" nr 6.

OPTYMALIZACJA WIELOKRYTERIALNA SYSTEMÓW FOTOWOLTAICZNYCH DLA OBIEKTÓW KOMUNALNYCH

Streszczenie. W pracy przedstawiono analizę techniczno-ekonomiczną elektrowni fotowoltaicznej pracującej na potrzeby gminnej oczyszczalni ścieków. Produkcję energii w elektrowni fotowoltaicznej rozpatrzono w dwóch aspektach tj. włączonej do sieci z możliwością oddawania energii do sieci w czasie jej nadprodukcji, oraz w układzie autonomicznym, w którym energia będzie tylko na potrzeby oczyszczalni ścieków bez możliwości oddawania do sieci. Na podstawie analizy stwierdzono, że lepszym rozwiązaniem jest praca elektrowni fotowoltaicznej w sieci energetycznej. Pomimo, niewielkich jednostkowych zysków z inwestycji, przynosi ona korzystny efekt ekologiczny w podstacji kosztów ograniczenia emisji CO2. Gmina chcąc implementować instalację fotowoltaiczną w swoich obiektach powinna ubiegać się o różnego typu subwencje na ten cel, ze względu na to, że jedynie dotacja wyższa niż 50% kosztów inwestycji pozwoli na uzyskanie minimalnej rentowności przedsięwzięcia.

Słowa kluczowe: elektrownia fotowoltaiczna, analiza techniczno-ekonomiczna instalacji fotowoltaicznych, oczyszczalnia ścieków, dotacje na odnawialne źródła energii.

TEKA. COMMISSION OF MOTORIZATION AND ENERGETICS IN AGRICULTURE – 2013, Vol. 13, No. 2, 97–102

CFD modelling of diesel engine at partial load

Wojciech Tutak

Czestochowa University of Technology, Poland
42-201 Czestochowa, Dabrowskiego 69, tutak@imc.pcz.czest.pl

Received April 9.2013; accepted June 18.2013

Summary. The paper presents the results of CFD modelling of thermal cycle of compression ignition IC engine. The turbocharged 6CT107 engine powered by diesel oil was the object of investigations. The results of model validation at partial load are presented. Model of CI engine was used to the optimization of thermal cycle of the test engine. The simulations of the combustion process have provided information on the spatial and time distributions of selected quantities within the combustion chamber of the test engine.
Key words: diesel engine, combustion, modelling, mesh, CFD.

INTRODUCTION

CFD modelling of internal combustion engines has been greatly developing along with the increasing computational power that allows modelling flow processes, combustion processes, emissions and injection fuel using any computational meshes. To model a complete engine cycle with intake and exhaust stroke, some commercial programs are most often used. Internal combustion engine is such a complex object of modelling that building its model including all the important processes is becoming very difficult. Early models of the thermal cycle of the compression ignition engine appeared in the twenties of the last century. In 1926 Schweitzer published a model of heat release in the compression ignition engine. In the sixties, the development of computation models followed. At the beginning, the models were single-zone, and later they were extended to multi-zone direct-injection models. Models based on the fuel injection characteristics were created. One of the first advanced multi-dimension combustion process models for engines with liquid fuel injection to the combustion chamber was the CONCHAS-SPRAY model developed at the Los Alamos Scientific Laboratory in the USA . Since the seventies this model has been modified and complemented with a number of sub-models and has become a basis for creating the KIVA program [2, 3, 5, 6, 7, 8, 9, 10, 11, 12, 13]. The KIVA program was used by the author to model the thermal and flow processes with combustion and fuel injection into the combustion chamber. During the model researches the commercial programme was used. For the last few years the modelling of thermal cycle of IC engine is performed using AVL Fire program. This program allows the modelling of flows and thermal processes occuring in the intake and exhaust manifold and in combustion chamber of internal combustion engine. It also allows modelling the transport phenomena, mixing, ignition and turbulent combustion in internal combustion engine. Homogeneous and inhomogeneous combustion mixtures in spark ignition and compression ignition engine can be modelled using this software, as well. Kinetics of chemical reactions phenomena is described by combustion models which take oxidation processes in high temperature into consideration. Several models apply to modelling auto ignition processes. This program allows for creating three-dimensional computational mesh, describing boundary conditions of surfaces as well as the initial conditions of simulation [14, 15, 16, 17, 18, 19].

Modelling is one of the most effective and readily used research methods. Advanced numerical models allow for researches to analyze the flow processes coupled with combustion and spray. These models require a number of initial and boundary parameters. Therefore, before using the model to optimize the engine cycle, it should be verified experimentally. Renganathan et. al. in their work presented reacting flow simulations performed in a single cylinder direct injection diesel engine with an improved version of the ECFM-3Z (extended coherent flame model – 3 Zones) model using ES-ICE and STAR-CD codes. Combustion and emission characteristics were studied in the sector of engine cylinder, which eliminates the tedious experimental task with conservation in resources and time. It was found that higher NOx emissions occur at peak temperatures, while soot and CO emissions occur at peak pressures. Additionaly, they stated that the numerical modelling of the combustion

and emissions give clear understanding in the heat release and formation of reactant species in the direct injection Diesel engine [20, 21, 22, 23, 24, 25, 26].

Binesh et. al. present the results of modelling fuel mixture formation and combustion in the turbocharged direct-injection compression-ignition engine. The numerical analysis was performed using the Fire program. As a result of computations, cylinder pressure variations and the curves of NO_x and soot formation in the engine exhaust gas were obtained; these results were then compared with the result of research work carried out on the real engine. As a result, fairly good agreement between the modelling results and experimental test results were achieved; and what the engine model reflected best was the variation of pressure in the engine. Hélie and Trouvé presented modifications of the coherent flame model (CFM) to account for the effects of variablemixture strength on the primary premixed flame, as well as for the formation of a secondary non-premixed reaction zone downstream of the premixed flame. The modelling strategy was based on a theoretical analysis of a simplified problem by Kolmogorov, Petrovskii, and Piskunov (KPP). The KPP problem corresponds to a one-dimensional, turbulent flame propagating steadily into frozen turbulence and frozen fuel-air distribution, and it provides a convenient framework to test the modified CFM model. In this simplified but somewhat generic configuration, two radically different situations were predicted: for variations in mixture strength around mean stoichiometric conditions, unmixedness tends to have a net negative impact on the turbulent flame speed: in contrast, for variations in mixture strength close to the flammability limits, unmixedness tends to have a net positive impact on the turbulent flame speed.

This paper presents results of thermal cycle modelling of turbocharged internal combustion diesel engine at full and partial loads [27, 28, 29, 30].

OBJECT OF INVESTIGATION

Contemporary engines are designed to minimize exhaust emissions while maximizing power and economy. Emissions can be reduced by equipping the engine with advanced exhaust after-treatment systems or by controlling the combustion process occurring in the cylinder of internal combustion engine. In order to improve the performance of the engine, research and optimization of the combustion process are carried out. This is dictated by growing concern about decreasing energy resources and environmental protection. Therefore, intensive research is being carried out towards development of internal combustion engine systems. It involves improving the combustion process, introduction of a new fuel such as hydrogen as well as the optimization of engine parameters. The engine should operate with the greatest efficiency possible and with the least toxic compounds emissions [31, 32, 33].

Modelling of the thermal cycle of an auto-ignition internal combustion supercharged engine was carried out within the study. The object of investigation was a 6CT107 internal combustion engine powered by diesel oil, installed on an ANDORIA-MOT 100 kVA/ 80 kW power generating set. The engine was equipped with pressure sensors in each cylinder. The measurements results were used to the model validation. Based on the recorded results of indication, thermodynamic analysis of the engine was performed. Inter alia, the mean cylinder pressure and efficiency of the test engine were determined. It should be noted that in this engine the peak pressures in all the six cylinders are not significantly different from one another.

Table 1. Engine specification

Parameters	Value	
displacement	6.54	dm^3
rotational speed	1500	rpm
stroke	120	mm
cylinder bore	107	mm
connecting-rod length	245	mm
compression ratio	16.5	-
intake valve opening	10±4° BTDC	deg
intake valve closure (IVC)	50±4° ABDC	deg
exhaust valve opening	46±4° BBDC	deg
exhaust valve closure (EVC)	14±4° ATDC	deg
injection angle	9°±1.5°	deg

MODEL ASSUMPTIONS

The Fire program contains many submodels which are necessary to solve processes occurring in the combustion chamber of IC engine. The most important submodel is combustion model. The ECFM (Extended Coherent Flame Model) model was developed especially for modelling the combustion process in a compression ignition engine. The ECFM-3Z model belongs to the group of advanced combustion process models in a compression ignition engine. For several years ECFM-3Z combustion model has been successfully used, constantly modified and improved by many researchers. Together with turbulence process sub-models (e.g. the k-zeta-f), exhaust gas component formation, knock combustion and other sub-models, they constitute a useful tool for modelling and analysis of the thermal cycle of the compression ignition internal combustion engine. To adapt the model for the modelling of the combustion process in the auto-ignition engine, a sub-model was added, which describes the process of mixing fuel to be injected to the combustion chamber. The flame front is formed by the turbulent effect of load vortices and interaction between the burned zone and the unburned part of the load. This model is based on the concept of laminar flame propagation with flame velocity and flame front thickness as the average flame front values. It is also assumed that the reactions occur in a relatively thin layer separating unburned gases from the completely burned gases . The model relies on the flame front transfer equation, as well as on the mixing model describing the combustion of an inhomogeneous mix and the diffusion combustion model. The model assumes the division of the combustion region into three zones: a fuel zone, a zone of air with a possible presence of exhaust gases

remained from the previous engine operation cycle, and an air-fuel mixture zone, where combustion reactions occur following the ECFM concept. The air-fuel mixture formation model provides for gradual mixing of fuel with air. The created combustion model is called ECFM-3Z (3-Zones Extended Coherent Flame Model). In this model, the mixture zone is additionally divided into a burned and an unburned zone. To initiate the combustion process, the auto-ignition model for the forming mixture zone and for the diffusion flame zone is used . The ECFM makes use of the 2-stage fuel oxidation mechanism ($C_{13}H_{23}$). The fuel oxidation occurs in two stages: the first oxidation stage leads to the formation of large amounts of CO and CO2 in the exhaust gas of the mixture zone, at the second stage in the mixture zone exhaust gas, the previously formed CO is oxidized to CO2.The combustion model for the auto-ignition engine was complemented with the unburned product zone. The exhaust gas contains unburned fuel and O_2, N_2, CO_2, H_2O, H_2, NO, CO. The fuel oxidation occurs in two stages: the first oxidation stage leads to the formation of large amounts of CO and CO_2 in the exhaust gas of the mixture zone, the second stage in the mixture zone exhaust gas, the previously formed CO is oxidized to CO_2. The reaction of formation of CO and H2 is taken into account for stoichiometric and fuel-rich mixtures, while for lean mixtures this reaction is omitted. In the ECFM-3Z model, transport equations for the chemical components O2, N2, CO2, CO, H2, H2O, O, H, N, OH and NO are also solved. The concept of the injected fuel and air mixing model relies on the characteristic time-scale of the turbulence model. Because of the occurring process of fuel evaporation, it is necessary to determine the amount of fuel entering the mixture zone and to the pure fuel zone. In the injected fuel stream, fuel droplets are situated so close to one another as to form altogether a fuel zone. After the fuel has evaporated, a specific time is still needed for mixing of the pure fuel zone fuel with air and formation of the combustible mixture. It is additionally assumed that the composition of gas, fuel + EGR is identical both in the mixture zone and in the zone which remins unmixed. The mixture auto-ignition delay is calculated from the empirical correlation. The combustion model for the auto-ignition engine was complemented with the unburned product zone. The exhaust gas contains unburned fuel and O2, N2, CO2, H2O, H2, NO, CO.

Table 2. Modelling parameters

Parameters	Value		
Load	100% (80kW)	70% (58kW)	45% (37kW)
Initial pressure	0.164 MPa	0.137 MPa	0.124 MPa
Initial temperature	317 K	314 K	311 K
Injection angle	-9 deg BTDC		
Fuel temperature	330 K		

Table 3. Submodels

Model	Name
Combustion model	ECFM-3Z
Turbulence model	k-zeta-f
NO formation model	Extended Zeldovich Model
Soot formation model	Lund Flamelet Model
Evaporation model	Dukowich
Breakup model	Wave

The above-mentioned submodels were used during modelling. The parameters shown in Table 1 were taken from the experiment and then these were used as input values for modelling.

RESULTS OF MODELLING

Modelling of the thermal cycle of the test supercharged compression ignition engine using the FIRE software was conducted. The object of research was the internal combustion test engine 6CT107, operated at constant rotational speed equal to 1500 rpm. The researches were conducted for three loads. The initial parameters were taken from the previous experiment. The boundary conditions such as temperature of combustion chamber parts, valves and ports were taken from literature .

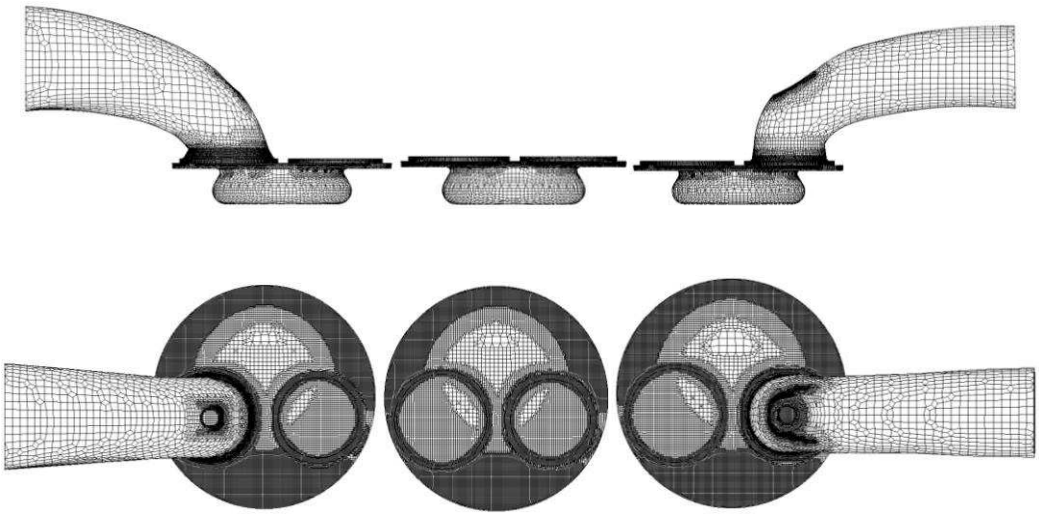

Fig. 1. Computational mesh domains

Figure 1 shows the computational domains for, respectively, intake stroke, compression and work stroke and exhaust stroke. During the calculation the program uses them consecutively.

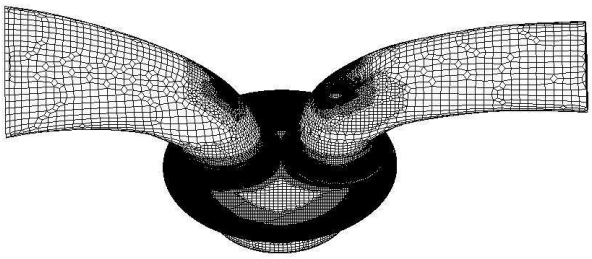

Fig. 2. Computational mesh which was created as a combination of three computational domains

Figure 2 shows computational domain for complete engine work space connected during calculation. The presented domain consists of 350000 cells and the density of this mesh was optimized.

Figure 3 shows the pressure and heat release rate courses. The courses for real test engine were taken on the basis of engine indication process and these courses were compared with courses achieved by modelling. Also, the satisfactory consistency of results was obtained. Of course, there are some differences occurring, but considering the complexity of the processes taking place in the cylinder, the results of the verification of the model can be considered as satisfactory.

Figure 4 shows indicated mean effective pressure and break thermal efficiency calculated on the basis of indication results of six cylinders of the test engine compared

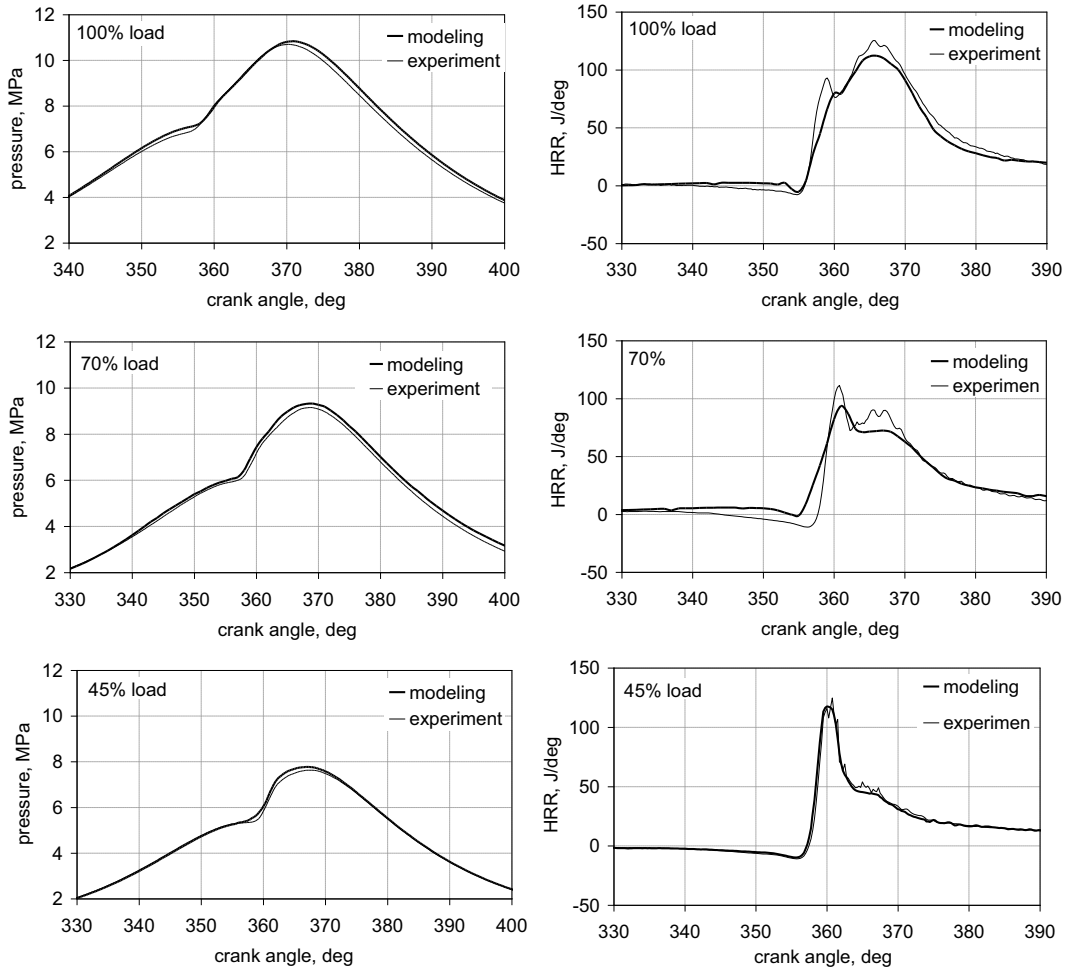

Fig. 3. Pressure and heat release rate courses

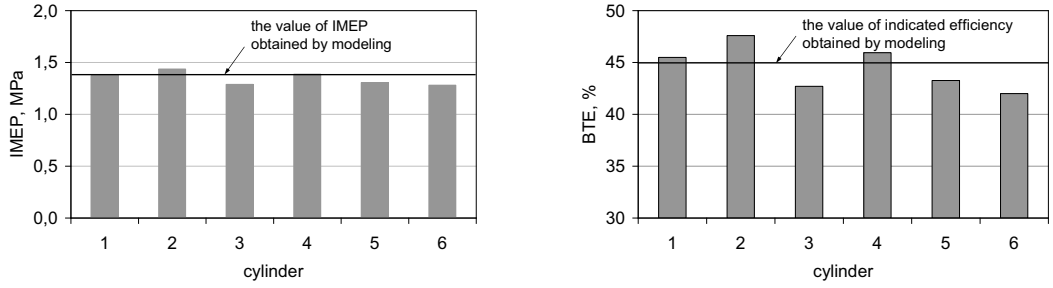

Fig. 4. Indicated mean effective pressure and break thermal efficiency

with the values obtained by the modelling of engine at full load (100%). In the case of modelling the indicated mean effective pressure was equal 1.4 MPa and break thermal efficiency was equal to 45%. The real engine parameters are varied in each cylinder. This could be due to different degrees of filling cylinders and other phenomena. At partial loads the similar correlations were obtained.

CONCLUSIONS

The paper presents results of modelling of supercharged IC compression ignited test engine at partial loads. The calculation was carried out using the Fire software . Pressure, temperature, heat release rate and other parameters in function of crank angle as well as spatial distribution of the above mentioned quantities at selected crank angles were determined. The biggest problem during modelling is to generate adequate mesh which will not affect the results. Obtaining the independence of the results on the density of the mesh is a key issue here. Local and temporary densification of the mesh was used in order to improve the results while reducing cost of calculations. The created model of diesel engine was successfully verified. The resulting differences are acceptable taking into account the complexity of the problem. The results of modelling allows the analysis of engine operation both in terms of thermodynamic and flow. Such verified engine model can be used to model and optimize the engine thermal cycle.

REFERENCES

1. **Schweitzer P, 1926**: The tangent method of analysis of indicator cards of internal combustion engines. Bulletin nr 35, Pennsylvania State University, September
2. **Heywood J. B., 1988**: Internal combustion engine fundamentals. McGraw-Hill.
3. **Rychter T., Teodorczyk A., 1990**: Modelowanie matematyczne roboczego cyklu silnika tłokowego. PWN, Warsaw.
4. **Amsden A.A., O'Rourke P.J., Butler T.D., 1989**: KIVA-II, A computer program for Chemically Reactive Flows with Sprays. Los Alamos National Laboratory LA-11560-MS.
5. **Jamrozik A., Tutak W., Kociszewski A., Sosnowski M., 2013**: Numerical simulation of two-stage combustion in SI engine with prechamber. Applied Mathematical Modelling, Volume 37, Issue 5, 2961–2982.
6. **Szwaja S., Jamrozik A., Tutak W., 2012**: A Two-Stage Combustion System for Burning Lean Gasoline Mixtures in a Stationary Spark Ignited Engine. Applied Energy, 105 (2013), 271-281, 2013.
7. **Tutak W., 2012**: An analysis of EGR impact on combustion process in the SI test engine. Combustion Engines, Vol 148, No. 1/2012, 11-16.
8. **Tutak W., 2011**: Modelling and analysis of some parameters of thermal cycle of IC engine with EGR. Combustion Engines 4/2011 (147), 43-49.
9. **Tutak W., 2011**: Numerical analysis of some parameters of SI internal combustion engine with exhaust gas recirculation. Teka Kom. Mot. i Energ. Roln. – OL PAN T. 11, 407-414.
10. **Tutak W., 2011**: Numerical analysis of the impact of EGR on the knock limit in SI test engine. Teka Kom. Mot. i Energ. Roln. – OL PAN T.11, 397-406.
11. Tutak W., 2011: Possibility to reduce knock combustion by EGR in the SI test engine. Journal of KONES, Powertrain and Transport, No 3, 485-492.
12. **Tutak W., 2008**: Thermal Cycle of Engine Modeling with Initial Swirl Proces Into Consideration, Combustion Engines, 1/2008 (132), 56-61.
13. **Tutak W., 2011**: *Modelling and analysis of some parameters of thermal cycle of IC engine with EGR.* Combustion Engines 4/2011 (147), 43-49.
14. **Tutak W., Jamrozik A., 2010**: *Modeling of thermal cycle of gas engine using AVL FIRE software.* Combustion Engines, R.49 nr 2 (141), 105-113.
15. C**upiał K., Tutak W., Jamrozik A., Kociszewski A., 2011**: The accuracy of modelling of the thermal cycle of a compression ignition engine. Combustion Engines, R.50 nr 1 (144), 37-48.
16. **Tutak W., Jamrozik A., Kociszewski A., Sosnowski M., 2007**: Numerical analysis of initial swirl profile influence on modelled piston engine work cycle parameters. Combustion Engines, 2007-SC2, 401-407.
17. **Tutak W., 2008**: Thermal Cycle of Engine Modeling with Initial Swirl Proces Into Consideration, Combustion Engines, 1/2008 (132), pp. 56-61.
18. **Renganathan Manimaran, Rajagopal Thundil Karuppa Raj and Senthil Kumar K., 2012**: Numerical Analysis of Direct Injection Diesel Engine Combustion using Extended Coherent Flame 3-Zone Model. Research Journal of Recent Sciences, Vol. 1(8), 1-9.
19. **Binesh A.R., Hossainpour S., 2008**: Three dimensional modeling of mixture formation and combustion in a direct injection heavy-duty diesel engine, World Academy of Science, Engineering and Technology 41, 207-212.
20. **Hélie J., Trouvé A., 2000**: A modified coherent flame model to describe turbulent flame propagation in mixtures with variable composition. Proceedings of the Combustion Institute, Volume 28, Issue 1, 193-201.
21. AVL FIRE, VERSION 2009ICE, Physics & Chemistry. Combustion, Emission, Spray, Wallfilm, 2009, Users Guide.
22. **Colin O., Benkenida A., 2004**: The 3-Zones Extended Coherent Flame Model (ECFM3Z) for Computing Premixed/Diffusion Combustion, Oil & Gas Science and Technology.
23. **Tatschl R., Priesching P., Ruetz J., 2007**: Recent Advances in DI-Diesel Combustion Modeling in AVL FIRE – A Validation Study. International Multidimensional Engine Modeling User's Group Meeting at the SAE Congress, Detroit, MI.
24. **Tutak W., Jamrozik A., Kociszewski A., 2011**: Three Dimensional Modelling of Combustion Process in SI Engine with Exhaust Gas Recirculation. International Conference on Heat Engines and Environmental Protection, 203-208.

25. **Tutak W., 2009**: Modelling of flow processes in the combustion chamber of IC engine. Perspective Technologies and Methods in MEMS Design, MEMSTECH 2009. 45-48.
26. **Szwaja S., 2011**: Knock and combustion rate interaction in a hydrogen fuelled combustion engine. Journal of KONES Powertrain and Transport, T. 18, 431-438.
27. **Tutak W., 2012:** Influence of exhaust gas recirculation on the ignition delay in supercharged compression ignition test engine. ECONTECHMOD, An International Quartely Journal on Economics of Technology and Modelling Processes. Vol 1, No 2, 57-62.
28. **Jamrozik A. Tutak W., 2010**: Numerical analysis of some parameters of gas engine. Polish Academy of Science Branch in Lublin, TEKA, Commission of Motorization and Power Industry in Agriculture, Vol. X, 491-502.
29. **Szwaja S., Jamrozik A., Tutak W., 2013**: A Two-Stage Combustion System for Burning Lean Gasoline Mixtures in a Stationary Spark Ignited Engine. Applied Energy, 105 (2013), 271-281, 2013.
30. **Szwaja S., 2009**: Combustion Knock – Heat Release Rate Correlation of a Hydrogen Fueled IC Engine Work Cycles. 9th International Conference on Heat Engines and Environmental Protection. Proceedings. Balatonfured, Hungary.
31. **Szwaja S, Jamrozik A., 2009**: Analysis of Combustion Knock in the SI Engine. PTNSS KONGRES. International Congress of Combustion Engines. The Development of Combustion Engines.
32. **Jamrozik A., 2009**: Modelling of two-stage combustion process in SI engine with prechamber. MEMSTECH 2009, V-th International Conference PERSPECTIVE TECHNOLOGIES AND METHODS IN MEMS DESIGN, Lviv-Polyana, 22-24.
33. **Jamrozik A., 2008**: Analiza numeryczna procesu tworzenia i spalania mieszanki w silniku ZI z komorą wstępną. Teka Komisji Motoryzacji Polskiej Akademii Nauk oddział w Krakowie. Konstrukcja, Badania, Eksploatacja, Technologia Pojazdów Samochodowych i Silników Spalinowych, Zeszyt Nr 33-34.

MODELOWANIE CFD SILNIKA O ZAPŁONIE SAMOCZYNNYM PRZY OBCIĄŻENIACH CZĘŚCIOWYCH

Streszczenie. W pracy przedstawiono wyniki modelowania CFD obiegu cieplnego tłokowego silnika spalinowego o zapłonie samoczynnym. Przedstawiono siatkę obliczeniową modelowanego silnika oraz weryfikację przyjętego modelu dla trzech obciążeń silnika 100, 70 i 45%. Weryfikacja modelu polegała na porównaniu przebiegu ciśnienia w cylindrze silnika modelowanego z przebiegami uzyskanymi drogą eksperymentalną, porównano także przebiegi szybkości wydzielania ciepła. Szybkość wydzielania ciepła w silniku jest bardzo miarodajnym parametrem obiegu cieplnego silnika tłokowego. W prezentowanym modelowaniu uzyskano niezależność wyników od gęstości siatki, co jest zagadnieniem kluczowym w modelowaniu. Uzyskaną zgodność wyników uznano za satysfakcjonującą.
Słowa kluczowe: silnik tłokowy, spalanie, modelowanie, siatka obliczeniowa.

ACKNOWLEDGEMENTS

The authors would like to express their gratitude to AVL LIST GmbH
for Providing a AVL Fire software under the University Partnership Program.

TEKA. COMMISSION OF MOTORIZATION AND ENERGETICS IN AGRICULTURE – 2013, Vol. 13, No. 2, 103–106

Heating value of seeds of leguminous plants and their mixes with seeds of tussock-grass subfamily cereals

Grzegorz Wcisło[1], Andrzej Żabiński[2], Urszula Sadowska[2]

[1]Department of Power Engineering and Automation of Agricultural Processes
[2]Institute of Machinery Management, Ergonomics and Production Processes
University of Agriculture in Krakow, No. 6 Łupaszki Street, 30-198 Kraków, POLAND
e-mail: zabinski@ur.krakow.pl

Received April 10.2013; accepted June 18.2013

Summary. The purpose of undertaken research was to determine and compare heating values for seeds of selected leguminous plant species and their mixes with cereal seeds. The tests were carried out using a calorimeter according to the applicable standard: PN-EN ISO 9831:2005. It has been observed that highest average heating value of 20.19 MJ·kg^{-1} is characteristic for yellow lupine seeds, and lowest – for field pea (17.91 MJ·kg^{-1}). Moreover, the tests have proven that seeds of selected leguminous plants do not burn entirely, as a result of which deposit remains on crucible bottom.
Key words: seeds of leguminous plants, combustion heat, calorimetric method.

INTRODUCTION AND PURPOSE OF THE RESEARCH

Biomass will be more and more frequently used as fuel for heating purposes in houses and public facilities. Among other things, this is fostered by increasing prices of gas and heating oil, and the obligation imposed on Poland to increase the share of energy derived from renewable sources. In the world, grains of cereals, mainly oat and corn are used quite commonly for energy production purposes. Easier transport and storage are among the advantages of using this biomass type, as compared to straw or wood. Moreover, there are technical possibilities to fully automate the process of fuel feeding into boiler [5].

In Poland, using plant seeds or fruit for energy purposes is not widespread yet due to the fears of competitiveness regarding production of food and feeds. However, in case of energy production it is possible to use material of lower quality, not qualified for eating. In agricultural practice, material used for these purposes requires storing for shorter or longer time, while its quality is quite often deteriorating. This effect may result from activity of pests, which have adapted to feeding in closed rooms [9]. There are many reasons why fighting them is not easy. First, it is their high vitality and reproduction rate; moreover, development stages of some of them are hidden inside the seeds, thus limiting access for fumigants. Storage pests not only destroy materials, on which they feed, but also deteriorate their quality contaminating them with excreta, skins, and/or dead specimens. Moreover, they change physical properties of stored materials. Life-processes occurring in pest organisms (release of water, thermal energy) cause increase in material humidity and temperature, which in turn creates favourable conditions for growth of microorganisms, e.g. mildew fungi. Their metabolism products may be the reason for acute intoxications, and they also prove to have mutagenic, carcinogenic, teratogenic and estrogenic properties [8]. Cereal plantations captured by Fusarium genus fungi contaminated with mycotoxins may constitute another source of grain for energy production purposes [2].

The purpose of undertaken studies was to determine and analyse heating values for seeds of selected leguminous plant species and their mixes with cereal seeds.

MATERIAL AND METHOD

Material for tests was taken from a field experiment established using the method of randomly selected blocks in four repetitions. The experiment was carried out in soil with grain composition of strong clayey sand, belonging to good rye complex. White mustard was the forecrop. The tests covered seeds of the following leguminous plants: *Mister* variety yellow lupine, *Sonet* variety narrow-leaved lupine, *Titus* variety horse bean, *Eureka* variety field pea. Tested cereal-leguminous mixes include: seeds of *Mister* variety yellow lupine with seeds of *Kier* variety rye – ratio 1:1, seeds of *Eureka* variety field pea with *Furman* variety oat seeds – ratio 1:1.

The tests were carried out in the humidity of leguminous plant seeds close to 8.5 %, and cereal seeds: 10 %. Examined

material humidity was determined using the dryer-weight method according to Polish Standard PN-R-65950 of December 1994 [12]. Samples were dried for 1 hour at the temperature of 130°C.

Heating value for seeds was determined using the KL-10 calorimeter (Fig. 1) according to applicable standard PN-EN [13-15].

The experiment involved complete combustion of samples weighing 1g (+/-0.0002) in oxygen atmosphere under pressure of 2.8 MPa in a bomb calorimeter, immersed in water (2.7 dm^3 in volume), in calorimetric vessel. Subsequently, water temperature rise was determined. Kanthal resistance wire was used to ignite samples.

Calorimeter operation is based on the measurement of characteristic thermal balance temperatures for the following setup: bomb calorimeter with combusted fuel and calorimetric vessel with water.

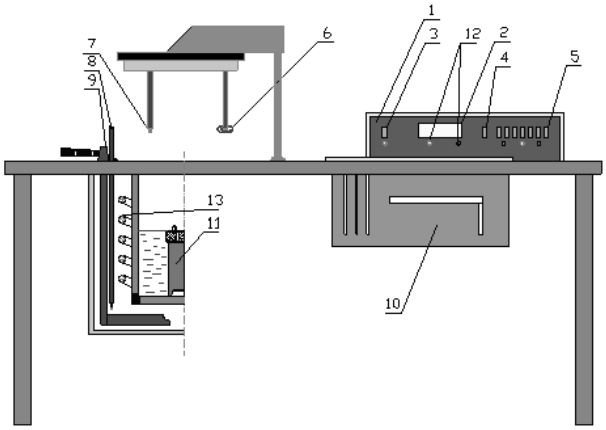

1. control device
2. digital display
3. power switch
4. start of measurement
5. read heat of combustion
6. mixer
7. thermometer
8. thermometer water jacket
9. mixer the water jacket
10. computerized measuring system
11. bomb calorimeter
12. LEDs
13. coil

Fig. 1. Calorimeter schematic diagram

Fuel sample heating value was computed automatically according to an internal device program using the following formula:

$$Q_s = K\,(T_3 - T_2 - k), \qquad (1)$$

where:

K – calorimeter heat capacity [kJ/kg],

T_2, T_3 – characteristic balance temperatures [K],

k – allowance for heat exchange between calorimeter and environment,

$$k = 0.5\,[0.2\,(T_2 - T_1) + 0.2\,(T_4 - T_3)] + 0.2\,(n-1)\,(T_4 - T_3), \qquad (2)$$

where:

n – number of minutes in cycle no. 2 (main period),

T_1, T_4 – characteristic balance temperatures, [K].

The results were processed statistically with variance analysis method for significance level 0.05, using Statistica 9 application. Homogeneous groups were separated according to Duncan's test in case of occurrence of significant differences.

TEST RESULTS AND THEIR ANALYSIS

Currently, available literature includes studies on the subject related to using different plant biomass types for fuel purposes. However, most frequently they refer to vegetative organs of plants only. Whereas, relatively few concern seeds or fruit, while they mostly focus on cereal seeds and primarily refer to one species only – oats [7,10]. Completed studies included leguminous plants as well, in order to compare heating value of their seeds and determine the chances to possibly use them for energy production purposes through combustion.

Obtained heating values for seeds of leguminous plants and their mixes with seeds of tussock-grass subfamily cereals range from 17.9 to 20.2 $MJ \cdot kg^{-1}$. The highest heating value was shown by yellow lupine seeds, the lowest – by field pea (Fig. 2). Heating value for leguminous plants was higher compared to seeds of tussock-grass subfamily cereals, for which it was ranging from 16.2 to 18.6 $MJ \cdot kg^{-1}$ [19]. Probably, this is due to high protein concentration in leguminous seeds (in general 26.9% of dry matter), and in particular yellow lupine (on average 42.75% in dry matter) [6,11]. Protein is characterised by higher heating value (24 $MJ \cdot kg^{-1}$) than starch (17.5 $MJ \cdot kg^{-1}$), which prevails in chemical constitution of cereal seeds [3]. Heating values for cereal-leguminous mixes were ranging between the values obtained for leguminous seeds and cereal seeds used in these mixes.

As opposed to cereal seeds, during combustion of leguminous plant seeds, especially yellow lupine, the researchers observed a residue in form of hard, glassy substance on crucible bottom. This is probably due to higher ash content in leguminous plant seeds, compared to cereal seeds, on average 4.3% in dry matter (cereal grain: 2.4%) [6,17]. Moreover, leguminous plant seeds are characterised by high content of alkaline metals, especially potassium, (cereal grain: 0.5% of dry matter). Potassium reduces ash fusibility temperature. As a result of this, the mixture of chemical compounds characterised by low melting point generated during combustion process forms a good binder for all ash particles and unburned fuel particles. In practice, using fuels of this type makes boiler operation harder, since it leads to formation of hard and difficult to remove deposits inside combustion chamber. They disturb heat exchange process and accelerate high-temperature corrosion. It seems that good solution for this problem would be using co-combustion of leguminous plant seeds with other biomass type. This effect may be also partially prevented by adding to fuel those substances, which increase ash fusibility temperature, e.g. potassium-bonding silicon and aluminium compounds [4]. The first of the proposed solutions will also allow to use ashes as fertilisers, thus closing the entire cycle from agricultural production to energy production [1].

CONCLUSIONS

1. Among the examined leguminous plant seeds, the highest average heating value of 20.19 $MJ \cdot kg^{-1}$ was observed for yellow lupine seeds, and the lowest for field pea seeds (17.91 $MJ \cdot kg^{-1}$).

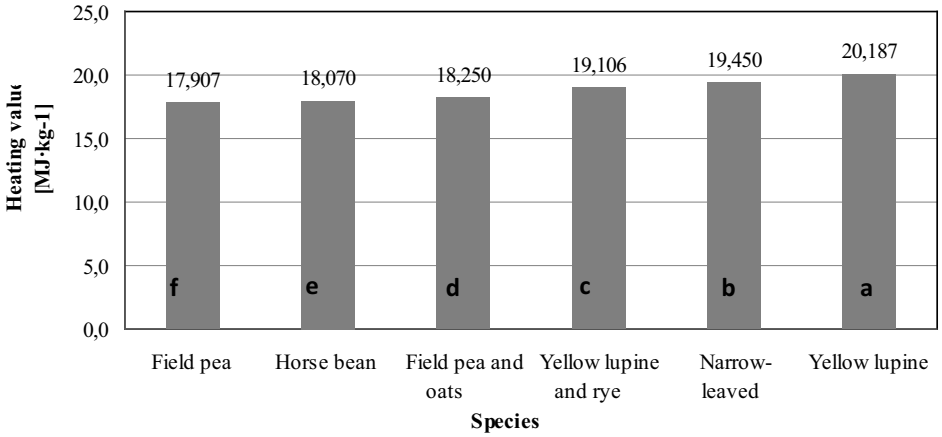

*a, b, c, d, e, f – homogeneous groups according to Duncan's test

Fig. 2. Heating values for leguminous plant seeds and their mixes with cereal seeds.

2. Heating values for cereal-leguminous mixes were within range limited by values obtained for individual species, for field pea and oats: 18.25 MJ·kg^{-1}, and for yellow lupine and rye: 19.11 MJ·kg^{-1}.
3. Seeds of leguminous plants do not combust entirely, leaving deposit on crucible bottom.

REFERENCES

1. **Andersson D., Klasa A., 2009**: Pellet production from wastes in sowing material production. 'Hodowla Roślin i Nasiennictwo' Quarterly No. 3, 34-37
2. **Arseniuk E., Góral T., 2005**: Fusariose of ears – causative factors and economic effects of the disease. IV Forum Zbożowe. http.//WWW.pin.org.pl/hrin/txt/2005/3_6.rtf).
3. **Chachułowa J., Fabijańska M., Karaś J., Skomiał J., Sokół J., 1997**: Feeds. SGGW Warszawa. ISBN 83-86900-22-2
4. **Hardy T., Kordylewski W., Mościcki K., 2009**: Threat of chloride corrosion due to biomass combustion and co-combustion in boilers, Vol.9 (), No. 3-4, 181-195
5. **Janowicz L., 2006**: Heat from grain. 'Agroenergetyka' Quarterly No. 1(15), 39-41
6. **Jasińska Z., Kotecki A., 1993**: Leguminous plants. PWN Warszawa.
7. **Kwaśniewski D., 2010**: Production and use of oat seeds as a renewable energy source. 'Problemy Inżynierii Rolniczej' Quarterly No. 3, 95 – 101.
8. **Maćkiw E., 2010**: Filamentous fungi, mycotoxins and human health. 'Żywienie Człowieka i Metabolizm' Quarterly XXXVII No. 4, 300-309
9. **Nawrot J., 2001**: Storage pests of leguminous seeds. Agrochemia Monthly No. 11, 23
10. **Niedziółka I., Zuchniarz A., 2006**: Energy analysis of selected biomass types from plants. Motorol 8A, 232 -237.
11. **Osek M., 1996**: Rape and horse bean as national source of protein in swine feeding. WSRP. Siedlce
12. Polish Standard PN-R-65950:1994: Sowing material. Seed testing methods.
13. Polish Standard PN-EN ISO 9831:2005: Feeds, animal products, faeces and urine.
14. Polish Standard PN-80/G-04511 – Paliwa stale. Oznaczanie zawartości wilgoci.
15. Polish Standard PN-80/G-04512 – Paliwa stałe. oznaczania zawartości popiołu w paliwach stałych metodą spalania.
16. Polish Standard PN-81/G-04513 – Paliwa stale. Oznaczenie ciepła spalania i wyznaczenie wartości opałowej.
17. **Starczewski J., 2006**: Cultivation of land and plants. P. II. Field cultivation plants. Land and plants cultivation technologies. Akademia Podlaska. Siedlce.
18. **Wcisło G. 2004**. Wyznaczenie ciepła spalania oraz wartości opałowej olejów rzepakowych (paliw rzepakowych). Inżynieria Rolnicza 2 (57). Kraków. 323-332.
19. **Żabiński A., Sadowska U., Wcisło G., 2011**: Heating value of seeds of tussock-grass subfamily cereals. 'Inżynieria Rolnicza' Quarterly 5(130), 307-31

CIEPŁO SPALANIA NASION ROŚLIN STRĄCZKOWYCH I ICH MIESZANEK Z ZIARNIAKAMI ZBÓŻ Z PODRODZINY WIECHLINOWATYCH

Streszczenie. Celem przeprowadzonych badań było określenie i porównanie wartości opałowych nasion wybranych gatunków roślin strączkowych i ich mieszanek z nasionami zbóż. Badania przeprowadzono za pomocą kalorymetru według obowiązującej normy: PN-EN ISO 9831:2005. Stwierdzono, że największą średnią wartością opałową 20,19 MJ · kg-1 charakteryzuje się żółte nasiona łubinu, a najniższą – groch zwyczajny (17,91 MJ · kg-1). Co więcej, badania wykazały, że nasiona wybranych roślin strączkowych nie palą się w całości, w wyniku czego pozostaje popiół na dnie tygla.
Słowa kluczowe: nasiona roślin strączkowych, wartość opałowa, metoda kalorymetryczna.

TEKA. COMMISSION OF MOTORIZATION AND ENERGETICS IN AGRICULTURE – 2013, Vol. 13, No. 2, 107–112

Analysis of damage to an operator caused by mobile parts of the machines used in farms

Magdalena Wójcik[1], Grzegorz Jordan[2], Witold Jordan[1,3], Andrzej Mruk[1]

[1]Krakow University of Technology, Poland
[2]Jagiellonian University in Krakow, Medical College, Poland
[3]Institute of Forensic Research in Krakow, Poland

Received April 11.2013; accepted June 18.2013

Summary. Application of modern tools and machines in agricultural farms facilitates the work, but the lack of skills in managing the machines often leads to accidents causing injuries of different degree of seriousness. The paper presents the investigation on the injuries sustained during the accidents involving tools and farm machines in the Krakow County in 2005-2010. It was examined what kinds of injuries were the commonest and in which group of machines the number of accidents was the highest. Also, the degree of seriousness of injuries was considered. The most frequent were the accidents involving sawing machines. The second group were angle grinders. Among the typically agricultural machines, the most frequent were the accidents involving combine-harvesters. The part of body mostly injured during the accidents was an upper limb. The most frequent type of injuries amid all the accidents was laceration. In case of the group of sawing machines and angle grinders, the injuries mostly caused rather low percentage of permanent health damage. In the accidents involving combine-harvesters, the percentages increased significantly and reached the values that indicated important health damage leading to the limitation of independent existence. The most frequent cause of accidents was carelessness, lack of concentration, inattention or the operator's tiredness.
Key words: agricultural farm, tools and machines, accidents, injuries.

INTRODUCTION

The agricultural engineering develops continuously involving a necessity to launch more and more modified agricultural machines of different kinds. Using the agricultural machines in farms facilitates the work and enables doing the farming better and faster. Nowadays, the farmer's work consists mainly in running the machines, so it is important that every operator is skilled at their management. The lack of such skills often leads to accidents causing injuries of different degree of seriousness.

The purpose of the study was an analysis of operators injuries sustained during the accidents involving agricultural machines within Krakow County in 2005-2010. It was investigated what kind of injuries were the commonest, in which group of machines the accidents occurred most frequently and what the level of damage severity was.

CHARACTERISTICS OF THE REGION UNDER INVESTIGATION

The investigation included the accidents which took place in Krakow County. Krakow County is situated in North-West Małopolska directly within Krakow environment, bordering eight other counties and a town on the rights of the county. The area of Krakow County is 1231 km^2, which is about 8% of the Province's total area. In terms of size, this County occupies the fourth place in Małopolska Province. In Krakow County there is a great diversity of soil kinds and types. The most common soil is loess. 80% of all soils in the county are used agriculturally – it is one of the greatest shares of arable lands amid the counties of Małopolska province [4, 5].

The districts within Krakow County have an agricultural character. According to the statistical data, more than 40% of Krakow County population work in the agricultural sector. The arable lands constitute definitely a predominant part of the County area, that is about 81.5 thousands of hectares. The remaining lands and wastelands constitute more than 20% of the County area. A characteristic feature of Krakow County is a high degree of farm fragmentation. The area of many farms does not exceed 1 ha. There are 50% of such farms in the County, while only about 1% of farms have the area larger than 10 ha. Because of the high fragmentation of farms, their economic condition is poor. That is why the main task of the farms is the production for family needs, then to deliver the products to the shops and markets in Krakow. Only 20% of the farms in Krakow County are oriented at the market production. Among 40% of the County inhabitants working in agriculture, only about

16% of households treat agricultural activity as their main source of income [5].

Because of the agricultural character of the districts and the significant amount of inhabitants with agricultural traditions, Krakow County is a place with a large number of accidents involving machines used in farms.

MACHINES USED IN FARMS

1. FARM MACHINES

Farm machines and devices are necessary components of modern farm equipment. The term 'farm machines' includes a whole range of technical means used in the agriculture production for mechanization of production and works in farms. The farm machines, in the strict sense of the word, are the group of machines, where the working process is the consequence of the motion both of the whole unit in the field and of the active interior gear driving the working elements of the machine.

An appropriate connection of the machines to the energy sources, which enables mechanization of many activities in a farm, makes a unit. The farm tractors are the source of energy for the machines moving in the field, while in the case of stationary machines, the sources of energy are electric motors or stationary combustion engines. The degree of the diversity of the tasks realized in the farms is very high. Therefore, the agricultural machines and devices must include a wide range of possibilities of working in different production processes [5].

The manure spreader is a farm machine used to deliver, grind down and spread evenly the manure in the field. The machines used to haul hay and other green fodders from the field are the mowers, which can be divided, according to their destination, into lawnmowers (electric, petrol) and tractor mowers. In both mower groups, the working set is a cutting set. Shear or rotational cutting set is a piece of equipment of the tractor mowers and it is used to cut stalks of plants [6, 8].

The harvester is a farm machine destined to combine the cereals and root crops. The use of a harvester reduces the transport way of the plant processing and resultant losses. Depending on the prime mover, the combine harvesters divide into self-propelled harvesters (with the own prime mover) and tractor harvesters (semi-mounted or trailed) [11, 12].

The hay presses are farm machines for gleaning hay, straw and green fodders. The press, besides collecting, presses hay or straw (bale forming), which significantly facilitates the collection and transport, and allows to save storage space used to store these materials [8].

The binder is a farm machine for automatically reaping rye and some kinds of rape. This machine also binds the reaped materials into sheaves [4].

Potato sorters are farm machines, which grade dug potatoes according to size.

Cutters for clean and healthy potatoes, beet shredders and grain mills are used to prepare and deliver feed. Straw cutters are used to cut green fodder and straw. Grain mills serve to grind the seeds of cereals and leguminous plants.

2. SAWING MACHINES AND OTHER MACHINES USED IN FARMS

In farms, besides the crop and harvest works, many activities are connected with logging and woodworking. Sawing machines are the main machines used to cut wood. There are different models of sawing machines. Diversity of equipment and design of these machines allow using them not only as professional machines for forest work, but also for other farm tasks, for home-garden work, for the urban greenery cultivation etc. Sawing machines can be classified, considering the type of engine, as combustion machines and electric machines [9]. Considering the cutting tool, they can be classified as chain machines and circular machines.

Many accidents in the farms involve the angle grinders. They are used for cutting, grinding and polishing.

Moreover, among the accidents involving machines there are the accidents with planers and lathes. A planer is a cutting machine used to plane wood. In planers, the machining tools can be flat cutters, saw blade discs, shafts or cutter heads. The lathe is a machine tool for machining the objects with a surface of revolution. The machining tool in the lathe is a turning tool, drill or a tool for threads.

SCALES OF ASSESSING THE SEVERITY OF INJURIES

1. CLASSIFICATION OF THE SCALES OF INJURY SEVERITY

Many point scales have been developed to assess the severity of injuries. Some of them are based on anatomical assessment (structural injuries, for example fractures), the others – on physiological assessment (function changes due to the injury, for example change in the eye reaction to the light). There is also a scale based on the assessment of the disability and social losses.

Anatomical scales are used to describe the injury, considering its anatomic location, the type of injury and the severity level. These scales classify rather the injuries than their consequences. The most popular anatomical scale is Abbreviated Injury Scale (AIS). The anatomical scales distinguish the degree of human damage severity, depending on the fact if it is damage to one part of human body or to several parts. This scale has been modified, now the scale in force is"AIS 90" [13].

Physiological scales, describing physiological condition of a patient, are based on information about function changes due to the injuries. This condition and, in consequence, the numbers assigned to it, can change during the treatment of the patient. Therefore, such scales are applied mainly in clinics.

The last group of scales are the scales of disability and social losses. In this case, neither the injury itself nor physiological changes due to the injury are assessed. The assessment concerns the long-lasting consequences, also these relating to the economic situation. Illustrative scales are Injury Cost Scale (ICS), Injury Priority Rating (IPR) and HARM. All these scales are based on assigning economic values to different injuries [13].

2. SCALE OF THE PERCENTAGE OF PERMANENT DAMAGE TO HEALTH

The scale of the percentage of permanent damage to health is used by the insurance firms, for instance by Agricultural Social Insurance Fund. On the reason that during the accidents people sustain permanent damage to health, these scales are applied wherever the compensation is awarded. For a percentage of permanent damage to health, a determined sum of money is awarded as compensation. The greater the permanent damage to health is. the higher the compensation. The percentage of permanent damage to health is determined by a medical commission. Determining the permanent damage to health, the doctors rely on the tables "Principles of assessing permanent damage to health". The tables contain all possible injuries with percentage values of damage. The doctors determine permanent damage to health assessing individual damage to physical fitness in medical terms. In the case of disturbance of many physical and mental body functions as a result of an accident, the degrees of damage to health for all the impairments are summarized. The only condition is that the value after summarizing does not exceed the percentage of permanent damage to health responsible for the total loss of the damaged part of a limb [3].

RESEARCH METHODOLOGY

Necessary information about the accidents in agriculture was developed and analysed using the documentation from Agricultural Social Insurance Fund (KRUS) – regional unit in Krakow. Studies include years 2005-2010.

ANALYSIS OF INJURIES SUSTAINED DURING ACCIDENTS

The principal purpose of the analysis is to determine the most frequent injuries caused by mobile parts of machines used in farms, as well as the severity of these injuries. The relations between the number of accidents and the type of the farm machine, the percentage of damage to health and the kind of the injured body part were analysed.

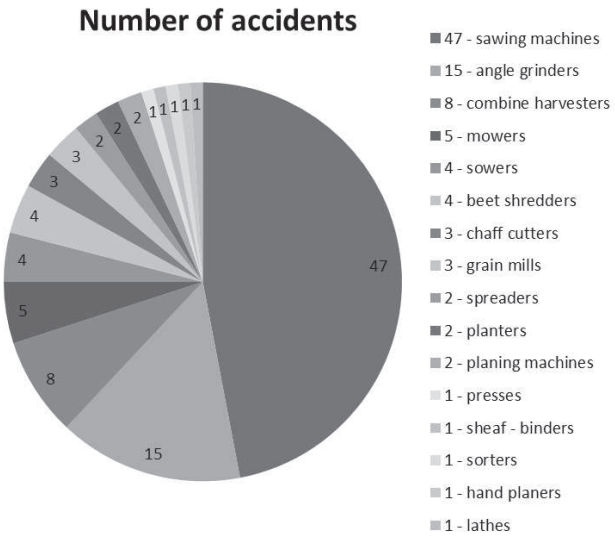

Fig. 1. Number of accidents in different groups of machines used in farms

The analysis of the number of accidents in different groups of farm machines used in the farms shows clearly that in the group of sawing machines, the number of accidents was the highest, i.e. 47 for 100 examined accidents. Many accidents (15) were involved with grinding machines. The analysis of the accidents run showed that the main cause of accidents was the ignorance of the rules of work safety, tiredness, carelessness, inattention of the operator or inefficiency of the machine. A frequent cause of the injuries was the effect called 'rebound of sawing machine'. It occurred when a moving saw suddenly touched the wood causing a violent turn of the sawing machine. The accidents often happened during the approaches to jerk out a saw jammed in wood, or during the work using a chain saw which was too blunt or improperly stretched. A frequent cause of the accidents was the incorrect, forced position of the operator during work (mostly bending), causing tiredness of the operator and break of the cutting disk.

The most frequent accidents involving farm machines were these with the combine harvesters. In 2005-2010 there were eight accidents involving combine harvesters. A harvester is composed of many active working elements, so the harvester operator should have a considerable knowledge on the operation of these elements. Most accidents resulted from the lack of knowledge about the work of the harvester elements or from the lack of a full cover of a working part in the machine. Most of the accidents with combine harvesters were caused by the carelessness, inattention or lack of experience of the operator, often leading to widespread injuries and sometimes even to the operator's death. In the case of tractor harvesters, the cause was the lack of or bad signalling between the operator of the harvester and the driver of the tractor.

The lowest number of accidents – one in each group – involved presses, sheaf-binders, sorters, planers and lathes. The main cause of these accidents was insufficient concentration during the work and lack of covers for mobile machine mechanisms. The carelessness of the machine operators, even during the simplest operations, can lead to accidents and to permanent health damage.

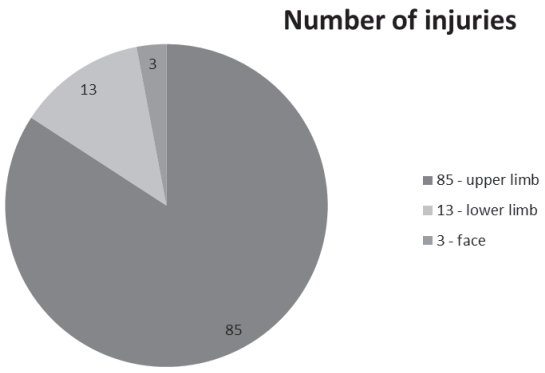

Fig. 2. Number of injuries to different body parts

Based on the analysed accidents, it can be confirmed that the part of the body mostly injured is an upper limb. Upper

limbs were injured in up to 85 accidents. It is so because most of the accidents occur during the works involving sawing and grinding machines, where the operations are performed using the upper limbs – hands. Moreover, most of farm works, like repair or adjustment of machines, are done using upper limbs. Another body part that sustains frequent injuries is a lower limb. There were 13 accidents causing damage to lower limbs. The face is the part, which is the most rarely injured. For a hundred of accidents, there was only one causing more than one injury. This was the situation during an accident involving a spreader, when an upper and a lower limb were injured.

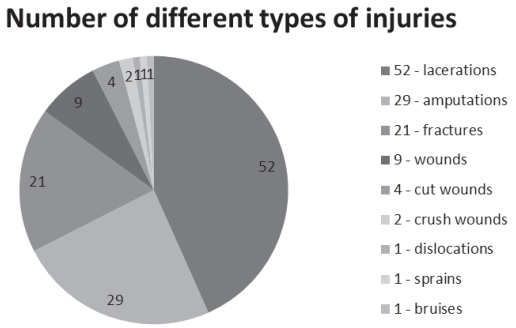

Fig. 3. Number of different types of injuries

The analysis results concerning the relation between the number of accidents and the type of injury are presented graphically in Fig. 3. Amid all injuries, the most frequent were: lacerations – in 52 accidents, amputations – in 29 accidents and fractures – in 21 accidents. The rarest were the following injuries: bruise – 1, sprain – 1, dislocation – 1. In total, the number of injuries in 100 accidents came up to 120. There were accidents with many different injuries for one body part. Frequent were both the amputations with fracture and the lacerations with fracture.

The wounds are caused by breaking anatomical continuity of the skin, of deeper tissue or of organs. The most frequent reason is a mechanical injury. Wounds can be divided depending on the force's acting way and its mechanism, into lacerations, cut wounds, bruises, puncture wounds, crush wounds and many others [1, 10].

The lacerations are inflicted with the objects tearing the tissues. A laceration has uneven, jagged edges, walls and bottom. In case of a cut wound, the skin was cut with a sharp object. The break of the skin occurs throughout the thickness, it can also damage the tissues lying deeper.

The cut wounds are distinguished by smooth edges, while a bruise is caused by a blow made with a blunt-ended object. In case of a bruise, besides breaking anatomical continuity of the skin, the tissues adjacent to the wound are crushed. Afterwards, the necrosis spreads on the crushed tissues. A bruise has uneven and swollen edges.

The crush wounds are kind of bruises with the difference that the injury surface is larger. Crushing causes a strong injury to tissues surrounding the wound.

The amputation also is a kind of wound, caused by the action of a crushing force resulting in partial or total detachment of a perimeter body part such as upper limb, lower limb, ear, nose, from the whole organism.

The fracture is an interruption of the bone continuity under the influence of the inside or outside factors. A fracture occurs when the force acting on the bone is too great. Among the analysed injuries, frequent types of fractures are multiple fractures. It is a very grave type of fracture caused by high forces, in which the bone has broken into several pieces and the bone fragments are driven into each other. A dislocation is a displacement of the bones in the articular capsule under the action of the force causing a transposition of articulation surfaces [1, 2, 10, 13].

A sprain consists in damaging the articular capsule as a result of surpassing the allowed limit of the articulation motion.

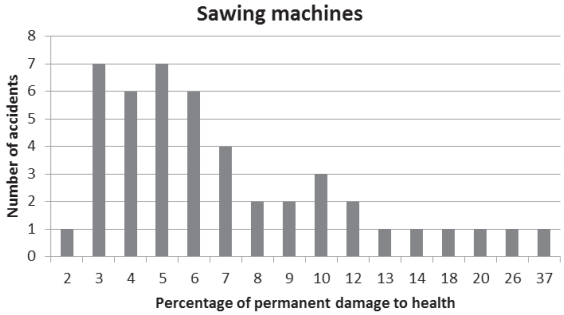

Fig. 4. Relation between the number of accidents involving sawing machines and the percentage of permanent damage to the operator health

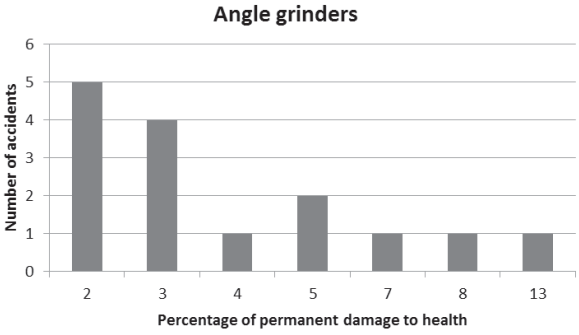

Fig. 5. Relation between the number of accidents involving angle grinders and the percentage of permanent damage to the operator health

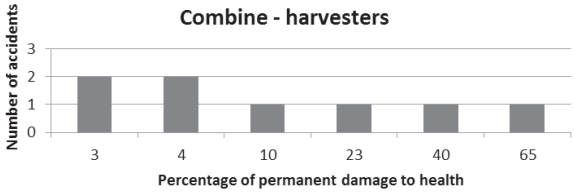

Fig. 6. Relation between the number of accidents involving combine-harvesters and the percentage of permanent damage to the operator health

The analysis of the relation between the number of accidents and the percentage of permanent damage to health was done for three groups of machines with the highest number of accidents, i.e. for sawing machines, angle grinders and combine-harvesters. The analysis results are presented graphically in Figs. 4, 5 and 6. In the analysis, the scale of the percentage of permanent damage to health was used. The analysis using the AIS scale showed that the injuries in all examined acci-

dents belonged to the same group – AIS I. However, applying the scale of percentage of permanent damage to health, we can distinguish accidents in terms of the intensity level of sustained injuries. In case of the group of sawing machines, we can note, that most of accidents caused, in principle, not very large permanent damage to health, within 3-7%. However, there were more serious accidents, involving more severe consequences, where the permanent damage to health came up to 20% – 37%. Accidents with sawing machines also caused small permanent damage to health, usually 2-3%. The highest damage to health caused by an angle grinder was 13%. The accidents involving combine-harvesters, because of their complexity, cause different damages to health. They can be small damages of 3-4%, but they can also be damages coming up to 40% or 65%, resulting even in the limitation of independent existence of the accident's victim.

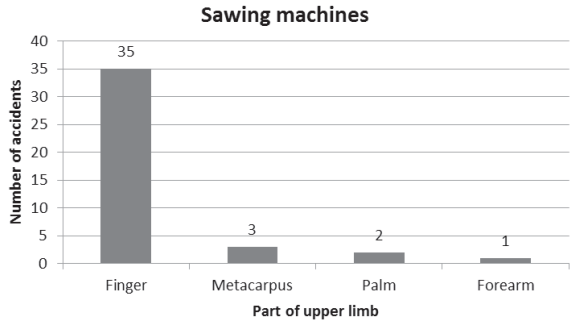

Fig. 7. Relation between the number of accidents involving sawing machines and an injured part of the upper limb

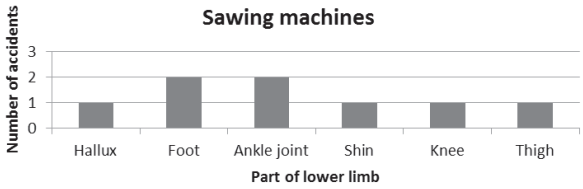

Fig. 8. Relation between the number of accidents involving sawing machines and an injured part of the lower limb

For the sawing machines, as it is a group of machines with the highest number of accidents, an additional analysis was made – which of the limbs sustained injuries and on what area. The results of the analysis are presented in Figs. 7 and 8. In most of the accidents involving sawing machines, 38 for 47 accidents, the upper limb was injured. The most frequent were the injuries to the upper limb fingers. It results from the fact that most of accidents involving sawing machines concern stationary circular saws, where the operator shifts the cut wood with his hands. There were some more dangerous accidents, in which more than one part of the upper limb is injured.

The accidents in which the lower limb was injured were less numerous – 8 accidents. There was however a great diversity among them. Almost all parts of the lower limb were injured in the same number of accidents. The foot and the ankle joint appeared only in two accidents. Injuries to the lower limb occurred during the works using portable chain sawing machines, where the operator was injured when trying to jerk out a jammed chain. In one accident with a sawing machine, the operator's face was injured.

CONCLUSIONS

- On the area of Krakow County in 2005-2010, most of accidents involved the sawing machines. It is due to the fact that the number of such machines used in farms is the highest. These machines, apparently simple, often are operated by people without proper acquaintance with such work and this leads to accidents. Another group of machines with numerous accidents were the angle grinders. Among the typically agricultural machines, the frequent accidents were those involving combine-harvesters.
- The part of the body frequently injured in the accidents was the upper limb. In the accidents involving sawing machines, most of the damage to an upper limb concerned fingers.
- The most frequent types of injuries amid all accidents were the lacerations. Also, frequent types of injuries were amputations (occurring mainly during the works with the sawing machines) and fractures.
- In case of the group of sawing machines and angle grinders, the injuries sustained involved, in majority, a low percentage of permanent damage to health.
- In the accidents involving combines, the percentages were significantly higher and reached the value that indicated important damage to health leading to the limitation of independent existence.
- The most frequent causes of all the accidents were carelessness, lack of concentration, inattention or the operator's tiredness.

REFERENCES

1. **Driscoll P., Skinner D., Earlan R.: 2010**, ABC postępowania w urazach, Górnicki Wydawnictwo Medyczne Wrocław.
2. **Kapandji I.: 2013**, Anatomia funkcjonalna stawów – kończyna dolna, Wydawnictwo Elsevier Urban and Partner, Wrocław.
3. Kasa Rolniczego Ubezpieczenia Społecznego: 2009, Informacje podstawowe, Warszawa.
4. **Kawiorski J.: 1990**, Księga powiatów, Wydawnictwo Kurier Press, Kraków.
5. **Kozłowska B., Apacki Sz., Komarnicka K.: 2007**, Raport z analizy obecnej sytuacji na obszarze Powiatu Krakowskiego, LEM Projekt Sp. z o. o., Kraków.
6. **Kuczewski J., Waszkiewicz Cz.: 1997**, Mechanizacja rolnictwa. Maszyny i urządzenia do produkcji roślinnej i zwierzęcej, Wyd. SGGW, Warszawa.
7. **Pike J. A.: 1990**, Automotive Safety. Anatomy, Injury, Testing & Regulation. Chapter 3: Injury Scaling, Society of Automotive Engineers, Inc.
8. **Praca zbiorowa pod red. Regulski St.: 1986**, Maszyny rolnicze, Państwowe Wydawnictwo Rolnicze i Leśne, Warszawa.
9. **Praca zbiorowa pod red. Więsik J.: 2005**, Pilarki przenośne. Budowa i eksploatacja, Wydawnictwo Fundacja „Rozwój SGGW", Warszawa.
10. **Thompson J., Netter F.: 2007**, 16. Atlas anatomii ortopedycznej, Wydawnictwo Elsevier Urban and Partner, Wrocław.

11. UNIQA Towarzystwo Ubezpieczeń Spółka Akcyjna, UNIQA Towarzystwo Ubezpieczeń na Życie Spółka Akcyjna: 2008, Tabela oceny procentowej trwałego uszczerbku na zdrowiu.
12. **Waszkiewicz Cz., Kuczewski J.: 1998**, Maszyny rolnicze. Maszyny i urządzenia do produkcji roślinnej, Wydawnictwa Szkolne i Pedagogiczne, Warszawa.
13. **Wismans J.S.H.M. et al.: 1994**, Injury Biomechanics, Eindhoven University of Technology.
14. **Wójcik M.: 2012**, Analiza obrażeń operatora spowodowanych przez ruchome części maszyn rolniczych, Praca dyplomowa inżynierska, Politechnika Krakowska Wydział Mechaniczny.

ANALIZA OBRAŻEŃ OPERATORA SPOWODOWANYCH PRZEZ RUCHOME CZĘŚCI MASZYN UŻYWANYCH W GOSPODARSTWACH ROLNICZYCH

Streszczenie. W gospodarstwach rolniczych użytkowane są coraz to nowsze narzędzia i maszyn, które ułatwiają pracę. Brak umiejętności do ich obsługiwania prowadzi często do wypadków, których efektem są urazy o różnym stopniu nasilenia ciężkości. Przeprowadzono badania obrażeń powstałych podczas wypadków z udziałem narzędzi i maszyn rolniczych na terenie Powiatu Krakowskiego w latach 2005-2010. Zbadano jakie rodzaje obrażenia występują najczęściej, w jakiej grupie maszyn jest najwięcej wypadków, a także oceniono stopień nasilenia ciężkości obrażeń. Najwięcej wypadków miało miejsce z udziałem pilarek, drugą grupą są szlifierki kątowe. Wśród maszyn typowo rolniczych najczęściej zdarzały się wypadki z udziałem kombajnów. Częścią ciała, która najczęściej doznawała obrażeń w wypadkach jest kończyna górna. Najczęstszym rodzajem obrażenia wśród wszystkich wypadków były rany szarpane. W przypadku grupy pilarek i szlifierek kątowych występujące obrażenia w większości mają niewielki procent trwałego ubytku na zdrowiu. W wypadkach z udziałem kombajnów wskaźniki procentowe ulegają znacznemu wzrostowi i osiągają wartość procentową, która wskazuje na znaczne ubytki na zdrowiu prowadzące do ograniczenia samodzielnej egzystencji. Najczęstszą przyczyną wszystkich wypadków jest brak zachowania należytej ostrożności, brak koncentracji, nieuwaga, a także zmęczenie operatora.

Słowa kluczowe: narzędzia i maszyny gospodarstw rolniczych, wypadki, obrażenia.

The study was performed within the framework of a PK WM M-4/84/2013/DS Project.

TEKA. COMMISSION OF MOTORIZATION AND ENERGETICS IN AGRICULTURE – 2013, Vol. 13, No. 2, 113–118

Oil leaks intensity in variable-height gaps

Tadeusz Zloto, Konrad Kowalski

Institute of Mechanical Technologies
Częstochowa University of Technology

Received April 8.2013; accepted June 18.2013

Summary. The paper deals with issues of oil flow intensity in variable-height flat and ring gaps in hydraulic machines. On the basis of the Navier-Stokes equations and the continuum equation a formulas are given describing leaks in gaps. It is demonstrated that the volumetric loss in gaps depends on the dimensions and exploitation parameters of hydraulic machines.
Key words: variable-height gaps, hydraulic oil leaks.

INTRODUCTION

Hydraulic systems are applied in numerous branches of industry [1, 3, 13, 19]. In hydraulic machines there are oil-filled spaces between surfaces of neighbouring parts, called gaps [2, 4, 11, 14, 15, 17, 20]. The phenomena occurring in gaps are of great practical importance, since most energy losses in hydrostatic machines is associated with complex processes taking place in gaps [9]. Examining and understanding these processes makes it possible for designers and constructors of hydraulic machines to create more and more effective, reliable and durable devices [6, 7, 12, 15].

In the majority of cases, a gap is not of constant height, which may be caused by the inevitable imprecision of construction, or non-uniform wear [14]. Fig. 1 presents a classification of variable-height gaps dealt with in this paper. Wedge-shaped gaps are a typical case of flat gaps. Cone-shaped gaps, on the other hand, are typical representatives of ring gaps. Such gaps occur between the piston and cylinder block in axial piston pumps and hydraulic motors.

Among variable-height gaps one can distinguish confusor gaps (the height decreases with the flow direction) and diffuser gaps (the height increases) [16, 18].

Each gap is a source of volumetric losses, and the leak can be caused by various kinds of flow [8]:
– pressure flow (there is a pressure difference between the ends of a gap)
– friction flow (the piston or the cylinder wall is moving),
– pressure-friction flow (both phenomena occur).

The gap height is usually 1 ÷ 50 μm, but the fluid flow is not disrupted even for 0.1 μm. Despite the fact that the gap height is so small, the laws of the fluid mechanics still hold [2].

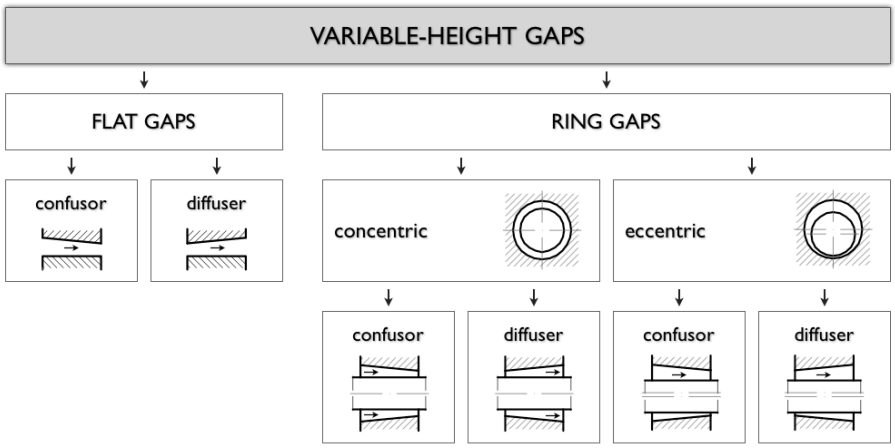

Fig. 1. Classification of variable-height gaps

APPLICATION OF THE NAVIER-STOKES EQUATIONS FOR DETERMINING VOLUMETRIC LOSSES IN LIQUID FLOWING THROUGH GAPS

Fig. 2 presents a diagram of a flat gap and a ring gap of a variable height h and the known length l. At the entrance to the gap of height h_1 the pressure is p_1 and at the exit from the gap of height h_2 the pressure is smaller and equals p_2. One of the walls of a gap can move with respect to the other with a relative velocity v. The direction of the liquid flow intensity Q is marked with an arrow.

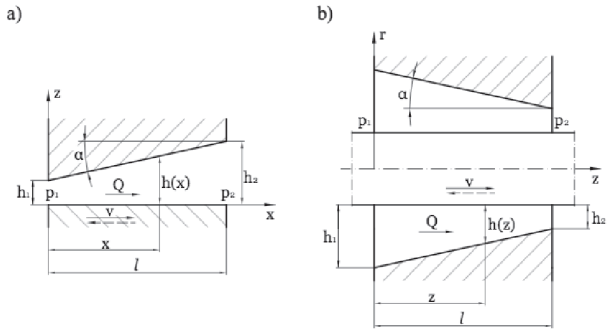

Fig. 2. Variable-height gaps: a) flat diffuser gap, b) ring confusor gap

The confusor and diffuser type gaps can be described by means of convergence m or convergence parameter k [8]:

$$m = tg\alpha = \frac{h_2 - h_1}{l}, \tag{1}$$

$$k = \frac{h_2 - h_1}{h_1}. \tag{2}$$

Pressure changes in the flat gap are accounted for by the Navier-Stokes equations and the flow continuum equation represented in the cylindrical coordinate system x, y, z [5, 10]:

$$\frac{\partial v_x}{\partial t} + v_x\frac{\partial v_x}{\partial x} + v_y\frac{\partial v_x}{\partial y} + v_z\frac{\partial v_x}{\partial z} = \nu\left(\frac{\partial^2 v_x}{\partial x^2} + \frac{\partial^2 v_x}{\partial y^2} + \frac{\partial^2 v_x}{\partial z^2}\right) - \frac{1}{\rho}\frac{\partial p}{\partial x}, \tag{3}$$

$$\frac{\partial v_y}{\partial t} + v_x\frac{\partial v_y}{\partial x} + v_y\frac{\partial v_y}{\partial y} + v_z\frac{\partial v_y}{\partial z} = \nu\left(\frac{\partial^2 v_y}{\partial x^2} + \frac{\partial^2 v_y}{\partial y^2} + \frac{\partial^2 v_y}{\partial z^2}\right) - \frac{1}{\rho}\frac{\partial p}{\partial y}, \tag{4}$$

$$\frac{\partial v_z}{\partial t} + v_x\frac{\partial v_z}{\partial x} + v_y\frac{\partial v_z}{\partial y} + v_z\frac{\partial v_z}{\partial z} = \nu\left(\frac{\partial^2 v_z}{\partial x^2} + \frac{\partial^2 v_z}{\partial y^2} + \frac{\partial^2 v_z}{\partial z^2}\right) - \frac{1}{\rho}\frac{\partial p}{\partial z}, \tag{5}$$

$$\frac{\partial v_x}{\partial x} + \frac{\partial v_y}{\partial y} + \frac{\partial v_z}{\partial z} = 0. \tag{6}$$

The following assumptions were adopted in the analysis:
- the flow is laminar, uniform, steady and isothermal [9],
- inertia forces of the liquid are negligible,
- the liquid is incompressible and completely fills the gap,
- tangent stress is Newtonian,
- liquid particles directly adjacent to the moving surface retain its velocity,
- the gap surfaces are rigid,
- cavitation phenomena in gaps were not taken into consideration.

When $v_x = v_x(x,z)$, $v_y = 0$ and $v_z = 0$ is assumed, equations (3 ÷ 6) become simplified:

$$v_x\frac{\partial v_x}{\partial x} = \nu\left(\frac{\partial^2 v_x}{\partial x^2} + \frac{\partial^2 v_x}{\partial z^2}\right) - \frac{1}{\rho}\frac{\partial p}{\partial x}, \tag{7}$$

$$0 = \frac{\partial p}{\partial y}, \tag{8}$$

$$0 = \frac{\partial p}{\partial z}, \tag{9}$$

$$\frac{\partial v_x}{\partial x} = 0. \tag{10}$$

It follows from equations (7 ÷ 10) that $v_x = v_x(z)$ and $p = p(x)$. Thus, the liquid motion in the gap is described by the following differential equation:

$$0 = \nu\frac{\partial^2 v_x}{\partial z^2} - \frac{1}{\rho}\frac{\partial p}{\partial x}. \tag{11}$$

With the dynamic viscosity coefficient μ, equation (11) becomes:

$$\frac{\partial^2 v_x}{\partial z^2} = \frac{1}{\mu}\frac{\partial p}{\partial x}. \tag{12}$$

To obtain a formula for the liquid flow velocity in the gap, equation (12) was integrated twice and boundary conditions for a gap with a moving wall were assumed:

$$v_x = \frac{1}{2\mu}\frac{\partial p}{\partial x}\left(z^2 - hz\right) - \frac{v}{h}z + v. \tag{13}$$

The liquid flow intensity through a gap of width b can be represented as:

$$Q = b\int_0^h v_x dz. \tag{14}$$

The pressure of the liquid in the gap is:

$$p(x) = \int\frac{dp}{dx}dx. \tag{15}$$

The differential dp/dx occurring in equation (15) was obtained as:

$$\frac{dp}{dx} = \frac{6\mu v}{h^2} - \frac{12\mu Q}{bh^3}, \tag{16}$$

where h is the gap height equal to:

$$h = \left(h_2 - h_1\right)\frac{x}{l} + h_1. \tag{17}$$

Substituting (16) into (15) and taking (17) into consideration:

$$p(x) = \int\left[\frac{6\mu v}{\left(\left(h_2 - h_1\right)\frac{x}{l} + h_1\right)^2} - \frac{12\mu Q}{b\left(\left(h_2 - h_1\right)\frac{x}{l} + h_1\right)^3}\right]dx. \tag{18}$$

After integrating equation (18), determining the integration constant and applying transformations:

$$p(x)=\frac{6\mu x}{h_1 h}\left(\pm \mathrm{v}-\frac{Q}{b}\cdot\frac{h+h_1}{hh_1}\right)+p_1. \tag{19}$$

Further to the operations stated above, assuming the boundary conditions as $x=l$, $p=p_2$, $h=h_2$, the leak flow intensity Q was obtained from (19):

$$Q=\frac{b\left(p_1-p_2\right)\left(h_1h_2\right)^2}{6\mu l\left(h_1+h_2\right)}\pm\frac{\mathrm{v}bh_1h_2}{h_1+h_2}. \tag{20}$$

An analogous procedure was conducted for the ring gap and the following formula was obtained for the leak flow intensity in a cone-shaped gap [8]:

$$Q=\frac{\pi dh_1\left(p_1-p_2\right)}{12\mu l}\left[1+1.5\left(\frac{e}{h_1}\right)^2+0.5k\left(3+0.5k-0.25k^2\right)+0.75k\left(\frac{e}{h_1}\right)^2+\frac{1}{8}\frac{k^4}{\sqrt{\left(2+k\right)^2-4\left(\frac{e}{h_1}\right)^2}}\right]\pm$$
$$\pm\frac{\pi dh_1\mathrm{v}}{4}\left(2+k-\frac{k^2}{\sqrt{\left(2+k\right)^2-4\left(\frac{e}{h_1}\right)^2}}\right), \tag{21}$$

where: e is a centrifugal displacement of the piston with diameter d.

RESULTS OF SIMULATION EXPERIMENTS ON LEAK FLOW INTENSITY OF OIL IN VARIABLE-HEIGHT GAPS

Simulation experiments on leaks in typical hydraulic oil were performed for a flat diffuser gap (convergence parameter k = 0.8) and for a ring confusor gap (convergence parameter k = -0.5). It was assumed that the oil flow is of pressure-friction type. One of the gap walls is moving with respect to the other with velocity v = 1 [m/s] in the direction reverse to the oil flow in the gap. Similarly, the piston is moving in the cylinder with velocity v = 1 [m/s] in the direction reverse to the oil flow in the gap.

The following parameters were assumed in the computations for the flat gap:

- pressure at the gap entrance p1 = 25 [MPa],
- pressure at the gap exit p2 = 0 [MPa],
- the gap length l = 0,032 [m],
- the gap width b = 0,01 [m],
- dynamic viscosity coefficient μ = 0.0253 [Pas].

For the ring gap, the parameters were as follows:

- pressure at the gap entrance p1 = 25 [MPa],
- pressure at the gap exit p2 = 0 [MPa],
- the gap length l = 0,02 [m],
- the piston diameter d = 0,015 [m],
- dynamic viscosity coefficient μ = 0.0253 [Pas].

Fig. 3 presents the results obtained in a flat diffuser gap for various dimensions and exploitation parameters. It can be observed that leaks grow with decreasing values of the dynamic viscosity coefficient of oil (Fig. 3a). At the same time, as the mean gap height increases, leaks grow exponentially (Fig. 3b). When the gap wall is moving in the direction reverse to that of oil flow, increase in the gap wall velocity contributes to decreasing leaks (Fig. 3c). Besides, leaks grow with the growth of the pressure difference between the two ends of the gap (Fig. 3d).

Fig 4 presents the results obtained in a ring confusor gap for various dimensions and exploitation parameters. By changing the value of the centrifugal displacement of the piston from 0 (concentric position in the cylinder) to 16 μm (the maximal displacement of the piston in the case under consideration), its impact on volumetric losses was examined. The analysis demonstrate that as the piston displacement increases, the value of leaks in the gap increases too (Fig. 4a). The leaks are the greater, the bigger the mean gap height is (Fig. 4b). Increase in the gap length l is accompanied by decreasing leaks (Fig. 4c). Oil viscosity is a crucial factor: when viscosity increases, leaks decrease (Fig. 4d). Besides, leaks grow with the growth in the pressure difference between the two ends of the gap (Fig. 4e). When the piston is moving in the reverse direction to that of oil flow, then increase in the velocity of the piston motion causes leaks to decrease (Fig. 4f). Thus, it is evident that piston velocity influences the quantity of leaks due to the operation of molecular friction forces in oil.

CONCLUSIONS

The study leads to the following conclusions:

1. Computational models discussed in the present analysis provide adequate tools for determining the flow intensity of oil leaks in flat and ring gaps.
2. The intensity of oil leaks depends on a number of parameters, such as dimensions or exploitation factors. Their occurrence negatively affects the efficiency of hydraulic machines and devices.
3. The laminar flow occurs in hydraulic gaps, and the Reynolds number increases with the growth of leaks.

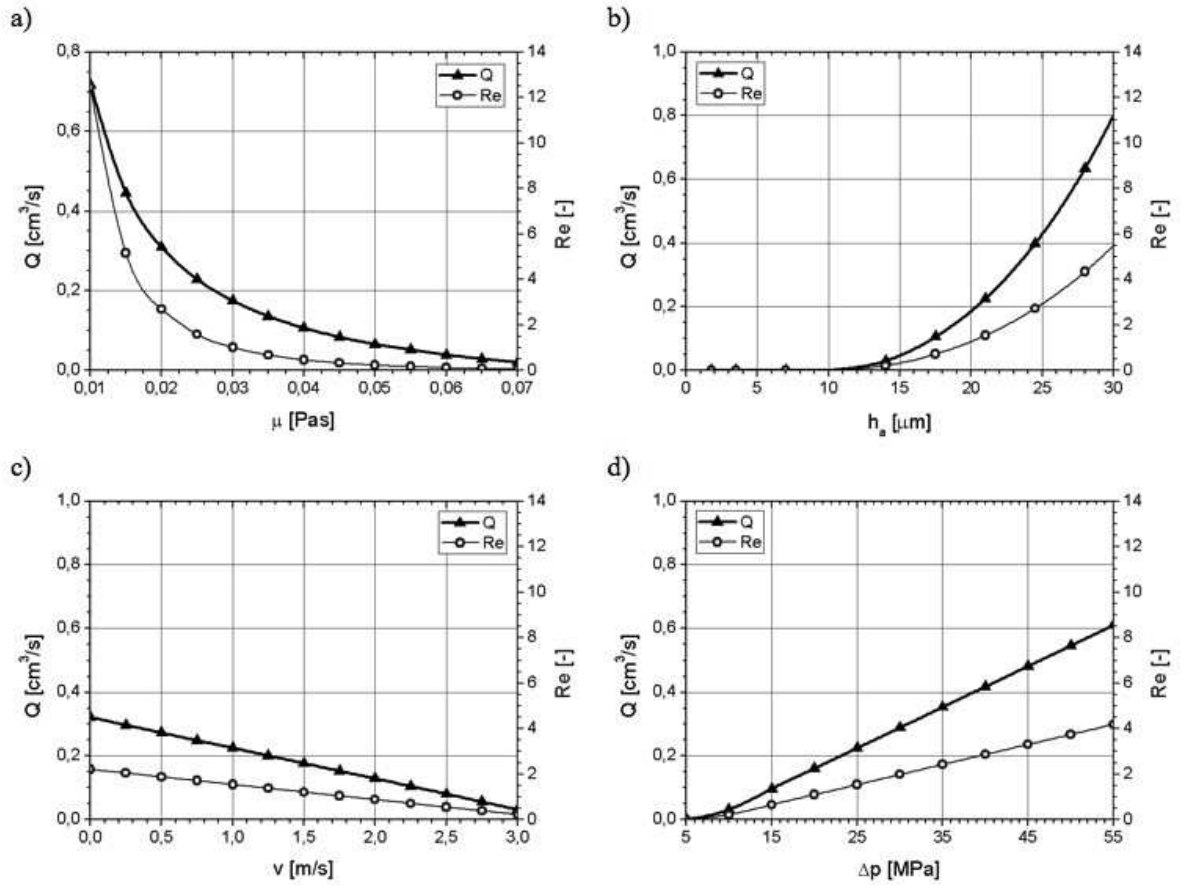

Fig. 3. Leaks and Reynolds numbers in a flat gap depending on: a) dynamic viscosity coefficient μ of oil, b) mean gap height $h_a = (h_1+h_2)/2$, c) velocity v of one of the gap walls, d) pressure drop Δp between the two ends of the gap

REFERENCES

1. **Greczanik T., Stryczek J., 2005**: The concept of the bus fluid power system of the mining machine. Polska Akademia Nauk, Teka Komisji Motoryzacji i Energetyki Rolnictwa, Tom V, s. 72-79, Lublin.
2. **Ivantysyn J., Ivantysynova M., 2001**: Hydrostatic Pumps and Motors. Academia Books International, New Delhi.
3. **Ivantysynova M., 2009**: Design and Modeling of Fluid Power Systems. Purdue University.
4. **Kleist A., 2002**: Berechnung von Dicht- und Lagerfugen in hydrostatischen Maschinen. Reihe Fluidtechnik, Band 25. Shaker Verlag, Aachen.
5. **Kondakow L. A., 1975**: Uszczelnienia układów hydraulicznych. WNT, Warszawa.
6. **Lasaar R., 2000**: The Influence of the Microscopic and Macroscopic Gap Geometry on the Energy Dissipation in the Lubricating Gaps of Displacement Machines. Proc. of 1-st FPNI-PhD Symposium, Hamburg.
7. **Murrenhoff H., 2005**: Grundlagen der Fluidtechnik. Teil 1: Hydraulik, Shaker Verlag, Aachen.
8. **Nikitin G. A., 1982**: Szczielewyje i łabirintnyje upłotnienia gidroagregatow. Maszinostrojenie, Moskwa.
9. **Osiecki A., 2004**: Hydrostatyczny napęd maszyn. WNT, Warszawa.
10. **Osipow A. F., 1966**: Objemnyje gidrowliczieskie maszyny. Maszinostrojenie, Moskwa.
11. **Otremba J., 1967**: Przepływ laminarny cieczy lepkich w szczelinach pierścieniowych. Archiwum Budowy Maszyn, Tom XIV, Zeszyt 3, Warszawa.
12. **Podolski M. E., 1981**: Upornyje podszipniki skolżenia, Leningrad.
13. **Ryzhakov A., Nikolenko I., Dreszer K., 2009**: Selection of discretely adjustable pump parameters for hydraulic drives of mobile equipment. Polska Akademia Nauk, Teka Komisji Motoryzacji i Energetyki Rolnictwa, Tom IX, 267-276, Lublin.
14. **Stryczek S., 1984**: Napęd hydrostatyczny. Elementy i układy. WNT, Warszawa.
15. **Szydelski Z., Olechowicz J., 1986**: Elementy napędu i sterowania hydraulicznego i pneumatycznego. PWN, Warszawa.
16. **Trifonow O. N., 1974**: Gidrawliczieskie sistemy mietałorieżuszczych stankow. MSI, Moskwa.
17. **Wieczorek U., 2000**: Simulation of the gap flow in the sealing and bearing gaps of axial piston machines. Proc. Of 1-st FPNI-PhD Symposium, 493-507, Hamburg.
18. **Will D., Gebhardt N., 2011**: Hydraulik: Grundlagen, Komponenten, Schaltungen. Springer, Berlin.
19. **Zloto T., 2007**: Analysis of the hydrostatic load of the cylinder block in an axial piston pump. Polska Akademia

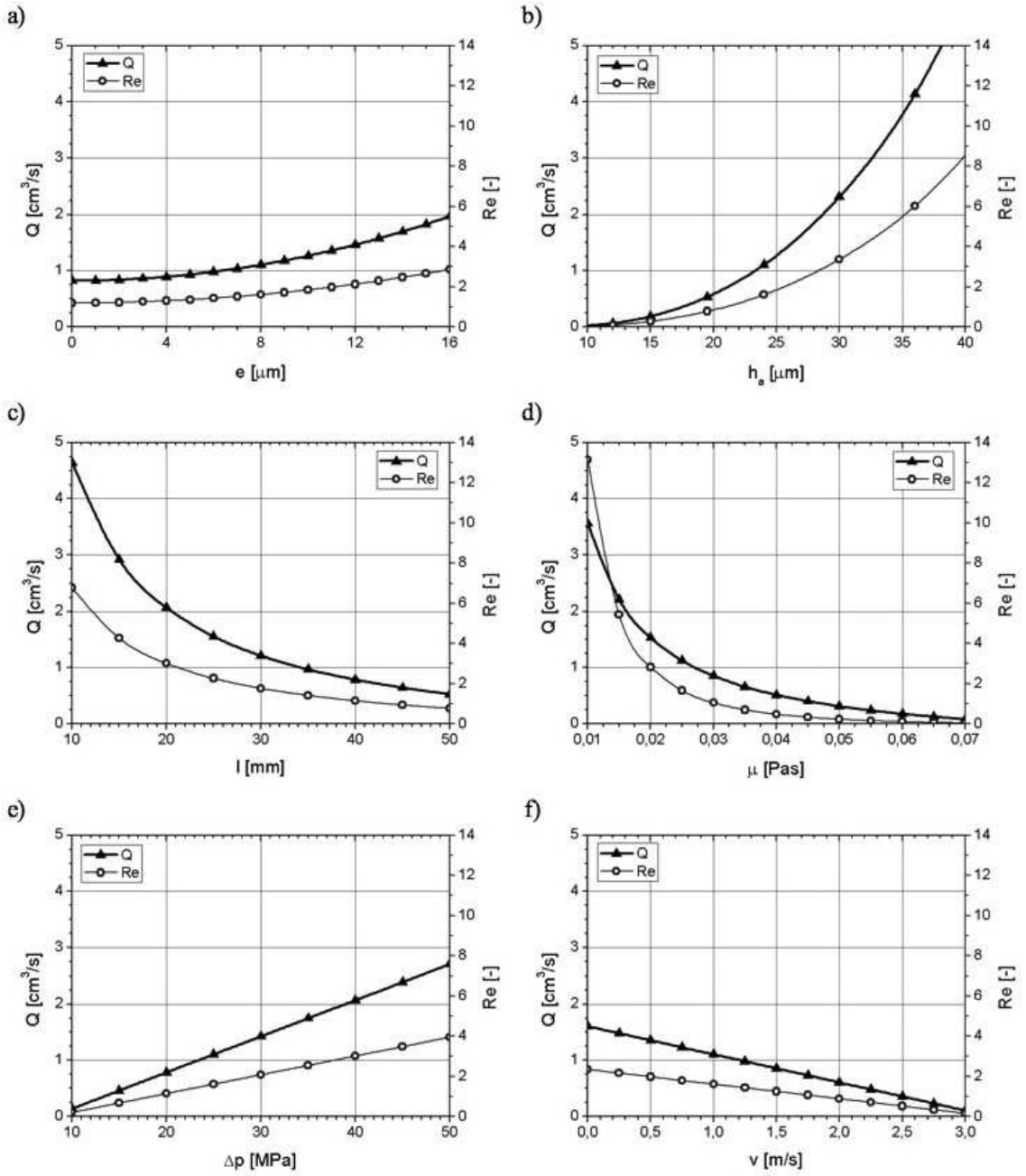

Fig. 4. Leaks and Reynolds numbers in a ring gap depending on: a) centrifugal displacement e of the piston, b) mean gap height $h_a = (h_1+h_2)/2$, c) gap length l, d) dynamic viscosity coefficient μ of oil, e) pressure drop Δp between the two ends of the gap, f) piston velocity

Nauk, Teka Komisji Motoryzacji i Energetyki Rolnictwa, Tom VII, 302-309, Lublin.

20. **Zloto T., Kowalski K., 2011**: Oil pressure distribution in variable height gaps. Polska Akademia Nauk, Teka Komisji Motoryzacji i Energetyki Rolnictwa, Tom XIC, 343-352, Lublin.

NATĘŻENIE PRZEPŁYWU PRZECIEKÓW OLEJU W SZCZELINACH O ZMIENNEJ WYSOKOŚCI

Streszczenie. W artykule przedstawiono problematykę związaną z natężeniem przepływu oleju przez szczeliny płaskie i pierścieniowe o zmiennej wysokości, które występują w różnego rodzaju maszynach hydraulicznych. W oparciu o równania Naviera-Stokesa i równanie ciągłości wyznaczono zależności określające przecieki w szczelinach. Rezultaty obliczeń strat wolumetrycznych występujących w szczelinach przedstawiono w zależności od parametrów geometrycznych i eksploatacyjnych.

Słowa kluczowe: szczelina o zmiennej wysokości, przecieki oleju hydraulicznego.

TEKA. COMMISSION OF MOTORIZATION AND ENERGETICS IN AGRICULTURE – 2013, Vol. 13, No. 2, 119–124

Modelling the load of the piston system in an axial piston pump by means of the adina software

Tadeusz Zloto, Piotr Stryjewski

Insitute of Mechanical Technologies
Częstochowa University of Technology

Received April 11.2013; accepted June 18.2013

Summary. The paper analyses the load of the kinematic pair piston-cylinder block in an axial piston pump. The surface compressive stress occurring between the piston and the cylinder block were determined by means of the commercially available software Adina, which was used for constructing numerical models and representing results of the research.
Key words: axial piston pump, piston load, software Adina.

INTRODUCTION

Axial piston pumps have numerous industrial applications. Since they can operate by high pressures and power, they are characterized by high values of power efficiency, defined as the ratio of power to mass or volume [11, 12, 19]. Axial piston pumps are most often used in the drives of complex devices requiring high efficiency [13, 20]. Needless to say, attempts are constantly made at improving the design and exploitation parameters of pumps to further increase their efficiency and reliability [6, 7, 9, 10, 14, 17, 18, 21].

As was mentioned, axial piston pumps have a constantly growing range of industrial applications, including such branches as

- aircraft industry,
- automotive industry (presses, CNC systems, injection molding machines),
- heavy industry (pressure foundries, rolling machines, cokeries),
- building industry (excavators, loaders, extension arms),
- agriculture and forestry (cranes, elevators, grill rigs, mowers, harvesters),
- military vehicles (multifunction vehicles, constructing bridges).

LOAD OF A PISTON IN AN AXIAL PISTON PUMP

From among all hydraulic machines, the highest pressures are attested in axial piston pumps [1, 8, 22]. High pressures cause high loads of the basic kinematic pairs in these machines. Fig. 1 presents forces acting on the piston system in an axial piston pump.

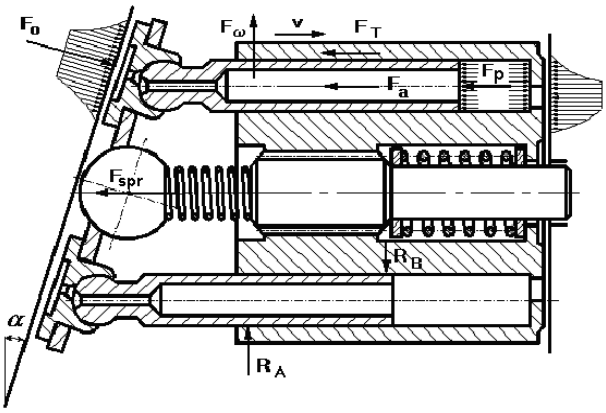

Fig. 1. Load of an axial piston pump

The following forces can be observed: Force F_p originating from pressure in the displacement chamber, dynamic force F_a of the piston system, centrifugal force F_w and friction F_T. The friction force F_T operates between the cylinder and the piston when the latter is moving in the course of the work. In the pump work cycle, friction increases load of the valve plate, but in the motor work cycle it causes relief of the valve plate.

One of the main sources of energy losses in axial piston pumps is the system piston-cylinder block. The two types of cylinder lining and the corresponding piston motions are presented below [3, 5, 16]:

- piston travels in a sleeveless cylinder (Fig. 2a),
- piston travels in a sleeved cylinder (Fig. 2b).

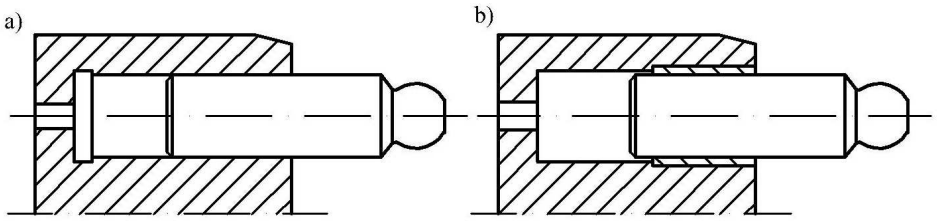

Fig. 2. Piston moving in: a) sleeveless cylinder, b) sleeved cylinder

ANALYSIS OF STRESS FORCES IN THE PISTON SYSTEM

In the piston-cylinder system in axial piston pumps operating on the swash plate principle, a radial force F_{Wy} coming mostly from the force of displacement pressure acts on the piston joint. This causes the piston to skew, and subsequently, significant reactions R_A, R_B occur between the piston and the cylinder.

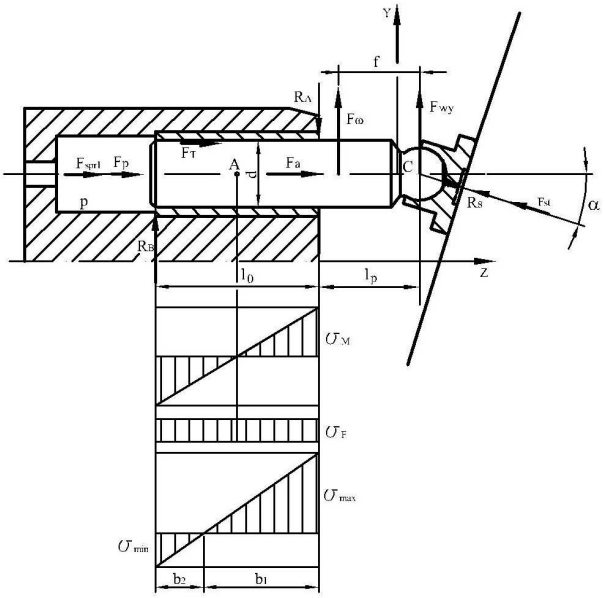

Fig. 3. Computational model of surface compressive stress

The surface compressive stress coming from the radial force are represented by the following formula [2, 4, 19]:

$$\sigma_F = \frac{F_{wy}}{d \cdot l_0}, \tag{1}$$

and the surface compressive stress coming from the torque of the radial force are represented as [4]:

$$\sigma_M = \frac{6 \cdot \left[F_{wy} \cdot \left(l_p + \frac{1}{2} \cdot l_0\right)\right]}{d \cdot {l_0}^2}. \tag{2}$$

The maximum surface compressive stress between the piston and the cylinder are [4, 19]:

$$\sigma_{max} = \sigma_M + \sigma_F. \tag{3}$$

Fig. 4 presents the maximal and minimal values of surface compressive stress as the function of the angle φ of the cylinder block rotation in the model under consideration.

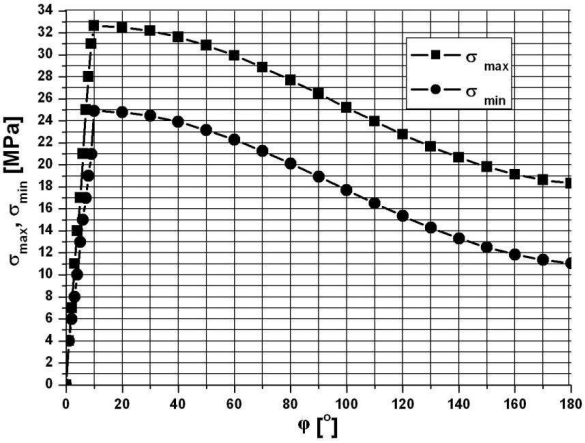

Fig. 4. Maximal and minimal surface compressive stress as the functions of the angle φ of the cylinder block rotation

MODELLING THE PISTON-CYLINDER CONTACT ZONE

In the study, the ADINA (Automatic Dynamic Incremental Nonlinear Analysis) system was used to simulate numerically the effective stress distribution of the kinematic pair piston-cylinder in an axial piston pump. The software is designed as a dedicated tool for solving problems related to fluid mechanics and heat flow.

Fig. 5 presents the algorithm of the simulation subsequently applied in the Adina system.

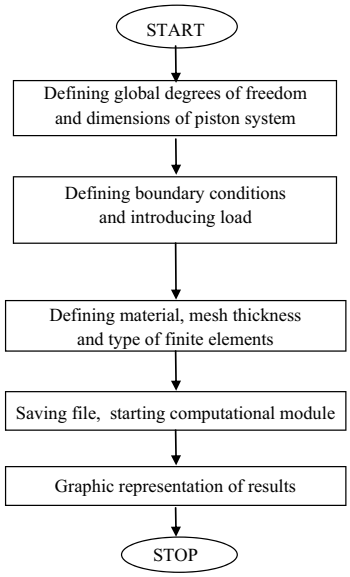

Fig. 5. Algorithm of the simulation in the Adina system

The piston-cylinder contact is analysed as a case of flat deformation in a two-dimensional space. Such a model includes some simplifications, but on the other hand, it offers important advantages, such as simplicity of modelling, compact size, and consequently, short computation time. Therefore, the model proves to be useful for testing computations related to various problems.

Fig. 6 presents the discretization region of the piston system.

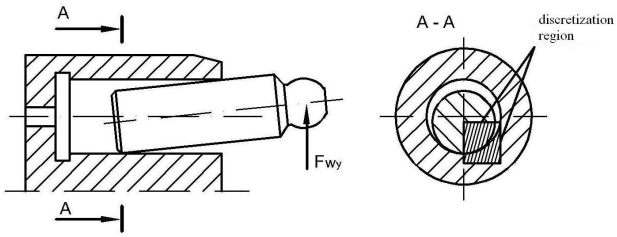

Fig. 6. Discretization region

The discretization uses 4-nod elements of the type 2D-SOLID.

Fig. 7 presents a mesh of the two-dimensional model of the steel piston-steel cylinder system.

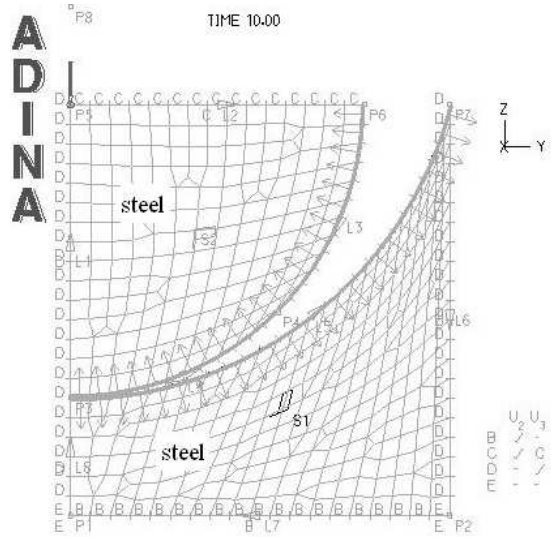

Fig. 7. Two-dimensional model mesh (steel-steel)

Fig. 8 presents smoothed field of effective stress in the contact zone, obtained for the piston-cylinder system.

Fig. 9 shows a mesh of the two-dimensional model of the steel piston-bronze cylinder system.

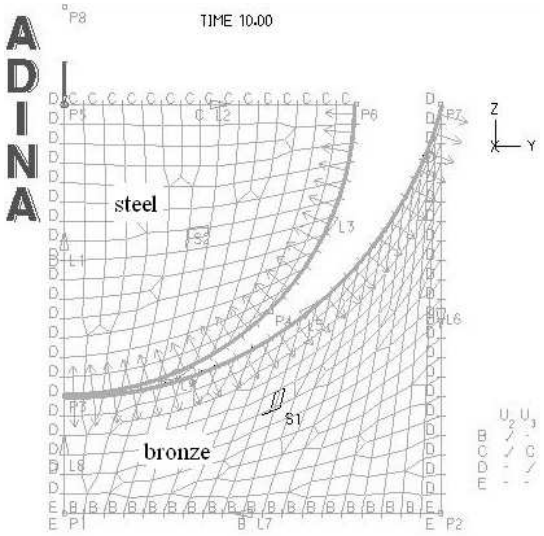

Fig. 9. Two-dimensional model mesh (steel-bronze)

Fig. 10 presents smoothed field of effective stress in the contact zone, obtained for the steel piston-bronze cylinder system.

Table 1 presents selected stress values obtained in the piston-cylinder contact zone in an axial piston pump for the analytic model not taking into account the material of which the parts are made and the numerical models of the steel piston-steel cylinder system and the steel piston-bronze cylinder system.

The absolute differences in unitary stress were obtained for the numerical models and the analytic model with respect to the analytic model. The relative values for the numerical model in the steel piston-steel cylinder case are 1.6 – 13.6 %, whereas in the case steel piston-bronze cylinder the relative values are 1.9 – 8.7% [15].

The study carried out therefore lends support to the thesis that the construction with a steel piston and a bronze cylinder should be preferred over the alternative construction of a pump in which both the piston and cylinder are made of steel.

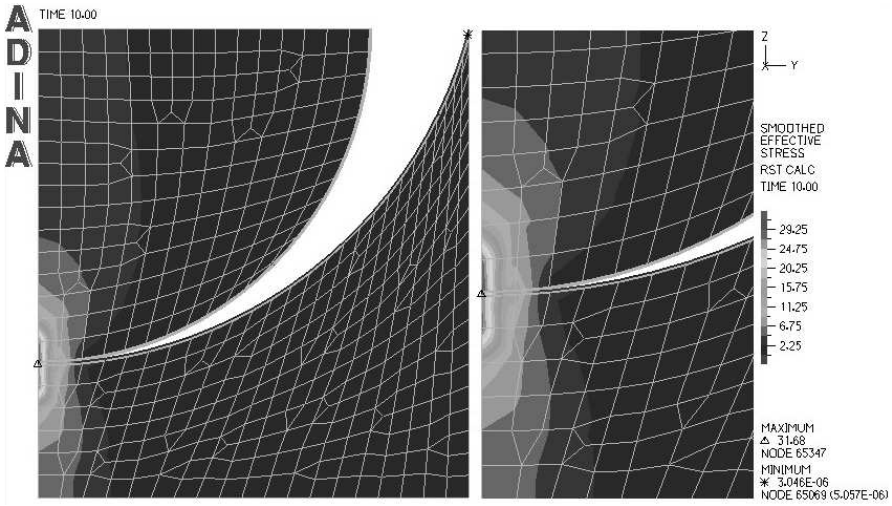

Fig. 8. Huber-von Mises smoothed effective stress distribution in the contact zone, obtained for the steel piston-steel cylinder system

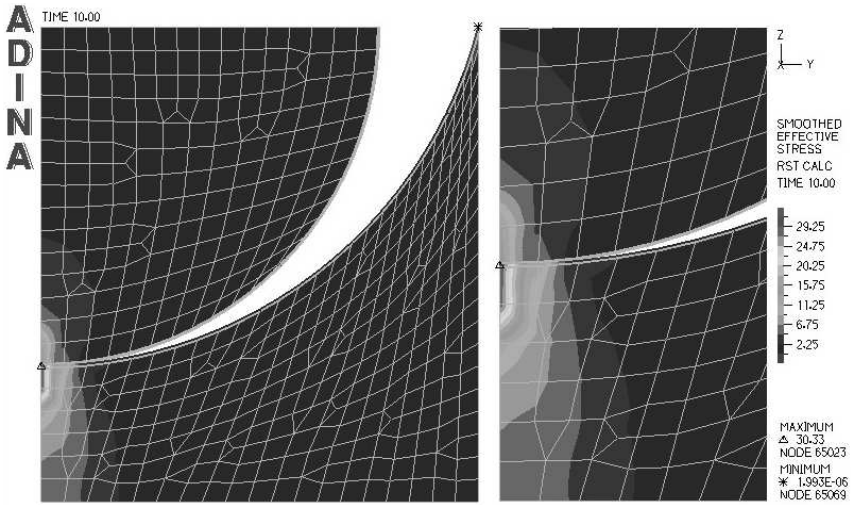

Fig. 10. Huber-von Mises smoothed effective stress distribution in the contact zone, obtained for the steel piston-bronze cylinder system

Table 1.

No.	Cylinder block rotation angle φ [°]	Radial force F_{wy} [N]	Analytic model σ [MPa]	Numerical models			
				Steel piston and cylinder σ [MPa]	Relative values [%]	Steel piston and bronze cylinder σ [MPa]	Relative values [%]
1	0	1864.11	32.21	31.68	1.6	30.33	5.8
2	45	1835.63	30.42	31.18	2.5	29.85	1.9
3	90	1774.53	26.55	30.15	13.6	28.86	8.7

CONCLUSIONS

On the basis of the present study, the following conclusions can be put forward:

1. The numerical models developed with the use of the software Adina enable determining the values of stress forces in the kinematic pair piston-cylinder of an axial piston pump.
2. In the case when the piston is made of steel and the cylinder block is made of bronze the surface compressive stress are significantly smaller than in the case when both the piston and the cylinder are made of steel. Supposedly it is caused by different strain and material properties of steel and bronze.

REREERENCES

1. **Balas W. 1966**: Łożyska hydrostatyczne w osiowych pompach tłokowych. Przegląd Mechaniczny, Nr 11, 329-331.
2. **Bronsztejn I.N., Siemiendiajew K.A., Musiol G., Mühlig H. 2004**: Nowoczesne compendium matematyki. WN PWN, Warszawa.
3. **Heyl W. 1979**: Ermittlung der optimalen Kolbenanzahl bei Schrägscheiben-Axialkolbeneinheiten. Ölhydraulik und Pneumatik, 23, Nr 1, 31-35.
4. **Ivantysyn J., Ivantysynova M.**: Hydrostatic Pumps and Motors. Akademia Books International, New Delhi 2001.
5. **Jang D.S. 1997**: Verlustanalise an Axialkolbeneinheiten. Dissertation RWTH, Aachen.
6. **Kögl Ch. 1995**: Verstellbare hydrostatische Verdrängereinheiten im Drehzahl- und Drehmomentregelkreis am Netz mit angepaβtem Versorgungsdruck. Dissertation RWTH, Aachen.
7. **Kraszewski D. 1975**: Dobieranie parametrów konstrukcyjnych łożyska hydrostatycznego o powierzchni płaskiej i sferycznej w zastosowaniu do maszyn tłokowych. Rozprawa doktorska. Pol. Wrocławska, Wydział Mechaniczny, Wrocław.
8. **Murrenhoff H. 2005**: Grundlagen der Fluidtechnik. Teil 1: Hydraulik, Shaker Verlag, Aachen.
9. **Niegoda J. 1978**: Badanie możliwości zastosowania tłoków z bezprzegubowym podparciem hydrostatycznym w pompach i silnikach wielotłoczkowych osiowych. Rozprawa doktorska. Pol. Gdańska, Wydz. Budowy Maszyn, Gdańsk.
10. **Olems L. 1999**: Berechnung des Spaltes der Kolben-Zylinderbaugruppe bei Axialkolbenmaschinen. Ölhydraulik und Pneumatik, 43, Nr 11-12, 833-839.
11. **Osiecki A. 1998**: Hydrostatyczny napęd maszyn. WNT, Warszawa.
12. **Орлов Ю.М. 1993**: Авиационные объемные гидромашины с золотниковым распределением. ПГТУ, Пермь.
13. **Osiecki L. 1999**: Badanie zjawisk zachodzących w zespole tłoczek-stopka hydrostatyczna-dławik śrubowy

maszyny wielotłoczkowej osiowej. Rozprawa doktorska. Pol. Poznańska, Wydz. Budowy Maszyn i Zarządzania, Poznań.
14. **Osiecki A., Osiecki L. 1998**: Prace rozwojowe nad nową konstrukcją pomp wielotłoczkowych osiowych. Hydraulika i Pneumatyka, Nr 4, 4-9.
15. **Paleczek W. 2003**: Mathcad Professional. Akademicka Oficyna Wydawnicza EXIT, Warszawa.
16. **Полозов А.В. 1976**: Выбор оптимальных параметров объемного роторного насоса. Вестник Машиностроения , № 1, 3-8.
17. **Renius K.H. 1973**: Experimentelle Untersuchungen an Gleitschuhen von Axialkolbenmaschinen. Ölhydraulik und Pneumatik, 17, Nr 3, 75-80.
18. **Renius K.H. 1975**: Reibung zwischen Kolben und Zylinder bei Schrägscheiben-Axialkolbenmaschinen. Ölhydraulik und Pneumatik, 19, Nr 11, 821-826.
19. **Stryczek S. 1995**: Napęd hydrostatyczny. Tom 1, WNT, Warszawa.
20. **Ryzhakov A., Nikolenko I., Dreszer K. 2009**: Selection of discretely adjustable pump parameters for hydraulic druves of mobile equipment. Polska Akademia Nauk, Teka Komisji Motoryzacji i Energetyki Rolnictwa, Vol. IX, 267-276.
21. **Złoto T., Stryjewski P. 2012**: Load of the kinematic pair piston-cylinder block in an axial piston pump , PAN, TEKA Komisji Motoryzacji i Energetyki Rolnictwa, Vol. 12, No 2, 269-274.
22. **Zhang Y. 2000**: Verbesserung des Anlauf- und Langsamlaufverhaltens eines Axialkolbenmotors in Schrägscheibenbauweise durch konstruktive und materialtechnische Maβnahmen. Dissertation RWTH, Aachen,.

MODELOWANIE OBCIĄŻENIA ZESPOŁU TŁOCZKA POMPY WIELOTŁOCZKOWEJ Z WYKORZYSTANIEM PROGRAMU ADINA

Streszczenie. Praca zawiera analizę obciążenia pary kinematycznej tłoczek-cylinder pompy wielotłoczkowej osiowej. Do określenia nacisków powierzchniowych występujących pomiędzy tłoczkiem i cylindrem w pompie wielotłoczkowej wykorzystano komercyjny program komputerowy Adina. Zbudowano modele numeryczne w tym programie i zaprezentowano wyniki badań.
Słowa kluczowe: pompa wielotłoczkowa osiowa, obciążenie tłoczka, program Adina.

Table of contents

List of the Reviewers

1. U. A. Abdulgazis
2. Kazimierz Dreszer
3. Mieczysław Dziubiński
4. Andrzej Kornacki
5. Elżbieta Kusińska
6. Andrzej Kusz
7. Andrzej Marciniak
8. Janusz Mysłowski
9. Ignacy Niedziółka
10. Mariusz Szymanek
11. Wojciech Tanaś
12. Janusz Wojdalski
13. Daniela Żuk

Editors of the „TEKA" quarterly journal of the Commission of Motorization and Energetics in Agriculture would like to inform both the authors and readers that an agreement was signed with the Interdisciplinary Centre for Mathematical and Computational Modelling at the Warsaw University referred to as "ICM". Therefore, ICM is the owner and operator of the IT system needed to conduct and support a digital scientific library accessible to users via the Internet called the "ICM Internet Platform", which ensures the safety of development, storage and retrieval of published materials provided to users. ICM is obliged to put all the articles printed in the "Motrol" on the ICM Internet Platform. ICM develops metadata, which are then indexed in the "Agro" database.

Impact factor of the TEKA quarterly journal according to the Commission of Motorization and Energetics in Agriculture is 3,01 (June 2013).

GUIDELINES FOR AUTHORS (2013)

The journal publishes the original research papers. The papers (min. 8 pages) should not exceed 12 pages including tables and figures. Acceptance of papers for publication is based on two independent reviews commissioned by the Editor.

Authors are asked to transfer to the Publisher the copyright of their articles as well as written permissions for reproduction of figures and tables from unpublished or copyrighted materials.

Articles should be submitted electronically to the Editor and fulfill the following formal requirements:
- Clear and grammatically correct script in English,
- Format of popular Windows text editors (A4 size, 12 points Times New Roman font, single interline, left and right margin of 2,5 cm),
- Every page of the paper including the title page, text, references, tables and figures should be numbered,
- SI units should be used.

Please organize the script in the following order (without subtitles):
Title, Author(s) name (s), Affiliations, Full postal addresses, Corresponding author's e-mail
Abstract (up to 200 words), Keywords (up to 5 words), Introduction, Materials and Methods, Results, Discussion (a combined Results and Discussion section can also be appropriate), Conclusions (numbered), References, Tables, Figures and their captions

Note that the following should be observed:
An informative and concise title; Abstract without any undefined abbreviations or unspecified references; No nomenclature (all explanations placed in the text); References cited by the numbered system (max 5 items in one place); Tables and figures (without frames) placed out of the text (after References) and figures additionally prepared in the graphical file format jpg or cdr.

Make sure that the tables do not exceed the printed area of the page. Number them according to their sequence in the text. References to all the tables must be in the text. Do not use vertical lines to separate columns. Capitalize the word 'table' when used with a number, e.g. (Table1).

Number the figures according to their sequence in the text. Identify them at the bottom of line drawings by their number and the name of the author. Special attention should be paid to the lettering of figures – the size of lettering must be big enough to allow reduction (even 10 times). Begin the description of figures with a capital letter and observe the following order, e.g. Time(s), Moisture (%, vol), (%, $m^3m^{-3)}$ or (%, gg^{-1}), Thermal conductivity ($W\ m^{-1}K^{-1}$).

Type the captions to all figures on a separate sheet at the end of the manuscript.

Give all the explanations in the figure caption. Drawn text in the figures should be kept to a minimum. Capitalize and abbreviate 'figure' when it is used with a number, e.g. (Fig. 1).

Colour figures will not be printed.

Make sure that the reference list contains about 30 items. It should be numbered serially and arranged alphabetically by the name of the first author and then others, e.g.
7. Kasaja O., Azarevich G. and Bannel A.N. 2009. Econometric Analysis of Banking Financial Results in Poland. Journal of Academy of Business and Economics (JABE), Vol. IV. Nr 1, 202–210.

References cited in the text should be given in parentheses and include a number e.g. [7].

Any item in the References list that is not in English, French or German should be marked, e.g. (in Italian), (in Polish).

Leave ample space around equations. Subscripts and superscripts have to be clear. Equations should be numbered serially on the right-hand side in parentheses. Capitalize and abbreviate 'equation' when it is used with a number, e.g. Eq. (1). Spell out when it begins a sentence. Symbols for physical quantities in formulae and in the text must be in italics. Algebraic symbols are printed in upright type.

Acknowledgements will be printed after a written permission is sent (by the regular post, on paper) from persons or heads of institutions mentioned by name.